https://doi.org/10.35662/unine-thesis-2922

UNIVERSITÉ DE NEUCHÂTEL

Compound-Specific Carbon and Chlorine Isotope Analysis of Organic Contaminants in Soil and Groundwater

A thesis submitted to the
Faculty of Science
Centre for Hydrogeology and Geothermics (CHYN)
University of Neuchâtel (Switzerland)

for the degree of
Docteur ès sciences

by
Jeremy Zimmermann

Defended on
June 30, 2021
Public presentation on
September 24, 2021

Accepted on the recommendation of
Prof. Daniel Hunkeler
Prof. Mario Schirmer
Dr. Jordi Palau

UNIVERSITÉ DE NEUCHÂTEL

Faculté des Sciences
Secrétariat-décanat de Faculté
Rue Emile-Argand 11
2000 Neuchâtel – Suisse
Tél : + 41 (0)32 718 21 00
E-mail : secretariat.sciences@unine.ch

IMPRIMATUR POUR THESE DE DOCTORAT

La Faculté des sciences de l'Université de Neuchâtel autorise l'impression de la présente thèse soutenue par

Monsieur Jeremy ZIMMERMANN

Titre:

"Compound-specific carbon and chlorine isotope analysis of organic contaminants in soil and groundwater"

sur le rapport des membres du jury composé comme suit:

- Prof. Daniel Hunkeler, directeur de thèse, Université de Neuchâtel, Suisse
- Prof. titulaire Mario Schirmer, Université de Neuchâtel, Suisse
- Dr Jordi Palau, Université de Barcelone, Espagne

Neuchâtel, le 12 octobre 2021

Le Doyen, Prof. A. Bangerter

Abstract

Chlorinated aliphatic hydrocarbons and aromatic petroleum hydrocarbons belong to the group of volatile organic compounds (VOC) and are common subsurface contaminants. They are naturally attenuated by dilution, sorption and degradation. Classical approaches in contaminant hydrogeology are often limited in their potential for monitoring attenuation processes, as they require that initial contaminants and degradation products be adequately captured by the sampling and analysis methods. Compound specific stable isotope analysis (CSIA) has emerged in recent decades as a versatile tool for tracking these processes. CSIA does not rely on concentration measurements. Degradation causes an isotopic enrichment in the initial contaminants and an isotopic depletion in degradation products. In addition to carbon isotope ratios, additional isotope system such as chlorine can be monitored for mechanistic insights. While carbon CSIA has established itself in the routine assessment of contaminated sites, studies incorporating chlorine isotopes have only recently become more common.

The aim of this work was to demonstrate the potential of compound-specific carbon and chlorine isotope analysis. It focuses on analytical aspects, isotope fractionation for different processes, and field applications. A review provides an overview of chlorine isotope fractionation of chlorinated contaminants in the subsurface by different processes and presents analytical techniques in chlorine isotope analysis. A summary of successful field applications illustrates the potential of using chlorine isotope data. Approaches in modelling chlorine isotope fractionation are also discussed.

An analytical method was developed for lowering method detection limits of chlorine isotope ratio measurements to the sub-$\mu g\,L^{-1}$ range for tetrachloroethene (PCE) and trichloroethene (TCE) in aqueous solution using headspace solid-phase microextraction (HS-SPME) coupled to gas chromatography (GC) quadrupole mass spectrometry. The novel SPME Arrow system featuring an increased sorptive phase volume was used. SPME parameters were optimized with a design of experiments approach to achieve maximum intensity. Mass spectrometric parameters and chlorine isotope ratio calculation schemes were also investigated and optimized. Any chlorine isotope fractionation was accounted for through a two-point calibration with externally referenced standards. Precise $\delta^{37}Cl$

measurements (standard deviations below 0.5‰) were achieved for concentrations of $0.4\,\mu g\,L^{-1}$ (PCE) to $0.8\,\mu g\,L^{-1}$ (TCE).

Another analytical method was developed to extend the applicability of carbon CSIA to complex volatile organic compound mixtures in soil samples. Soil extraction methods were compared and a heart-cutting two-dimensional GC-GC isotope-ratio mass spectrometry (IRMS) method developed. Good chromatographic separation for the target compounds in difficult matrices and high accuracy (trueness and precision) for carbon isotopic analysis were achieved. The use of purge and trap concentration allowed high volumes of extraction solvents to be analyzed, hereby lowering method detection limits of carbon CSIA in soil.

In a laboratory study, isotope fractionation during abiotic degradation of chlorinated ethenes was investigated. As opposed to many biodegradation processes, abiotic degradation is likely to yield non-chlorinated, generally non-toxic degradation products. However, this is difficult to demonstrate in the field. Dual carbon-chlorine isotope slopes are useful to investigate abiotic degradation in the field mediated by naturally occurring reactive iron phases. The degradation of chlorinated ethenes *cis*-1,2-dichloroethene (DCE), TCE and PCE by iron(II)sulfide (FeS) was investigated. FeS was found to be reactive with TCE and PCE, but not with *cis*-1,2-DCE. Carbon-chlorine isotope enrichment slopes $\Delta\delta^{13}C/\Delta\delta^{37}Cl$ were 11.0 ± 0.8 for PCE and 4.1 ± 0.2 for TCE. For PCE, the obtained slope is sufficiently distinct from those measured for biodegradation and can thus be applied to distinguish degradation processes in the field.

In a field study, the effect of source isolation on contaminant longevity was assessed at a site contaminated by a complex mixture of benzene, toluene, ethylbenzene and xylenes (BTEX) and chlorinated ethanes, ethenes and methanes. Through soil and groundwater concentration profiles over time and space, the importance of forward diffusion into low-permeability zones, degradation, and back-diffusion of initial contaminants and degradation products after source isolation was highlighted. Compound-specific carbon- and chlorine isotope analysis of groundwater and soil extracts showed that chloroform is degraded to dichloromethane through hydrogenolysis, while 1,1,2,2-tetrachloroethane is degraded to trichloroethene and *cis*-1,2-dichloroethene. The study demonstrated the potential of applying compound-specific isotope analysis not only to groundwater, but also to soil. Soil is shown to be an important matrix that often controls the long-term fate of contaminants.

In conclusion, the improvements in analytical methods and understanding of isotopic fractionation processes presented in this thesis offer an important contribution to the field of compound-specific isotope analysis, and shall further advance its routine application in contaminated site management. The approaches developed and discussed herein may be

adapted to other organic compounds and applied in future investigations that aim to track the environmental fate of organic contaminants.

Keywords volatile organic compounds, contaminants, compound-specific isotope analysis, chlorinated hydrocarbons, stable carbon isotopes, stable chlorine isotopes, abiotic degradation, biotic degradation, monitored natural attenuation, degradation pathways, isotope fractionation, gas chromatography, isotope-ratio mass spectrometry

Synthèse

Les hydrocarbures aliphatiques chlorés et les hydrocarbures pétroliers aromatiques appartiennent au groupe des composés organiques volatils et sont fréquemment retrouvés comme polluants dans le sous-sol. Naturellement, leurs concentrations sont atténuées par la dilution, la sorption et la dégradation. Les approches classiques de l'hydrogéologie des contaminants sont souvent limitées en tant qu'outil de surveillance des processus d'atténuation, car elles exigent que les contaminants d'origine et les produits de dégradation soient correctement capturés par les méthodes d'échantillonnage et d'analyse. L'analyse des isotopes stables de composés spécifiques s'est avérée être un outil polyvalent pour suivre ces processus au cours des dernières décennies. La méthode ne repose pas sur des mesures de concentration. La dégradation entraîne un enrichissement des isotopes lourds dans les polluants d'origine et un appauvrissement dans les produits de dégradation. Outre les rapports isotopiques du carbone, d'autres systèmes isotopiques, comme ceux du chlore, peuvent être mesurés pour obtenir des informations sur les mécanismes. Alors que l'analyse des isotopes du carbone est bien établie dans l'évaluation de routine des sites contaminés, les études intégrant les isotopes du chlore ne sont devenues courantes que récemment.

L'objectif de cet article était de démontrer le potentiel de l'analyse isotopique du carbone et du chlore de composés organiques spécifiques. Il se concentre sur les aspects analytiques, le fractionnement isotopique pour différents processus et les applications sur le terrain. Un article de synthèse donne une image complète du fractionnement isotopique du chlore des contaminants chlorés dans le sous-sol par différents processus et présente les techniques analytiques de l'analyse isotopique du chlore. Un résumé des applications de terrain réussies illustre le potentiel des données isotopiques du chlore. Les approches de la modélisation du fractionnement isotopique du chlore sont également discutées.

Une méthode analytique a été mise au point pour réduire les limites de détection des mesures du rapport isotopique du chlore à la gamme sub-$\mu g\,L^{-1}$ pour le tétrachloroéthène (PCE) et le trichloroéthène (TCE) en solution aqueuse par microextraction sur phase solide par espace de tête (*headspace solid-phase microextraction*, HS-SPME) en combinaison avec la chromatographie gazeuse couplée avec la spectrométrie de masse quadripolaire. Le nouveau système SPME Arrow avec un volume accru des phases sorptives a été utilisé.

Les paramètres de la SPME ont été optimisés par un plan d'expériences afin d'obtenir une intensité maximale. Les paramètres de spectrométrie de masse et les schémas de calcul du rapport isotopique du chlore ont également été étudiés et optimisés. L'éventuel fractionnement isotopique du chlore pendant l'extraction et l'analyse a été pris en compte par un étalonnage en deux points avec des standards de référence externes. Des mesures précises de δ^{37}Cl (écarts types inférieurs à 0.5‰) ont été obtenues pour des concentrations allant de $0.4\,\mu g\,L^{-1}$ (PCE) à $0.8\,\mu g\,L^{-1}$ (TCE).

Une autre méthode analytique a été mise au point pour étendre le champ d'application de l'analyse des isotopes du carbone de composés spécifiques à des mélanges complexes de composés organiques volatils dans des échantillons de sol. Les méthodes d'extraction du sol ont été comparées et une méthode bidimensionnelle de spectrométrie de masse du rapport isotopique GC-GC utilisant la *coupe à cœur* a été développée. Une bonne séparation chromatographique pour les composés cibles dans des matrices difficiles et une grande exactitude (justesse et précision) pour l'analyse des isotopes du carbone ont été obtenues. En utilisant la concentration par purge et piégeage, de grands volumes de solvants d'extraction ont pu être analysés, ce qui a permis d'abaisser les limites de détection de la méthode d'analyse des isotopes du carbone de composés spécifiques dans le sol.

Dans une étude de laboratoire, le fractionnement isotopique pendant la dégradation abiotique des éthènes chlorés a été étudié. Contrairement à de nombreux processus de dégradation biologique, des produits de dégradation non chlorés et généralement non toxiques sont formés au cours de la dégradation abiotique. Cependant, ceux-ci sont difficiles à détecter dans la pratique. Les pentes des enrichissements isotopiques du carbone et du chlore sont utiles pour étudier la dégradation abiotique par les phases ferreuses réactives naturelles sur les sites pollués. La dégradation des éthènes chlorés *cis*-1,2-dichloroéthène (DCE), TCE et PCE par le sulfure de fer(II) (FeS) a été étudiée. Le FeS s'est révélé réactif avec le TCE et le PCE, mais pas avec le *cis*-1,2-DCE. Les pentes des enrichissements isotopiques du carbone et du chlore $\Delta\delta^{13}C/\Delta\delta^{37}Cl$ étaient de 11.0 ± 0.8 pour le PCE et de 4.1 ± 0.2 pour le TCE. La pente déterminée pour le PCE est suffisamment différente des valeurs mesurées pour la biodégradation et peut donc être utilisée pour distinguer les processus de dégradation sur le terrain.

Une étude de terrain a été menée pour étudier les effets de l'élimination des foyers de contamination sur la longévité des contaminants sur un site contaminé par un mélange complexe de benzène, toluène, ethylbenzène, xylènes (BTEX) et d'éthanes, éthènes et méthanes chlorés. Les profils de concentration du sol et des eaux souterraines dans le temps et l'espace ont été utilisés pour mettre en évidence l'importance de la diffusion vers l'avant dans les zones de faible perméabilité, de la dégradation et de la rétrodiffusion

des contaminants d'origine et des produits de dégradation après l'élimination de la source de contaminants. L'analyse isotopique du carbone et du chlore de composés spécifiques des extraits d'eaux souterraines et de sols a montré que le chloroforme est dégradé par hydrogénolyse en dichlorométhane, tandis que le 1,1,2,2-tétrachloroéthane est dégradé en trichloroéthène et en *cis*-1,2-dichloroéthène. L'étude a montré le potentiel de l'analyse isotopique de composés spécifiques non seulement pour les échantillons d'eaux souterraines mais aussi pour les échantillons de sol. Le sol s'avère être une matrice importante qui influence souvent le devenir à long terme des contaminants.

En résumé, les améliorations des méthodes analytiques et de la compréhension des processus de fractionnement isotopique présentées dans cette thèse apportent une contribution importante à l'analyse isotopique de composés spécifiques et peuvent faire progresser son application de routine dans la restauration des sites contaminés. Les approches développées et discutées ici peuvent être transférées à d'autres composés organiques et utilisées dans des études futures pour suivre les polluants organiques dans l'environnement.

Mots-clés composés organiques volatils, contaminants, composés organochlorés, analyse des isotopes de composés organiques spécifiques, isotopes stables du carbone, isotopes stables du chlore, dégradation abiotique, biodégradation, atténuation naturelle surveillée, fractionnement isotopique, voies de dégradation, chromatographie en phase gazeuse, spectrométrie de masse à rapport isotopique

Kurzfassung

Chlorierte aliphatische Kohlenwasserstoffe und aromatische Mineralölkohlenwasserstoffe gehören zu der Gruppe der flüchtigen organischen Verbindungen und sind häufig als Schadstoffe im Untergrund anzutreffen. Auf natürliche Weise werden ihre Konzentrationen durch Verdünnung, Sorption und Abbau gemindert. Klassische Ansätze in der Schadstoffhydrogeologie stossen als Werkzeug zur Überwachung von Minderungsprozessen oft an ihre Grenze, da sie voraussetzen, dass die Schadstoffe und Abbauprodukte durch die Probenahme- und Analysemethoden angemessen erfasst werden. Die komponentenspezifische Analyse stabiler Isotopen hat sich in den letzten Jahrzehnten als vielseitiges Instrument zur Nachverfolgung dieser Prozesse erwiesen. Die Methode beruht nicht auf Konzentrationsmessungen. Der Abbau verursacht eine Anreicherung der schweren Isotope in den ursprünglichen Schadstoffen und eine Abreichung in den Abbauprodukten. Zusätzlich zu den Kohlenstoffisotopenverhältnissen können weitere Isotopensysteme wie jene des Chlors gemessen werden, um mechanistische Erkenntnisse zu erlangen. Während die Kohlenstoff-Isotopenanalyse bei der routinemässigen Bewertung von kontaminierten Standorten etabliert ist, werden Studien, die Chlorisotope einbeziehen, erst seit kurzem häufiger durchgeführt.

Ziel dieser Arbeit war es, das Potenzial der komponentenspezifischen Kohlenstoff- und Chlorisotopenanalyse aufzuzeigen. Sie behandelt analytische Aspekte, die Isotopenfraktionierung bei verschiedenen Prozesse und Feldanwendungen. Ein Übersichtsartikel gibt ein umfassendes Bild über die Chlorisotopenfraktionierung von chlorierten Schadstoffen im Untergrund durch verschiedene Prozesse und stellt analytische Techniken der Chlorisotopenanalyse vor. Eine Zusammenfassung erfolgreicher Feldanwendungen veranschaulicht das Potenzial von Chlorisotopendaten. Herangehensweisen zur Modellierung der Chlorisotopenfraktionierung werden ebenfalls diskutiert.

Im Rahmen dieser Arbeit wurde eine Analysemethode entwickelt, mit der die Nachweisgrenzen von Messungen des Chlorisotopenverhältnisses für Tetrachlorethen (PCE) und Trichlorethen (TCE) in wässriger Lösung durch Dampfraum-Festphasen-Mikroextraktion (*headspace solid-phase microextraction*, HS-SPME) in Verbindung mit Gaschromatographie (GC) Quadrupol-Massenspektrometrie auf den Sub-µg L^{-1}-Bereich gesenkt werden konnten. Es wurde das neuartige SPME-Arrow-System mit einem erhöhten sorptiven Phasenvolumen

verwendet. Die SPME-Parameter wurden mittels statistischer Versuchsplanung optimiert, um eine maximale Intensität zu erreichen. Massenspektrometrische Parameter und Berechnungsschemata für das Chlorisotopenverhältnis wurden ebenfalls untersucht und optimiert. Mögliche Chlorisotopenfraktionierung während der Extraktion und Analyse wurde durch eine Zweipunktkalibrierung mit extern referenzierten Standards berücksichtigt. Hiermit sind präzise δ^{37}Cl-Messungen (Standardabweichungen unter 0.5‰) für Konzentrationen von $0.4\,\mu g\,L^{-1}$ (PCE) bis $0.8\,\mu g\,L^{-1}$ (TCE) möglich.

Eine weitere Analysemethode wurde entwickelt, um den Anwendungsbereich der komponentenspezfischen Kohlenstoffanalyse auf komplexe Mischungen flüchtiger organischer Verbindungen in Bodenproben auszuweiten. Es wurden Bodenextraktionsmethoden verglichen und eine zweidimensionale GC-GC-Isotopenverhältnis-Massenspektrometrie-Methode mittels *heart-cutting* entwickelt. Es wurden eine gute chromatographische Trennung für die Zielverbindungen in schwierigen Matrizen und eine hohe Genauigkeit (Richtigkeit und Präzision) für die Kohlenstoffisotopenanalyse erreicht. Durch den Einsatz von *purge & trap*-Konzentration konnten grosse Volumina an Extraktionslösungsmitteln analysiert werden, wodurch die Nachweisgrenzen der Methode für komponentenspezifische Kohlenstoffanalyse im Boden gesenkt werden konnten.

In einer Laborstudie wurde die Isotopenfraktionierung während des abiotischen Abbaus von chlorierten Ethenen untersucht. Im Gegensatz zu vielen biologischen Abbauprozessen entstehen beim abiotischen Abbau meistens nicht-chlorierte, allgemein nicht-toxische Abbauprodukte. Diese lassen sich jedoch in der Praxis nur schwer nachweisen. Duale Kohlenstoff-Chlor-Isotopenanreicherungsgeraden sind nützlich, um den abiotischen Abbau durch natürlich vorkommende reaktive Eisenphasen an Geländestandorten zu untersuchen. Der Abbau der chlorierten Ethene *cis*-1,2-Dichlorethen (DCE), TCE und PCE durch Eisen(II)-sulfid (FeS) wurde untersucht. FeS war reaktiv mit TCE und PCE, aber nicht mit *cis*-1,2-DCE. Die Steigungen der Kohlenstoff-Chlor-Isotopenanreicherungsgeraden $\Delta\delta^{13}C/\Delta\delta^{37}Cl$ betrugen 11.0 ± 0.8 für PCE und 4.1 ± 0.2 für TCE. Die für PCE ermittelte Steigung unterscheidet sich hinreichend von den für den biologischen Abbau gemessenen Werten und kann daher zur Unterscheidung von Abbauprozessen im Feld verwendet werden.

In einer Feldstudie wurden die Auswirkungen der Beseitung des Schadstoffherdes auf die Langlebigkeit von Schadstoffen an einem Geländestandort untersucht, der mit einer komplexen Mischung aus Benzol, Toluol, Ethylbenzol, Xylolen (BTEX) und chlorierten Ethanen, Ethenen und Methanen kontaminiert war. Anhand von Boden- und Grundwasserkonzentrationsprofilen über Zeit und Raum wurde die Bedeutung der Vorwärtsdiffusion in Zonen mit geringer Durchlässigkeit, des Abbaus und der Rückdiffusion von ursprünglichen Schadstoffen und Abbauprodukten nach der Beseitung des Schadstoffherdes veranschaulicht.

Die komponentenspezifische Kohlenstoff- und Chlorisotopenanalyse von Grundwasser- und Bodenextrakten zeigte, dass Chloroform durch Hydrogenolyse zu Dichlormethan abgebaut wird, während 1,1,2,2-Tetrachlorethan zu Trichlorethen und *cis*-1,2-Dichlorethen abgebaut wird. Die Studie zeigt das Potenzial der verbindungsspezifischen Isotopenanalysen nicht nur für Grundwasserproben, sondern auch für Bodenproben. Der Boden erweist sich als massgeblich für die langfristige Speicherung von Schadstoffen.

Zusammenfassend betrachtet, leisten die in dieser Arbeit vorgestellten Verbesserungen von Analysemethoden und des Verständnisses von Isotopenfraktionierungsprozessen einen wichtigen Beitrag für die komponentenspezifische Isotopenanalyse. Die hier entwickelten und diskutierten Ansätze können auf andere organische Verbindungen übertragen und in zukünftigen Untersuchungen zur Nachverfolgung organischer Schadstoffe in der Umwelt eingesetzt werden.

Stichwörter flüchtige organische Verbindungen, Schadstoffe, chlorierte Kohlenwasserstoffe, komponentenspezifische Isotopenanalyse, stabile Kohlenstoffisotope, stabile Chlorisotope, abiotischer Abbau, biotischer Abbau, überwachte natürliche Schadstoffminderungsprozesse, Gaschromatographie, Isotopenverhältnis-Massenspektrometrie, Isotopenfraktionierung, Abbaupfade

Acknowledgments

I would like to express my gratitude to the people who supported me and my work in one way or the other.

First, I would like to thank my supervisor Daniel Hunkeler for giving me the opportunity to work on this topic. I appreciate the trust given to me in completing the tasks, and I greatly benefited from his decades of wisdom in the field of isotope fractionation. I also thank Jordi Palau and Mario Schirmer for accepting to be members of the thesis committee and for their valuable feedback.

I am very grateful to Violaine Ponsin and Clara Torrentó for their patience in familiarizing me with the mass spectrometric instrumentation. I would like to thank you for sharing your *savoir-faire* that eventually enabled me to take over responsibility of the isotope laboratory. I think I took good care of it.

I would like to thank my students Emilie Sammali, Flavia Isenschmid and intern Ouassim Boukaroum for their outstanding work in the isotope laboratory. I learned a lot from Ouassim's perspective as a chemist that formed the basis of one the chapters of this thesis.

I would like to express my appreciation for my collaborative partners Mette M. Broholm, Cecilie B. Ottosen and Alexandra M. Murray from Danmarks Tekniske Universitet for several successful research projects.

It was a pleasure to work at the CHYN during the last years, and I would like to thank my friends and colleagues for creating a great work atmosphere featuring numerous *apéros* (back in the day): Adeline, Álvaro, Asmae, Celia, Chiara, Claire, Clémence, Dan, Hannah, James, Kalliopi, Landon, Laurent, Lucile, Maria, Marion, Nathan, Przemek, Roberto, Simone, Stefanie and Vincent. Danke, Simone, für die vielen schönen Ausflüge in der Schweiz.

Thanks, Mom, for the final proofreading.

This work was funded by the Swiss National Science Foundation (SNSF) project *Tracking reactive processes in low permeability sediments and their effect on contaminant longevity in aquifers using compound-specific isotope analysis* [grant number 166233].

Contents

Abstract **I**

Synthèse **V**

Kurzfassung **IX**

Acknowledgments **XIII**

List of Figures **XIX**

List of Tables **XXI**

List of Abbreviations **XXIII**

List of Publications **XXV**

1. General introduction **1**

1.1. Context and aim of the thesis 1

1.2. Research approach and structure of the thesis 4

2. Tracking chlorinated contaminants in the subsurface using compound-specific chlorine isotope analysis: A review of principles, current challenges and applications **7**

2.1. Introduction 8

2.2. Measuring chlorine isotope ratios 9

2.3. Current knowledge about chlorine isotope fractionation 20

2.4. Field applications 29

2.5. Modelling chlorine fractionation processes 32

2.6. Conclusions and outlook 37

3. A design of experiments to optimize solid-phase microextraction for compound-specific chlorine isotope analysis of chlorinated ethenes 39
3.1. Introduction . . . 40
3.2. Material and methods . . . 42
3.3. Results and discussion . . . 48
3.4. Conclusions . . . 56

4. Compound-specific carbon isotope analysis of volatile organic compounds in complex soil extracts using purge and trap concentration coupled to heart-cutting two-dimensional gas chromatography–isotope ratio mass spectrometry 57
4.1. Introduction . . . 58
4.2. Material and methods . . . 62
4.3. Results and discussion . . . 67
4.4. Conclusions . . . 77

5. Carbon and chlorine isotope fractionation during abiotic degradation of chlorinated ethenes by ferrous sulfide (FeS) 79
5.1. Introduction . . . 80
5.2. Material and methods . . . 83
5.3. Results and discussion . . . 87
5.4. Environmental significance . . . 91

6. Assessing the impact of reactive back-diffusion on a complex chlorohydrocarbon plume using compound-specific isotope analysis 95
6.1. Introduction . . . 96
6.2. Site description . . . 97
6.3. Material and methods . . . 99
6.4. Results and discussion . . . 102
6.5. Conclusions . . . 112

7. General conclusions and outlook 115

Bibliography 119

Appendix 147

A. Supporting Information for Chapter 2 **149**
A.1. Supplementary tables 150
A.2. Supplementary figures 151

B. Supporting Information for Chapter 3 **153**
B.1. Modified multiple ion method 154
B.2. Influence of split ratio on peak shape for SPME injection 155
B.3. Central composite design 156
B.4. Response surface validation 157

C. Supporting Information for Chapter 4 **159**
C.1. Concentration measurement 160
C.2. Purge & trap parameters 160
C.3. GC-GC parameters 161
C.4. Physical properties of the extraction solvents 162
C.5. Method detection limit determination 162
C.6. Calculation of soil MDL 164

D. Supporting Information for Chapter 6 **165**
D.1. Soil profiles from source zone 166

List of Figures

1.1. Origins and behavior of VOC in the subsurface. 2

2.1. Overview of common offline and online chlorine isotope measurement methods for chlorinated hydrocarbons. 11
2.2. Potential biotic and abiotic degradation pathways for PCE. 25

3.1. Effect of factors on measured response. 50
3.2. Comparison between peak shapes obtained for different extraction temperatures. 51
3.3. Comparison between peak shapes obtained for different desorption temperatures. 51
3.4. Three-dimensional response surface for PCE intensity. 53
3.5. Three-dimensional response surface for PCE desirability. 54

4.1. GC-GC-C-IRMS configuration. 64
4.2. Chromatograms of target compounds. 68
4.3. Comparisons of target compound method detection limits and isotopic deviations in different matrices. 71
4.4. Chromatogram of methanol soil extract from field site. 72
4.5. Chromatogram of target compounds spiked with TGDE. 74
4.6. Chromatogram of TGDE soil extract from field site. 75
4.7. Comparison of extraction efficiency of TGDE compared to methanol. . . . 76

5.1. Potential biotic and abiotic degradation pathways for PCE. 82
5.2. Single and dual element isotope plots for abiotic degradation by FeS. . . . 88
5.3. Comparison of carbon and chlorine bulk enrichment factors for biotic degradation and abiotic degradation. 91
5.4. Hypothesized dichloroelimination pathways for the abiotic reductive dechlorination of PCE and TCE. 92

6.1. Map and cross section of the study site. 98

6.2. Possible reductive degradation pathways for the initial contaminants. . . . 100
6.3. Aqueous concentrations of CT, CF and DCM. 103
6.4. Aqueous concentrations of 1,1,2,2-TeCA, TCE, *cis*- and *trans*-1,2-DCE. . 105
6.5. Soil concentrations of CT, CF and DCM. 106
6.6. Soil concentrations of 1,1,2,2-TeCA, TCE, *cis*- and *trans*-1,2-DCE. 107
6.7. Carbon CSIA of CF and DCM. 109
6.8. Carbon CSIA of 1,1,2,2-TeCA, TCE and *cis*-1,2-DCE. 111
6.9. Dual carbon-chlorine isotope plot for chloroform. 112

List of Tables

2.1. Comparison of offline and online δ^{37}Cl analytical precision for organic compounds. 12
2.2. Bulk carbon and chlorine isotope enrichment factors by physical processes. 22
2.3. Bulk carbon and chlorine isotope enrichment factors as well as dual element isotope slopes (C/Cl) by biotic and abiotic degradation. 28
2.4. Field studies where chlorine CSIA has been applied. 29
2.5. Studies that have modelled isotopic fractionation of chlorine in groundwater contaminants. 34

3.1. Experimental domain with factors influencing SPME efficiency. 46
3.2. Comparison of evaluation methods for calculating chlorine isotope ratios. . 48
3.3. Experimental response for the full factorial design. 49
3.4. Experimental domain established by CCD and measured responses for SPME. 52
3.5. Factors and responses of the desirability function. 53
3.6. Performance evaluation for SPME extraction at optimized parameters. . . 55

4.1. Properties of the investigated target compounds. 62
4.2. Theoretically required purge times. 65

List of Abbreviations

BTEX	benzene, toluene, ethylbenzene, xylenes
CF	chloroform/trichloromethane
CHC	chlorinated hydrocarbons
CSIA	compound-specific isotope analysis
CT	carbontetrachloride/tetrachloromethane
DCA	dichloroethane
DCE	dichloroethene
DCM	dichloromethane
DDIW	double deionized water
DDT	dichlorodiphenyltrichloroethane
DoE	design of experiments
EA	elemental analyzer
EI	electron ionization
GC	gas chromatography
GC-GC	heart-cutting 2D gas chromatography
GCxGC	comprehensive 2D gas chromatography
HES	high-efficiency source
HS	headspace
HTC	high-temperature conversion
ICP	inductively coupled plasma
IRMS	isotope ratio mass spectrometry
KIE	kinetic isotope effect
MC	multicollector
MDL	method detection limit
NAPL	non-aqueous phase liquid
PAH	polycyclic aromatic hydrocarbons
PCB	polychlorinated biphenyl
PCE	tetrachloroethene/perchloroethene
PCP	pentachlorophenol
pcGC	preparative capillary gaschromatography
qMS	quadrupole mass spectrometry
RSM	response surface methodology
SIM	selected/single ion mode
SMOC	Standard Mean Ocean Chloride
SPME	solid-phase microextraction
TCA	trichloroethane
TeCA	tetrachloroethane
TCE	trichloroethene
TGDE	tetraethylene glycol dimethyl ether
TI	thermal ionization
VC	vinyl chloride
VOC	volatile organic compound
VPDB	Vienna Pee Dee Belemnite
ZVI	zero-valent iron

List of Publications

A. M. Murray, C. B. Ottosen, J. Maillard, C. Holliger, A. Johansen, L. Brabæk, I. L. Kristensen, J. Zimmermann, D. Hunkeler, and M. M. Broholm (2019): "Chlorinated ethene plume evolution after source thermal remediation: Determination of degradation rates and mechanisms". In: *Journal of Contaminant Hydrology* 227, p. 103551. DOI: 10.1016/j.jconhyd.2019.103551

J. Zimmermann, L. J. S. Halloran, and D. Hunkeler (2020): "Tracking chlorinated contaminants in the subsurface using compound-specific chlorine isotope analysis: A review of principles, current challenges and applications". In: *Chemosphere* 244, p. 125476. DOI: 10.1016/j.chemosphere.2019.125476

C. B. Ottosen, P. L. Bjerg, D. Hunkeler, J. Zimmermann, N. Tuxen, D. Harrekilde, L. Bennedsen, G. Leonard, L. Brabæk, I. L. Kristensen, and M. M. Broholm (2021): "Assessment of chlorinated ethenes degradation after field scale injection of activated carbon and bioamendments: Application of isotopic and microbial analyses". In: *Journal of Contaminant Hydrology* 240, p. 103794. DOI: 10.1016/j.jconhyd.2021.103794

J. Zimmermann, P. Wanner, and D. Hunkeler (2021): "Compound-specific carbon isotope analysis of volatile organic compounds in complex soil extracts using purge and trap concentration coupled to heart-cutting two-dimensional gas chromatography–isotope ratio mass spectrometry". In: *Journal of Chromatography A* 1655, p. 462480. DOI: 10.1016/j.chroma.2021.462480

1. General introduction

1.1. Context and aim of the thesis

Volatile organic compounds (VOC) are organic chemicals that have a high vapor pressure. They include chlorinated aromatic and aliphatic hydrocarbons (CHC) and the aromatic petroleum hydrocarbons benzene, toluene, ethylbenzene and xylenes, which are together referred to as BTEX. CHC are used in the synthesis of solvents and pesticides (Panagos et al. 2013). Aliphatic CHC or chlorinated solvents have been in the past widely utilized as industrial degreasing agents. BTEX are abundantly present in petroleum products. The presence of these VOC in soil and groundwater is of great concern as many of them have been shown to be harmful to the environment and human health (Lawrence 2006). Across contaminated sites in Europe, Panagos et al. (2013) reported the distribution of contaminants in soil as 8.3% CHC and 10.2% BTEX, while in groundwater the percentages are 10.0% for CHC and 14.8% BTEX.

VOC may be released into the subsurface through accidental spills (Figure 1.1A), illegal disposal, or leakages from storage tanks (Figure 1.1B). Due to their generally low solubility in water, VOC form non-aqueous phase liquids (NAPL) (Figure 1.1C) in the subsurface (Chapelle et al. 2003). Depending on the density of the NAPL in relation to the density of water, the compounds form either a light non-aqueous phase liquid (LNAPL) or a dense non-aqueous phase liquid (DNAPL). Due to their low density, BTEX spills result in an LNAPL which floats on the water surface. Chlorinated hydrocarbons on the other hand have a higher density than water and will sink (Fitts 2013).

LNAPL contaminant sources can be remediated by extracting them from the water table surface at shallow depth. This kind of recovery is not easily possible for DNAPL sources (Fitts 2013). The DNAPL will migrate downward through the topsoil, the unsaturated zone (Figure 1.1D) and the saturated zone (Figure 1.1E), and can diffuse into low-permeability zones or aquitards (Figure 1.1F). The DNAPL will then slowly dissolve into the groundwater constituting a long-term contaminant source.

In order to protect potential receptors, that is water catchments (Figure 1.1 G) and the population they serve, from contaminants, it is necessary to understand the behavior of

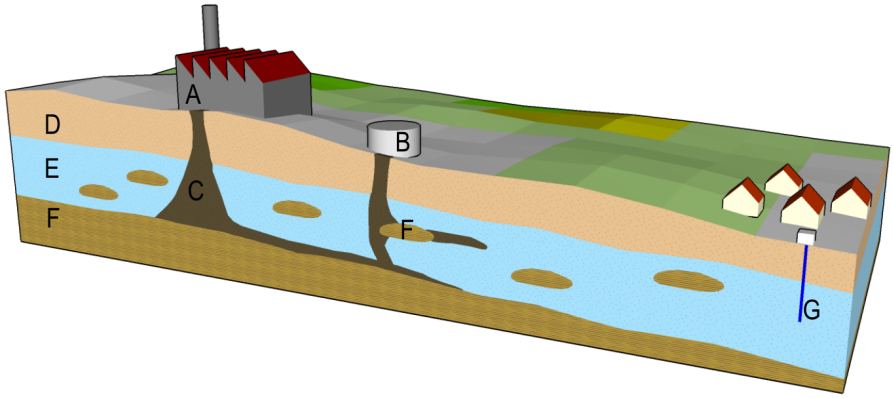

Figure 1.1.: Possible origins and behavior of VOC in the subsurface and potential receptors. (A) contaminant spill at factory (B) contaminant leakage from storage tank (C) DNAPL (D) unsaturated zone (E) saturated zone (F) low-permeability zone, aquitard (G) water catchment.

VOC in the subsurface. The VOC can migrate as said DNAPL, dissolve into the aqueous phase, and also volatilize into the pores of the unsaturated zone (Fitts 2013).

As DNAPL are more persistent than LNAPL, the focus of this thesis is set on methods of investigating the long-term fate of DNAPL source zones involving mainly the particularly problematic chlorinated compounds. The contaminant plume is subject to different physico-chemical processes, which over time will lead to an attenuation of the inital contaminant concentrations, provided the source has been identified and removed. The main attenuation processes are dilution, sorption and degradation. Even the most persistent chemicals are naturally degraded over time, though the time scale that is required varies widely between contaminants (Chapelle et al. 2003).

Classical approaches in contaminant hydrology are often limited in their potential for tracking attenuation processes and fingerprinting contaminant sources. An example is the identification of degradation processes and rates through mass balance calculations. An important criterion needs to be met for a successful mass balance calculation: Concentrations of the initial contaminants and degradation products must be known, requiring that they are adequately captured by the sampling and analysis methods. Given the volatile nature of the contaminants and the potential for many different degradation pathways, this may prove impossible.

Compound-specific stable isotope analysis (CSIA) has emerged in recent decades as a powerful tool in contaminant hydrology (Heraty et al. 1999; Hunkeler and Aravena 2000; Elsner et al. 2005; Zwank et al. 2005b; Abe and Hunkeler 2006; Jochmann and Schmidt 2015). CSIA does not rely on concentration measurements. The principle is based on the difference in bond strength between light and heavy isotopes within a compound. In a pool of contaminants, the molecules containing only the light isotope(s) will be preferentially degraded, causing a heavy isotope enrichment in the remaining pool. In addition to carbon isotope ratios, additional isotope system such as chlorine can be monitored. Dual carbon-chlorine CSIA opens up new possibilities for identifying processes and sources. The use of dual element CSIA in the routine assessment of contaminated sites has so far been held back by analytical challenges and the lack of isotope fractionation factors for different processes. The analytical challenges are rooted in the higher detection limits for chlorine isotopic measurements compared to those for carbon isotope measurements. Fractionation factors for chlorine istopes are not known for as many processes as for carbon isotopes, making data interpretation difficult. This is especially true for abiotic transformation of chlorinated hydrocarbons by naturally occurring phases.

This thesis aims to explore some of the untapped potential of single and dual element CSIA by focusing on three principal aspects of CSIA: Analytical improvements for lowering

detection limits and applying CSIA to complex mixtures, better understanding of isotope fractionation during abiotic degradation, and the application of CSIA in the field for evaluating the role of low-permeability zones on contaminant persistence. The main aim of this thesis is to improve the current understanding of CHC transformation processes in the subsurface and their effect on contaminant longevity. Specific objectives are to develop isotope-based methods for tracking transformation processes in both groundwater and soil and applying said methods in the field, with a focus on investigating the prevalence of degradation of CHC in low-permeability zones. The improved understanding of these transformation processes gained in this thesis shall help in promoting the widespread application of CSIA in contaminated site management.

1.2. Research approach and structure of the thesis

The research approach of this thesis is based on reviewing principles and applications of chlorine CSIA, exploring laboratory methods for carbon and chlorine CSIA of VOC, investigating isotope effects during abiotic degradation and the potential of applying CSIA in the field. The high detection limits of chlorine CSIA were lowered by developing an extraction and concentration method. The challenge of demonstrating contaminant degradation in low-permeability zones was faced by improving extraction and chromatographic separation of target compounds. The lack of dual carbon-chlorine slopes for abiotic degradation of CHC was addressed by laboratory batch experiments and the question of the prevalence of contaminant degradation in low-permeability zones was answered by investigations on a field site. The described studies are presented in the form of articles in the following chapters:

Chapter 1 serves as a brief general introduction to the topic of contaminant hydrology and the method of CSIA.

Chapter 2 reviews the principles of compound-specific chlorine isotope analysis of chlorinated contaminants, the history and recent developments in analytical methods, subsurface processes that cause chlorine isotope effects, field applications and modeling of chlorine isotope effects.

Chapter 3 reports a novel instrumental approach for lowering the method detection limits for chlorine CSIA of chlorinated ethenes using an online and easily automated preconcentration method, solid-phase microextraction. An approach of design of experiments is used to optimize the extraction of chlorinated ethenes.

Chapter 4 addresses the applicability of carbon CSIA to complex VOC mixtures in soil extracts. Soil extraction methods are compared and an analytical setup developed

that uses two chromatographic columns of different selectivity to achieve the necessary chromatographic resolution.

Chapter 5 investigates the carbon and chlorine isotope fractionation during abiotic degradation of chlorinated ethenes. For this purpose, laboratory batch experiments are conducted and dual carbon-chlorine isotope slopes obtained.

Chapter 6 demonstrates the application of CSIA to a field site contaminated by a complex mixture of BTEX and aliphatic CHC. The importance of low-permeability zones on plume longevity after source removal and the ongoing degradation and back-diffusion processes are studied with detailed isotope profiles over depth, spanning several years. Dual carbon-chlorine analysis is also applied for identifying transformation processes.

Chapter 7 aims to be a comprehensive summary of the work, discussing the limitations of the approaches and future research questions.

2. Tracking chlorinated contaminants in the subsurface using compound-specific chlorine isotope analysis: A review of principles, current challenges and applications

Jeremy Zimmermann[1], Landon J.S. Halloran[1], Daniel Hunkeler[1]
This chapter is based on the article published in *Chemosphere 244 (2020) 125476*

Abstract

Many chlorinated hydrocarbons have gained notoriety as persistent organic pollutants in the environment. Engineered and natural remediation efforts require a monitoring tool to track the progress of degradation processes. Compound-specific isotope analysis (CSIA) is a robust method to evaluate the origin and fate of contaminants in the environment and does not rely on concentration measurements. While carbon CSIA has established itself in the routine assessment of contaminated sites, studies incorporating chlorine isotopes have only recently become more common. Although some aspects of chlorine isotope analysis are more challenging than carbon isotope analysis, having additional isotopic data yields valuable information for contaminated site management. This review provides an overview of chlorine isotope fractionation of chlorinated contaminants in the subsurface by different processes and presents analytical techniques and unresolved challenges in chlorine isotope analysis. A summary of successful field applications illustrates the potential of using chlorine isotope data. Finally, approaches in modelling chlorine isotope fractionation due to degradation, diffusion, and sorption processes are discussed.

[1]Centre for Hydrogeology and Geothermics, University of Neuchâtel, Rue Emile-Argand 11, 2000 Neuchâtel, Switzerland

2.1. Introduction

Chlorinated hydrocarbons (CHC) are a diverse group of compounds, occurring as both aliphatic and aromatic hydrocarbons. These compounds have at least one covalently bonded chlorine atom in place of a hydrogen atom. Synthetic organochlorines have found widespread use as pesticides, pharmaceuticals, plastics, refrigerants, industrial solvents, lubricants, dielectric and dry-cleaning agents. They also appear as intermediates in chemical syntheses or as the result of combustion processes (Häggblom and Bossert 2004).

The chemical inertness, stability and lipid solubility of chlorinated hydrocarbons make them suitable for many industrial processes and have led to their large-scale production. These properties dominate the behavior of these compounds in the environment and are the reason that many of them have become known as persistent organic pollutants (POP). In addition to resisting degradation for long periods, many of these pollutants accumulate in the fatty tissue of organisms and show various degrees of toxicity for humans and ecosystems (Häggblom and Bossert 2004; Koenig et al. 2015).

Volatile chlorinated aliphatic hydrocarbons are short hydrocarbon chains containing at least one covalently bonded chlorine atom and include chlorinated methanes, ethanes and ethenes (Stroo and Ward 2010). These volatile organic compounds (VOCs) have been used in the past for degreasing, cleaning and dry-cleaning on the basis of their apolar nature, rapid evaporation and low flammability (Doherty 2000). Chlorinated solvents are among the most common persistent contaminants in the environment, owing to their extensive application and often improper handling and disposal (Philp 2007; Cincinelli et al. 2012). Although certain chlorinated solvents such as chloroform (CF) have been proven to occur naturally (Häggblom and Bossert 2004; Gribble 2010), the natural production for many of these compounds is dwarfed by their release from anthropogenic sources (Lecloux 2003; Hunkeler et al. 2012).

Among chlorinated solvents, chlorinated ethenes or ethylenes have been the subject of great interest in the field of contaminant hydrochemistry. They include vinyl chloride (VC), *trans*- and *cis*-dichloroethene (DCE), trichloroethene (TCE), and tetrachloroethene/perchloroethene (PCE). Chlorinated ethenes, especially TCE and PCE, have been used as industrial degreasing agents with PCE continuing to be used as a solvent in dry-cleaning applications. All chlorinated ethenes display some degree of toxicity, with TCE and VC being classified as known human carcinogens (Bradley 2003; Guha et al. 2012).

Being able to differentiate sources and understand transformation processes is key in assessing the impact of contamination by chlorinated solvents on groundwater and ecosystems (Cincinelli et al. 2012). Compound-specific isotope analysis (CSIA) has emerged as a

powerful tool to track contaminants in the subsurface. The concept involves measuring variations in the isotopic composition of each compound of interest and/or their degradation products by combining a mass spectrometer with a chromatographic separation system. Using this approach, additional information can be gathered that allows a deeper understanding of transformation processes when compared with measuring concentration levels exclusively. While carbon CSIA has become a routine technique in the assessment of contaminant degradation, studies incorporating chlorine CSIA are still relatively rare.

This review provides an overview of the current knowledge about isotope fractionation effects of chlorinated contaminants in the subsurface, as well as the analytical challenges in using Cl CSIA as a routine approach in the assessment of contaminated sites. Field applications, including source differentiation, tracking, degradation pathway evaluation, and degradation quantification, are also discussed. Finally, considerations related to modelling Cl isotope fractionation due to various subsurface processes are detailed.

2.2. Measuring chlorine isotope ratios

Chlorine has two stable isotopes, ^{35}Cl with a natural abundance of 75.8% and ^{37}Cl with an abundance of 24.2%. This ratio can vary slightly due to various physico-chemical processes. Since miniscule differences can be resolved, the ^{37}Cl/^{35}Cl isotope ratio of a sample R_{sample} is reported using the δ notation as per mille (‰) difference from the ^{37}Cl/^{35}Cl isotope ratio in a reference standard R_{SMOC}, which is standard mean ocean chlorine (SMOC):

$$\delta^{37}\mathrm{Cl} = \frac{R_{sample}}{R_{SMOC}} - 1 \qquad (‰) \tag{2.1}$$

Similarly, in any chlorinated compound, chlorine atoms can either be of the light (^{35}Cl) or the heavy (^{37}Cl) variety. Molecules of the same compound that differ in their isotopic composition are referred to as isotopologues.

Chlorine isotope ratios in compounds are obtained using mass spectrometric techniques. Measuring the molecular mass of a molecule is a three step process, which is shared by every type of mass spectrometer. In the first step, the ionization step, the molecules of interest are converted to ions. Different ionization methods are used depending on the volatility and ionization potential of the molecule or atom of interest. Electron ionization is a common method for ionizing molecules of relatively volatile compounds. Thermal ionization can be used to create atomic as well as molecular ions of inorganic analytes. Inductively coupled plasma ionization is a versatile method than can be applied to solid as well as dissolved samples. In the ionized argon plasma, the analyte undergoes a complete

vaporization, atomization and ionization. The ionization energy of this method is adequate to ionize many elements, while ensuring that in general only single-charged species are produced (Dass 2007; Westman-Brinkmalm and Brinkmalm 2008; Sparkman et al. 2011).

The second step is the acceleration and separation of the species according to their ratio of mass to charge (m/z) in a mass analyzer. Common mass analyzers are the magnetic sector mass spectrometer and the quadrupole mass spectrometer (qMS). Magnetic sector mass analyzers include isotope ratio mass spectrometers (IRMS), where it is possible to compare the obtained isotope ratios to those of standardized reference values by introducing a reference gas. The two common types of IRMS are continuous flow (CF-IRMS) and dual-inlet (DI-IRMS). In the former, the reference gas is introduced into a stream of carrier gas before and after the sample gas. In the latter, sample gas and reference gas are introduced alternately in a rapid succession, leading to a higher precision. Quadrupole mass spectrometers are compact benchtop instruments, where masses are separated according to their trajectory through an oscillating electromagnetic field.

In the third and final step, the mass spectrum is obtained by measuring the mass-resolved ion current in a detector, either consecutively in a single collector (common for quadrupole MS) or simultaneously with a multicollector (MC) setup.

Prior to chlorine mass spectrometric analysis of organic compounds, an extraction and conversion of the chlorine in the compound to an inorganic chloride may be necessary. This so-called offline measurement (Figure 2.1a) has the advantage that the extraction/conversion steps are independent of the kind of mass spectrometer that will be used to determine the isotope ratio, but for mixtures usually only bulk isotope ratios and not compound-specific isotope ratios can be reported. The counterpart, an online measurement (Figure 2.1b), allows analyzing samples directly in real-time and offers the possibility for compound-specific isotope measurements, a larger potential for automation and a higher sample throughput, but has the disadvantage that the extraction/conversion step is directly linked to the isotope measurement, thereby limiting the choice of mass spectrometer. Table 2.1 gives an overview of off- and online methods, including sample sizes and precisions obtained.

2.2.1. Offline chlorine isotope measurements

There exist several sample preparation paths for offline chlorine isotope analysis of chlorinated hydrocarbons (Figure 2.1a). Most offline methods require cryogenic, chromatographic or ion exchange purification of the product to remove unwanted reagents and byproducts prior to mass spectrometric analysis. Table 2.1 gives an overview of offline δ^{37}Cl measurements of organic compounds presented in this section. Apart from the limited possibilities of

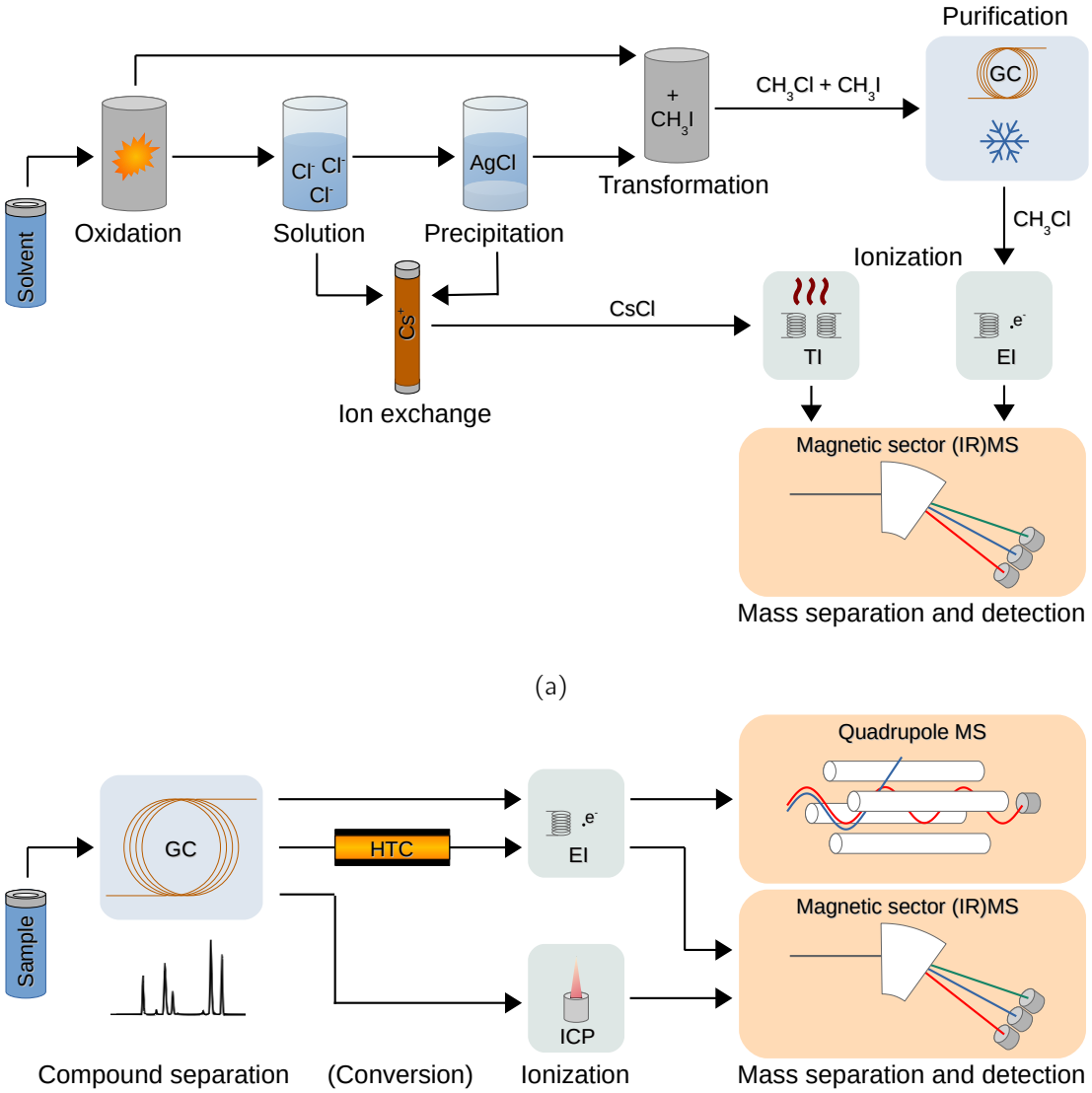

Figure 2.1.: Overview of common (a) offline and (b) online chlorine isotope measurement methods for chlorinated hydrocarbons. TI, thermal ionization; EI, electron ionization; MS, mass spectrometer; GC, gas chromatograph; HTC, high temperature conversion; ICP, inductively coupled plasma; IR, isotope ratio; MS, mass spectrometer.

Table 2.1.: Comparison of offline and online $\delta^{37}Cl$ analytical precision for organic compounds (only cases where SMOC-referenced $\delta^{37}Cl$ values were reported and $n \geq 3$). TCA, trichloroethane; DDT, dichlorodiphenyltrichloroethane; PCP, pentachlorophenol; DCM, dichloromethane; CF, chloroform; CT, carbon tetrachloride.

MS method	Compound	Analyzed ions / masses	Sample size	Repl. $n =$	Best 1σ (‰)	Reference
Offline						
DI (+)-ion IRMS	1,1,1-TCA	$CH_3{}^{35}Cl^+$, $CH_3{}^{37}Cl^+$	1500 µmol Cl	21	0.29	van Warmerdam et al. (1995)
DI (+)-ion IRMS	1,1,1-TCA	$CH_3{}^{35}Cl^+$, $CH_3{}^{37}Cl^+$	not reported	4	0.17	Beneteau et al. (1999)
DI (+)-ion IRMS	1,1,1-TCA	$CH_3{}^{35}Cl^+$, $CH_3{}^{37}Cl^+$	150 µmol Cl	3	0.07	Shouakar-Stash et al. (2003)
DI (+)-ion IRMS	TCE	$CH_3{}^{35}Cl^+$, $CH_3{}^{37}Cl^+$	1700 µmol Cl	3	0.26	van Warmerdam et al. (1995)
DI (+)-ion IRMS	TCE	$CH_3{}^{35}Cl^+$, $CH_3{}^{37}Cl^+$	33 µmol to 66 µmol Cl	8	0.15	Jendrzejewski et al. (1997)
DI (+)-ion IRMS	TCE	$CH_3{}^{35}Cl^+$, $CH_3{}^{37}Cl^+$	not reported	3	0.08	Beneteau et al. (1999)
DI (+)-ion IRMS	TCE	$CH_3{}^{35}Cl^+$, $CH_3{}^{37}Cl^+$	166 µmol Cl	4	0.05	Shouakar-Stash et al. (2003)
DI (+)-ion IRMS	PCE	$CH_3{}^{35}Cl^+$, $CH_3{}^{37}Cl^+$	2000 µmol Cl	6	0.10	van Warmerdam et al. (1995)
DI (+)-ion IRMS	PCE	$CH_3{}^{35}Cl^+$, $CH_3{}^{37}Cl^+$	40 µmol to 80 µmol Cl	4	0.10	Jendrzejewski et al. (1997)
DI (+)-ion IRMS	PCE	$CH_3{}^{35}Cl^+$, $CH_3{}^{37}Cl^+$	not reported	4	0.15	Beneteau et al. (1999)
DI (+)-ion IRMS	Lindane	$CH_3{}^{35}Cl^+$, $CH_3{}^{37}Cl^+$	250 µmol Cl	3	0.04	Gilevska et al. (2015)
DI (+)-ion IRMS	Various CHC	$CH_3{}^{35}Cl^+$, $CH_3{}^{37}Cl^+$	10 µmol to 70 µmol Cl	8	0.07	Holt et al. (1997)
(+)-ion TIMS	TCE	$Cs_2{}^{35}Cl^+$, $Cs_2{}^{37}Cl^+$	2.8 µmol Cl	3	0.22	Numata et al. (2002b)
(+)-ion TIMS	PCE	$Cs_2{}^{35}Cl^+$, $Cs_2{}^{37}Cl^+$	2.8 µmol Cl	4	0.08	Numata et al. (2002b)
(+)-ion TIMS	DDT	$Cs_2{}^{35}Cl^+$, $Cs_2{}^{37}Cl^+$	85 nmol Cl	3	0.46	Holmstrand et al. (2004)
Online						
GC-IRMS	DCE isomers	96, 98	6 nmol to 9 nmol Cl	15	0.08	Shouakar-Stash et al. (2006)
GC-IRMS	TCE	95, 97	6 nmol to 9 nmol Cl	30	0.06	Shouakar-Stash et al. (2006)
GC-IRMS	TCE	95, 97	40 pmol Cl	10	< 0.15	Bernstein et al. (2011)
GC-IRMS	PCE	94, 96	6 nmol to 9 nmol Cl	30	0.12	Shouakar-Stash et al. (2006)
GC-qMS	TCE	60, 62, 95, 97, 130, 132	150 pmol Cl	10	< 0.5	Bernstein et al. (2011)
GC-qMS	TCE	60, 62, 95, 97, 130, 132	75 pmol Cl	10	< 0.5	Bernstein et al. (2011)
GC-qMS	TCE	60, 62, 95, 97, 130, 132	95 pmol Cl	5	< 1.0	Bernstein et al. (2011)
GC-qMS	TCE	60, 62, 95, 97, 130, 132	3 pmol Cl	5	< 0.85	Bernstein et al. (2011)
GC-qMS	TCE	130, 132	>275 pmol Cl	10	< 0.5	Bernstein et al. (2011)
GC-qmS	PCE	164, 166	1.6 pmol Cl	10	0.6	Aeppli et al. (2010)
GC-qMS	DDT	352, 354	1100 pmol Cl	9	1.2	Aeppli et al. (2010)
GC-qMS	PCP	264, 266	40 pmol Cl	9	1.3	Aeppli et al. (2010)
GC-HTC-IRMS	TCE	36, 38	30 nmol Cl	16	0.24	Renpenning et al. (2015)
GC-HTC-IRMS	PCE	36, 38	30 nmol Cl	16	0.37	Renpenning et al. (2015)
GC-MC-ICPMS	DCM	35, 37	2 nmol to 3 nmol Cl	10	0.15	Horst et al. (2017)
GC-MC-ICPMS	CF	35, 37	2 nmol to 3 nmol Cl	10	0.15	Horst et al. (2017)
GC-MC-ICPMS	CT	35, 37	2 nmol to 3 nmol Cl	10	0.13	Horst et al. (2017)
GC-MC-ICPMS	VC	35, 37	2 nmol to 3 nmol Cl	8	0.14	Horst et al. (2017)
GC-MC-ICPMS	*cis*-1,2-DCE	35, 37	2 nmol to 3 nmol Cl	8	0.10	Horst et al. (2017)
GC-MC-ICPMS	TCE	35, 37	200 nmol to 1300 nmol Cl	26	0.06	van Acker et al. (2006)
GC-MC-ICPMS	TCE	35, 37	2 nmol to 3 nmol Cl	34	0.12	Horst et al. (2017)
GC-MC-ICPMS	PCE	35, 37	175 nmol to 350 nmol Cl	10	0.09	van Acker et al. (2006)
GC-MC-ICPMS	PCE	35, 37	2 nmol to 3 nmol Cl	9	0.12	Horst et al. (2017)

automating the conversion process, a main drawback is that offline methods cannot be coupled to a simple method that allows isotopically resolving mixtures of contaminants. There is the possibility of using preparative capillary gas chromatography (pcGC) to extract target analytes from mixtures at amounts sufficiently high for offline analysis. This method has so far been only applied to chlorine CSIA of semi-volatile organochlorine compounds such as the insecticide dichlorodiphenyltrichloroethane (DDT) by Holmstrand et al. (2006) and polychlorinated biphenyls (PCB) by Reddy et al. (2000) and Mandalakis et al. (2008). All three aforementioned works did not observe a significant chlorine isotope fractionation during this preparative step. Holmstrand et al. (2006) and Mandalakis et al. (2008) emphasize that the complete eluting peak must be collected due to slight differences in the GC retention times between isotolopogues. Gas chromatographic isotope effects are a well-known phenomenon (Brand 1996) and have also been observed for carbon (Ricci et al. 1994; Meier-Augenstein et al. 1996) and hydrogen isotopes (Jancsó and Van Hook 1974). As an alternative method, Numata et al. (2002b) suggest that there is the possibility of using compound-specific degradation techniques to resolve chlorine isotope data in complex mixtures. Direct coupling of a separation device, e.g. a gas chromatograph, to a mass spectrometer is however reserved for online methods. Nevertheless, offline methods are still essential to reference organic molecules to molecularly different, even inorganic molecules (Gilevska et al. 2015).

Some of the first measurements of organic chlorine isotope ratios were reported by Baertschi et al. (1953), who studied the chlorine isotope fractionation in chloroform and carbon tetrachloride during distillation. The chlorine isotope analysis was performed using a magnetic sector mass spectrometer with two collectors. The conversion step involved having the organic compounds undergo a reaction to yield gaseous hydrogen chloride (HCl).

Bartholomew et al. (1954) were the first to observe reactive isotope effects in a chlorinated organic compound, *tert*-butyl chloride ($(CH_3)_3CCl$). The compound was allowed to react with silver nitrate, and the kinetic isotope effect ($^{35Cl}k/^{37Cl}k$) for light and heavy chlorine isotopes was observed by converting the initial compound and the silver nitrate to chlorine gas (Cl_2), which was subsequently measured in a magnetic sector mass spectrometer. Masses of 70 ($^{35}Cl^{35}Cl$), 72 ($^{35}Cl^{37}Cl$), and 74 ($^{37}Cl^{37}Cl$) u were recorded. Bartholomew et al. (1954) also pointed out the memory effect that is observed when using chlorine gas in a mass spectrometer – a disadvantage it shares with hydrogen chloride, as both tend to adhere to the interior of the mass spectrometer (Eggenkamp 2014).

Being aware of this memory effect, Owen and Schaeffer (1955) were – together with Langvad et al. (1954) – some of the first researchers to establish chloromethane / methyl chloride (CH_3Cl) as a suitable gas in mass spectrometric analysis of chlorine isotopes.

Chloromethane remains the gas of choice in modern offline chlorine isotope ratio mass spectrometry. When using chloromethane in an IRMS, either positively or negatively charged ions can be analyzed, by switching the acceleration voltage to either a negative or a positive value respectively. Taylor and Grimsrud (1969) undertook some promising studies using negatively charged ions in DI-IRMS, since it results in a very simple mass spectrum consisting mainly of $^{35}Cl^-$ and $^{37}Cl^-$ ions. The downside is a lower intensity. Tanaka and Rye (1991) used this method to measure referenced chlorine isotope ratios in anthropogenic chlorinated hydrocarbons, at the same time being one of the first to propose the use of chlorine isotope mass spectrometry as a tool in fingerprinting of pollutants. Nowadays, it has become common practice to analyze positively charged ions of chloromethane, as most IRMS are set up like this for routine measurements of other compounds.

Jendrzejewski et al. (1997) developed an offline conversion technique to measure chlorine isotope ratios in chlorinated organic compounds by oxidizing them with cupric oxide, yielding inorganic chloride which was then measured as described by Long et al. (1993) by precipitation as AgCl and conversion to chloromethane, which was measured in positive ion mode. The method was also applied to a mixture of chlorinated hydrocarbons, but as there was no prior separation step only a bulk chlorine isotope ratio was reported. Positive ion IRMS was also the method of choice for van Warmerdam et al. (1995) and Beneteau et al. (1999) for organic compounds, though the offline conversion step differed. The compounds were oxidized offline and the resulting chloride trapped in a calcium carbonate solution.

Holt et al. (1997) developed a non-aqueous offline conversion process especially for VOC which is still in widespread use, since it also allows offline measuring of carbon isotope ratios. Here, the compound of interest undergoes a high-temperature reaction with cupric oxide to yield copper(I) chloride (CuCl), which further reacts with methyl iodide (CH_3I) in the same reaction tube resulting in chloromethane (CH_3Cl), omitting the step of precipitation of the chlorine as silver chloride. Yields of CH_3Cl from a variety of chlorinated organic compounds were $89 \pm 4\%$. Shouakar-Stash et al. (2003) used a modified Holt method to convert 1,1,1-trichloroethane (1,1,1-TCA) and TCE to chloromethane for isotopic analysis. The chloromethane was separated chromatographically from the excess methyl iodide and measured in a DI-IRMS.

Gilevska et al. (2015) identified the incomplete dissolution of the chlorine salt after the oxidation step to be the main reason leading to inaccurately lower $\delta^{37}Cl$ values when measuring chlorine isotope ratios of the insecticide γ-hexachlorocyclohexane (Lindane).

A different approach to offline chlorine isotope ratio measurements of chlorinated hydrocarbons that does not require transformation to chloromethane was brought up by Numata et al. (2002b), using the thermal ionization (TI) method developed by Magenheim et al.

(1994) for inorganic chlorides. Numata et al. (2002b)'s method involves a step where free chlorine is extracted from the compounds by treating them with sodiumbiphenyl. This chlorine is then transformed to CsCl by ion exchange. The solution is deposited directly onto a filament, the thermal ionization source of the mass spectrometer, and masses 301 ($^{133}Cs_2{}^{35}Cl^+$) and 303 ($^{133}Cs_2{}^{37}Cl^+$) are measured. The method required only 2.8 µmol Cl for highly precise measurements.

TIMS was also applied to more complex chlorinated hydrocarbons such as (DDT) by Holmstrand et al. (2004, 2006) and PCBs by Reddy et al. (2000) and Mandalakis et al. (2008). Holmstrand et al. (2004) observed that TIMS is very sensitive to impurities and matrix effects which stem from the intricate offline conversion.

2.2.2. Online chlorine isotope measurements

Compound-specific isotope analysis is simplified by online coupling of a separation device to a mass spectrometer. The prior separation step before measuring the isotope ratios has several benefits, including being able to report isotope ratios of the initial compounds as well as of the degradation products in the same sample. Different separation techniques and mass spectrometers are usually only applicable to certain groups of compounds.

Figure 2.1b gives an overview of the methods that so far have been applied in chlorine CSIA of (semi-)volatile compound mixtures. The mixture is separated chromatographically, after which each compound is ionized by either electron ionization or inductively coupled plasma ionization, and finally the fragment ions are separated by m/z ratio and detected in a quadrupole or magnetic sector mass spectrometer. High-temperature conversion of the compounds after separation is also an option; however, an online conversion interface that would yield the desired chloromethane has not yet been developed. Table 2.1 gives an overview of the results obtained with some of the online methods discussed here.

It has become possible to obtain compound-specific chlorine isotope ratios of organic compounds directly by analyzing fragment ions in a mass spectrometer. The fragment ions are produced by the ion source of a mass spectrometer during electron ionization. The isotope ratio of the compound is then related to the isotope ratio of the fragment ion. Shouakar-Stash et al. (2006) used an IRMS that was equipped for both continuous flow and dual inlet operation and reported chlorine isotope ratios for several chlorinated ethenes. The gaseous reference standards, identical to the compounds, were referenced to SMOC in dual-inlet operation by the Holt et al. (1997) method. Compound mixtures were separated by means of gas chromatography, and by injecting a reference gas peak at appropriate times during the chromatographic run in continuous flow operation, it was possible to report

compound-specific SMOC-referenced chlorine isotope ratios. This however also required adjusting the tuning parameters for each compound before a run. In addition to using headspace analysis for pure phase samples, chlorinated ethenes could also be extracted from aqueous samples and measured with the help of a solid-phase micro-extraction (SPME) fiber.

The work of Sakaguchi-Söder et al. (2007) paved the way for a simple online approach to measuring chlorine isotope ratios of chlorinated volatile organic compounds, analyzing the headspace of the samples. This approach uses a quadrupole mass spectrometer coupled to a gas chromatograph (GC-qMS) and is made possible by the high relative abundance of the ^{37}Cl isotope. Compound-specific fragment ions are analyzed in the mass detector, and the chlorine isotope ratio of the compound is calculated from intensities of these fragment ions through sets of stochastically derived Equations (2.2) and (2.3). Using the example of PCE, the ratio R_{PCE} of ^{37}Cl to ^{35}Cl in the molecule can be calculated as a weighted average by taking into account the measured intensities or peak areas I of the fragment ions produced in the mass spectrometer (Sakaguchi-Söder et al. 2007; Jin et al. 2011):

$$R_{PCE} = a \cdot \frac{1}{4} \cdot \frac{I_{166}}{I_{164}} + b \cdot \frac{1}{3} \cdot \frac{I_{131}}{I_{129}} + c \cdot \frac{1}{2} \cdot \frac{I_{96}}{I_{94}} + d \cdot \frac{1}{1} \cdot \frac{I_{61}}{I_{59}} \tag{2.2}$$

The weight factors a, b, c, d can be calculated through different means taking into account some or all fragment ion intensities (Jin et al. 2011). Alternatively, the ratio R_{PCE} can be calculated by only taking into account the measured intensities or peak areas I_{166} and I_{164} of the two most abundant fragment ions with masses 166 respectively 164 (Aeppli et al. 2010) or any pair of isotopologues (Elsner and Hunkeler 2008):

$$R_{PCE} = \frac{1}{4} \cdot \frac{I_{166}}{I_{164}} = \frac{1}{3} \cdot \frac{I_{131}}{I_{129}} = \frac{1}{2} \cdot \frac{I_{96}}{I_{94}} = \frac{1}{1} \cdot \frac{I_{61}}{I_{59}} \tag{2.3}$$

It has been shown by Elsner and Hunkeler (2008) that this proportionality remains valid even if isotopologue ratios change due to reactive processes. It is, however, important to note that Equation (2.3) is based on the assumption that all isotopes are distributed stochastically, i.e. randomly, among all possible isotopologues of a compound. A non-stochastic distribution of isotopes may occur when isotopologues contain more than one heavy isotope, which is referred to as isotope clumping (Eiler 2007). The relevance of this effect for chlorinated hydrocarbons and, consequently, the question of whether all or only the most abundant pairs of isotopologue fragment ions need be taken into account during mass spectrometric analysis has not yet been conclusively answered. Given the elevated temperatures of >400 °C at which most organochlorine compounds are synthesized (Dreher et al. 2011), it can be argued that the influence of clumped isotopes effects on the distribution of isotopes among

isotopologues is of minor importance, as clumped isotope effects become less pronounced at higher temperatures (Wang et al. 2004; Eiler 2007). Furthermore, clumped isotope effects decrease with mass (Eiler 2007). Hence, they are expected to be much smaller for isotopologues where chlorine is multiply isotopically substituted, compared to, e.g., the multiple substitution of hydrogen by deuterium.

Sakaguchi-Söder et al. (2007) did not report δ^{37}Cl values relative to SMOC but relative to the internal standard trichlorofluoromethane ($CFCl_3$), not providing an estimate for the trueness of the values by comparing them to those obtained by established offline methods. The required sample size of about 1 nmol makes this a sensitive method, at the expense of a lower precision than most other offline and online methods exhibit.

Aeppli et al. (2010) refined this method, realizing that in order to produce accurate results the samples need to be analyzed together with a molecularly identical SMOC-referenced standard. In addition to PCE, more complex molecules such as the pesticides dichlorodiphenyltrichloroethane (DDT) and pentachlorophenol (PCP) could also be analyzed with this approach. The chlorinated hydrocarbons were injected on-column following dilution in solvents. Only the two most abundant fragment ions were taken into account when calculating the chlorine isotope ratio, e.g. masses 164 and 166 for PCE (Equation (2.3)). To assess the trueness, δ^{37}Cl values were compared to those obtained by offline TIMS. It was shown that the concentrations of the standards and the samples had to be within 20% of each other, otherwise the accuracy of the obtained δ^{37}Cl values was compromised.

This necessity of matching the concentrations of standards and samples was also observed by Bernstein et al. (2011). The reproducibility of the direct qMS method was investigated in an interlaboratory study, comparing qMS and CF-IRMS methods coupled to GC. The IRMS instruments generally achieved a higher precision which was attributed to their multiple detector configuration. The qMS instruments exhibited a temporal drift in the instrument $^{37}Cl/^{35}Cl$ ratio. The effect of this drift on the δ^{37}Cl values was however negligible when samples were bracketed with two referenced, molecularly identical standards of differing isotopic composition. Further, a mismatch between the difference in δ^{37}Cl values and the known δ^{37}Cl difference of the two standards was observed, which could however also be corrected when using two standards. The authors advised against drawing any kind of conclusions about isotope enrichments based on raw, non-referenced isotope ratios.

A qMS can furthermore be coupled to an online thermal conversion interface. Hitzfeld et al. (2011) developed a setup for combusting chlorinated ethenes at a high temperature (HTC) of >1300 °C, yielding gaseous HCl which was analyzed in the mass detector as $^{1}H^{35}Cl^{+}$ and $^{1}H^{37}Cl^{+}$. No SMOC-referencing procedure was implemented at the time and the precision (1σ) for non-referenced ^{37}Cl was on the order of 1‰. Renpenning et al.

(2015) later used this HTC interface in combination with an IRMS to report referenced values of TCE and PCE. The severe memory effects that are linked to using HCl as analyte in a mass spectrometer (see Section 2.2.1) were not resolved, though.

An entirely different method was brought up by van Acker et al. (2006), using an inductively coupled plasma (ICP) ionization source which made it possible to directly measure $^{35}Cl^+$ and $^{37}Cl^+$ ions of TCE and PCE in the multicollector (MC) setup. The method offered high sensitivity and precision. No sample concentration step was applied, so only pure compounds were injected. PCE was referenced to SMOC by comparison to TCE of known $\delta^{37}Cl$ value, and both compounds were separated by GC. As the ionization source runs on argon, the author points out one of the drawbacks of this kind of ionization source: There is the possibility of interference of $^1H^{36}Ar^+$, which has a similar m/z (36.97537) as $^{37}Cl^+$ (36.96590). A high mass resolution was needed to overcome this issue.

The issue was solved with Horst et al. (2017)'s approach to GC-MC-ICPMS. Care was taken to inhibit the ingress of water into the ionization source to avoid the formation of $^1H^{36}Ar^+$. The hydrogen atoms bonded to the chlorinated hydrocarbons were shown to have a negligible influence on its formation. As a lower mass resolution could be applied, a better sensitivity was achieved. The referenced standards used in the two-point calibration were not always identical to the analyte.

As for offline pcGC (see Section 2.2.1), a chlorine isotope effect may occur during online GC separation of organochlorine compound mixtures due to slight differences in retention times for different isotopologues. Similarly, care must be taken during integration of the eluting peaks in order to register the complete signal of all isotopologues (Tang et al. 2017). Chlorine isotope fractionation also takes place during ionization (Tang et al. 2019). The effects can, however, be mitigated when bracketing with molecularly identical standards (Aeppli et al. 2010), which are expected to fractionate in the same manner as the samples when ionized.

Online methods do not only simplify compound-specific isotope analysis, but also require a far lower amount of target compound. GC-qMS is a versatile routine method as it makes it possible to analyze a wide range of masses, providing a good sensitivity and acceptable precision. Difficulties lie in obtaining suitable sets of molecularly identical reference standards which have shown to be indispensable (Bernstein et al. 2011; Elsner et al. 2012; Ebert et al. 2017), since most instruments do not allow introduction of a reference gas. GC-IRMS uses detector configurations specific to each compound, which allows for better precision but limits the compounds that can be analyzed. Online mass spectrometric methods employing a combustion interface have not yet proved themselves for routine chlorine isotope ratio measurements. They could, however, be applicable to a wide range of compounds, while

at the same time their mass detectors only need to be optimized for a single analyte – an advantage they share with GC-MC-ICPMS.

2.2.3. Accuracy, linearity and calibration strategies

Positive evidence that degradation processes are occurring is given when the isotopic fractionation as shift in δ^{37}Cl exceeds a certain threshold. An important question when comparing the capability of analytical methods to resolve this shift is hence that of the measurement uncertainty or accuracy of the method, which takes into account both the precision and the trueness. While some mass spectrometers report δ values by comparison with a working gas of known isotopic composition, this so called single point anchoring versus the working gas often does not yield sufficiently accurate results (Paul et al. 2007). Therefore, isotopically referenced standards, preferably molecularly identical to the compound of interest, are used. These isotopic standards must be stable and homogeneous in isotopic composition (Coplen 2011). They are required for two principal reasons. Firstly, they serve to account for isotopic fractionation processes during sample preparation and analysis. These processes may occur for example during incomplete conversion of the compound of interest to a molecule suitable for mass spectromety. Under the principle of identical treatment, standard and sample are prepared and analyzed in the same way yielding *repeatable* results. Secondly, they enable reporting of *reproducible* and standardized results across laboratories.

Depending on the accuracy of the instrument, two or more isotopically different reference standards can be necessary due to a distortion of instrument isotope ratios relative to the SMOC scale (Bernstein et al. 2011). These standards are analyzed within a run to bracket the samples, i.e. the samples should have an isotope ratio that lies within the range given by the standards' isotope ratios. Obtaining said standards can often prove challenging.

In isotopic analysis, the term linearity describes whether the measured isotope ratio is independent of the quantity that is injected into the measuring device (Sherwood Lollar et al. 2007; Hunkeler et al. 2008; Jochmann and Schmidt 2015). A large linearity range is advantageous as samples and standards are often not measured at exactly the same concentration or signal intensity. The limit of detection of an isotopic measurement method therefore involves identifying the lower limit of the linearity range or the lowest concentration for which no amount dependency is observed. Jochmann et al. (2006) have published guidelines to determine this so-called method detection limit using a moving mean approach, which gives the lower limit for which both the precision *and* trueness criteria are met. With all instruments, amount dependency effects of isotope measurements must be evaluated, in some cases requiring that the concentrations of samples and standards be closely matched.

2.3. Current knowledge about chlorine isotope fractionation

2.3.1. Basic concepts

The minor mass difference of isotopes leads to small changes in the physical and chemical properties of the molecules they are part of, which, in turn, is the cause of isotope fractionation or isotope effects. Isotope fractionation is described using the isotope ratio R_A in phase/educt A and R_B in phase/product B as the fractionation factor α:

$$\alpha = \frac{R_B}{R_A} = \frac{\delta^{37}\mathrm{Cl}_B + 1}{\delta^{37}\mathrm{Cl}_A + 1} \qquad (‰) \tag{2.4}$$

or, since α is generally close to 1, as the enrichment factor ε:

$$\varepsilon = \alpha - 1 \qquad (‰) \tag{2.5}$$

During a reversible equilibrium reaction $A \rightleftarrows B$, different isotopologues have a slightly different equilibrium constant, which in turn causes an isotopic fractionation of isotopologues between the phases/educts A and phases/products B. This equilibrium isotope effect (EIE), expressed as the equilibrium fractionation factor α_{eq}, is often not very large, though highly temperature-dependent.

Isotope effects for a non-equilibrium reaction $A \rightarrow B$ are caused by differences in the reaction rates for isotopologues having a light (^{35}Cl) or a heavy (^{37}Cl) isotope at the reactive position and are expressed as the kinetic fractionation factor α_{kin}. The difference in reaction rates k is expressed as the kinetic isotope effect (KIE):

$$KIE = \frac{k_{35\mathrm{Cl}}}{k_{37\mathrm{Cl}}} \tag{2.6}$$

A normal kinetic isotope effect is observed if $KIE > 1$, i.e. the isotopologue with the lighter isotope(s) at the reactive position(s) will react more rapidly, while the isotopologue with the heavier isotope(s) at the reactive position(s) will accumulate in the educt. The opposite is true if $KIE < 1$, which is denoted as a inverse kinetic isotope effect. In addition to this primary isotope effect, secondary isotope effects are observed when isotopic substitution takes place at non-reactive positions. Secondary isotope effects are however usually at least one order of magnitude weaker than primary isotope effects (Meckenstock et al. 2004; Elsner et al. 2005; Aelion 2010).

Using the isotope enrichment factor ε, the isotope fractionation during a transformation process can be described by the *Rayleigh* equation (Elsner and Hunkeler 2008):

$$\frac{R_t}{R_0} = f^{\varepsilon} = f^{(\alpha-1)} \tag{2.7}$$

where R_0 describes the initial isotope ratio at the beginning of the transformation process, R_t the isotope ratio and f the remaining fraction of the compound at a point in time t.

In a well-constrained, homogeneous system, Equation (2.7) is the basis to calculate a compound-specific bulk chlorine isotope enrichment factor $\varepsilon_{Cl,bulk}$, specific to a given transformation mechanism. This bulk enrichment factor accounts for the change in isotope ratios averaged over the whole compound. Crucially, the remaining concentration of the compound must only be influenced by the transformation process, thus laboratory batch experiments are preferable for obtaining said enrichment factors over field studies where processes such as dilution and dispersion affect the measured concentration data (Abe and Hunkeler 2006). If the transformation process on the field site is known, the degree of degradation can be quantified by inserting $\varepsilon_{Cl,bulk}$ and the measured shift in isotope ratios into Equation (2.7). Uncertainties in field data due to multiple unconstrained processes at play can be reduced when isotopic data of multiple elements is considered (Zwank et al. 2005b). More specifically, the ratio of the shift in delta values ($\Delta\delta$) for the isotopes of two elements during a transformation process is, for the most part, not affected by non-reactive processes, as well as being specific to the reaction pathway (Palau et al. 2017a). This ratio corresponds to the slope of a fitted linear relationship using least squares or, preferably, the *York* method (Ojeda et al. 2019b), obtained by plotting the δ values for the two elements, e.g. $\delta^{13}C$ and $\delta^{37}Cl$ against each other (Abe et al. 2009b), and provides a good approximation of the ratio of enrichment factors:

$$\frac{\Delta\delta^{13}C}{\Delta\delta^{37}Cl} = \frac{\varepsilon_{C,bulk}}{\varepsilon_{Cl,bulk}} \tag{2.8}$$

The dual element approach is useful for identifying the dominant degradation process, which allows constraining the element-specific range of enrichment factors to be inserted into Equation (2.7).

CSIA has been widely used for low molecular mass compounds. In larger chlorinated molecules such as certain aromatic compounds and pesticides, the isotope effect can be diluted as the heavy isotope is more likely to be at a non-reactive position in the molecule (see Section 2.5), leading to a smaller bulk isotope enrichment factor than would be expected from cleavage of a bond involving the heavier isotope. Another process, which is especially relevant to biotic degradation reactions, is masking. Being enzyme-catalyzed, biotic degradation reactions always involve multiple steps, where the isotope effect from the actual catalytic reaction can be masked by preceding rate-limiting steps such as extra- and intracellular mass transfer (Elsner 2010).

2.3.2. Chlorine isotope fractionation by physical processes

Physical processes, such as evaporation (volatilization / liquid-vapor partioning), diffusion, sorption and dissolution can lead to an isotopic fractionation due to slight differences in the thermodynamic properties of isotopologues (Aelion 2010). Table 2.2 summarizes the chlorine isotope enrichment factors caused by physical processes that have been obtained through laboratory studies.

Table 2.2.: Bulk carbon and chlorine isotope enrichment factors by physical processes based on laboratory experiments.

Mechanism	Compound	$\varepsilon_{C,bulk}$ (‰)	$\varepsilon_{Cl,bulk}$ (‰)	Reference
Continuous evaporation (of pure compound)	DCM	$+0.65 \pm 0.02$	-0.48 ± 0.06	Huang et al. (1999)
Continuous evaporation (of pure compound)	TCE	$+0.31 \pm 0.04$	-1.82 ± 0.22	Huang et al. (1999)
Continuous evaporation (of pure compound)	TCE	$+0.24 \pm 0.06$ to $+0.35 \pm 0.02$	-1.64 ± 0.13	Poulson and Drever (1999)
Continuous evaporation (of pure compound)	TCE	$+0.28 \pm 0.03$	-1.35 ± 0.03	Jeannottat and Hunkeler (2012)
Stepwise evaporation (of pure compound)	TCE	$+0.75 \pm 0.04$	-0.39 ± 0.03	Jeannottat and Hunkeler (2012)
Diffusion-controlled evaporation (of pure compound)	TCE	$+0.10 \pm 0.05$	-1.39 ± 0.06	Jeannottat and Hunkeler (2012)
Stepwise evaporation (of aqueous phase compound)	TCE	$+0.38 \pm 0.04$	-0.06 ± 0.05	Jeannottat and Hunkeler (2012)
Aqueous phase back-diffusion (enrichment in reservoir)	*cis*-1,2-DCE		-0.28 to -1.33	Vakili (2017)
Aqueous phase back-diffusion (enrichment in reservoir)	1,2-DCA	-0.23 ± 0.04	-0.61 ± 0.03	Wanner and Hunkeler (2015)
Aqueous phase sorption (enrichment in solution)	1,2-DCA	-0.40 ± 0.06	-0.55 ± 0.13	Wanner et al. (2017)
Aqueous phase sorption (enrichment in solution)	*cis*-1,2-DCE	< 0.1	-0.2	Vakili (2017)
Aqueous phase sorption (enrichment in solution)	TCE	< 0.1	-0.85	Vakili (2017)

Liquid-vapor chlorine isotope fractionation in chlorinated VOCs has been studied from an early date in the laboratory. Baertschi et al. (1953) and Bradley (1954) observed that for carbon tetrachloride (CT) and chloroform (CF), the liquid phase became enriched in ^{37}Cl, while δ^{13}C showed an inverse isotope trend, leading to an enrichment in the vapor phase. These opposite trends were confirmed by Huang et al. (1999) for TCE and dichloromethane (DCM) as well as by Poulson and Drever (1999) and Jeannottat and Hunkeler (2012) for TCE. They are believed to be caused by the differing effects of isotopic substitution on intermolecular forces in the condensed phase. In general, heavy isotope substitution leads to weaker intermolecular forces and thus a lower boiling point due to lower frequencies of internal vibration (Van Hook 2005), however the effect of ^{13}C substitution is considerably

larger than that of ^{37}Cl substitution (Jancsó and Van Hook 1974). The weak inverse chlorine isotope effect is thus counteracted by other intermolecular forces in the condensed phase, while it is possible to observe the strong inverse carbon isotope effect. When the chlorinated VOC is dissolved in water, hydrogen bonding and dipole-dipole interactions, which are relevant between the more polar molecules, may become strong enough to completely cancel out the inverse carbon isotope effect (Horst et al. 2016).

Vapor-phase diffusion has been shown to cause a significant chlorine isotope fractionation in laboratory experiments (Jeannottat and Hunkeler 2012). This arises due to heavier isotopocules generally being less mobile than their lighter counterparts. The difference of two atomic units between stable chlorine isotopes compared to only one atomic unit between stable carbon isotopes explains the pronounced chlorine isotope fractionation.

Isotope fractionation due to aqueous-phase diffusion also occurs in the subsurface. Several models for the diffusion coefficient have been proposed. Wanner and Hunkeler (2019) presented a comprehensive review of five relevant models and existing experimental data that have been obtained for several compounds. In general, models for the mass dependency of a compound's diffusion coefficient reduce to the form:

$$D \propto m^{-\beta} \tag{2.9}$$

where m is the isotopologue molecular mass and β is a number generally between 0 and $\sim 1/2$. This relation is sometimes written as a function of the reduced mass ($\mu_r = m \cdot m_{\text{solvent}}/(m + m_{\text{solvent}})$). However, as many theories that assume that the water molecule network acts as a massive effective particle ($m_{\text{solvent}} \gg m$) (Bourg and Sposito 2007; Wanner and Hunkeler 2019), Equation (2.9) is generally valid.

Various models such as the well-known *Chapman-Enskog* relation (Chapman and Cowling 1970) have been developed for diffusion. However, only some are relevant in the case of aqueous solutions in porous media. Extensions of classical *Fickian* kinetic theory (Fick 1855) imply that $\beta = 1/2$ in Equation (2.9) (Alder et al. 1974). The *Einstein* (Einstein 1905) and *Langevin* (Langevin 1908) models of diffusion are based on the random trajectory of a single solute particle (i.e., Brownian motion), but do not integrate mass effects. The *Maxwell-Stefan* diffusion model (Maxwell 1867), like the *Fick* model, considers the ensemble behaviour of solute particles. In this model, mass is explicitly taken into account with the resulting relationship of $\beta = 1/2$. This theory assumes that solute molecules move according to solute concentration gradients, but are subject to a friction-like force from the solvent molecules. A final theory of note is mode-coupling theory analysis (MCTA) (Bhattacharyya and Bagchi 1997; Ali et al. 2001) wherein $0 < \beta < 1/2$. In MCTA, the diffusion coefficient depends on the interplay between extremely frequent intermolecular

collisions, which are strongly mass-dependent, and longer-term hydrodynamic modes which exhibit little mass dependence (Wanner and Hunkeler 2019).

Finally, sorption can also induce isotopic fractionation in the adsorbed and desorped substances. While Vakili (2017) detected only an insignificant carbon isotope effect, the chlorine isotope enrichment in the solution reached −0.2‰ for *cis*-1,2-DCE and −0.85‰ for TCE, which may also be explained by the difference of two atomic units between stable chlorine isotopes compared to only one atomic unit between stable carbon isotopes. The preferential sorption of the light isotopologues leads to an enrichment of ^{37}Cl in the solution. Similarly to evaporation, this may be explained by the weaker intermolecular forces between heavy isotopologues and the sorbent compared to light isotopologues. Sorption is of concern primarily in organic-rich sediments as well as low-permeability sediments with small pore sizes, such as shales and clays, due to their high specific surface area. It is also relevant in zero-valent iron systems (Dries et al. 2007) which are of increasing interest in remediation efforts (Crane and Scott 2012).

Physical processes are often not well constrained to a single process. In laboratory experiments, Jeannottat and Hunkeler (2012) found a cumulative normal chlorine isotope effect by both liquid-vapor partioning and vapor phase diffusion. Vakili (2017) investigated chlorine isotope effects caused by back-diffusion from a low-permeability zone as well as sorption on the laboratory scale, although it is unclear how the set-up discriminated between diffusion and sorption processes. Wanner et al. (2017) attempted to isolate the isotopic effects of these processes by including field data into a numerical model. The theoretical sorption-induced isotope shift was calculated to reach up to 2‰.

Chlorine isotope effects caused by physical processes have not been widely studied on the field scale. While gas-phase diffusion (Jeannottat and Hunkeler 2012) may cause a significant chlorine isotope effect, its relevance in vadose zone transport has not been established (Hunkeler et al. 2011b). The isotope effects of physical processes are believed to have a minor influence compared to the isotope effects observed during (bio-)chemical degradation processes, and are less pronounced once steady-state conditions are reached (Schmidt and Jochmann 2012). Numerical considerations related to modelling physical processes are discussed in Section 2.5.

2.3.3. Chlorine isotope fractionation during biotic processes

Biotic degradation of chlorinated contaminants in the subsurface is a process that causes isotope fractionation due to bond cleavage. Chemical bonds involving the heavier isotope are slightly stronger than those involving the light isotope, thus the lighter isotopologue of

a molecule degrades preferentially resulting in a heavy isotope enrichment in the residual compound. Figure 2.2 gives an overview of potential degradation pathways for the example of PCE. One advantage of compound-specific isotope analysis is that degradation can be proven even if there are no characteristic degradation products. If they however do occur, it is advisable to monitor them, also their isotope ratios, to provide confirmation about the degradation path.

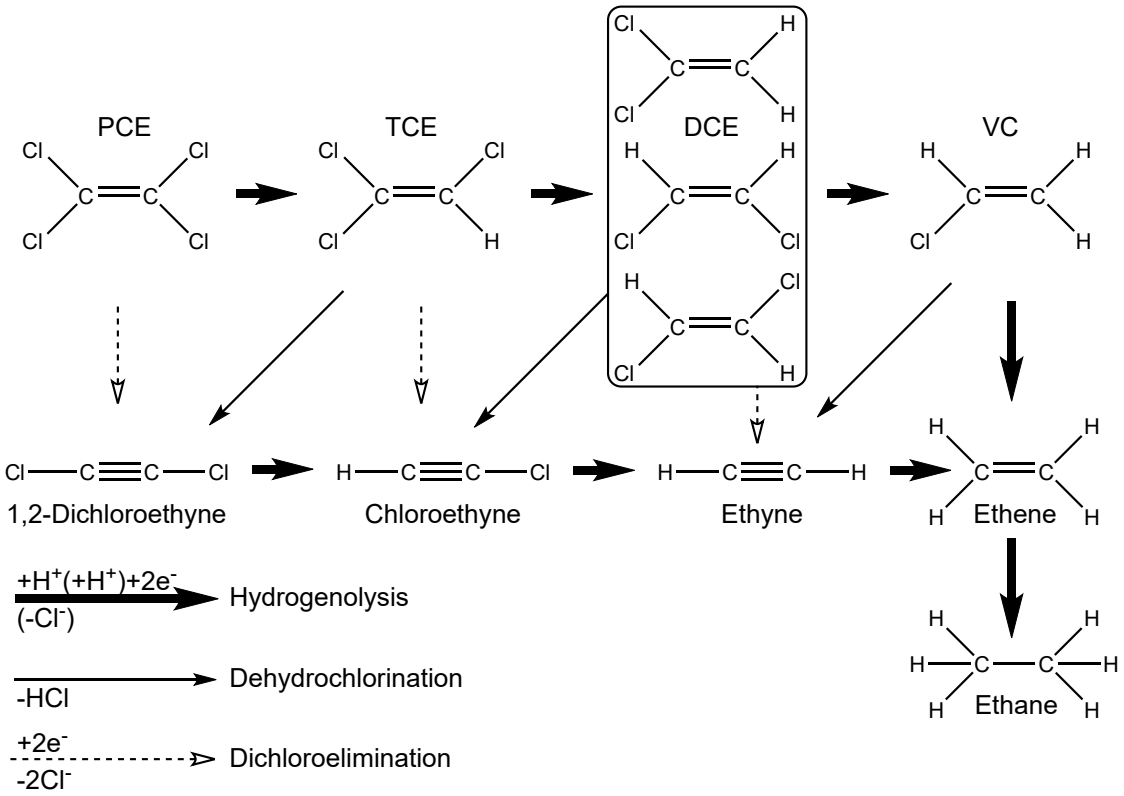

Figure 2.2.: Potential biotic and abiotic degradation pathways for PCE adapted from Brown et al. (2006). Biotic degradation typically takes the hydrogenolysis pathway from PCE to VC.

The biotic degradation pathway is a function of the redox potential in the soil and the availability of electron donors and adapted bacteria. Chlorinated hydrocarbons either serve as electron acceptors during anaerobic organohalide respiration or else as electron donors during anaerobic as well as aerobic metabolic degradation (Dolinová et al. 2017). If degradation of xenobiotics is not the primary metabolic process, it is referred to as co-metabolism and attributed to the activity of non-specific enzymes. Anaerobic dechlorination is usually the predominant process in biotic degradation on the field scale, as aerobic dechlorination is limited by the lack of electron acceptors, specifically molecular oxygen (Numata et al. 2002a).

The aerobic process does however become more relevant with decreasing chlorination, e.g. during the sequential degradation of PCE, where a purely anaerobic process would stall at the highly toxic degradation product VC (Tiehm and Schmidt 2011). Aerobes on the other hand have the potential to further degrade VC to non-chlorinated, non-toxic compounds through epoxide formation.

Table 2.3 gives an overview of some of the chlorine isotope enrichment factors that were measured in laboratory microcosms. It is noticeable that the chlorine isotope fractionation is almost always smaller in magnitude than the carbon isotope fractionation, as opposed to the trends observed for physical processes. Furthermore, different reactive processes lead to remarkably different carbon and chlorine isotope enrichment factors for the same compound. As commonly observed, the *exact* reaction mechanism dictates whether a large primary or lower secondary chlorine isotope effect is observed or whether dilution and masking (see Section 2.3.1) have an influence on the magnitude of fractionation.

During aerobic oxidation of DCM, a considerable carbon and chlorine isotope effect was observed by Heraty et al. (1999). The first and rate-limiting step was proposed to involve breaking of a C-Cl bond by nucleophilic substitution (S_N2), leading to CH_2O (formaldehyde) and HCl via the unstable intermediate CH_2ClOH. VC and *cis*-1,2-DCE on the other hand undergo a different reaction mechanism during aerobic oxidation, which manifests itself in the smaller enrichment factors (Abe et al. 2009a). Here, the first step does not involve C-Cl bond cleavage but C-C bond cleavage and the formation of an epoxide between the two carbon atoms.

Two distinct aerobic degradation pathways for 1,2-DCA can be distinguished using dual carbon-chlorine isotope plots (Palau et al. 2014a). Only a small carbon isotope effect is measured with C-H bond cleavage as the initial step, which is the case for the reaction with the monooxygenase enzyme used by the *Pseudomonas* sp. strain. The dehalogenase enzyme that is employed by *Xanthobacter autotrophicus* and *Ancylobacter aquaticus* causes a large carbon isotope effect, as here the initial step is C-Cl bond cleavage via nucleophilic S_N2 substitution. For both pathways, Palau et al. (2014a) observed a similar chlorine isotope effect $\varepsilon_{Cl,bulk}$. During anerobic degradation by *Dehalococcoides* and *Dehalogenimonas*, 1,2-DCA exhibits a significant chlorine isotope effect (Palau et al. 2017a). The reason is thought to be a dichloroelimination pathway, where not one but two C-Cl bonds are cleaved. This dichloroelimination pathway also appears during anaerobic degradation of 1,1,2-TCA to VC (Rosell et al. 2019). Compared to 1,2-DCA, the chlorine isotope effect is not quite as pronounced due to masking effects (see Section 2.3.1) caused by differences in the enzyme kinetics.

The anaerobic reductive dechlorination of chlorinated ethenes can proceed either via

single-electron transfer or nucleophilic addition as initial step (Aelion 2010). The former would lead to primary carbon and chlorine isotope effects due to C-Cl bond cleavage, while the latter would attack the C=C double bond resulting in a large primary carbon isotope effect and secondary chlorine isotope effects (Cretnik et al. 2014). For TCE, Kuder et al. (2013) applied triple element hydrogen-carbon-chlorine isotope analysis and observed secondary chlorine isotope effects consistent with the nucleophilic addition pathway.

Masking effects may also have a major impact on the observed isotope fractionation during reductive dechlorination. For PCE, Renpenning et al. (2014) obtained significantly different dual carbon-chlorine isotope slopes for the culture *Sulfurospirillum multivorans* ($\varepsilon_C/\varepsilon_{Cl}$ ranging from 2.2 to 2.8) versus the culture's enzyme corrinoid cofactor ($\varepsilon_C/\varepsilon_{Cl}$ ranging from 4.6 to 7.0), which was attributed to the preceding rate-limiting steps. Interestingly, this masking effect was not observed during reductive dechlorination of TCE.

While considerable work has been done in measuring chlorine isotope fractionation during biotic degradation, the masking effects that are inherent to biotic processes as well as the ambiguity of some dual carbon-chlorine isotope slopes can complicate the attribution of specific mechanisms to observed isotope fractionations. Improvements in analytical methods (see Section 2.2) can assist in lowering the uncertainty of chlorine CSIA data, especially for TCE.

2.3.4. Chlorine isotope fractionation during abiotic processes

Abiotic degradation of chlorinated contaminants in soil is usually slower than biotic degradation, but has the advantage that it is likely to result in completely dechlorinated, generally non-toxic compounds (Tobiszewski and Namieśnik 2012). There are many different constituents of natural soil that can be relevant to abiotic degradation during natural remediation, namely iron-bearing sulfide, oxide, hydroxide and clay minerals (He et al. 2015). Additionally, engineered remediation at polluted sites often involves reactive barriers that employ zero-valent metals or compounds that contain metals at their reduced state (Hara 2012). Table 2.3 gives an overview of some the chlorine isotope enrichment factors that were measured in the laboratory for abiotic degradation.

The isotope effects associated with abiotic degradation in chlorinated hydrocarbons are often very pronounced for carbon isotopes (Slater et al. 2003; Liang et al. 2007) and for chlorine isotopes. Audí-Miró et al. (2013) studied the chlorine isotope effect during degradation of chlorinated ethenes by zero-valent iron (ZVI). The process is based on an electron transfer where the chlorinated ethenes are dechlorinated reductively, while the ZVI is oxidized. Abiotic TCE degradation yielded *cis*-1,2-DCE via a hydrolysis pathway as well

Table 2.3.: Bulk carbon and chlorine isotope enrichment factors as well as dual element isotope slopes (C/Cl) by biotic and abiotic degradation based on laboratory microcosm studies.

Compound	Proposed mechanism (rate-limiting step)	Culture (enzyme) for biotic or reactant for abiotic degradation	$\varepsilon_{C,bulk}$ (‰)	$\varepsilon_{Cl,bulk}$ (‰)	C-Cl isotope slope	Reference
Biotic						
DCM	aerobic oxidation (nucleophilic substitution)	*Methylobacterium/ Ochrobactrum* MC8b	-42.4 ± 1.5	-3.8 ± 0.3	11.2	Heraty et al. (1999)
1,2-DCA	aerobic oxidation (C-H bond cleavage)	*Pseudomonas* sp.	-3.5 ± 0.1	-3.8 ± 0.2	0.78 ± 0.03	Palau et al. (2014a)
1,2-DCA	aerobic oxidation (nucleophilic substition)	*Xanthobacter autotrophicus* GJ10 & *Ancylobacter aquaticus* AD20	-31.9 ± 0.7 to -32.0 ± 0.9	-4.2 ± 0.1	7.7 ± 0.2	Palau et al. (2014a)
1,2-DCA	dichloroelimination	*Dehalococcoides*	-33.0 ± 0.4	-5.1 ± 0.1	6.8 ± 0.2	Palau et al. (2017a)
1,2-DCA	dichloroelimination	*Dehalogenimonas*	-23 ± 2	-12.0 ± 0.8	1.89 ± 0.02	Palau et al. (2017a)
1,1,2-TCA	dichloroelimination	*Dehalogenimonas* sp.	-6.9 ± 0.4	-2.7 ± 0.3	2.5 ± 0.2	Rosell et al. (2019)
VC	aerobic oxidation (epoxide formation)	*Nocardioides* strain JS614	-7.2 ± 0.16	-0.3 ± 0.04	25.6 ± 3.6	Abe et al. (2009a)
VC	reductive dechlorination	*Dehalococcoides*	-25.0 ± 0.72	-1.7 ± 0.12	13.7 ± 0.3	Abe et al. (2009a)
VC	reductive dechlorination	*Dehalococcoides*	-26.7 ± 1.9 to -28.1	-2.7 ± 0.4	10 ± 10	Kuder et al. (2013)
cis-1,2-DCE	aerobic oxidation (epoxide formation)	β-Proteobacterium strain JS666	-8.5 ± 0.10	-0.3 ± 0.07	32.3 ± 6.4	Abe et al. (2009a)
cis-1,2-DCE	reductive dechlorination	*Dehalococcoides*	-18.5 ± 1.80	-1.6 ± 0.14	11.4 ± 0.6	Abe et al. (2009a)
cis-1,2-DCE	reductive dechlorination	*Dehalococcoides*	-26.8	-3.2	8.3	Kuder et al. (2013)
TCE	reductive dechlorination	*Geobacter lovleyi*	-12.2 ± 0.5	-3.6 ± 0.1	3.4 ± 0.2	Cretnik et al. (2013)
TCE	reductive dechlorination	*Desulfitobacterium hafniense*	-9.1 ± 0.6	-2.7 ± 0.6	3.4 ± 0.2	Cretnik et al. (2013)
TCE	reductive dechlorination	*Desulfitobacterium* sp.	-12.2 ± 1.0	-3.6 ± 0.2	3.4 ± 0.2	Cretnik et al. (2014)
TCE	reductive dechlorination	*Clostridium* sp.& *Desulfitobacterium aromaticivorans*	-8.8 ± 0.2	-3.5 ± 0.5	2.7 ± 0.8	Wiegert et al. (2013)
TCE	reductive dechlorination	*Dehalococcoides*	-15.3 to -16.4 ± 0.4	-3.6 ± 0.3	4.8 ± 4.5	Kuder et al. (2013)
TCE	reductive dechlorination	*Sulfurospirillum multivorans* (PceA-norpseudo-B12 enzyme)	-20.0 ± 0.5	-3.7 ± 0.2	5.3 ± 0.3	Renpenning et al. (2014)
TCE	reductive dechlorination	*Sulfurospirillum multivorans* (PceA-nor-B12 enzyme)	-20.2 ± 1.1	-3.9 ± 0.6	5.0 ± 0.8	Renpenning et al. (2014)
PCE	reductive dechlorination	*Desulfitobacterium* sp.	-19.0 ± 0.9	-5.0 ± 0.1	3.8 ± 0.2	Cretnik et al. (2014)
PCE	reductive dechlorination	*Clostridium* sp. & *Desulfitobacterium aromaticivorans*	-5.6 ± 0.7	-2.0 ± 0.5	2.9 ± 0.9	Wiegert et al. (2013)
PCE	reductive dechlorination	*Sulfurospirillum multivorans* (PceA-norpseudo-B12 enzyme)	-1.4 ± 0.1	-0.6 ± 0.2	2.2 ± 0.7	Renpenning et al. (2014)
PCE	reductive dechlorination	*Sulfurospirillum multivorans* (PceA-nor-B12 enzyme)	-1.3 ± 0.05	-0.4 ± 0.1	2.8 ± 0.5	Renpenning et al. (2014)
PCE	reductive dechlorination	consortium SL2-PCEc *Sulfurospirillum* ($PceA_{TCE}$)	-3.6 ± 0.2	-1.2 ± 0.1	2.7 ± 0.3	Badin et al. (2014)
PCE	reductive dechlorination	consortium SL2-PCEb *Sulfurospirillum* ($PceA_{DCE}$)	-0.7 ± 0.1	-0.9 ± 0.1	0.7 ± 0.2	Badin et al. (2014)
Abiotic						
CF	oxidation (C-H bond cleavage)	persulfate	-8 ± 1	-0.44 ± 0.06	17 ± 2	Torrentó et al. (2017)
CF	hydrolysis (E1cB elimination)	pH 12 buffer	-57 ± 5	-4.4 ± 0.4	13.0 ± 0.8	Torrentó et al. (2017)
CF	hydrogenolysis (C-Cl bond cleavage)	ZVI pH 7	-33 ± 11	-3 ± 1	8 ± 2	Torrentó et al. (2017)
CF	hydrogenolysis/reductive elimination	ZVI pH 12	-20 ± 9	-2 ± 1	8 ± 1	Rodríguez-Fernández et al. (2018a)
CT	hydrogenolysis	ZVI pH 7	-3.7 ± 0.1	-0.58 ± 0.04	6.1 ± 0.5	Rodríguez-Fernández et al. (2018a)
CT	hydrogenolysis	ZVI pH 12	-3.4 ± 0.1	-0.55 ± 0.03	5.8 ± 0.4	Rodríguez-Fernández et al. (2018a)
CT	hydrogenolysis/hydrolysis	magnetite pH 12	-2 ± 1	-0.8 ± 0.2	2 ± 1	Rodríguez-Fernández et al. (2018a)
CT	hydrogenolysis/thyolithic reduction	pyrite pH 7	-5 ± 2	-1.5 ± 0.4	2.9 ± 0.5	Rodríguez-Fernández et al. (2018a)
CT	hydrogenolysis/thyolithic reduction	pyrite pH 12	-4 ± 1	-0.9 ± 0.4	3.7 ± 0.9	Rodríguez-Fernández et al. (2018a)
1,1,1-TCA	hydrolysis/ dehydrohalogenation	water	-1.6 ± 0.2	-4.7 ± 0.1	0.33 ± 0.04	Palau et al. (2014b)
1,1,1-TCA	(C-Cl bond cleavage)	ZVI	-7.8 ± 0.4	-5.2 ± 0.2	1.5 ± 0.1	Palau et al. (2014b)
cis-1,2-DCE	dichloroelimination & hydrogenolysis	ZVI	-20.5 ± 1.8	-6.2 ± 0.8	3.1 ± 0.2	Audí-Miró et al. (2013)
TCE	dichloroelimination & hydrogenolysis	ZVI	-14.8 ± 0.6	-2.6 ± 0.1	5.2 ± 0.3	Audí-Miró et al. (2013)
TCE	(nucleophilic addition)	magnetite + H_2O_2	-2.9 ± 0.3	-0.9 ± 0.1	3.1 ± 0.2	Liu et al. (2014)

as ethene and ethane via dichloroelimination (Figure 2.2). This additional pathway is often observed during abiotic degradation and involves the simultaneous cleavage of two chlorine substituents, explaining the large chlorine isotope effect. Torrentó et al. (2017) explored different abiotic degradation mechanisms for chloroform (CF). The oxidiation reaction was proposed to involve C-H bond cleavage as the initial step, hence only a small secondary chlorine isotope effect was observed (Table 2.3). Rodríguez-Fernández et al. (2018a) investigated the suitability of different iron minerals in engineered remediation, and observed a pronounced pH dependence of the chlorine isotope enrichment factors (Table 2.3), which was suspected to be caused by surface passivation of the iron minerals at alkaline pH.

Most chlorine isotope enrichment data for abiotic processes have so far been obtained with a focus on zero-valent iron in engineered remediation. The question of which pathways are taken during reaction of chlorinated contaminants with natural constituents of soils could be investigated using dual carbon-chlorine isotope analysis.

2.4. Field applications

Chlorine CSIA has rarely been used in source differentiation field applications. A more common field application is the tracking of reactive processes, usually in combination with carbon isotope analysis. Table 2.4 provides an overview of field studies where chlorine CSIA has been applied.

Table 2.4.: Field studies where chlorine CSIA has been applied.

Compound	Isotopes		Objective			Reference
	^{13}C	^{37}Cl	Source differentiation	Process assessment	Quantification of degradation	
1,2-DCA	✓	✓		✓		Wanner et al. (2017)
1,2-DCA	✓	✓		✓		Palau et al. (2017a)
1,1,1-TCA	✓	✓		✓		Palau et al. (2016)
cis-1,2-DCE	✓	✓		✓		Hunkeler et al. (2011a)
cis-1,2-DCE	✓	✓		✓		Hunkeler et al. (2011b)
TCE		✓		✓		Sturchio et al. (1998)
TCE	✓	✓		✓		Hunkeler et al. (2011b)
TCE	✓	✓	✓	✓	✓	Wiegert et al. (2012)
TCE	✓	✓		✓	✓	Wiegert et al. (2013)
TCE	✓	✓		✓		Badin et al. (2016)
TCE	✓	✓	✓	✓		Palau et al. (2014c)
PCE	✓	✓	✓			Beneteau et al. (1999)
PCE	✓	✓		✓		Hunkeler et al. (2011b)
PCE	✓	✓	✓	✓	✓	Wiegert et al. (2012)
PCE	✓	✓		✓	✓	Wiegert et al. (2013)
PCE	✓	✓		✓	✓	Badin et al. (2014)
PCE	✓	✓	✓	✓		Palau et al. (2014c)
PCE	✓	✓		✓		Badin et al. (2016)
PCE	✓	✓		✓	✓	Murray et al. (2019)

2.4.1. Source differentiation

Due to differences in the methods and raw materials used in manufacturing, certain chlorinated hydrocarbons can exhibit a range of δ^{37}Cl values. For example, van Warmerdam et al. (1995) reported δ^{37}Cl SMOC values from −2.4‰ to 4.4‰ for TCE sourced from different manufacturers. Based on these findings, Beneteau et al. (1999) used isotopic methods to distinguish two potential sources of PCE at a field site, with δ^{37}Cl SMOC values ranging from 0.2 to 1.1‰. The plume at this particular field site was however not affected by biodegradation. To assess whether a plume could be affected by biodegradation, where the resulting isotopic fractionation would hamper fingerprinting applications, a field site should be first characterized geochemically with regard to the redox conditions (Aelion 2010). Furthermore, a dual element isotope approach should be employed to exclude degradation. Dual carbon and chlorine isotope analysis was applied to a field site in a fractured bedrock aquifer by Palau et al. (2014c). Here, multiple sources as well as biodegradation had to be identified. The initial contaminants could be sampled at several different potential sources, yielding δ^{13}C values ranging from −40.5‰ to −15.6‰ for TCE, while δ^{37}Cl only varied between 0.53‰ and 0.66‰, though. The isotope ratios in groundwater samples downgradient of the sources showed that certain parts of the plumes were affected by biodegradation, while in others the isotope ratios remained stable. A systematic study of the δ^{37}Cl range is still lacking for many compounds, some of the values that have so far been reported are summarized in Table S1 in the supporting information (Appendix A).

2.4.2. Assessing reactive processes

In contaminated sites, isotope effects can be caused by physical processes (see Section 2.3.2) or reactive processes (see Sections 2.3.3 and 2.3.4). For assessing reactive processes, the typical analytical uncertainties for chlorine isotope analysis as discussed in Section 2.2 need to be considered carefully, in view of the generally smaller magnitudes of chlorine isotope fractionation compared to carbon isotope fractionation. A compound for which it is especially feasible to differentiate biotic and abiotic pathways using dual carbon-chlorine isotope slopes (see Table 2.3) is *cis*-1,2-DCE, while for TCE the slopes for both processes may fall into the same range. For 1,2-DCA, VC, *cis*-1,2-DCE and PCE different biotic pathways can easily be distinguished, and abiotic pathways can be differentiated for CF and CT. Data on abiotic degradation of PCE is still lacking.

As a basis for assessing reactive processes, the effect of non-reactive processes has to be taken into account. Chlorine isotope effects due to physical processes on the field scale were investigated by Hunkeler et al. (2011b), who observed neither carbon nor chlorine

isotopic fractionation by either liquid-vapor partitioning at the boundary layer or vapor phase diffusion in the unsaturated zone of a sandy aquifer for *cis*-1,2-DCE, TCE and PCE. This was taken as justification to relate isotope ratios measured in soil gas to those measured in groundwater, under the condition of a steady-state system. Wanner et al. (2017) used dual carbon-chlorine isotope plots to find out whether sorption of 1,2-DCA is associated with an isotope effect, this was however only possible because degradation could be excluded. Desorption from saturated low-permeability sediments was shown to have normal isotope effect for carbon and for chlorine, as expected from laboratory experiments (see Section 2.3.2).

Reactive processes on the field scale were assessed by Sturchio et al. (1998) using compound-specific chlorine isotope analysis at a site contaminated with TCE, where an enrichment in ^{37}Cl provided evidence for natural attenuation. Hunkeler et al. (2011a) measured stable isotope fractionation at a field site that exhibited varying redox conditions and the potential for abiotic degradation. Dual carbon-chlorine isotope plots made it possible to exclude an abiotic degradation pathway for TCE and PCE, while the fate of the degradation product *cis*-1,2-DCE remained unclear. In a follow-up study at this field site, Badin et al. (2016) applied dual carbon-chlorine isotope plots, giving evidence for abiotic degradation of *cis*-1,2-DCE by pyrite (FeS_2) or other iron sulfide species as suggested by Hunkeler et al. (2011a) for this field site. A difficulty was observed here when investigating a compound that is a degradation product as well as a primary contaminant. It is possible to resolve these issues with dual carbon-chlorine isotope plots of both the initial contaminant and the degradation product, where both will follow a linear trend if no further degradation of the product is occurring (Hunkeler et al. 2009). Further dual carbon-chlorine isotope analysis by Murray et al. (2019) at this field site confirmed the biotic degradation pathway for PCE.

Wiegert et al. (2012) encountered a wide range of chlorine isotope enrichment factors for chlorine when calculating it through dual carbon-chlorine isotope slopes from field data and $\varepsilon_{C,bulk}$ literature values according to Equation (2.8), hence in their following study Wiegert et al. (2013) used bacteria culture from the field site in batch reactors to help constrain $\varepsilon_{Cl,bulk}$ for TCE and PCE and hereby lowering the uncertainty in calculating the degree of degradation. Badin et al. (2014)'s field study showed that similar bacterial culture do not necessarily lead to similar dual carbon-chlorine isotope plots during reductive dechlorination. This was attributed to a different reaction mechanism, which resulted in either primary or secondary isotope effects. Applying dual element isotope analysis when quantifying the degree of degradation proved advantageous at this field site. Taking into

account the chlorine isotope data helped to narrow down the choice of enrichment factor when quantifying the degree of degradation.

A common problem that was encountered during the application of chlorine CSIA at the aformentioned field studies is the lack of published dual carbon-chlorine isotope slopes for different compounds and processes. If laboratory-derived reaction-specific enrichment values for the isotopes of multiple elements are available, even relative contributions of different reactive processes, such as aerobic and anaerobic degradation, can be assessed (Palau et al. 2016; Palau et al. 2017a). New developments in modelling degradation and physical processes (e.g., Jin et al. 2014; Badin et al. 2018; Halloran et al. 2019) show promise for more robust integration of chlorine CSIA data into quantitative assessments.

2.5. Modelling chlorine fractionation processes

2.5.1. General considerations

Interpretation of CSIA data requires an understanding of the fractionation processes. Two major factors differentiate the modelling of chlorine isotopic fractionation from that of carbon. Firstly, the ratio of heavy to light chlorine atoms in nature ($\sim$0.320) is far higher than that of heavy to light carbon atoms ($\sim$0.0112). Secondly, for chlorinated compounds of interest in contaminant hydrology, relevant degradation reactions involve dechlorination. Thus, for most molecules, including all of those considered here, a chlorine atom can be in a reactive position.

One of the implications of the $^{37}Cl/^{35}Cl$ ratio is that for a compound with multiple chlorine atoms (e.g., PCE) significant proportions of the molecules will have one or more heavy isotopes present (Figure S1 in supporting information Appendix A). Thus, while considering only two species (i.e., "heavy" and "light" molecules) may introduce negligible error for carbon isotope modelling, for chlorine, a greater number of species will need to be considered. For example, in modelling PCE, to avoid errors in $\delta^{37}Cl$ (Figure S1 in supporting information Appendix A), isotopologue modelling would need to include five isotopologues (if only chlorine is of interest). While a large body of work exists on the modelling of carbon isotope fractionation (e.g. Clayton 1991; Cramer et al. 1998; Yu and Semprini 2004), the explicit treatment of chlorine isotopes has become of interest only more recently, corresponding to advances in chlorine CSIA methods.

As discussed in Section 2.3, both degradation and physical processes lead to detectable isotope fractionation. Thus, a comprehensive modeling approach needs to take both processes into account. Degradation effects stem from the relative differences of reaction

rates involving heavy and light Cl isotopes. Similarly, diffusive effects are caused by the relative effects of heavy and light Cl isotopes on diffusive transport. Sorption effects stem from the relative tendency of compounds with heavy or light Cl isotopes to adsorb onto or desorb from the matric surfaces of porous media.

The behaviour of concentration C of a given species γ_i (e.g., a given isotopocule or isotopologue) can be described by the convection-diffusion-degradation equation:

$$\frac{\partial(\varepsilon C_{\gamma_i})}{\partial t} = \nabla \cdot (D_{\gamma_i} \nabla C_{\gamma_i}) - \vec{v} \cdot \nabla C_{\gamma_i} + \left[\frac{\partial C_{\gamma_i}}{\partial t}\right]_{\text{reactions}} + Q_{s,\gamma_i} \tag{2.10}$$

where D is the diffusion coefficient; ε, porosity; $\vec{v}$, the advective velocity; and Q_s, a source term. Here, the subscript i is used to refer to a single species.

2.5.2. Chemical and physical processes

Degradation is often the primary cause of isotopic fractionation in groundwater contaminants (Barth et al. 2002; Abe and Hunkeler 2006). Degradation will generally result in relative isotopic enrichment in the parent compound and relative isotopic depletion in the daughter compound due to heavier species being degraded more slowly than lighter ones. To illustrate, consider a simple case where compound A is degraded to stable compound B, and where each compound has a light (A_L and B_L) and a heavy (A_H and B_H) species. If the reactions

$$A_H \xrightarrow{k_H} B_H \tag{2.11a}$$

$$A_L \xrightarrow{k_L} B_L \tag{2.11b}$$

where k_H and k_L denote the reaction rates, are possible, then compound A will become enriched and B depleted if $k_L > k_H$. In practice, this condition is nearly always true because bonds with heavier isotopes generally have lower energy levels and consequently higher activation energies for bond cleavage.

As noted above, when chlorine is considered, more than two isotopocules or isotopologues may be present in non-negligible quantities (e.g. PCE, Figure S1 in supporting information Appendix A). There may also be multiple isotopocules to which a parent isotopocule can be degraded. Furthermore, compounds of interest may be both parent and daughter compounds in different reactions. These considerations necessitate a more rigorous mathematical definition of the mechanism for fractionation stemming from degradation (i.e., the $\left[\partial C_{\gamma_i}/\partial t\right]_{\text{reactions}}$ term in Equation (2.10)).

To date, investigations involving modelling of isotopic fractionation in chlorinated compounds have focused on chlorinated ethenes (Table 2.5). Numata et al. (2002a) presented

Table 2.5.: Studies that have modelled isotopic fractionation of chlorine in groundwater contaminants. "*(ind.)*" denotes independent modelling of multiple elements. * indicates that a correction factor was used.

Level of modelling	Molecules	Secondary effects?	Diffusion effects?	Reference
isotope, Cl	PCE, TCE	no	no	Numata et al. (2002a)
isotope, Cl/C *(ind.)*	PCE, TCE, *cis*-1,2-DCE, VC	no	no	Hunkeler et al. (2009)
isotopologue, Cl/C *(ind.)*	PCE, TCE, *cis*-1,2-DCE, VC	no	no	Hunkeler et al. (2009)
isotopologue, Cl/C	TCE, *cis*-1,2-DCE, VC	no	no	Jin et al. (2014)
isotope, Cl/C *(ind.)*	PCE, TCE, *cis*-1,2-DCE, VC	yes*	no	Höhener (2016)
isotopologue, Cl/C/H *(ind.)*	TCE, *cis*-1,2-DCE, VC	yes	no	van Breukelen et al. (2017)
isotopologue, Cl/C *(ind.)*	PCE, TCE, *cis*-1,2-DCE	yes	no	Badin et al. (2018)
isotopomer, Cl/C	PCE, TCE, *cis*-1,2-DCE	yes	no	Badin et al. (2018)
isotopologue, Cl/C	PCE, TCE, *cis*-1,2-DCE	yes	$D \propto \mu_r^{-1/2}$	Halloran et al. (2019)

the first modelling study for chlorine isotope fractionation using the Rayleigh equation (Equation (2.7)).This equation holds for a first order degradation in a system without transport, but for more complex systems error may be introduced in using it (Abe and Hunkeler 2006).

Further progress in Cl isotope fractionation modelling was made by Hunkeler et al. (2009), who described a modelling scheme for Cl isotopologues of chlorinated ethenes and another for simplified "light" and "heavy" molecules. The models included a single kinetic isotope effect for Cl and could be combined with similar models of C isotopologues, evaluated in parallel, to produce $\delta^{37}Cl/\delta^{13}C$ plots (e.g. Wanner et al. 2016). Later, van Breukelen et al. (2017) used the independent isotopologue approach of Hunkeler et al. (2009) for Cl while also introducing δ^2H modelling and Monod kinetics (Kompala et al. 1984). Crucially, this study determined position-specific isotope enrichment factors in the model based on experimental data from Kuder et al. (2013).

Jin et al. (2013) developed a model that considered the four isotopically different combinations of Cl-C bonds and the differential rates at which each would be cleaved. This work was the first that considered Cl and C isotopes as interdependent. The authors used data from Aeppli et al. (2009) to show how their combined modelling method could describe $\delta^{13}C$ trends better than the separate C/Cl isotopologue model of Hunkeler et al. (2009).

Recognising the practical aspects of independent isotope-level modelling, as well as the need for more detail to account for relative molecular positions of isotopes, Höhener (2016) presented a correction factor to the isotope model of Hunkeler et al. (2009) based on the results of Cretnik et al. (2014). This "Cretnik" correction factor accounted for the fact that in the degradation step TCE $\rightarrow$ *cis*-1,2-DCE, only one position can be reactive.

Badin et al. (2018) proposed a generalised model, including secondary isotope effects, for

degradation-induced fractionation for a given isotopocule i of compound γ in the degradation sequence $\gamma - 1 \rightarrow \gamma \rightarrow \gamma + 1$:

$$\left[\frac{\partial C_{\gamma_i}}{\partial t}\right]_{\text{reactions}} = \left[\sum_{h=1}^{n_{\text{iso}}^{\gamma-1}} \boldsymbol{\kappa}_{h,i}^{\gamma-1\rightarrow\gamma} R_{\gamma-1} \frac{C_{(\gamma-1)_h}}{C_{(\gamma-1)}}\right] - \left[\sum_{j=1}^{n_{\text{iso}}^{\gamma+1}} \boldsymbol{\kappa}_{i,j}^{\gamma\rightarrow\gamma+1}\right] R_\gamma \frac{C_{\gamma_i}}{C_\gamma} \tag{2.12}$$

Here, R is the overall reaction rate, while $n_{iso}^{\gamma-1}$ and $n_{iso}^{\gamma+1}$ are the total number of isotopocules of compounds $\gamma - 1$ and $\gamma + 1$, respectively. The most critical parts of this equation are the $\boldsymbol{\kappa}$ matrices, which describe the difference in reaction rates arising from isotopic effects. The first term in the right side of Equation (2.12) describes production of isotopolocule γ_i from parent species, while the second term describes its degradation.

Halloran et al. (2019) presented an isotopologue-level version of this model, noting that for chlorinated ethenes this would reduce the number of modelled species from $2^{n_C}2^{n_{Cl}}$ to $(n_C + 1)(n_{Cl} + 1)$ (where n_C and n_{Cl} are the number of carbon and chlorine atoms in the molecule) when both Cl and C isotopes are considered concurrently.

The $\boldsymbol{\kappa}$ matrices integrate primary and secondary kinetic isotope effects in terms of apparent kinetic isotope effects (AKIEs), A. The apparent kinetic isotope effect can be evaluated from measured enrichment factors (Elsner et al. 2005):

$$A = \frac{1}{1 + z\varepsilon_r/1000} \tag{2.13}$$

where z is the number of indistinguishable reactive sites. The primary AKIE, $A_{Cl,p}$, and secondary AKIE, $A_{Cl,s}$, are used in the definition of $\boldsymbol{\kappa}$ matrices for degradation of compound γ to compound $\gamma + 1$. At the isotopocule level (i.e., all isotopomers of all possible isotopologues), considering both Cl and C isotopes, this matrix (see Equation (3) in Badin et al. 2018) can be defined in a generalised way that is not specific to chlorinated ethenes.

For isotopologues of chlorinated ethenes, chlorine and carbon isotopes can be considered separately and the matrix for Cl be evaluated (refer to Equation (7) in Badin et al. (2018)).

These matrices are generally sparse due to the limited number of daughter isotopologues for a given parent isotopocule. When considering isotopologues rather than isotopocules (Equation (3) in Badin et al. 2018)), these matrices reduce in size considerably (e.g., from 64×32 to 15×12 for PCE $\rightarrow$ TCE) and have been evaluated explicitly for degradation of chlorinated ethenes (Halloran et al. 2019).

In practical terms, the only cases where isotopocule-level models would be needed instead are those where significantly different secondary isotopic effects occur at different non-reacting positions (Badin et al. 2018). However, this may not necessarily be true for other compounds. Future laboratory investigations of secondary isotope effects using NMR (e.g.

Chan et al. 2010) or other tools may improve our understanding of these processes and the necessity of modelling them explicitly at the isotopocule or isotopologue level.

The degree to which diffusion contributes to isotopic fractionation is a current topic of interest (Wanner and Hunkeler 2019). Jin et al. (2014) performed laboratory experiments of *cis*-1,2-DCE and TCE in an agar gel, obtaining values of $\beta = 0.088 \pm 0.015$ for *cis*-1,2-DCE and $\beta = 0.043 \pm 0.008$ for TCE (see Equation (2.9)). Wanner and Hunkeler (2015) used a modified Stokes diffusion cell to measure diffusion coefficients of 1,2-DCA and TCE. They obtained values of $\beta = 0.031 \pm 0.002$ for 1,2-DCA and 0.024 ± 0.002 for TCE. With respect to modelling, only one study (Halloran et al. 2019) thus far has combined diffusion and degradation effects.

The limited amount of experimental studies on chlorine diffusive fractionation make it difficult to draw broad conclusions. For example, it is not yet known whether there are scale effects on diffusive fractionation in porous media. Nonetheless, it appears that $\beta = 1/2$ is not valid for the studied compounds and is unlikely to be valid for other similar compounds of concern here (e.g. PCE, TCA). In future modelling studies, it is therefore advisable to model diffusive fractionation with empirical β values (Jin et al. 2014; Wanner and Hunkeler 2015), or, ideally, to allow β to vary over some reasonable range when performing parameter optimization.

Finally, for sorption-induced fractionation, there have been modelling studies on carbon, but nothing yet on chlorine. For carbon, Slater et al. (2000) found that no significant fractionation effects were present for several compounds in equilibrium sorption with graphite and activated carbon. It is known that sorption is dependent on pH, salinity, temperature, and other factors (e.g. Michot 1991; Oh et al. 2016) that are often difficult to constrain in field studies. Therefore, it is expected that future laboratory studies will provide the next advances in this domain.

In practical terms, modelling of sorption effects can be implemented by including additional adsorbed (immobile) isotopologues or isotopocules in a model which act as sources (the Q_s term in Equation (2.10)) of the individual isotopologues or isotopocules. For each isotopologue, the *Freundlich* isotherm (e.g., Dries et al. 2007) could be used to describe the equilibrium mass of the adsorbed material (m_{sorbed}):

$$m_{\text{sorbed}} = K_F C^{1/n_F} \tag{2.14}$$

where K_F is the *Freundlich* sorption capacity, which may depend on the isotopologue's mass, and n is an empirically-determined constant. Other models, such as the *Langmuir* isotherm could also be used, but in the absence of empirical data, constraining sorption processes with as few parameters as possible is advantageous.

2.6. Conclusions and outlook

As this review has shown, complementing carbon isotope data with chlorine isotope data has the potential to greatly improve our understanding of the fate of chlorinated contaminants in the subsurface. Additional efforts are needed to overcome the analytical challenges and lack of isotope fractionation factors in order to tap into this potential and further establish chlorine CSIA as routine method in the assessment of contaminated sites. In particular, there is an urgent need for a reliable method of producing isotopically different, compound-specific sets of reference standards.

While considerable progress has been made in δ^{37}Cl measurement methods and chlorine isotope fractionation process understanding, there remain several knowledge gaps. Further progress in filling these gaps will continue to improve and widen the applicability of chlorine CSIA.

While recent work on diffusion (Wanner and Hunkeler 2019) has shown its isotope effect to be generally weaker than previously thought, very few measurements (Jin et al. 2014; Wanner and Hunkeler 2015) of these effects have been made for chlorinated hydrocarbons. As back-diffusion (Parker et al. 2008) is a widely observed phenomenon at contaminated sites with aquifer-aquitard interfaces, further investigation of diffusion isotope effects in other chlorinated hydrocarbons is needed. Furthermore, as noted, isotope effects due to sorption have not yet been reliably measured. Adsorption and desorption processes occur in many low-permeability hydrogeological units such as clay-rich sediments. Measurements of sorption isotope effects are therefore crucial for comprehensive assessment of contaminated sites. Additionally, further measurements of isotope effects during degradation by various biotic or abiotic mechanisms are always welcome.

There also remain open questions related to modelling chlorine isotope fractionation. As few such studies currently exist (Table 2.5), the value of chlorine CSIA data in informing models – which may drive remediation decisions – is currently not well understood. There is also a need to understand the level of model complexity in modelling isotope effects that is required to make accurate assessments of degradation and transport of chlorinated hydrocarbons. Efforts to improve the modelling of chlorine isotope fractionation processes will be most effective when combined with data from laboratory and field studies. Additionally, there is significant scope for the expansion of chlorine CSIA to other, larger compounds, especially those with few chlorine atoms. Here, the applicability of chlorine CSIA will be pronounced as carbon isotope fractionation is less significant in larger organic molecules.

Finally, there is clearly major potential for further applications of chlorine CSIA to evaluate degradation in field sites. After all, this is one of the main motivations for the development of

the laboratory and modelling techniques discussed in depth here. In particular, chlorine CSIA in conjunction with carbon CSIA will surely see further applications in the differentiation of both sources and processes.

Chlorine CSIA is a relatively new tool for the assessment of groundwater contamination by chlorinated hydrocarbons. Research and development in this field is moving forward with continued progress on laboratory techniques, field applications, modelling approaches, and fundamental understanding.

Acknowledgments

The authors acknowledge the Swiss National Science Foundation (SNSF) (grant number: 166233, http://p3.snf.ch/Project-166233) for their financial support.

3. A design of experiments to optimize solid-phase microextraction for compound-specific chlorine isotope analysis of chlorinated ethenes

Jeremy Zimmermann[1,a], Ouassim M. Boukaroum[1,2,a], Daniel Hunkeler[1]
In preparation

Abstract

Compound-specific chlorine isotope analysis is a powerful tool to track the origin and fate of chlorinated ethenes in the environment. The aim of this study was to develop and evaluate a simple and easily automated method for lowering method detection limits of chlorine isotope ratio measurements to the sub-µg L^{-1} range for tetrachloroethene (PCE) and trichloroethene (TCE) in aqueous solution. We extracted target compounds using a novel headspace solid-phase microextraction (SPME) technique, SPME Arrow, which is characterized by a higher phase volume compared to classical SPME. Compounds were then separated and analyzed with gas chromatography hyphenated to quadrupole mass spectrometry. Using a modeled response surface, we optimized SPME parameters to achieve maximum intensity. Measured intensity values were in good agreement with predicted values. Mass spectrometric parameters and chlorine isotope ratio calculation schemes were also investigated and optimized. Any chlorine isotope fractionation was accounted for through a two-point calibration with externally referenced standards. Precise δ^{37}Cl measurements

[1]Centre for Hydrogeology and Geothermics, University of Neuchâtel, Rue Emile-Argand 11, 2000 Neuchâtel, Switzerland
[2]Laboratoire de Chimie Environnement, Aix-Marseille University, 3 Place Victor Hugo, 13331 Marseille, France

[a]These authors contributed equally to the work

(standard deviations below 0.5‰) were achieved for concentrations of 0.4 µg L^{-1} (PCE) to 0.8 µg L^{-1} (TCE).

3.1. Introduction

The chlorinated ethenes trichloroethene (TCE) and tetrachloroethene/perchloroethene (PCE) are volatile organic compounds (VOC) that have found extensive use as industrial degreasing and dry-cleaning agents. Due to their persistence and often improper disposal, they have become widespread soil and groundwater contaminants. As they are toxic and known or suspected to be carcinogenic, their regulatory limits in groundwater are in the µg L^{-1} range.

Engineered remediation efforts that aim to restore the affected aquifers to conditions below the regulatory limits are unfeasible at many sites contaminated with chlorinated hydrocarbons (Kent and Mosquera 2001). Even if the source of the chlorinated ethene contamination has been identified and contained, back-diffusion from low-permeability layers beyond the source zone can lead to persistent contaminant plumes (Liu and Ball 2002; Chapman and Parker 2005; Tatti et al. 2016).

Monitored natural attenuation is an in situ technique that relies on naturally occurring processes to decrease the concentration levels of contaminants. Under predominantly anaerobic conditions, PCE and TCE may degrade biotically or abiotically to toxic or non-toxic degradation products as a function of redox conditions and the availability of organohalide-respiring bacteria or certain minerals.

To determine which pathway is taken at a field site, a tool is required that does not solely rely on concentration measurements or the monitoring for characteristic degradation products, as these may be unspecific, highly volatile or not captured by the sampling method. Compound-specific isotope analysis (CSIA) has proven to be an integral tool in the assessment of sites contaminated by chlorinated hydrocarbons. Here, the isotopic ratio of one ($\delta^{13}C$) or more elements ($\delta^{37}Cl$, $\delta^{2}H$) of the parent compounds and/or degradation products is monitored. Chemical bonds involving the heavier isotope are more stable than those involving the light isotope, leading to a heavy isotope enrichment in the residual compound and an isotope depletion in the degradation products. CSIA is applied to identify different degradation mechanisms, to quantify the degree of degradation, and to differentiate contaminant sources (Schmidt and Jochmann 2012; Wiegert et al. 2012; Ojeda et al. 2019a; Zimmermann et al. 2020).

The dual carbon-chlorine isotope approach allows to better constrain degradation mecha-

nisms. The ratio of isotopic enrichment in both elements over time or space, the dual element isotope slope, is more specific to the reaction pathway and less affected by non-reactive processes than the isotopic enrichment observed in only one element of the compound in question.

As degradation should and will invariably lead to low contaminant concentrations, measuring the chlorine isotope ratio of the contaminant may prove challenging, since the analytical sensitivity for isotope analysis is generally inferior to that of simple quantification. It is necessary to concentrate the contaminant, while maintaining a high analytical precision in light of the generally smaller magnitude of chlorine isotope fractionation compared to carbon isotope fractionation. Different methods are available for extraction and concentration, including liquid-liquid extraction, headspace (HS) extraction, purge & trap concentration, stir bar sorptive extraction (SBSE) and solid-phase microextraction (SPME).

To simplify compound-specific chlorine isotope analysis of chlorinated VOC, an online method is preferable. Here, extraction, separation and mass spectrometric analysis are directly coupled. Gas chromatography (GC) is a suitable method for separation of VOC. Mass spectrometers that can be directly coupled to GC are isotope ratio mass spectrometers (IRMS) and quadrupole mass spectrometers (qMS). As opposed to IRMS, which requires dedicated detector configurations for each compound, a qMS offers a versatile possibility to detect a wide range of mass to charge (m/z) ratios of different compounds and is commonly available in laboratories. However, at least two isotopically differing molecularly identical reference standards are necessary due to an often-observed mismatch between the measured difference in δ^{37}Cl values and the known δ^{37}Cl difference (Bernstein et al. 2011; Ebert et al. 2017), which is caused by the single-detector configuration of qMS. The simplicity of qMS also comes at the expense of an inferior sensitivity compared to IRMS as well as a lower precision. The latter can be improved by increasing the number of repeat measurements.

Our objective was to lower method detection limits for compound-specific chlorine isotope analysis of PCE and TCE to the sub-microgram per liter range in aqueous samples. An efficient extraction technique is needed to reach sufficiently low detection limits. We chose SPME as it is a solvent-free, easily automated method that can be retrofitted to many autosampler systems. SPME was developed by Belardi and Pawliszyn (1989) and uses a sorptive fiber that can be either immersed directly into the aqueous sample, or, preferably for VOC analysis, exposed to the headspace. When the fiber is exposed, compounds will be sorbed and retained. Compounds are then thermally desorbed from the fiber by heating. Instead of classical SPME, we used the recently developed SPME Arrow system. Here, the sorptive phase has been coated onto a solid stainless steel core, which promises improved

mechanical robustness and a six times higher sorptive phase volume (Kremser et al. 2016). The improvement in sorptive phase volume is critical for measuring chlorine isotope ratios with qMS. The use of SPME concentration for CSIA of VOC has so far only been reported using an IRMS, for carbon isotopes (Hunkeler and Aravena 2000; Zwank et al. 2005b; Heckel et al. 2017), chlorine isotopes (Shouakar-Stash et al. 2009) and hydrogen isotopes (Palau et al. 2017b). The coupling of SPME to GC-qMS for compound-specific chlorine isotope analysis of VOC is a novel use of this technique.

Analytical variables that may influence headspace SPME efficiency are, e.g., the type of fiber, phase ratios, sample agitation, sample temperature and extraction time. Signal intensity is also affected by the peak shape, which is determined by GC split ratio and desorption temperature. To reach our objective of lowering detection limits for compound-specific chlorine isotope analysis, we first determined the mass spectrometric parameters best-suited for chlorine isotope measurements, and then optimized SPME parameters to improve peak shape and intensity. Due to the high number of factors that influence SPME efficiency, and the possible interactions between them, a multivariable optimization is justified (Marrubini et al. 2020). We applied a design of experiments (DoE) or experimental design approach (Leardi 2009) to evaluate and optimize these factors. We then evaluated precision, trueness and isotopic linearity for chlorine isotope ratio measurements and determined method detection limits (MDL).

3.2. Material and methods

3.2.1. Chemicals and standard preparation

Pure phase TCE and PCE standards that had been isotopically referenced to standard mean ocean chloride (SMOC) were obtained. For TCE, standards TCE EIL-1 ($\delta^{37}Cl = +3.05‰$) and TCE EIL-2 ($\delta^{37}Cl = -2.7‰$), and for PCE, standards PCE EIL-1 ($\delta^{37}Cl = +0.3‰$) and PCE EIL-2 ($\delta^{37}Cl = -2.5‰$) were used. Stock solutions were prepared gravimetrically in methanol (HPLC grade, purity $\geq 99.8\%$, Fisher Chemical). All aqueous solutions were prepared in ultrapure water from a Merck Millipore Direct-Q 3 water purification system. Intermediate aqueous solutions were prepared by diluting defined volumes of methanol stock solutions in 42 mL vials filled with water and capped with PTFE-coated silicone septa and screw caps without headspace. For static headspace and SPME headspace analysis, intermediate solutions were further diluted in 20 mL vials to obtain a liquid-phase volume of exactly 15 mL, leaving 5 mL of headspace, and capped with PTFE-coated butyl rubber

septa and magnetic screw caps. Nitrogen ($\geq$ 99.995% purity) and helium ($\geq$ 99.9999% purity) were purchased from Carbagas.

3.2.2. Instrumentation

For sample handling, a PAL3 Autosampler (CTC Analytics AG) with robotic tool change (RTC) was used. This allowed for both static headspace analysis using a syringe and SPME Arrow headspace analysis. The autosampler was equipped with a heated agitator (incubator) for headspace equilibration (5 minutes at 600 rpm), a heated vortex agitator for SPME (600 rpm), and an SPME fiber-conditioning module. The latter serves to condition SPME fibers and eliminate carryover between injections, achieving this by heating the fiber in an inert gas (N_2) flow to the same temperature that is also used for desorption.

SPME Arrow fibers (CTC Analytics AG) with an outside diameter of 1.1 mm, coated with a sorptive phase of 120 µm thickness and 20 mm length, were used. A carboxen (CAR) wide range (WR) polydimethylsiloxane (PDMS) fiber was used because preliminary tests showed that it was the only sorptive phase that considerably improved extraction efficiency over static headspace analysis. This is consistent with previous studies where the mixed mode CAR/PDMS phase SPME has been shown to exhibit a superior extraction efficiency for chlorinated VOC, e.g., Popp and Paschke (1997), Page and Lacroix (2000), Zwank et al. (2003), Palau et al. (2007), Wejnerowska and Gaca (2008), and Ziv-El et al. (2014)

For separation, we used an Agilent 7890B GC, equipped with an HP-5MS capillary column (30 m $\times$ 0.25 mm, 0.25 µm, Agilent J & W) and deactivated fused-silica pre-column (3 m $\times$ 0.25 mm). Injection took place through a split/splitless inlet, using a tapered liner with a volume of 900 µL for static headspace injections and a straight liner with an inside diameter of 1.3 mm and 52 µL volume for SPME injections. Carrier gas was helium at a constant flow of 1.2 mL min^{-1}. The GC temperature program was as follows: Initial temperature of 40 °C, held for 2 minutes, 40 °C to 85 °C at 15 °C min^{-1}, then 85 °C to 150 °C at 30 °C min^{-1}, with a final hold time of 2 minutes, for a total run time of 8.27 minutes. We determined through preliminary tests that a one-minute desorption at a split ratio of 1:5 produces the optimum peak shape for stable chlorine isotope analysis during desorption from SPME fibers (Figure S1 in supporting information Appendix B), with splitless injection leading to pronounced peak tailing.

The GC was coupled to an Agilent 5977B qMS equipped with a high-efficiency source (HES) for electron ionization (EI) at 70 eV. The source was kept at a temperature of 230 °C and the quadrupole at 150 °C. During our research we had determined an optimum dwell time of 30 ms for each m/z for measuring chlorine isotope ratios in selected ion mode

(SIM). We compared the ionization efficiency of the HES with that of the standard source of an Agilent 5975C qMS coupled to an Agilent 7890A GC, using identical parameters, and found about eight times lower MDL for chlorine isotope analysis when using the HES.

Due to the lower stability of qMS compared to IRMS, each standard is analyzed eight to ten times. For static headspace analysis, 1000 µL of headspace were removed five times from two headspace vials via syringe. For SPME, however, the number of vials had to be increased while reducing the number of extractions per vial. This was due to the highly efficient extraction, which caused a strongly decreasing intensity for multiple extractions from the same vial.

3.2.3. Calculation of chlorine isotope ratios

Chlorine isotope ratios R, defined according to Equation (3.1) as the ratio of ^{37}Cl to ^{35}Cl abundance, can be calculated for molecules from intensities I of certain molecular or fragment ions measured in SIM (Sakaguchi-Söder et al. 2007). This is made possible by the high natural abundance of the heavy ^{37}Cl isotope of 24.2%. The intensities were measured as peak areas, which were calculated with the software Chemstation (Agilent) using default peak integration parameters. For TCE, the possible ions to be measured are m/z of 60, 62, 95, 97, 130 and 132; for PCE m/z of 59, 61, 94, 96, 129, 131, 164 and 166. Here, one of the three (TCE) or four (PCE) chlorine atoms of a compound is substituted by its heavy isotope. The chlorine isotope ratios can be calculated from the molecular ion intensities, or any of the fragment ion intensities (Elsner and Hunkeler 2008), as follows for TCE with Equation (3.2) and for PCE with Equation (3.3):

$$R = \frac{^{37}Cl}{^{35}Cl} \tag{3.1}$$

$$R_{TCE} = \frac{1}{3} \times \frac{I_{132}}{I_{130}} = \frac{1}{2} \times \frac{I_{97}}{I_{95}} = \frac{1}{1} \times \frac{I_{62}}{I_{60}} \tag{3.2}$$

$$R_{PCE} = \frac{1}{4} \times \frac{I_{166}}{I_{164}} = \frac{1}{3} \times \frac{I_{131}}{I_{129}} = \frac{1}{2} \times \frac{I_{96}}{I_{94}} = \frac{1}{1} \times \frac{I_{61}}{I_{59}} \tag{3.3}$$

Alternatively, the chlorine isotope ratios can be calculated from weighted averages of both molecular and fragment ion intensities as follows for TCE with Equation (3.4) and for PCE with Equation (3.5):

$$R_{TCE} = a \times \frac{1}{3} \times \frac{I_{132}}{I_{130}} + b \times \frac{1}{2} \times \frac{I_{97}}{I_{95}} + c \times \frac{1}{1} \times \frac{I_{62}}{I_{60}} \tag{3.4}$$

$$R_{PCE} = a\frac{1}{4} \times \frac{I_{166}}{I_{164}} + b \times \frac{1}{3} \times \frac{I_{131}}{I_{129}} + c \times \frac{1}{2} \times \frac{I_{96}}{I_{94}} + d \times \frac{1}{1} \times \frac{I_{61}}{I_{59}} \tag{3.5}$$

The weight factors a, b, c, d were calculated according to the modified multiple ion method (Jin et al. 2011), taking into account all ion intensities (see section B.1 in supporting information Appendix B). For a discussion on the validity of these equations, which are based on the assumption of a stochastic distribution of isotopes amongst isotopologues of a compound, see Zimmermann et al. (2020).

To convert a measured isotope ratio to the δ notation, it is expressed as a per mille (‰) deviation from the isotope ratio of a standard (Equation (3.6)):

$$\delta^{37}\mathrm{Cl} = \frac{R_{measured}}{R_{standard}} - 1 \qquad (‰) \tag{3.6}$$

To obtain SMOC-referenced δ^{37}Cl values from raw, instrument-specific δ values, a two-point calibration is then performed using the two SMOC-referenced standards as anchor points as explained by Bernstein et al. (2011).

3.2.4. Evaluation of mass spectrometric calculation schemes

The most precise choice of calculation method (Equations (3.2) to (3.5)) for obtaining chlorine isotope ratios of TCE and PCE was determined with static headspace analysis, by calculating the standard deviation 1σ for replicate measurements ($n = 10$) of the EIL-1 standards for TCE and PCE. The aqueous concentration of TCE or PCE was fixed at $30\,\mu g\,L^{-1}$. Headspace partitioning was improved by agitating vials for five minutes in the incubator at 60 °C. A headspace volume of 1000 µL was removed and injected at 200 °C and a split ratio of 1:20. This corresponds to 14 pmol TCE or 11 pmol PCE on column, calculated using temperature-dependent partitioning constants published by Chen et al. (2012).

3.2.5. Quantitative analysis of factors influencing SPME efficiency

We optimized the factors extraction time, extraction temperature and desorption temperature. Through preliminary tests we had determined these factors to be most sensitive in influencing the extraction efficiency and, with it, signal intensity. This is in agreement with studies performed by Dron et al. (2002), Pawliszyn (2012), and Spietelun et al. (2013). The extraction time represents the time the fiber is exposed to sample headspace in the vortex agitator. Extraction was always preceded by a five minute headspace equilibration in the incubator. The relationship between extraction temperature and efficiency for SPME

is not as straightforward as for static headspace analysis; while an increased temperature will favor headspace partition of VOC, sorption on the fiber may be negatively influenced, as it is not actively cooled. Competitive sorption on the fiber between water vapor and target compounds may also play a role. Desorption temperature is especially relevant for CAR/PDMS due to the porosity of the phase, which requires high temperatures for efficient desorption of target analytes (Wercinski 1999).

3.2.6. Performance evaluation and validation of analytical methods for chlorine isotope measurements

In order to determine the influence and interaction of these factors on signal intensity, we applied factor analysis using the design of experiments (DoE) software *Azurad 1.3.2* (Azurad SAS 2020). These factors were varied independently over the experimental domain, which is shown in Table 3.1.

Table 3.1.: Experimental domain with factors influencing SPME efficiency.

	Factor	Unit	Lower level	Upper level
X_1	Extraction time	(min)	5	25
X_2	Extraction temperature	(°C)	40	60
X_3	Desorption temperature	(°C)	200	270

The upper limit of the extraction time was chosen as to avoid excessive analysis times, considering the large number of repeat measurements necessary for chlorine isotope ratio measurements using qMS. The upper limit of desorption temperature was set below the maximum permissible temperature of 300 °C for the CAR/PDMS fiber in order to increase its lifespan.

The factor analysis was performed using PCE standard EIL-1 at 0.5 µg L^{-1} for all possible combinations of these factors, a full factorial design, which required $2^3 = 8$ measurements. The measurements were performed in random order to preclude any memory effects, and repeated twice. The response in the form of intensity was measured as the sum of the molecular ions with m/z 164 and 166 of PCE in counts per second (cps).

3.2.7. Optimization of SPME efficiency using response surface methodology

After determining the two most sensitive SPME factors from those presented in Table 3.1 using factor analysis, we used the software *Azurad 1.3.2* to apply the response surface

methodology (RSM) in order to optimize the two factors, following the example of Dron et al. (2002) for SPME optimization.

A central composite design (CCD) was used to establish different combinations of these two factors which were to be experimentally investigated. The $2^2 = 4$ combinations of the lower and upper levels of the two factors were expanded with a point at the center of the experiment domain, and four additional points, so-called axial or star points, located at axial distances α of $\sqrt{2} \sim 1.414$ from the center, hereby generating new extreme levels for both factors and ensuring a rotatable design (Figure S2 of the supporting information Appendix B). As we measured the central combination of factors twice, the total number of measurements was ten.

The dependent or response variables were the signal intensity as sum of PCE m/z 164 and 166, which was to be maximized, and the total analysis time as the sum of extraction time and GC analysis, which was to be minimized. We postulate that the responses can be described using a second-order polynomial. We validated the response surface model by comparing measured values for three randomly generated combinations of factors with those given by the response surface, the criterion being a 95% confidence interval when performing a Student's t-test.

In order to determine the optimum conditions, we combined the two response variables into a desirability function (Harrington 1965; Derringer and Suich 1980; Khoder 2011). Here, each response is transformed into a scale-free individual desirability d_i, which is assigned a value from 0 to 1 (0 to 100%). The global desirability D is then calculated from the individual desirabilities according to Equation (3.7):

$$D = (d_1 \times d_2 \times ... \times d_r)^r \tag{3.7}$$

where r is the number of responses (here: $r = 2$). Using the software *Azurad 1.3.2*, we determined the global optimum, which is characterized by a value of D close to 1 (100%).

3.2.8. Performance evaluation and validation of analytical methods for chlorine isotope measurements

In order to validate the methods for chlorine isotope measurements, we defined accuracy (trueness and precision) criteria that had to be met. The precision of chlorine isotope measurements was measured by calculating the standard deviation 1σ, which for δ^{37}Cl values had to be equal or less than 0.5‰ for at least eight repeat measurements ($n \geq 8$). Trueness of isotope measurement is usually evaluated by analyzing independently referenced standards. As in our case the referenced standards themselves serve as anchor points, we

used the calibration slope between instrument δ^{37}Cl values and SMOC δ^{37}Cl values during a measurement sequence as indicator of trueness. If these calibration slopes remain over time stable and similar for both static and SPME headspace analysis, any results obtained for measurements of samples are expected to be true. Samples are expected to isotopically fractionate in the same manner as the molecularly identical standards during extraction, separation and ionization. A statistical treatment was performed on the obtained δ^{37}Cl datasets to remove possible outliers using Dixon's Q test with a 95% confidence interval.

3.3. Results and discussion

3.3.1. Evaluation of mass spectrometric calculation schemes

The precision of chlorine isotope ratios is affected by the choice of ions that are measured (Jin et al. 2011), as fragment ions usually produce a lower intensity than the molecular ions, and a high number of ions measured simultaneously affects the stability of the single detector of a qMS. For static headspace analysis at target compound concentrations of 30 µg L^{-1}, Table 3.2 shows the measured raw chlorine isotope ratios and standard deviations 1σ of δ^{37}C values for the EIL-1 standards, and the slope between the two standards.

Table 3.2.: Comparison of evaluation methods for calculating chlorine isotope ratios from molecular and/or fragment ions of target compounds. Ratios and standard deviations 1σ for δ^{37}Cl were calculated for the EIL-1 standards ($n = 10$). The slope is the measured difference between δ^{37}Cl values of the two standards divided by the difference between reference values.

			Molecular and fragment ion method			Modified multiple ion method		
Compound	m/z ^{35}Cl	m/z ^{37}Cl	R ^{37}Cl/^{35}Cl $\pm 1\sigma$	$1\sigma\delta^{37}$Cl (‰)	Slope	R ^{37}Cl/^{35}Cl $\pm 1\sigma$	$1\sigma\delta^{37}$Cl (‰)	Slope
PCE	164	166	0.3173 ± 0.0001	0.28	1.48	0.3207 ± 0.0001	0.23	1.19
	129	131	0.3193 ± 0.0001	0.18	1.15			
	94	96	0.3239 ± 0.0002	0.68	0.75			
	59	61	0.3309 ± 0.0003	1.07	0.86			
TCE	130	132	0.3183 ± 0.0001	0.17	1.14	0.3223 ± 0.0001	0.17	1.13
	95	97	0.3233 ± 0.0001	0.34	1.08			
	60	62	0.3311 ± 0.0002	0.42	1.16			

While the different evaluation methods all lead to different raw chlorine isotope ratios, a two-point calibration using the two standards as anchor points is expected to yield true

δ^{37}Cl SMOC values for any samples isotopically bracketed by these standards (Ebert et al. 2017). For PCE, the molecular ion method using ions 164 and 166, the fragment ion method using ions 129 and 131, and the modified multiple ion method feature a precision 1σ for δ^{37}Cl values of less than 0.5‰ and are thus suitable for chlorine isotope analysis. For TCE, all evaluation schemes are sufficiently precise at this concentration. Here, the slope is close to unity and does not vary much between evaluation schemes, which is a good indicator of trueness. Chlorine isotope method detection limits for static headspace analysis were 15 µg L^{-1} for both TCE and PCE, with an isotopic linearity range ranging from 15 µg L^{-1} to 90 µg L^{-1}. This corresponds to 5.6 pmol to 33.6 pmol on column for PCE, and to 7.1 pmol to 42.4 pmol on column for TCE, calculated using temperature-dependent partitioning constants published by Chen et al. (2012) and taking into account phase ratio, injection volume and split ratio. We chose the molecular ion methods for the following SPME optimization.

3.3.2. Quantitative analysis of factors influencing SPME efficiency

The eight measurements incorporating the factors from Table 3.1 and their lower and upper levels are presented in Table 3.3.

Table 3.3.: The eight SPME measurements of the full factorial design and the experimental response as PCE intensity of the first measurement round.

Measurement	Extraction time X_1 (min)	Extraction temperature X_2 (°C)	Desorption temperature X_3 (°C)	Intensity PCE m/z 164 + 166 (10^6 cps)
1	5	40	200	7.65
2	20	40	200	11.7
3	5	60	200	7.81
4	20	60	200	10.7
5	5	40	270	14.6
6	20	40	270	12.8
7	5	60	270	8.52
8	20	60	270	12.2

In order to investigate which of the three factors is the most influential on the measured response, we plotted the results of the factor analysis in Figure 3.1. The extraction time has the most significant positive influence on response, and an increase in desorption temperature also yields a higher response. In contrast, a higher extraction temperature decreases the response. As for the interactions between factors, Figure 3.1 shows that the

response does not significantly change for combinations of these factors. They can thus be varied independently across the experimental domain.

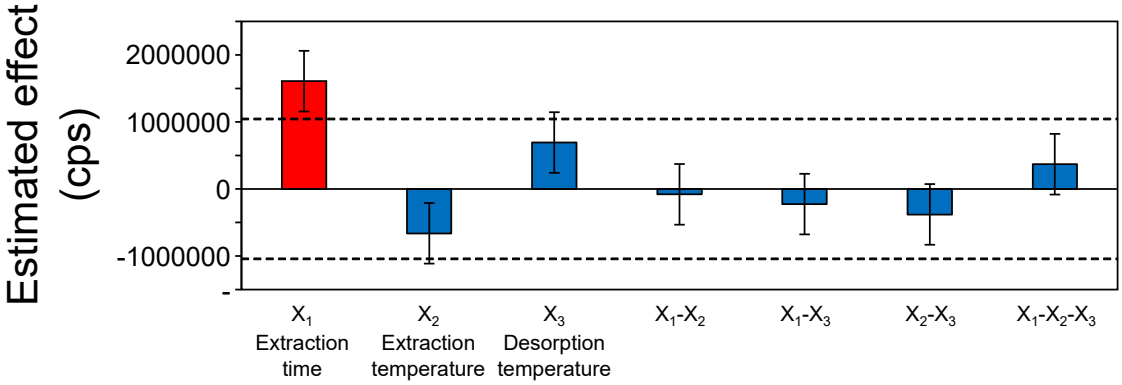

Figure 3.1.: Graphical plot of the effect of three factors on the measured response for PCE. The dashed lines represent the limits for a confidence interval of 95%, values beyond these limits indicate that a factor significantly influences response.

In addition to their effect on intensity, the effects of extraction and desorption temperature on peak shape must not be disregarded for chlorine isotope analysis. Figure 3.2 shows the chromatograms obtained for a PCE concentration of 0.5 µg L^{-1} when varying the extraction temperature. While a higher extraction temperature slightly improves peak shape, the effect is not very pronounced. At a higher desorption temperature, however, tailing is strongly reduced (Figure 3.3).

3.3.3. Optimization of SPME efficiency using response surface methodology

The two factors extraction time and desorption temperature were shown in the preceding section to be the most significant factors that influence intensity for SPME. These two factors are now varied using parameters from the CCD and the response measured in order to generate the response surface. The CCD of the two factors is shown in detail in Figure S2 of the supporting information Appendix B. Table 3.4 shows the two responses, the intensities and the analysis times, that were measured for the nine different combinations of factors. The validation of the response surface using three randomized measurements is shown in Table S1 of the supporting information Appendix B.

The three-dimensional response surface for the intensity is shown in Figure 3.4. As can be seen, the intensity is positively correlated with extraction time, while desorption temperature shows little influence on intensity. A maximum intensity is obtained for an extraction time of 25 minutes and a desorption temperature of 280 °C. The intensity reaches a plateau

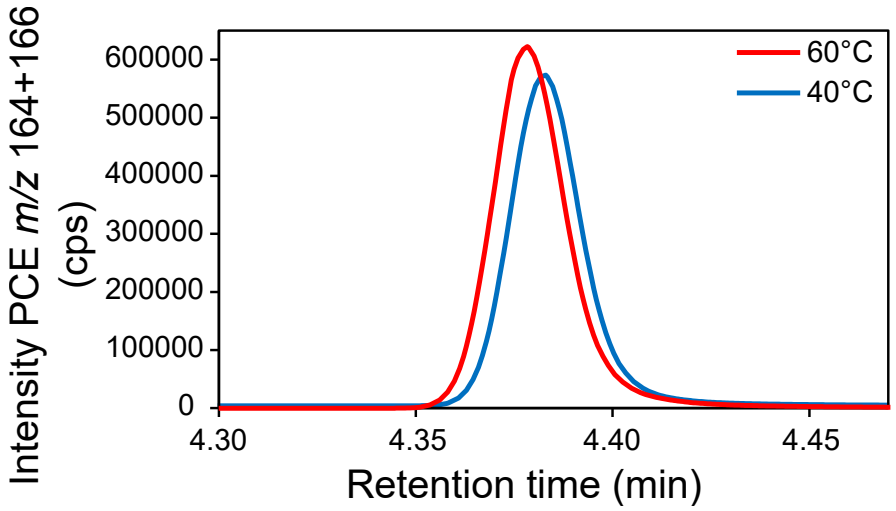

Figure 3.2.: Comparison between peak shapes obtained for extraction temperatures of 40 °C or 60 °C for a PCE concentration of 0.5 µg L^{-1}. Desorption temperature of 270 °C and extraction time of 15 min.

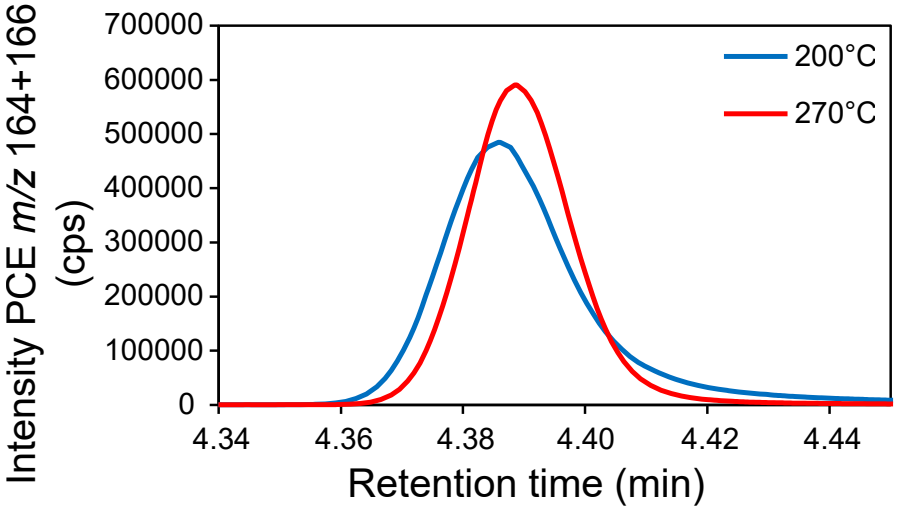

Figure 3.3.: Comparison between peak shapes obtained for desorption temperatures of 200 °C or 270 °C for a PCE concentration of 0.5 µg L^{-1}. Extraction temperature of 40 °C and extraction time of 15 min.

Table 3.4.: Experimental domain established by CCD and measured responses for SPME of PCE at $0.5\,\mu g\,L^{-1}$.

Measurement	Factors		Responses	
	Extraction time X_1 (min)	Desorption temperature X_2 (°C)	Intensity m/z 164 + 166 (10^6 cps)	Analysis time (min)
1	5	200	7.04	20
2	25	200	12.1	40
3	5	270	7.01	20
4	25	270	13.3	40
5	0.86	235	3.60	16
6	29.14	235	12.5	44
7	15	185.50	10.5	30
8	15	284.50	11.5	30
9-1 (Center)	15	235	12.1	30
9-2 (Center)	15	235	10.7	30

after 25 minutes, which may be an indication that SPME sorption equilibrium has been reached for PCE at the given concentration.

Two issues become apparent when relying solely on intensity as a response for chlorine isotope analysis. Firstly, the response surface only represents the peak area, but a good peak shape must also be ensured, which requires high desorption temperatures. Secondly, an extraction time of 25 minutes is not feasible for chlorine isotope analysis due to the necessary number of repeat measurements. The latter response is hence the focus of the next optimization step.

To this end, we simultaneously optimized intensity and total analysis time. While investigating isotopic linearity limits using static headspace analysis, we determined that the detector requires a minimum intensity of 6×10^6 cps for accurate chlorine isotope analysis of PCE. We assigned the highest desirability of 100% (Equation (3.7)) to a total analysis time of 20 minutes (Table 3.5). This includes SPME time, desorption time of one minute, GC run time of 8.27 minutes and fiber conditioning time of three minutes. The five minute headspace equilibration takes place during the GC run time and does not influence analysis time. The corresponding desirability response surface for the constraints is shown in Figure 3.5. A maximum global desirability that still ensures the minimum intensity for accurate chlorine isotope analysis can be achieved for an extraction time of 4.9 minutes (Table 3.5).

With an extraction time of about five minutes, a total analysis time of 20 minutes for one injection can be achieved, taking into account that GC run time and preparation of the subsequent sample can overlap. The global desirability is not strongly influenced by

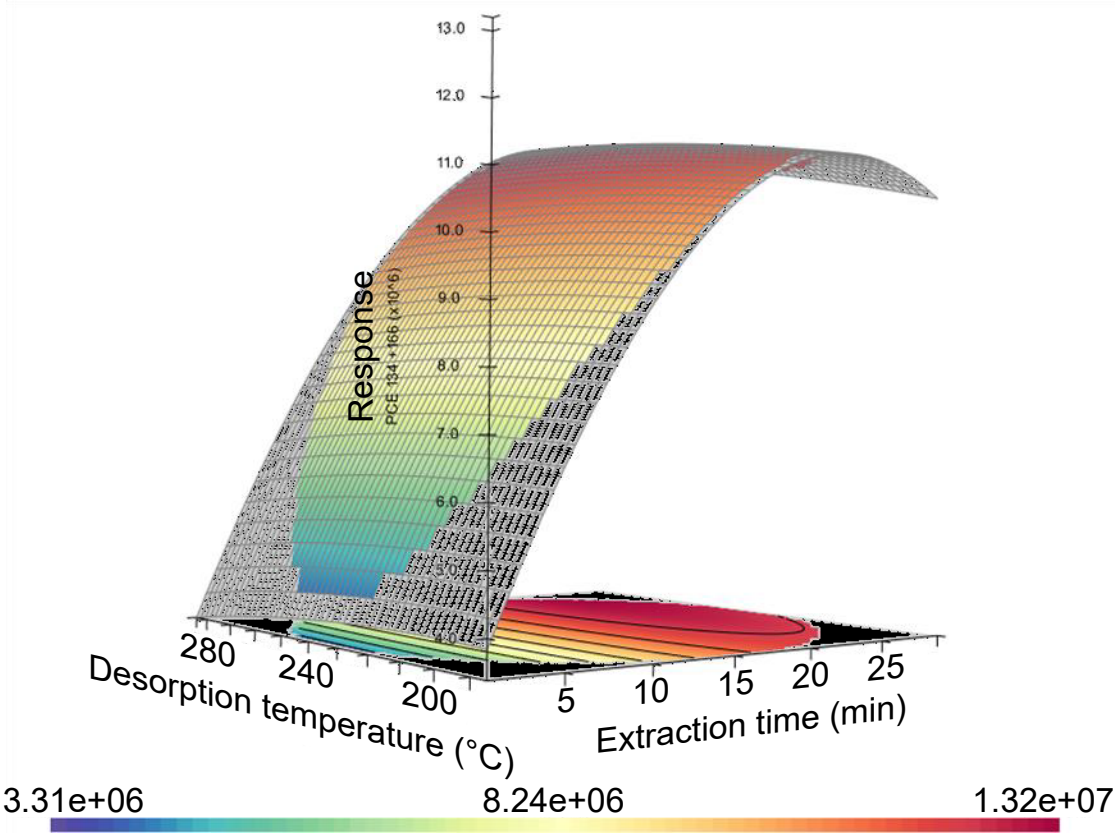

Figure 3.4.: Three-dimensional response surface for PCE intensity as a function of the factors desorption temperature and extraction time at an extraction temperature of 40 °C.

Table 3.5.: Factors and responses of the desirability function.

Factors for achieving maximum global desirability			Responses assigned to 100% individual desirability		
Factor	Unit	Value	Response	Unit	Value
Extraction time	(min)	4.9	Intensity PCE m/z 164 + 166	(cps)	6×10^6
Desorption temperature	(°C)	215	Total analysis time	(min)	20

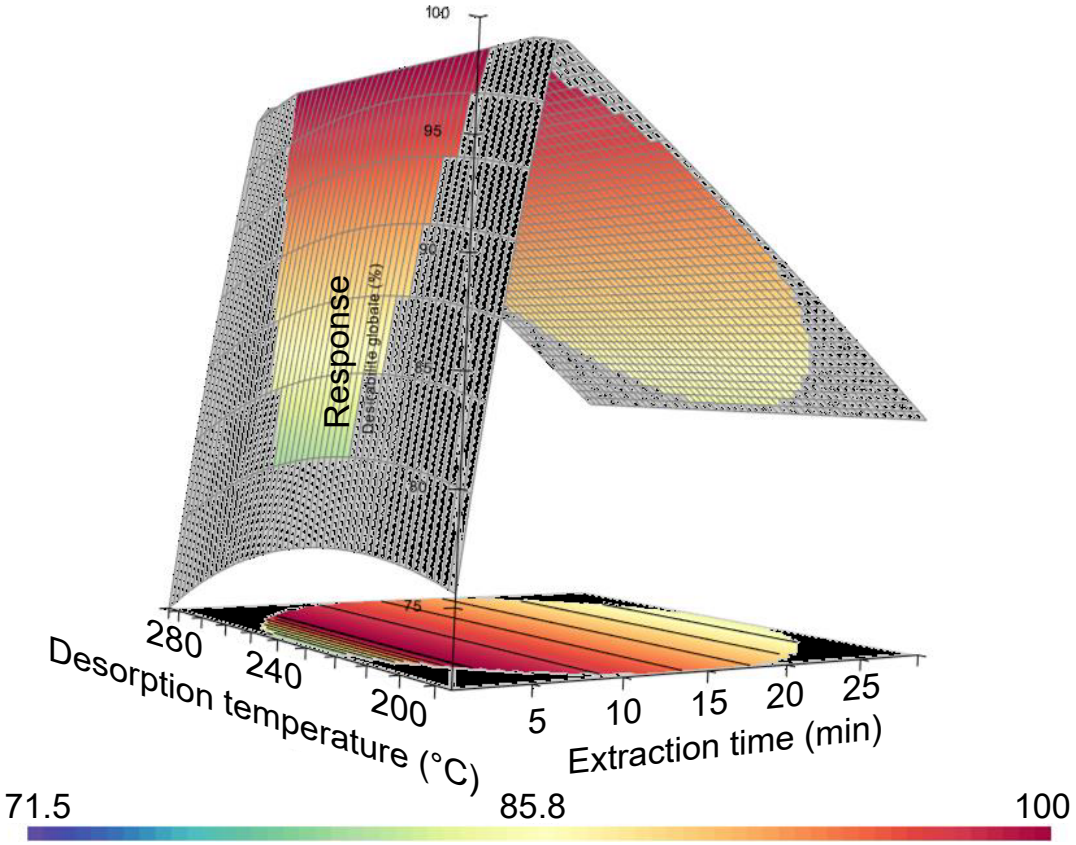

Figure 3.5.: Three-dimensional response surface for PCE SPME desirability as a function of the factors desorption temperature and extraction time at an extraction temperature of 40 °C.

desorption temperature, which can hence be further optimized in regards to peak shape without compromising analysis time. As static headspace analysis was shown to produce accurate results for chlorine isotope analysis of TCE (Table 3.2), we also applied the same optimized SPME parameters, a five minute headspace equilibration at 40 °C, five minute SPME at 40 °C, and a desorption at 270 °C for one minute at a split ratio of 1:5, for the analysis of TCE.

3.3.4. Performance evaluation of the optimized HS SPME Arrow GC-qMS method

We measured chlorine isotope ratios, slopes between standards and precisions for five concentration levels ranging from 0.07 µg L^{-1} to 2.24 µg L^{-1} for both PCE and TCE (Table 3.6). In order to achieve ten measurements, only one extraction per vial for PCE and two per vial for TCE were possible, due to the efficient extraction. This higher sample amount needs to be considered when taking samples from a field site.

Table 3.6.: Performance evaluation for SPME extraction at optimized parameters. Ratios and standard deviations 1σ for $\delta^{37}Cl$ were calculated for the EIL-1 standards. The slope is the measured difference between $\delta^{37}Cl$ values of the two standards divided by the difference between reference values.

Compound	Concentration (µg L^{-1})	$R\ ^{37}Cl/^{37}Cl \pm 1\sigma$	$1\sigma\delta^{37}Cl$ (‰)	Slope
PCE	0.07	0.3187 ± 0.0001	0.44	1.02
	0.37	0.3174 ± 0.0001	0.32	0.91
	0.75	0.3161 ± 0.0001	0.50	0.81
	1.50	0.3144 ± 0.0001	0.20	0.88
	2.24	0.3121 ± 0.0005	2.03	0.78
TCE	0.07	0.3199 ± 0.0008	3.56	0.65
	0.37	0.3190 ± 0.0002	0.48	1.31
	0.75	0.3186 ± 0.0002	0.47	1.02
	1.50	0.3193 ± 0.0001	0.33	1.01
	2.24	0.3191 ± 0.0001	0.22	0.98

The results in Table 3.6 show a clear isotopic enrichment trend for PCE with decreasing concentration. The precision 1σ for $\delta^{37}Cl \leq 0.5$‰ and the slope close to unity indicate that the SPME method can be applied for PCE concentrations of 0.07 µg L^{-1}. However, as the raw chlorine isotope ratio appears to be strongly dependent on signal intensity, concentrations of standards and samples have to be closely matched. As a consequence,

matrix effects must be considered and standard solutions matrix-matched to the samples to compensate for matrix effects that could influence the analytical response.

The concentration-dependent isotope fractionation effect seen in the raw isotope ratios (Table 3.6) is less pronounced for TCE, as the extraction is not as efficient as for PCE. Here, a precision of $\leq 0.5‰$ is achieved for concentrations $\geq 0.37 \mu g\,L^{-1}$, and a slope near unity for concentrations $\geq 0.75 \mu g\,L^{-1}$, which hence constitutes the MDL.

3.4. Conclusions

Our approach for lowering method detection limits for compound-specific chlorine isotope analysis of PCE and TCE allows the application of this technique at sub-$\mu g\,L^{-1}$ concentrations below most regulatory limits. The combination of SPME Arrow and qMS is easily automated and available in many laboratories. The design of experiments approach allowed easy identification and optimization of critical factors for SPME and preclusion of possible interactions between factors. Possible chlorine isotope fractionation due to the extraction can be accounted for by bracketing with two molecularly identical, isotopically different standards, and by carefully evaluating isotopic linearity limits. It is crucial that the concentrations of samples and standards be closely matched. The effects of different sample matrices and competitive sorption on the fiber when analyzing complex mixtures require further investigation. Our method allows further expansion of the application of compound-specific isotope analysis in the routine assessment of contaminated sites.

Acknowledgments

Dr. Stefan Cretnik and CTC Analytics AG (Zwingen, Switzerland) are acknowledged for their technical support and for providing the SPME Arrow tool. This work was supported by the Swiss National Science Foundation (SNSF) [grant number 166233].

4. Compound-specific carbon isotope analysis of volatile organic compounds in complex soil extracts using purge and trap concentration coupled to heart-cutting two-dimensional gas chromatography–isotope ratio mass spectrometry

Jeremy Zimmermann[1], Philipp Wanner[2], Daniel Hunkeler[1]

This chapter is based on the article published in *Journal of Chromatography A 1655 (2021) 462480*

Abstract

Compound-specific carbon isotope analysis (CSIA) is a powerful tool to track the origin and fate of organic subsurface contaminants including petroleum and chlorinated hydrocarbons and is typically applied to water samples. However, soil can form a significant contaminant reservoir. In soil samples, it can be challenging to recover sufficient amounts of volatile organic compounds (VOC) to perform CSIA. Soil samples often contain complex contaminant mixtures and gas chromatography combustion isotope ratio mass spectrometry (GC-C-IRMS) is highly dependent on good chromatographic separation due to the conversion to a single analyte. To extend the applicability of CSIA to complex volatile organic compound mixtures in soil samples, and to recover sufficient amounts of target compounds for carbon

[1]Centre for Hydrogeology and Geothermics, University of Neuchâtel, Rue Emile-Argand 11, 2000 Neuchâtel, Switzerland
[2]Department of Earth Sciences, University of Gothenburg, Guldhedsgatan 5a, 41320 Göteborg, Sweden

CSIA, we compared two soil extraction solvents, tetraglyme (TGDE) and methanol, and developed a heart-cutting two-dimensional GC-GC-C-IRMS method. We used purge & trap concentration of solvent-water mixtures to increase the amount of analyte delivered to the column and thus lower method detection limits. We optimized purge & trap and chromatographic parameters for twelve target compounds, including one suffering from poor purge efficiency. By using a 30 m thick-film non-polar column in the first and a 15 m polar column in the second dimension, we achieved good chromatographic separation for the target compounds in difficult matrices and high accuracy (trueness and precision) for carbon isotopic analysis. Tetraglyme extraction was shown to offer advantages over methanol for purge & trap concentration, leading to lower target compound method detection limits for CSIA of soil samples. The applicability of the developed method was demonstrated for a case study on soil extracts from a former manufacturing facility. Our approach extends the applicability of CSIA to an important matrix that often controls the long-term fate of contaminants in the subsurface.

4.1. Introduction

Compound-specific isotope analysis (CSIA) is a powerful method to track the origin and fate of contaminants in the subsurface and is often applied to volatile organic compounds (VOC) in groundwater samples (Braeckevelt et al. 2012; Wiegert et al. 2012; Palau et al. 2014c; Badin et al. 2016). The principle is based on monitoring the isotopic ratio of one or more elements (e.g. carbon, chlorine, hydrogen) of the parent compounds and/or degradation products. For carbon, the ratio of ^{13}C to ^{12}C of a sample R_{sample} is expressed using the delta (δ) notation as per mille (‰) difference from the isotope ratio in the reference standard Vienna Pee Dee Belemnite (VPDB):

$$\delta^{13}C = \frac{R_{sample} - R_{VPDB}}{R_{VPDB}} = \frac{R_{sample}}{R_{VPDB}} - 1 \qquad (‰) \tag{4.1}$$

Chemical bonds involving the heavier isotope are slightly stronger than those involving the light isotope, leading to a heavy isotope enrichment in the residual compound and a depletion in the degradation products. CSIA is applied to identify different degradation mechanisms, to quantify the degree of degradation, and to differentiate contaminant sources (Ojeda et al. 2019a; Schmidt and Jochmann 2012; Wiegert et al. 2012; Zimmermann et al. 2020)

Compound-specific carbon isotope analysis of VOC is typically performed by separating the target compounds with a gas chromatograph (GC), followed by combustion (C) to a single analyte, CO_2, and isotopic analysis in an isotope ratio mass spectrometer (IRMS).

In GC-C-IRMS systems, no mass fragments of the original compounds can be monitored, hence baseline chromatographic separation is required (Zhang et al. 2012; Leeuwen et al. 2014). In order to achieve a precision of $< 0.5‰$ for $\delta^{13}C$ measurements, Zhang et al. (2012) recommend that peak areas of any interferences remain below 5% of the target analyte peak area. Further complications arise due to chromatographic isotope effects, as isotopologues of target compounds travel at different velocities through the GC column. Isotopologues containing ^{13}C have been shown to migrate more rapidly compared to the isotopically light isotopologues, which causes the beginning of a peak to become isotopically enriched and its end to become depleted (Ricci et al. 1994). Hence, the isotopic ratio is not constant across the whole peak, which explains the need for integrating the complete peak area. For these reasons, Zhang et al. (2012) and Leeuwen et al. (2014) also advise against attempting to resolve co-eluting peaks by using algorithms.

At field sites with complex VOC mixtures that include monocyclic aromatic hydrocarbons (BTEX) and chlorinated aliphatic hydrocarbons, the baseline chromatographic separation can prove challenging. The analysis of VOC in soil samples adds an additional difficulty. Groundwater samples will only contain a limited range of VOC in solution, due to their generally low solubility in water, and a lower solubility of BTEX compared to chlorinated aliphatic compounds (Lawrence 2006). Soil samples on the other hand can contain a variety of contaminants, as in this case water cannot assume the role of a selectively extracting medium.

For quantification of VOC concentrations in solid samples, advances have been made that allow quantitative static or dynamic headspace extraction of VOC from solid samples (Jakubowska et al. 2009), resolving the severe matrix dependencies of these techniques that have been observed in the past, such as low recoveries and low reproducibility (Charles and Simmons 1987; Jenkins and Schumacher 1987; Minnich et al. 1997; Hewitt 1998).

However, none of these solvent-free extraction methods are suited for compound-specific carbon isotope analysis of complex mixtures, as method detection limits are generally higher than those required for simple quantification, and, most importantly, the linearity ranges for measuring isotope ratios with an IRMS hyphenated with a conversion step are much smaller than those for the detectors typically used in quantification. While flame ionization detectors (FID) allow quantifying concentrations spanning five orders of magnitude (Dettmer-Wilde and Engewald 2014), isotope ratio measurements using an IRMS are typically performed over a limited concentration range of only one order of magnitude (Sherwood Lollar et al. 2007). The pronounced amount dependence of isotopic measurements may be due to pressure fluctuations in the mass spectrometer itself or isotope fractionation at the open split of the combustion furnace (Ohlsson and Wallmark 1999). Hence, samples need to be

diluted to different levels and analyzed multiple times to ensure that the concentration of each target compound lies within the narrow linearity range inherent to GC-C-IRMS.

Therefore, a prior extraction step is necessary to make compound-specific carbon isotope analysis possible. Different extractants, e.g. organic solvents, are available for this task. A suitable solvent should be able to extract a wide range of contaminants, as well as be miscible in water to facilitate sample preparation and to accelerate the desorption rate of target compounds from soil, with methanol being the solvent of choice (Ball et al. 1997; Hewitt 1998). Methanol extraction has not only been applied for quantification of VOC in soil (Parker et al. 2004), but has also been shown to be suitable for carbon CSIA for tracking degradation processes of VOC in low-permeability zones (Wanner and Hunkeler 2015; Wanner et al. 2016, 2017).

The analysis of target compounds extracted from soil using solvents becomes challenging at low concentration levels of target compounds. This is especially relevant for CSIA, as the most pronounced isotope effects will first emerge after a large proportion of the initial contaminant has been degraded. Offline pre-concentration of soil extracts by evaporation of the extraction solvent is limited to high-boiling target compounds such as polycyclic aromatic hydrocarbons (PAH) and cannot be applied to VOCs. Furthermore, large solvent peaks may interfere with target VOCs during chromatographic separation.

For sample introduction into the GC using a standard splitless injector with a liner volume limited to 1 mL, the maximum permissible liquid injection volume is generally in the low µL-range, in order to avoid overloading the glass inlet liner when the sample is evaporated (Dettmer-Wilde and Engewald 2014). Wilcke et al. (2002), Kim et al. (2005), Graham et al. (2006), and Bosch et al. (2015) have applied carbon CSIA to PAH in soil extracts. Due to the small injection volumes, extensive pre-concentration and purification were required in all cases. Using programmable temperature vaporizing (PTV), the injection volume can be increased to 100 µL or even 1000 µL (large-volume injection), at the risk of losing low-boiling compounds during the necessary solvent evaporation step (Dettmer-Wilde and Engewald 2014). Blessing (2008) and Blessing et al. (2015) applied a large-volume injection of up to 150 µL for carbon CSIA of PAH in soil, requiring solid-liquid and liquid-liquid extraction and purification steps prior to analysis.

In order to avoid these laborious offline steps and associated possible losses when applied to VOC, and to allow the injection of much larger amounts of extraction solvents, we propose diluting the soil extracts in water and concentrating target compounds using a purge & trap concentrator. In addition, cryogenic focusing allows us to use a splitless injection. This ensures quantitative transfer of compounds, which is of particular importance for IRMS due to the lower sensitivity. At a methanol proportion of 1% (v/v) in water and

a purge volume of 25 mL, 250 µL of soil extract can be analyzed. This is an improvement by a factor of 125 to 250 over classical solvent injection. The dilution is necessary as high proportions of methanol may interfere with target compounds due to competitive sorption on the trap and/or the GC separation. The maximum permissible methanol content for carbon CSIA using purge & trap has so far been limited to 1% (v/v) (Wanner and Hunkeler 2015). As a high boiling-point alternative to methanol, the use of tetraethylene glycol dimethyl ether (TGDE, tetraglyme) has been proposed (Jenkins and Schumacher 1987; Hewitt 1998; Troost 1999; Bouchard et al. 2017).

As mentioned, the efficient extraction of target as well as non-target compounds may lead to problems in achieving a high chromatographic resolution. Heart-cutting two-dimensional (2D) gas chromatography (GC-GC), not to be confused with comprehensive 2D gas chromatography (GCxGC), is a suitable method to separate a limited number of target compounds from interfering compounds (Tranchida et al. 2012). This method uses two GC columns of different selectivity connected in series through a valve system called the Deans' switch (Deans 1968), which allows target compound peaks eluting from the first column to be diverted to the second column for additional separation. Compound-specific carbon isotope analysis using GC-GC-C-IRMS has been applied, amongst others, to drug residues in human excreta (Brailsford et al. 2012), flavor compounds in truffle oils (Sciarrone et al. 2018), polychlorinated biphenyls (Horii et al. 2005), and aliphatic (Nara et al. 2006) as well as aromatic hydrocarbons (Ponsin et al. 2017) in groundwater and gas-phase environmental samples. To the best of our knowledge, GC-GC methods have not yet been applied to isotope analysis of VOCs in soil extracts.

The objective of our study was to develop a method that allows obtaining compound-specific carbon isotope ratios for complex mixtures of monocyclic aromatic hydrocarbons and chlorinated aliphatic hydrocarbons in soil samples. We determined the solvent best suitable for purge & trap analysis and optimized purge & trap parameters. We developed a GC-GC method for baseline separation of peaks, and determined accuracy, isotopic linearity and method detection limits for each target compound. Possible isotope fractionation effects during the analytical measurement (Meier-Augenstein et al. 1996; Jochmann et al. 2006; Tang et al. 2017) were also evaluated. The applicability of the developed method was illustrated with soil extracts from a field site, where soils had been contaminated by a complex mixture of organic contaminants.

4.2. Material and methods

4.2.1. Chemicals

Nitrogen purge gas ($\geq$ 99.995% purity) and helium carrier gas ($\geq$ 99.9999% purity) were obtained from Carbagas. Any aqueous solutions were prepared in ultrapure water from a Merck Millipore Direct-Q 3 water purification system. Two different tetraglyme products ($\geq$ 99% purity) were obtained from Sigma Aldrich and Thermo Fisher Scientific. Methanol ($\geq$ 99.8% purity) was obtained from Thermo Fisher Scientific. The extraction solvents and their physical properties are summarized in Table S4 in the supporting information (Appendix C).

Chlorinated aliphatic hydrocarbons and non-chlorinated aromatic hydrocarbons were obtained in high purities (Table 4.1). The choice of twelve target compounds coincided with those found at the field site. All target compounds with the exception of carbon tetrachloride had been previously referenced isotopically towards Vienne Pee Dee Belemnite (VPDB) with an elemental analyzer (EA) as pure liquid phase. Stock solutions of target compounds were prepared gravimetrically in methanol. The target compounds and their physical properties are summarized in Table 4.1.

Table 4.1.: Properties of the investigated target compounds. δ^{13}C VPDB values measured using an elemental analyzer, physicochemical data from Schwarzenbach et al. (2003).

Systematic name	Common name	Manufacturer	Purity	δ^{13}C VPDB (‰)	M (g mol^{-1})	ρ (g cm^{-3})	T_b (°C)
Dichloromethane	Methylene chloride	Merck	$\geq$ 99.8%	-30.17 ± 0.06	84.9	1.33	40.1
Trichloromethane	Chloroform	Fluka	$\geq$ 99.5%	-48.38 ± 0.07	119.4	1.48	61.4
Tetrachloromethane	Carbon tetrachloride	Fluka	$\geq$ 99.8%	–	153.8	1.59	76.7
trans-1,2-Dichloroethene		Fluka	$\geq$ 97.0%	-18.92 ± 0.10	96.9	1.27	48.0
cis-1,2-Dichloroethene		Fluka	$\geq$ 97.0%	-23.99 ± 0.07	96.9	1.27	60.0
Trichloroethene		Fluka	$\geq$ 99.5%	-26.70 ± 0.10	131.4	1.46	87.0
Tetrachloroethene	Perchloroethene	Riedel-de-Haën	$\geq$ 99.5%	-26.54 ± 0.07	165.8	1.62	121.1
1,1,2,2-Tetrachloroethane		Sigma	$\geq$ 98.0%	-8.63 ± 0.05	167.9	1.60	146.3
Methylbenzene	Toluene	Riedel-de-Haën	$\geq$ 99.5%	-27.49 ± 0.03	92.9	0.87	110.6
Ethylbenzene		Fluka	$\geq$ 99.0%	-29.29 ± 0.06	106.2	0.86	136.2
1,2-Dimethylbenzene	*ortho*-Xylene	Alfa Aesar	$\geq$ 99.0%	-28.55 ± 0.05	106.2	0.88	144.4
1,3-Dimethylbenzene	*meta*-Xylene	Fluka	$\geq$ 99.0%	-27.37 ± 0.12	106.2	0.86	139.1

4.2.2. Carbon isotope analysis

For compound-specific carbon isotope analysis, 25 mL of a 42 mL sample were purged with N_2 at 40 mL min^{-1} in a fritted sparge vessel using a Teledyne Tekmar Stratum purge & trap system and Aquatek 70 autosampler. The purged compounds were trapped onto a Vocarb K 3000 trap. Compounds were then desorbed by heating the trap to 250 °C, which

could be preceded by a dry purge cycle of 100 mL N_2 at ambient temperature to remove water. During desorption, the desorbed compounds were introduced into the helium carrier gas stream of an Agilent 7890A gas chromatograph (GC) through a 6-port valve, followed by cryogenic focusing at −120 °C. After two minutes of desorption, the cryogenic trap was rapidly heated to 180 °C, releasing the compounds completely onto the first capillary column. The purge & trap parameters are specified in detail in the supporting information (Table S2 in Appendix C).

The effluent of the first column was directed via the Deans' switch to either a flame ionization detector (FID) or to the second column. By first separating a standard mixture in the first column and diverting the complete flow to the FID, the switching times for the Deans' switch could be determined. For subsequent analytical runs, the switching times were adjusted accordingly to only divert the peaks of interest to the second column. The FID signal was still monitored to ensure that the complete target peak was diverted to the second column. The heart-cut valve after the second GC column allows additional cuts for target compounds that can only be fully separated in the second dimension. The effluent of the second GC column led to an Elementar Isoprime GC5 combustion furnace, where the hydrocarbons were transformed to CO_2. Subsequently, water was removed by a Nafion tube, semi-permeable to water vapor, and finally the CO_2 was analyzed in an Elementar Isoprime 100 continuous flow isotope ratio mass spectrometer (CF-IRMS). Figure 4.1 shows a scheme of the analytical setup.

The flow of the first column was controlled by the GC inlet and set to 1.5 mL min^{-1} in constant pressure mode, while the flow of the second column was controlled by a pressure control module (PCM) and set to 2.5 mL min^{-1} in constant pressure mode, each for the initial GC oven temperature. Proper operation of the Deans' switch requires the deactivated capillary leading to the FID, the so-called restrictor, to have the same pneumatic resistance as the second column (Boeker et al. 2013). To this end, its length had to be adjusted as a function of initial GC oven temperature, column flow and choice of second column. The parameters used are specified in detail in the supporting information (Table S3 in Appendix C).

4.2.3. Choice of GC-GC columns

Two-dimensional chromatography uses two columns of different selectivity, e.g. a polar and a non-polar column. We tested different combinations of columns before settling on a combination that would enable baseline separation of the twelve target compounds in

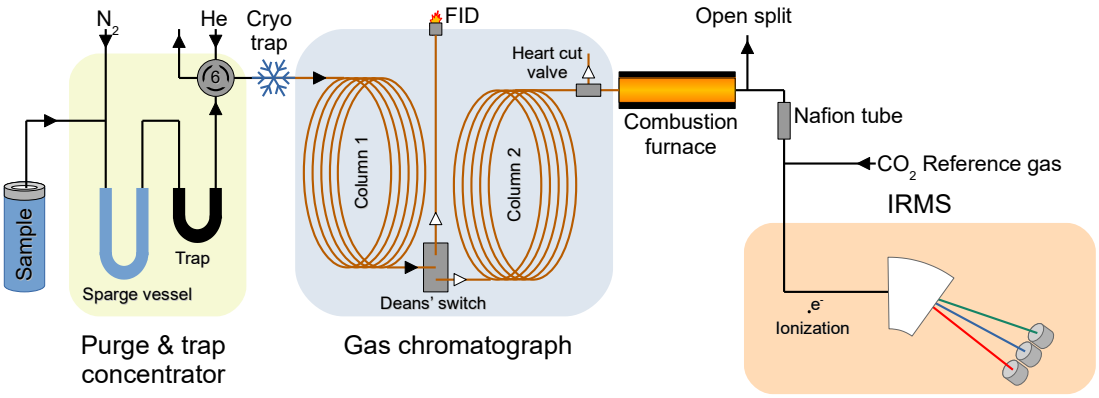

Figure 4.1.: GC-GC-C-IRMS configuration.

different matrices and at heavy column loading, while at the same time avoiding excessive GC runtimes.

A non-polar thick-film 100% polydimethylsiloxane (PDMS) phase column, Rtx-1 (30 m × 0.32 mm, 5 µm, Restek), was chosen in the first dimension for the following two reasons. Firstly, non-polar columns are not very selective for methanol, which would allow the extraction solvent peak to pass through the column without interfering with target compound separation. Secondly, thick-film columns have a high resolution for volatiles and a high sample loading capacity. The latter point is crucial in this study, as extraction solvents and a wide concentration range of target compounds are introduced into the system.

In the second dimension, a polar Rtx-Wax column (15 m × 0.32 mm, 1 µm, Restek) was used. As the first column already achieved the bulk of the separation work, a shorter column in the second dimension was deemed adequate to remove interfering compounds and to achieve the baseline separation necessary for C-IRMS.

4.2.4. Purge & trap and GC-GC optimization

The purge & trap and GC-GC parameters were first optimized for target compounds in water, in order to determine the limits of a basic application of the purge & trap and GC-GC-C-IRMS method, without concerns for matrix effects. An important purge & trap parameter to be optimized is the purge time for a given purge flow. A theoretical estimate of the time required to purge 90% of a target compound from water was calculated using Equation 4.2 (Schwarzenbach et al. 2003):

$$c_{iw}(t) = c_{iw}(0) \times \exp\left(\frac{-K_{iaw} \times G}{V_w} \times t\right) \tag{4.2}$$

where $c_{iw}(t)$ is the target compound concentration in water after a certain time t in $\mu g\,L^{-1}$, $c_{iw}(0)$ is the initial concentration in water in $\mu g\,L^{-1}$, G is the purge gas flow in $mL\,min^{-1}$ and V_w is the purge volume in mL. K_{iaw} is the dimensionless Henry or air-water partition constant that gives the ratio of the gaseous concentration in air to the dissolved concentration of a compound i in pure water. It can be approximated by the ratio of vapor pressure to aqueous solubility (Schwarzenbach et al. 2003). Setting $c_{iw}(t)/c_{iw}(0) = 0.1$, i.e. 10% of the compound still remain in water, and solving for t yields theoretically required purge times shown in Table 4.2.

Table 4.2.: Theoretical purge times required to purge 90% of a target compound from 25 mL of water at a purge flow of $40\,mL\,min^{-1}$ at 25 °C. Air-water partition constants (K_{iaw}) from Schwarzenbach et al. (2003). DCM, dichloromethane; CF, chloroform; CT, carbon tetrachloride; DCE, dichloroethene; TCE, trichloroethene; PCE, tetrachloroethene; TeCA, tetrachloroethane.

Compound	K_{iaw} (25 °C)	Purge time (25 °C) (min)
DCM	0.12	12.2
CF	0.14	10.0
CT	1.10	1.3
trans-1,2-DCE	0.26	5.6
cis-1,2-DCE	0.22	6.6
TCE	0.49	2.9
PCE	1.20	1.2
1,1,2,2-TeCA	0.02	86.7
Toluene	0.25	5.7
Ethylbenzene	0.32	4.6
o-Xylene	0.20	7.0
m-Xylene	0.30	4.9

An issue becomes evident when comparing the theoretical purge times. 1,1,2,2-TeCA would require almost one and a half hours for 90% of it to be purged from water, while all other compounds with the exception of DCM require less than 10 minutes of purging.

4.2.5. Standardization and method detection limit determination

The CO_2 reference gas had been previously referenced towards VPDB by dual inlet (DI) IRMS. It was introduced twice at the beginning and twice at the end of each analytical run. All target compounds were measured simultaneously during one analytical run. To test for possible isotopic fractionation during sample preparation, concentration, separation and combustion, the obtained $\delta^{13}C$ values were compared to the EA values.

The concentration range for which the pre-defined precision and trueness criteria are met is denoted the isotopic linearity range (Sherwood Lollar et al. 2007). We applied Jochmann et al. (2006)'s guidelines to determine method detection limits (MDL) for $\delta^{13}C$ analysis of each target compound. To this end, standards were injected five times over a range of concentration levels, and the mean $\delta^{13}C$ value as well as the standard deviation $1\sigma(n = 5)$ were plotted against the concentration. Subsequently, the mean $\delta^{13}C$ value for the highest concentration levels was calculated, and an interval of $\pm 0.5‰$ was set around this mean value. Next, the mean calculation was repeated, this time including the next lower concentration level. This process was repeated until the mean $\delta^{13}C$ value for a concentration level was either outside the $+0.5‰$ interval around the moving mean, or its 1σ was $> 0.5‰$. The lowest concentration level to still meet these criteria was defined as the MDL. We determined the isotopic MDLs for each target compound according to this scheme, which is shown for the examples of TCE and PCE in Figures S1 and S2 of the supporting information (Appendix C).

4.2.6. VOC standards spiked with extraction solvents

In order to demonstrate the applicability of the GC-GC and soil extraction methods for compound-specific $\delta^{13}C$ analysis, multiple concentration levels of target compounds were analyzed in water that had been spiked with different volumes of methanol and TGDE. Isotopic linearity ranges were determined for each compound.

VOC standards were prepared in 42 mL glass vials capped with PTFE-coated silicone septa and screw caps from the methanol stock via an intermediate aqueous solution. We observed a diminished 1,1,2,2-TeCA peak when analyzing the single compound in aqueous solution and the appearance of a TCE peak. As noted by Barani et al. (2006), 1,1,2,2-TeCA readily transforms to TCE via E2 elimination at neutral and alkaline pH. Hence, it was necessary to acidify all aqueous solutions to a pH of 2 to 3 with HNO_3.

4.2.7. VOC samples from field site

Soil extracts in water, methanol and TGDE were prepared from soil samples containing target compounds collected at a contaminated site. The site, previously characterized in detail by Wanner et al. (2018), is a former manufacturing facility, where 200 L of a complex mixture of chlorinated and petroleum hydrocarbons were introduced to the subsurface during the 1960s. These formed a downgradient plume in the heterogeneous sandy aquifer, further diffusing into a thin underlying aquitard. The contaminant source was isolated from the

active groundwater flow system by soil mixing with bentonite and zero-valent iron in 2008, and in 2018 a study was initiated to evaluate in detail the plume response to this source treatment.

Soil cores were drilled using a direct-push rig, followed by subsampling of the low-permeability zones using tube-and-piston subsamplers. Soil samples taken at the same depth were extracted in methanol, TGDE or water. The soil samples, weighing 10 g to 15 g, were dispersed in 42 mL glass vials capped with PTFE-coated silicone septa and screw caps containing 20 mL of the extraction medium (Parker et al., 2004). The vials were weighed empty, with the extraction medium, and with the extraction medium plus the soil sample (Isenschmid 2018).

The vials containing soil and extraction medium were sonicated, shaken, and centrifuged. Concentrations of VOC in the soil extracts were measured using a gas chromatograph coupled to a mass spectrometer (GC-qMS) based on EPA method 8260B, following pre-concentration with a purge & trap system (Table S1 in the supporting information Appendix C).

Selected matrix-rich samples in methanol and TGDE were analyzed after dilution in water and acidification using the developed GC-GC-C-IRMS method with optimized purge & trap parameters as described above.

4.3. Results and discussion

4.3.1. Purge & trap and GC-GC optimization

Figure 4.2(a) shows the chromatogram at a single concentration level that is obtained in the first dimension when diverting all compounds to the FID, while Figure 4.2(b) shows the chromatogram detected with the IRMS when diverting all compounds eluting from the first column onto the second column, each after a purge time of 10 minutes at 25 °C. The GC temperature program was developed in a manner that would achieve separation of most target compounds in a reasonable time frame, while limiting the retention of methanol. A co-elution was observed in the first dimension for *o*-xylene and 1,1,2,2-TeCA, but this could be resolved in the second dimension. This required a rather low final GC temperature, thereby prolonging run time. Eventually, the GC temperature program was as follows: Starting temperature of 70 °C, held for 2 minutes, 70 °C to 90 °C at 2 °C min^{-1}, held for 2 minutes, 90 °C to 165 °C at 15 °C min^{-1}, held for 12.5 minutes, for a total run time of 31.5 minutes. While having both columns in the same GC oven and undergoing the same temperature program is not an optimum approach in GC-GC analysis, the only drawback

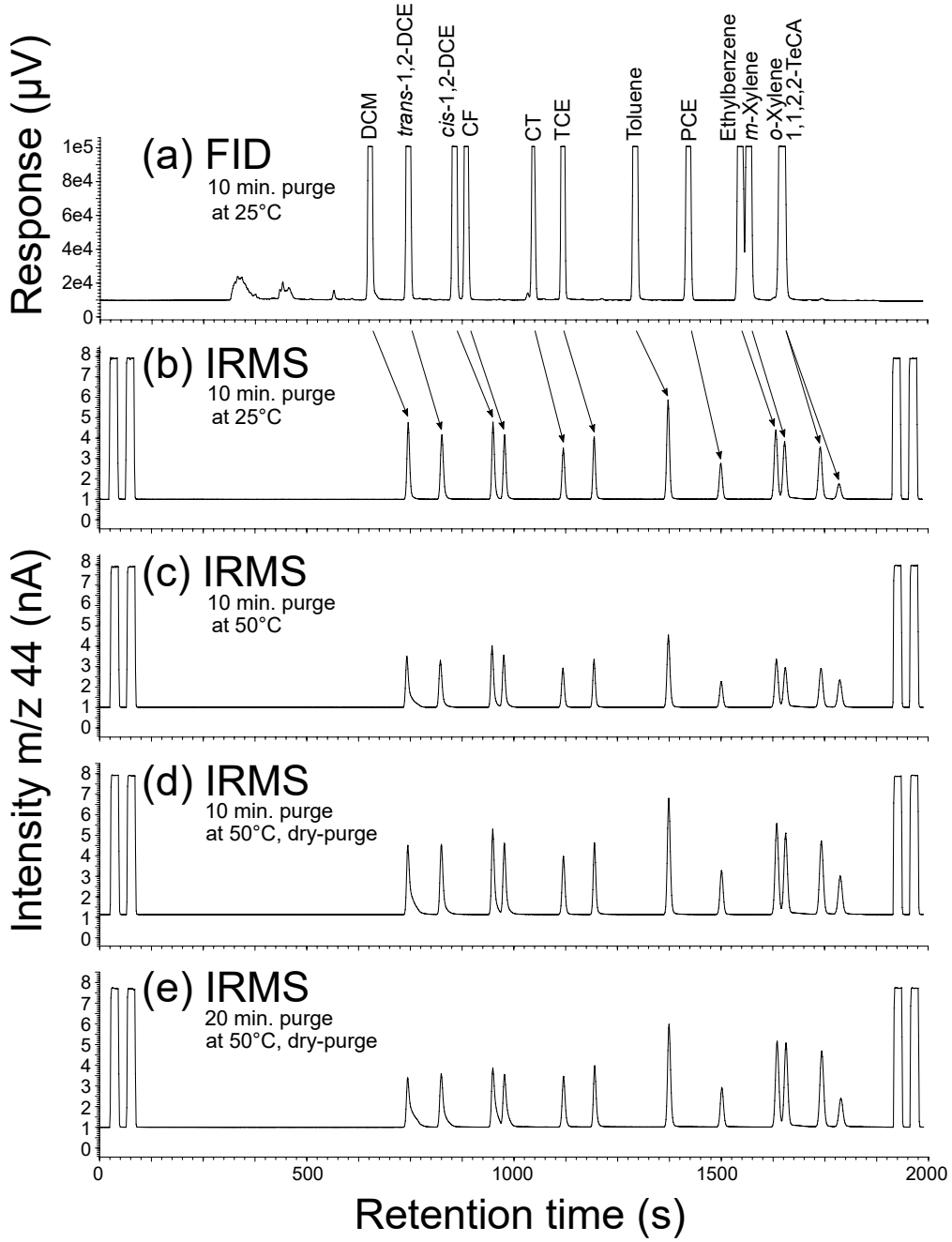

Figure 4.2.: Chromatograms of target compounds in water for the (a) first dimension, showing only the FID signal, and (b) – (e) second dimension, as detected by the IRMS after conversion to CO_2. Concentrations of 90 µg L^{-1} for DCM, CF, CT and 1,1,2,2-TeCA; 45 µg L^{-1} for *trans*-1,2-DCE, *cis*-1,2-DCE, TCE and PCE; 16 µg L^{-1} to 17 µg L^{-1} for toluene, ethylbenzene, *m*-xylene and *o*-xylene.

we observed for our contaminant mixture was an incomplete separation of *m*-xylene and ethylbenzene. The other peaks are well resolved and no undue peak broadening or tailing is observed.

To improve the purge efficiency of 1,1,2,2-TeCA, three possibilities were explored. Salting out, an increase in purge time, and an increase of purge temperature. By increasing the ionic strength of a solution through addition of salts, organic compounds may increasingly partition from the liquid phase towards the headspace. When adding sodium chloride, we observed salt build-up in the sparge vessel. Further after-effects may include blockage and corrosion of the purge & trap sample pathways (Manickum and John 2011). Most importantly, the method does not affect non-polar compounds such as 1,1,2,2-TeCA, as these are already poorly soluble in water (Wercinski 1999; Schwarzenbach et al. 2003). For these reasons, salting-out was quickly abandoned.

The effect of purge temperature was investigated using a thermostatically controlled custom water bath around the sparge vessel, held at 50 °C. As a rule-of-thumb, the Henry constant is expected to increase by a factor of 1.6 for a temperature increase of 10 °C in the ambient range (Staudinger and Roberts 1996), which in this case would cause an increase of the Henry constant by a factor of 4 for a purge temperature of 50 °C versus 25 °C and accordingly lower the time required to purge 90% of 1,1,2,2-TeCA to around 20 minutes.

The main drawback of increased purge temperature and time is an increase of the amount of water that is transferred to the trap. The effect can be observed in Figure 4.2(c), causing tailing peaks for early eluting compounds DCM, *trans*-1,2-DCE and *cis*-1,2-DCE and an overall reduced intensity. The latter can be remedied by a dry-purge cycle before release of the compounds from the trap (Lee et al. 2001). We applied a dry-purge of 1 minute at 100 mL min^{-1} N_2 for a total dry-purge volume of 100 mL. The effect can be seen in Figure 4.2(d), with an increased intensity for the late eluting compounds. The peak tailing of the early eluting compounds remains an issue. In general, DCM would benefit from a lower initial oven temperature and lower cryogenic focusing temperature. Figure 4.2(e) shows a combination of a longer purge time of 20 minutes with an increased purge temperature of 50 °C. Here, even for 1,1,2,2-TeCA, the intensity is further reduced, possibly requiring further investigations into the effect of dry-purging. While the technique removes water from the trap after purging is complete, a competitive sorption on the trap between water and target compounds during purging may be the underlying issue explaining the reduced intensity.

In conclusion, early eluting compounds should be purged at room temperature, and 1,1,2,2-TeCA is the only target compound that significantly benefits from an increased

purge temperature. Longer purge times than theoretically required are to be avoided, in order to inhibit the ingress of water to the trap.

4.3.2. Method performance for CSIA

Figure 4.3 (top) shows a comparison of method detection limits of target compounds for different extraction solvent spiking levels normalized to the MDL in water. Figure 4.3 (bottom) shows the deviation in ‰-points of our mean measured δ^{13}C values from the δ^{13}C VPDB values measured using an EA for the target compounds. Purge & trap parameters were a 10 minute purge time and a purge temperature of 25 °C. For 1,1,2,2-TeCA, the effect of an elevated purge temperature of 50 °C was also investigated.

Our measured δ^{13}C values in water are for most compounds higher than the EA value, indicating an isotopic enrichment during sample concentration and/or analysis. This systematic offset is inherent to purge & trap concentration (Zwank et al. 2003; Ponsin et al. 2017). An inverse ^{13}C isotope effect during volatilization of VOC has been observed by, e.g., Baertschi et al. (1953), Bradley (1954), Huang et al. (1999), Poulson and Drever (1999), and Jeannottat and Hunkeler (2012). If this offset remains constant within the limits of isotopic linearity for standards, the values measured for actual samples can be corrected by simple means.

Methanol as extraction solvent

Methanol and the target compounds were already well separated in the first dimension. We observed, however, a decreasing intensity for all compounds with increasing methanol content from 1% to 2% to 3% (v/v). This is reflected by a higher MDL for all target compounds at a methanol spiking level of 3% (Figure 4.3 top). The lower intensity is thought to be caused by competitive sorption between methanol and the target compounds on the trap. Target compounds could be resolved using the two-dimensional GC setup for methanol spiking levels of up to 3% (v/v). Beyond this value, the likelihood of saturating the first column increased and target compound peaks could not be resolved anymore. A combination of 3% (v/v) and heated purging caused strong shifts in retention times, making it difficult to set the correct timing for the Deans' switch. Hence, it was not possible to increase the purge efficiency of 1,1,2,2-TeCA at higher methanol proportions.

For most compounds, the carbon isotopic enrichment seen when purging target compounds from pure water is reduced when spiking with methanol (Figure 4.3 bottom). Hence, it would be necessary to match the amount of extraction solvent in standards and samples.

Figure 4.4 shows the chromatograms for a sample from the field site that required

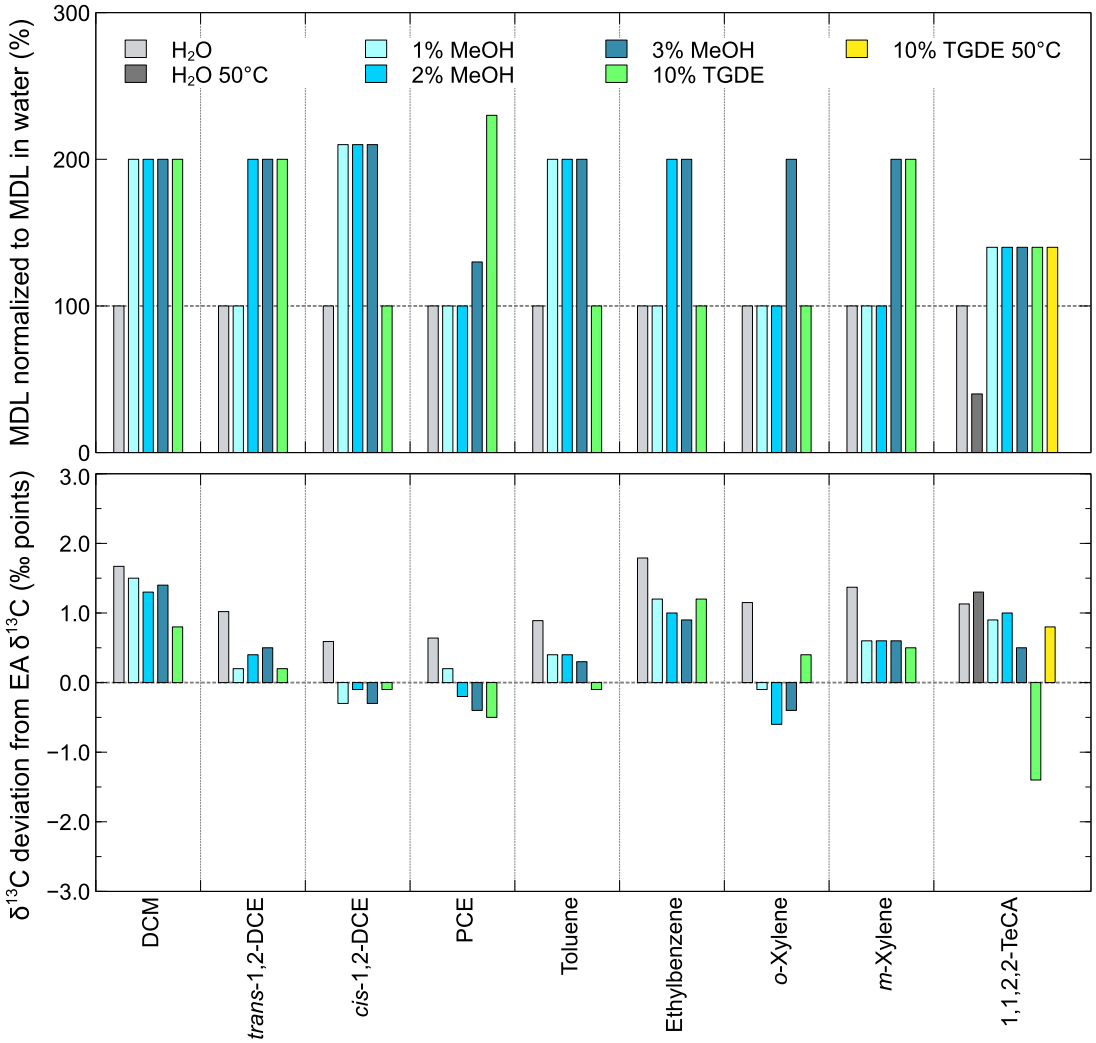

Figure 4.3.: (Top) Comparisons of target compound method detection limits in different matrices for optimized purge & trap parameters and, for 1,1,2,2-TeCA additionally purging at 50 °C. TCE, CF and CT have been omitted because of suspected contamination of the methanol used for spiking. (Bottom) Deviation in ‰-points of our mean measured δ^{13}C values from the δ^{13}C VPDB values measured using an EA for the target compounds.

analysis at a methanol content of 3% (v/v), due to the low concentrations of certain target compounds. The two-dimensional setup allowed separation of target peaks from non-target peaks, impurities in the methanol and the methanol itself.

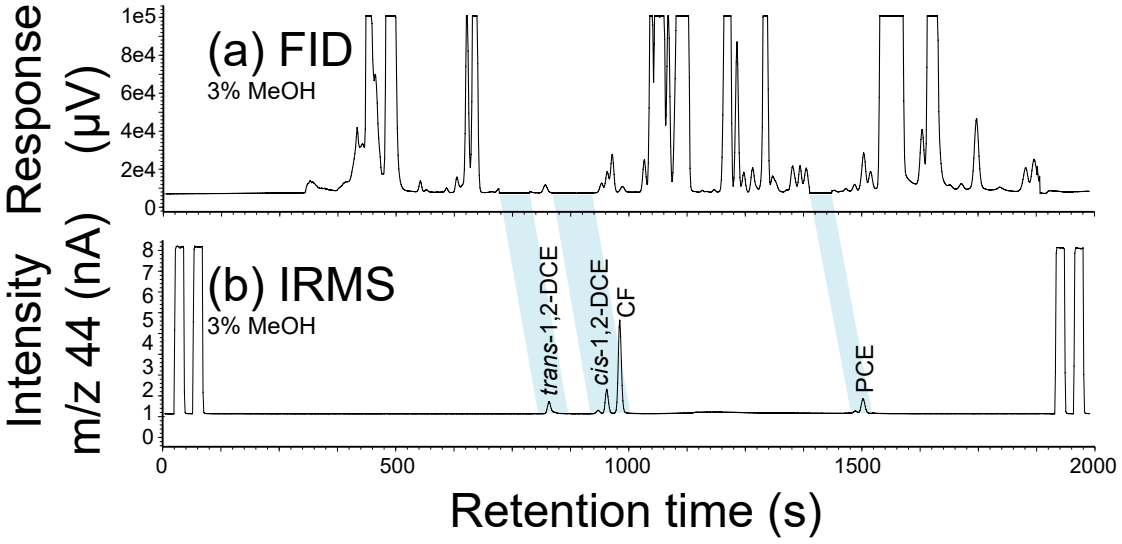

Figure 4.4.: Chromatograms for analysis of a sample from the field site that was extracted with methanol for (a) first dimension and (b) second dimension. Methanol proportion during purging is 3% (v/v).

TGDE as extraction solvent

We spiked aqueous solutions containing target compounds with different amounts of TGDE up to 10% (v/v) and purged them for 10 minutes at 25 °C and for 1,1,2,2-TeCA at 50 °C. For the sensitivity, we observed some major advantages of TGDE over methanol. For many of the compounds, the MDLs are on par with those measured in the best-case scenario, which is in pure water (Figure 4.3 top). Furthermore, with a TGDE spiking level of 10% (v/v), the maximum permissible extraction solvent level for purge & trap analysis can be increased by a factor of three over methanol, which in turn results in a lower MDL for soil extracts by a factor of three.

For some compounds, MDLs when spiking with TGDE are higher compared to purging from pure water (Figure 4.3 top). The peak intensity for all target compounds peaks is diminished when the sample is spiked with 10% TGDE (Figure 4.5) compared to when purged from pure water (Figure 4.2(b)). For 1,1,2,2-TeCA, MDLs are not any lower when increasing the purge temperature to 50 °C, in contrast to the heating effect observed in

pure water for 1,1,2,2-TeCA (Figure 4.3). As discussed by Staudinger and Roberts (1996), the presence of other organic solvents can decrease Henry's constants for target VOCs, especially those that are poorly soluble in water, which is the case for all of our studied target compounds. This so-called co-solvent effect occurs when another non-target organic solvent, in our case TGDE, is present at concentrations higher than 10% (v/v), causing it to not be fully hydrated. The molecules of interest will then dissolve into the co-solvent and thus cannot be purged efficiently. The effect is less severe for the aromatic hydrocarbons, which have a lower octanol-water coefficient than the aliphatic hydrocarbons (Schwarzenbach et al. 2003). This supports the hypothesis that it is indeed the dissolution of the analytes into the co-solvent that causes the decrease in purging efficiency.

At high spiking levels, it became apparent that both TGDE products that were used contained high amounts of volatile compounds. Jenkins and Schumacher (1987) and Troost (1999) purified the TGDE used in their purge & trap studies by rotary evaporation under vacuum at 97 °C or purging with an ultrapure gas at 80 °C, respectively. However, in these cases the TGDE was diluted in water by a factor of 60 or 50. A more sophisticated purification step is necessary for a higher proportion of TGDE. Huybrechts et al. (2001) investigated proportions of TGDE up to 20% in water, and purified the TGDE through an aluminum oxide column to remove peroxides. These peroxides are easily formed by reaction of the TGDE with ambient oxygen. An oxygen scavenger was also added to the purified TGDE. Bouchard et al. (2017) used TGDE proportions of up to 15% (v/v) without a prior purification step; however, the analysis was limited to only two target compounds.

We attempted to purify the TGDE as suggested by Troost (1999) by heating an aliquot to 80 °C and passing a flow of ultrapure nitrogen for several hours. Only one of the TGDE products improved significantly with regards to VOC contamination following this treatment. Although the baseline in the first dimension remained noisy, target compounds, with the exception of CT, could be isolated from the interfering compounds using the two-dimensional GC setup (Figure 4.5).

A frequently encountered downside of TGDE is its tendency to foam during purge & trap applications. This can be prevented by adding anti-foaming agents. We tested two commercial silicone anti-foaming agents, one of them specifically marketed for purge & trap analysis, and found both of them to contain unacceptable levels of interfering contaminants which could not be eliminated even using GC-GC. Erickson et al. (1981) studied several anti-foaming agents and determined that they require prior purification for purge & trap analysis. We dispensed with using anti-foaming agents and did not observe troublesome levels of foaming at TGDE proportions of up to 10% (v/v). Frequently analyzed blanks of ultrapure water did not indicate any carryover in the purge & trap system.

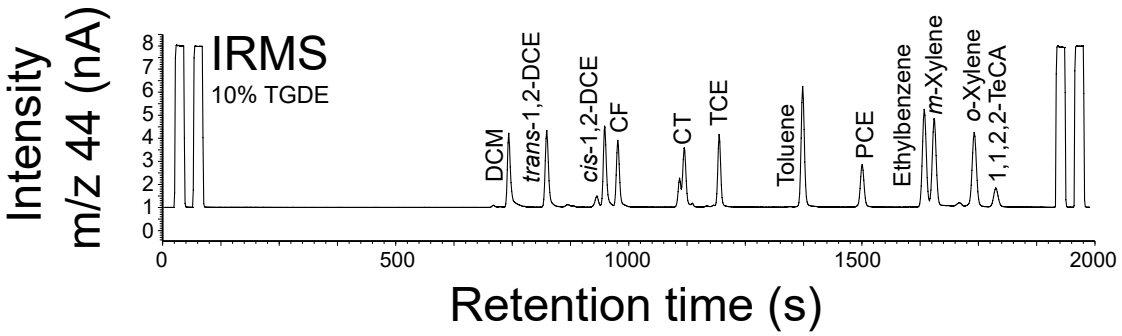

Figure 4.5.: Chromatogram in the second dimension of target compounds in water spiked with 10% TGDE (v/v) for purging at 25 °C. Concentrations of 90 µg L^{-1} for DCM, CF, CT and 1,1,2,2-TeCA; 45 µg L^{-1} for *trans*-1,2-DCE, *cis*-1,2-DCE, TCE and PCE; 16 µg L^{-1} to 17 µg L^{-1} for toluene, ethylbenzene, *m*-xylene and *o*-xylene. Purge time 10 minutes at 40 mL min^{-1}, dry purge 1 minute at 100 mL min^{-1}.

At a TGDE spiking level of 10% (v/v), the δ^{13}C offsets from δ^{13}C EA values are similar in magnitude to those measured when spiking with methanol (Figure 4.3 bottom). For 1,1,2,2-TeCA, however, the necessity of heating the sample during purging is demonstrated. In pure water, sensitivity of 1,1,2,2-TeCA analysis is considerably improved by heating. At a high TGDE spiking level, sensitivity is not improved by heating, however, it is required in order for the mean δ^{13}C value to show a similar offset to that measured in pure water and when spiked with methanol. Figure 4.6 shows the chromatograms for a sample from the field site that required analysis at a TGDE proportion of 10% (v/v), due to the low concentrations of certain target compounds. The two-dimensional setup allowed separation of target peaks from non-target peaks and impurities in the TGDE.

The δ^{13}C values for samples from the field site taken at same depths were in good agreement for both extraction solvents (data not shown). Furthermore, our values showed an isotopic enrichment of parent compounds 1,1,2,2-TeCA and CF in the aquitard, indicating that degradation is taking place. This is in accordance with the findings in the earlier study at this field site by Wanner et al. (2018), which had been performed on water extracts.

4.3.3. Comparison of soil extraction efficiency of water, methanol and TGDE for target compounds and implications for MDL

Normalized to the wet soil sample weight, we compared the target compound concentrations of up to 28 soil extracts from the field site in water, TGDE and methanol. Water was not able to extract a sufficient amount of VOC from the soil samples for δ^{13}C analysis, thus

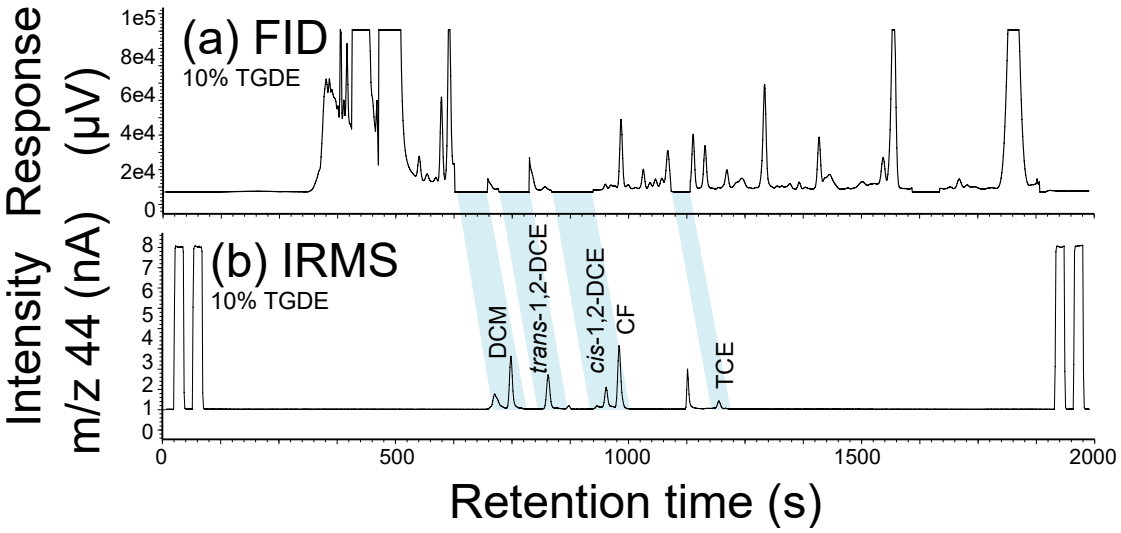

Figure 4.6.: Chromatograms for analysis of a sample from the field site that was extracted with TGDE for (a) first dimension and (b) second dimension. TGDE proportion during purging is 10% (v/v).

this extraction method is not discussed any further. We limited the statistical treatment to those samples for which the soil concentration in both methanol and TGDE was $>5\,\mu g\,g^{-1}$ (in wet soil), hence values for CT, PCE and toluene were rejected. As opposed to the isotopic measurements of soil extracts, concentrations were measured highly diluted in water, thus co-solvent effects are not expected to be relevant.

The mean extraction efficiency of TGDE was for all compounds lower than that achieved using methanol, but always above 75% of the methanol extraction efficiency (Figure 4.7). The performance of these two extraction solvents has been the focus of previous studies. Jenkins and Schumacher (1987) compared the extraction efficiency of TGDE for soils that had been spiked with VOCs through vapor equilibration, with methanol performing as well or better than TGDE. Hewitt (1998) spiked soil specimen with VOCs in aqueous solutions or through a process called vapor fortification. Here, methanol also achieved higher, quantitative recoveries of target VOCs compared to TGDE, independent of the spiking method. This discrepancy was found to become more pronounced with increasing organic carbon content of the soil specimen. As our study applied these extraction methods to natural soil samples from a contaminated site, some of our observed differences in recovery may also be due to soil and VOC distribution heterogeneities.

The use of TGDE as soil extraction solvent allows higher proportions of extraction solvent of up to 10% (v/v) during purge & trap analysis. Consequently, the lower soil extraction

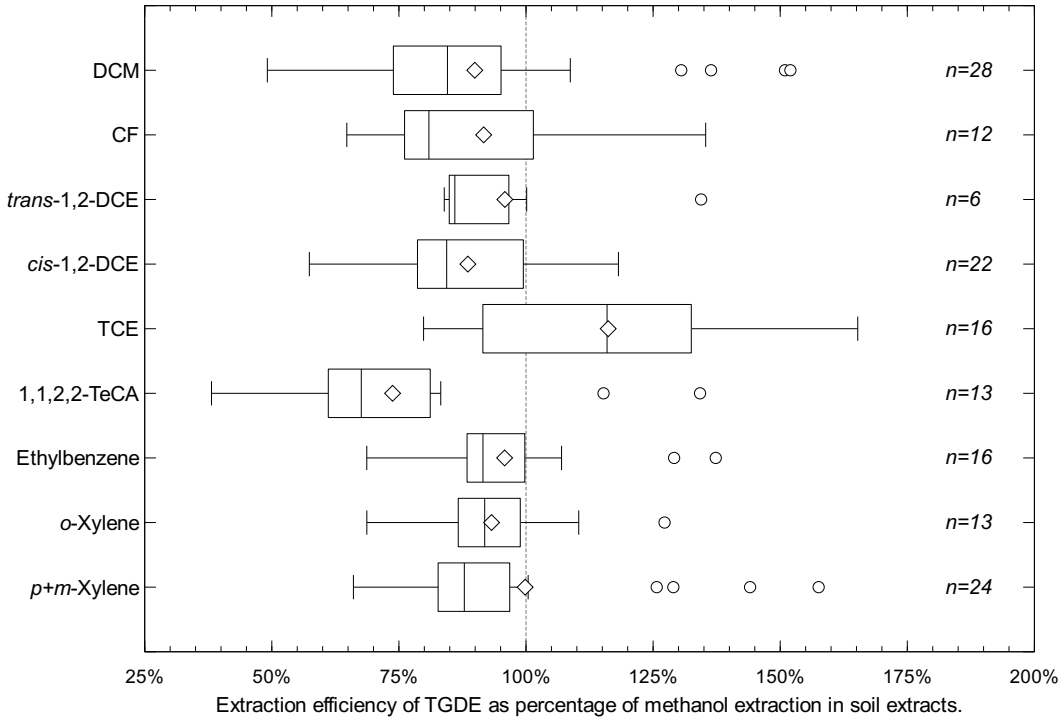

Figure 4.7.: Comparison of extraction efficiency of TGDE compared to methanol for soil extracts from the field site. Diamonds denote mean values, circles are outliers according to $\pm 1.5\times$ interquartile ranges.

efficiency of TGDE compared to methanol is offset by the higher permissible extraction solvent-to-water ratio. Even higher TGDE proportions might be possible when further purifying the TGDE before soil extraction. Compared to direct injection of soil extracts containing VOC, limited to a volume of a few µL for splitless injection, the use of purge & trap allows the analysis of 2.5 mL of TGDE soil extract, or 830 µL of methanol soil extract, in a 25 mL purge vessel, hereby lowering the MDL for compound-specific carbon isotope analysis in soil by up to three orders of magnitude. In comparison to this substantial improvement, the MDL increases by a factor of two for most compounds at high spiking levels of extraction solvents are of little consequence.

The samples from the field site were taken at a soil-to-extraction-solvent ratio of 10 g to 15 g of wet soil in 20 mL of solvent. This yields an MDL for soil of, e.g., 0.22 µg g^{-1} for TCE (calculation in Section C.5 of the supporting information Appendix C). Blessing (2008) obtained MDLs of 10 µg kg^{-1} to 20 µg kg^{-1} or 0.01 µg g^{-1} to 0.02 µg g^{-1} in soil for PAH using a large volume injection of 150 µL extraction solvent, not requiring dilution but rather concentration of the solvent, which is not easily possible for VOC as target compounds. As, for example, the PAH naphtalene contains five times as many carbon atoms as TCE, our MDLs are on a per carbon basis about $2 - -4$ times higher than those obtained by Blessing (2008). As explained in Section 4.1, methods that use a liquid injection of 1 µL solvent have MDLs several orders of magnitude higher. Herrero et al. (2021) have recently reported a carbon CSIA MDL for TCE in soil of 0.034 µg g^{-1} using dimethylacetamide as extraction solvent at a proportion of 20% in water (v/v) in combination with headspace solid-phase microextraction (SPME). The method was tested on a mixture of four aliphatic chlorinated hydrocarbons and might not be easily extended to complex VOC mixtures often found at contaminated sites.

Typical TCE levels encountered in an aquitard downgradient of a TCE source zone might range between 1 and 15 µg g^{-1} (Chapman and Parker 2005), and our method would allow measuring compound-specific $\delta^{13}C$ values even below this range. Depending on soil properties, water extraction might prove favorable as no further dilution is necessary and MDLs are generally lower (Figure 4.3 top). As noted, for our strongly sorbing soil, this extraction method did not yield sufficient recoveries of target compounds.

4.4. Conclusions

We compared the suitability of two different extraction solvents, methanol and TGDE, for compound-specific carbon analysis of a range of petroleum and chlorinated hydrocarbon

contaminants. Two-dimensional chromatography was necessary in order to achieve baseline separation of peaks at high extraction solvent-to-water ratios. Trueness and precision of $\delta^{13}C$ analysis were not compromised compared to pure water as a matrix, although MDLs were elevated for most compounds. A thick-film column capable of high column loading was required in order to keep retention times constant. The GC-GC setup required no additional oven.

TGDE turned out to be a viable alternative to methanol for GC-C-IRMS analysis of matrix-rich soil extracts. Its low vapor pressure is an advantage for purge & trap concentration and allows for a high extraction solvent-to-water ratio of up to 10% (v/v), which could possibly be increased.

The wide range of target compounds with different physicochemical properties that we investigated makes it difficult to draw broad conclusions on purge & trap optimization. For this method, water management must not be disregarded in any kind of matrix when attempting to maximize purge efficiencies. Hence, shorter purge times and lower temperatures may even prove favorable. Dry-purge has been shown to be an important parameter that could be further optimized. The method, as all headspace analysis methods, reaches its limit when semi-volatile compounds such as 1,1,2,2-TeCA need to be analyzed, but can be adapted to many volatile compound target analytes.

For environmental samples, our method allows demonstrating contaminant degradation in lower-permeability layers, broadening the application of carbon CSIA beyond groundwater samples.

Acknowledgments

We would like to thank Professor Tadeusz Górecki (University of Waterloo, Canada) and Professor Violaine Ponsin (Université du Québec à Montréal) for guidance in two-dimensional chromatography. We would also like to thank the field crew who collected the soil samples: Steven Chapman, Flavia Isenschmid, Ryan Kroeker and Nathan Glas. Funding: This work was supported by the Swiss National Science Foundation (SNSF) [grant number 166233].

5. Carbon and chlorine isotope fractionation during abiotic degradation of chlorinated ethenes by ferrous sulfide (FeS)

Jeremy Zimmermann[1], *Daniel Hunkeler*[1]

To be submitted to *Environmental Science & Technology*

Abstract

Chlorinated ethene degradation in the environment may proceed through either biotic or abiotic processes. The degree of degradation can be determined using compound-specific isotope analysis, which requires knowledge of the pathways and enrichment factors. By measuring stable chlorine isotope ratios in addition to stable carbon isotope ratios, pathway-specific and compound-specific dual element isotope slopes can be obtained over time or space. In order to relate slopes measured at a site with the respective pathways, well-constrained laboratory degradation experiments are set up. While dual carbon-chlorine isotope slopes have been measured for the biotic degradation of chlorinated ethenes, for abiotic degradation the focus has in the past been set towards zero-valent iron systems in engineered remediation. Abiotic degradation is preferable as it is likely to yield non-chlorinated, generally non-toxic degradation products. We investigated the degradation of chlorinated ethenes *cis*-1,2-DCE, TCE and PCE by a reactive iron phase that is also found naturally in the environment, iron(II)sulfide (FeS) or mackinawite. We found FeS to be reactive with TCE and PCE, but not with *cis*-1,2-DCE. Carbon-chlorine isotope slopes $\Delta\delta^{13}C/\Delta\delta^{37}Cl$ were 11.0 ± 0.8 for PCE and 4.1 ± 0.2 for TCE. We hypothesize that the difference in chlorine isotope enrichment between PCE ($\varepsilon_{Cl} = -1.5 \pm 0.1‰$) and TCE ($\varepsilon_{Cl} = -5.6 \pm 0.3‰$) may be due to different rate-limiting steps with a primary chlorine isotope effect for TCE and a secondary chlorine isotope effect for PCE. Our obtained

[1]Centre for Hydrogeology and Geothermics, University of Neuchâtel, Rue Emile-Argand 11, 2000 Neuchâtel, Switzerland

enrichment factors offer an important contribution to the applicability of dual element compound-specific isotope analysis at contaminated sites.

5.1. Introduction

Chlorinated ethenes have found many industrial uses. Due to their extensive application and often improper disposal, they have become widespread and persistent soil and groundwater contaminants. At many of these contaminated sites, containment in combination with in situ degradation may be the only viable option for remediation. Initial chlorinated ethene contaminants are usually tetrachloroethene/perchloroethene (PCE) or trichloroethene (TCE).

Degradation of chlorinated ethenes can proceed via a biotic or an abiotic pathway. Biotic degradation can occur naturally or may be stimulated by injecting suitable bacteria cultures and/or electron donors into the subsurface. Abiotic degradation is often the motivation behind reactive barriers, which employ compounds capable of reducing chlorinated ethenes, such as zero-valent iron (ZVI) or zero-valent zinc. In addition to these engineered remediation solutions, there is the potential for abiotic degradation by natural constituents of soil, such as iron-bearing minerals (He et al. 2015).

Various iron-bearing mineral phases have been observed to mediate the degradation of certain chlorinated ethenes at the laboratory scale. Among them are the iron sulfide mackinawite ($Fe(II)_{1.00}S$ to $Fe_{1.07}S$ (Butler and Hayes 1999, 2001; Elsner et al. 2004; Jeong et al. 2007; Liang et al. 2007; Scherer et al. 2007; He et al. 2010; Lan et al. 2016)and pyrite ($Fe(II)S_2$) (Weerasooriya and Dharmasena 2001; Lee and Batchelor 2002a). Further reactive minerals are the iron oxides Fe(II)O (Ingram et al. 2000) and magnetite (Fe_3O_4) (Lee and Batchelor 2002a; Ferrey et al. 2004), iron phyllosilicates such as biotite (Lee and Batchelor 2004) and the iron oxyhydroxide α-FeOOH or goethite (Liang et al. 2009). Green rusts have been reported to degrade chlorinated ethenes (Lee and Batchelor 2002b; Maithreepala and Doong 2005; Scherer et al. 2007; Liang et al. 2009; Choi et al. 2010; Jeong et al. 2011; Han et al. 2012; Jeong et al. 2013; Bhave and Shejwalkar 2018). These are mixed Fe(II)/Fe(III) hydroxides that consist of alternating iron hydroxide cation layers and hydrated anion layers, the latter typically being chloride, sulfate or carbonate (O'Loughlin and Burris 2004).

There is a strong interest in demonstrating abiotic degradation at contaminated sites. Engineered remediation only leads to a partial contaminant removal while the remainder is subject to monitored natural attenuation (Kent and Mosquera 2001). As opposed to

petroleum hydrocarbons, which may degrade in both aerobic and anaerobic environments, the degradation of PCE and TCE usually requires sufficiently reducing conditions. For this reason, the biotic dechlorination of PCE and TCE is often incomplete. Further obstacles may be a low electron donor availability and the absence of dehalogenating microorganisms (Chapelle et al. 2003). In this context, abiotic degradation can be a key factor, but it is difficult to demonstrate unequivocally. Though generally slower than biotic degradation (Tobiszewski and Namieśnik 2012), the abiotic degradation of chlorinated ethenes is likely to produce non-chlorinated, generally non-toxic degradation products (Figure 5.1) and is capable of fully eliminating residual contamination.

While a hydrogeochemical characterization of the aquifer can help to constrain the expected degradation pathway at a particular field site, it is not advisable to rely solely on this approach. The same holds true for the monitoring for characteristic degradation products, as these may be unspecific or not adequately captured by the sampling method. Compound-specific isotope analysis (CSIA) is an established method to distinguish degradation pathways and to calculate the fraction of degraded contaminant during monitored natural attenuation and has the advantage of not relying solely on concentration measurements. The reaction-, compound-, and isotope-specific enrichment factor ε that is required for these evaluations is obtained through controlled laboratory studies.

Carbon isotope enrichment ($\Delta\delta^{13}C$) during abiotic degradation of chlorinated ethenes by natural constituents of soil has been observed by Zwank et al. (2005a), Liang et al. (2007), Dong et al. (2009), and Liang et al. (2009) on the laboratory scale. By following the progression of the isotope ratio of an additional element, such as chlorine, the underlying processes during degradation can be better constrained. By plotting the shift Δ in δ values for two elements during degradation against each other, a dual element isotope plot is obtained. The combined shift in isotope ratios, i.e. $\Delta\delta^{13}C$ versus $\Delta\delta^{37}Cl$, forms the slope of the regression line. This slope is generally not affected by non-reactive processes and is specific to the reaction pathway.

For the abiotic degradation of chlorinated ethenes, this dual element carbon and chlorine isotope approach has so far only been applied to reactions with ZVI (Audí-Miró et al. 2013). Dual element carbon-chlorine isotope slopes for reactions of chlorinated ethenes with natural constituents of soil have not yet been reported. For the reaction of TCE with ZVI, Audí-Miró et al. (2013) observed a combined hydrogenolysis and dichloroelimination pathway with a cleavage of a C-Cl bond as the rate-limiting step and no masking of this isotope effect.

The primary objective of the present study was to obtain dual element isotope plots for the reaction of the chlorinated ethenes PCE, TCE, and *cis*-1,2-DCE with FeS in batch

reactors. In addition, chlorinated and non-chlorinated degradation products were monitored. Due to the generally slow process of abiotic degradation, the focus was set on an iron phase that has been proven to degrade chlorinated ethenes within a reasonable time-scale that would allow obtaining said dual element isotope plots. Studies by Butler et al. (2009) have shown FeS to be the most reactive iron phase for the degradation of PCE and TCE. We performed preliminary tests indicating that neither synthesized chloride green rust, in agreement with the findings reported by Mangayayam et al. (2018), nor pyrite, similar to what has been reported by Pham et al. (2008), were capable of reducing chlorinated ethenes at our experimental conditions.

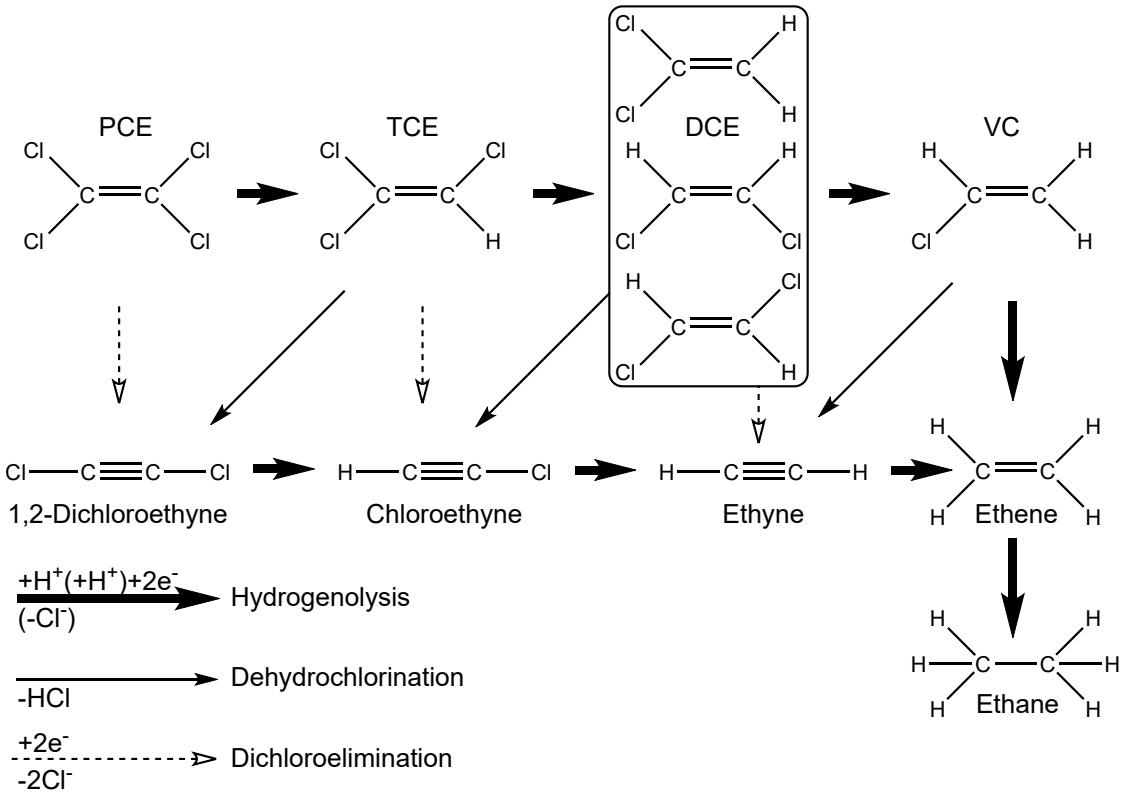

Figure 5.1.: Possible degradation pathways of the initial contaminants PCE and TCE and the chlorinated biotic degradation products DCE and VC. Abiotic degradation has been observed to yield non-chlorinated degradation products. Modified after Brown et al. (2006), first published in Zimmermann et al. (2020).

FeS occurs in the natural environment. It is a precursor of pyrite or greigite (Fe_3S_4) in sedimentary and hydrothermal systems (Rickard 1969; Lennie 1995), and may stem from

the reaction between iron minerals such as goethite and aqueous sulfide species (Butler and Hayes 2001).

5.2. Material and methods

5.2.1. Chemicals

The following chemicals were obtained: iron(II)chloride tetrahydrate ($FeCl_2{\cdot}4\,H_2O$) at $\geq$ 99% purity, sodium sulfide nonahydrate ($Na_2S{\cdot}9\,H_2O$) at $>$ 98% purity, analytical reagent grade tris(hydroxymethyl)aminomethane and hydrochloric acid. The chlorinated ethene *cis*-1,2-DCE was obtained at 99% purity, TCE at $\geq$ 99.5% purity, and PCE at $\geq$ 99.5% purity. For quantification of non-chlorinated hydrocarbons, a gaseous mixture of ethyne/acetylene, ethene and ethane in N_2 at 100 ppm v/v each was purchased from Messer. Standards for concentration and isotope analysis of chlorinated hydrocarbons were prepared gravimetrically in HPLC grade methanol. Ultrapure double deionized deoxygenated water (deox-DDIW) was used for all procedures. For deoxygenating, it was purged with N_2 in a 2 L laboratory bottle for at least one hour (Butler et al. 1994), while applying a vacuum and while submerged in an ultrasonic bath. 0.1 M Tris buffer was prepared in deox-DDIW and adjusted to pH 7.5 with 0.1 M HCl.

Stock solutions of chlorinated ethenes for spiking were prepared by measuring volumes of pure compound using microliter syringes and injecting them through a PTFE-coated septa into 0.1 M Tris buffer in a 250 mL bottle. After dissolution with a magnetic stirrer, the chlorinated ethene concentration of the respective stock solution was 130 mg L^{-1}.

5.2.2. Preparation of FeS

FeS was synthesized in a 1 L reaction vessel equipped with a magnetic stirrer, a pH probe, a burette and a gas bubbler for inert gas (N_2). Solid reagents were added through an opening against the counter flow of inert gas. The setup allowed the mineral precipitate to be transferred into other vessels through PTFE tubing without exposing them to oxygen, by applying an overpressure of N_2.

FeS was synthesized according to Scherer et al. (2007) by adding 1.1 M $Na_2S{\cdot}9\,H_2O$, prepared by dissolving 76.3 g of $Na_2S{\cdot}9\,H_2O$ in 300 mL deox-DDIW, to 0.57 M $FeCl_2$, prepared by dissolving 56.6 g of $FeCl_2{\cdot}4\,H_2O$ in 500 mL deox-DDIW. The black precipitate was transferred to centrifuge bottles and rinsed by undergoing several cycles of centrifuging, decanting of the supernatant and resuspending with deox-DDIW.

5.2.3. Maintenance of anoxic conditions

During synthesis and rinsing of iron phases, a constant flushing of N_2 was ensured. For FeS the unchanged black color and sulfide odor indicated that it was not oxidized during manipulations (Butler and Hayes 1998). The preparation of batch reactors was carried out inside a glovebox with an internal palladium catalyst regenerator (Plas-Labs 855-AC) filled with a mixture of 10% H_2 in N_2. Anoxic conditions were verified using anaerobic indicator test strips. Additionally, an active carbon filter fan was kept running inside the glovebox to remove traces of chlorinated ethenes, as these may decrease the performance of the catalyst.

5.2.4. Experimental setup

To avoid any effects of repetitive sampling from the same batch reactor on the isotope slopes (Buchner et al. 2017), a series of identical batch reactors were prepared. Batch reactors with FeS were prepared in 42 mL glass vials capped with a PTFE-coated septa and screw caps. The synthesized FeS was neither dried nor lyophilized to preclude any oxidation. Instead, it was handled as suspension or slurry, following the example of O'Loughlin and Burris (2004) and He et al. (2010).

The batch experiments were buffered to achieve pH values more similar to ones found in the natural environment. Preliminary experiments showed that Tris buffer does not inhibit the degradation of chlorinated ethenes by FeS. The FeS batches contained 20 mL Tris deox-DDIW, 5 mL of FeS slurry and 10 mL of stock solution of the respective solvent, prepared in Tris deox-DDIW. This resulted in a liquid volume of 35 mL and 7 mL of headspace. The initial solvent concentration in the batches was 37 mg L^{-1}. Controls were prepared by substituting the FeS slurry with an equivalent volume of Tris deox-DDIW.

Diffusion of chlorinated solvents is enhanced in headspace compared to the liquid phase. To limit losses of solvents through the septum cap, the batch reactors were kept with the cap towards the bottom, in order for the headspace to not be in contact with the septum. The batch reactors were put in a container filled with water to further limit diffusive losses, and the container was set on a laboratory shaker at room temperature in the dark. At selected intervals, batch reactors were sacrificed and analyzed in duplicate, together with a control. Concentrations of non-chlorinated C_2-hydrocarbons were measured in headspace, while concentrations and isotope ratios of chlorinated hydrocarbons were measured in the liquid phase of the batch reactors.

5.2.5. Concentration analysis

Acetylene/ethyne, ethene and ethane were analyzed by chilling the batch reactors to a temperature of 10 °C, then removing either 50 µL or 1000 µL of headspace gas through the septum using a gas-tight syringe, depending on the expected concentration level, and injecting it into an SRI 310 gas chromatograph equipped with a flame ionization detector. The compounds were separated isothermally at 35 °C on a packed Hayesep column using N_2 as carrier gas. Calibration standards were prepared using gas-tight syringes by diluting the gaseous standard in 120 mL septum-capped laboratory bottles that had been flushed with N_2. Separate 3-point calibration curves for the injection of either 50 µL or 1000 µL of the gaseous standard were obtained. To calculate aqueous concentrations of the compounds from the measured gaseous concentrations, standard operating procedure RSKSOP-175 (US EPA 2004) was applied, taking into account the sample temperature, headspace-to-liquid ratios and Henry coefficients of the solvents.

Chlorinated ethene concentrations were measured on an Agilent 7890A gas chromatograph (GC) coupled to an Agilent 5975C quadrupole mass spectrometer (qMS). The batch reactors were centrifuged, opened, part of the liquid phase removed and diluted in ultrapure water in septum-capped 20 mL headspace vials for a final liquid volume of 15 mL. A 5-point calibration curve was prepared by diluting the methanol standard in ultrapure water, then diluting this intermediate solution in headspace vials to a final liquid volume of 15 mL.

5.2.6. Carbon isotope analysis

For carbon isotope analysis, solutions from the batch reactors were diluted in ultrapure water in 42 mL glass vials capped with PTFE-coated septa. Compounds were concentrated by a Teledyne Tekmar Stratum purge & trap system, injected splitlessly into an Agilent 7890A GC, and converted to CO_2 in an Isoprime GC5 combustion interface. Carbon isotope ratios were measured with an Isoprime 100 IRMS. Samples were analyzed in duplicate. Standards that had been characterized isotopically using EA were analyzed during each sequence to correct for isotopic fractionation during measurements. Concentrations were kept within the previously determined isotopic linearity limits. For carbon, the ratio of ^{13}C to ^{12}C of a sample R_{sample} is expressed using the delta (δ) notation as per mille (‰) difference from the isotope ratio in the reference standard Vienna Pee Dee Belemnite (VPDB):

$$\delta^{13}C = \frac{R_{sample}}{R_{VPDB}} - 1 \qquad (‰) \tag{5.1}$$

5.2.7. Chlorine isotope analysis

For chlorine isotope analysis, liquid from the batch reactors was diluted in 15 mL ultrapure water in 20 mL glass headspace vials capped with PTFE-coated septa and analyzed for compound-specific chlorine isotope ratios using GC-qMS. After injection of 1 mL headspace using a CombiPAL (CTC Analytics) autosampler into an Agilent 7890A using a split ratio of 1:20, peaks were analyzed with an Agilent 5975C qMS in selected ion mode. For *cis*-1,2-DCE, masses 61, 63, 96 and 98, for TCE, masses 130 and 132 and for PCE, masses 129 and 131 were analyzed. Chlorine isotope ratios were calculated from the mass intensities using sets of stochastically derived equations (Jin et al. 2011).

For chlorine, the ratio of ^{37}Cl to ^{35}Cl of a sample R_{sample} is expressed using the delta (δ) notation as per mille (‰) difference from the isotope ratio in the reference standard Standard Mean Ocean Chloride (SMOC) according to Equation 5.2:

$$\delta^{37}\mathrm{Cl} = \frac{R_{sample}}{R_{SMOC}} - 1 \qquad (‰) \tag{5.2}$$

In order to obtain SMOC-referenced values, sets of two compound-specific standards of differing chlorine isotope ratio were analyzed at the beginning and end of each sequence. For *cis*-1,2-DCE, these were standards cDCE-F and IS63 with δ^{37}Cl SMOC values of -1.52‰ and $+0.07$‰, TCE standards EIL-1 ($+3.05$‰) and EIL-2 (-2.7‰) and PCE standards EIL-1 ($+0.3$‰) and EIL-2 (-2.5‰). Using a two-point isotopic calibration, SMOC-referenced δ^{37}Cl values were calculated from the chlorine isotope ratios. Each sample and standard was analyzed ten times, removing five times 1 mL from two vials each. Concentrations of samples and standards were kept within a narrow range of 80 µg L^{-1} to 120 µg L^{-1} in aqueous solution. Standard deviations 1σ for repeat measurements remained below 0.5‰.

5.2.8. Isotope data evaluation

Isotopic data was evaluated by calculating carbon and chlorine isotopic enrichment factors ε using the Rayleigh equation (5.3):

$$\frac{R_t}{R_0} = f^{\varepsilon} \tag{5.3}$$

Where R_0 describes the initial isotope ratio at the beginning of the transformation process, R_t the isotope ratio and f the remaining fraction of the compound at a point in time t. The isotopic specific bulk enrichment factor ε_C or ε_{Cl} is given by the slope of the least-squares

regression for a double-logarithmic plot of isotope ratios, calculated from δ values, over f (Equation 5.4):

$$ln(\frac{\delta_t + 1000}{\delta_0 + 1000}) = \varepsilon \times ln(f) \tag{5.4}$$

where δ_t refers to the isotopic composition at a point in time t and δ_0 to the initial isotopic composition. In accordance with Scott et al. (2004)'s guidelines, uncertainties in concentration measurements were not incorporated into the regression, and the regression was not forced through the origin. Due to losses of about 50% of the initial target compounds over the course of the experiments, the fraction f was calculated by dividing the concentration of the batch c_t by that of the control c_0. Dual element isotope slopes were obtained by plotting the δ values for carbon and chlorine against each other, taking into account isotopic measurement uncertainty in both axes.

5.3. Results and discussion

5.3.1. Carbon and chlorine isotope enrichment during degradation by FeS

PCE and TCE were degraded by FeS at pH 7.5–8.1. At the end of the experiment, PCE and TCE concentrations were at less than 10% of their initial concentrations. As opposed to PCE and TCE, *cis*-1,2-DCE showed no reaction, which is in agreement with Jeong et al. (2007) and Jeong et al. (2011)'s findings. Controls without FeS did not indicate any degradation of chlorinated ethenes.

No chlorinated ethene degradation products were detected; instead, both solvents reacted almost quantitatively to acetylene, with ethene and ethane appearing only at trace levels (data not shown). This is consistent with the studies performed by Butler and Hayes (2001), Jeong et al. (2007), Liang et al. (2007), Scherer et al. (2007), and He et al. (2010).

The formation of acetylene is indicative of a reductive dichloroelimination or β-elimination pathway, that first yields 1,2-dichloroacetylene in the case of PCE and chloroacetylene in the case of TCE (Figure 5.1), which are then further transformed to acetylene. While these chlorinated intermediates were not monitored, they are rarely found at detectable levels in degradation studies (O'Loughlin et al. 2003; Lee and Batchelor 2004). The reason is that chlorinated acetylenes are rapidly decaying, transient intermediates (Arnold and Roberts 2000; Schaefer et al. 2013). As no accumulation of the non-reactive *cis*-1,2-DCE was observed, the hydrogenolysis pathway can be ruled out. The large degree of degradation allowed obtaining carbon and chlorine isotopic enrichment factors and dual element slopes for PCE and TCE (Figure 5.2).

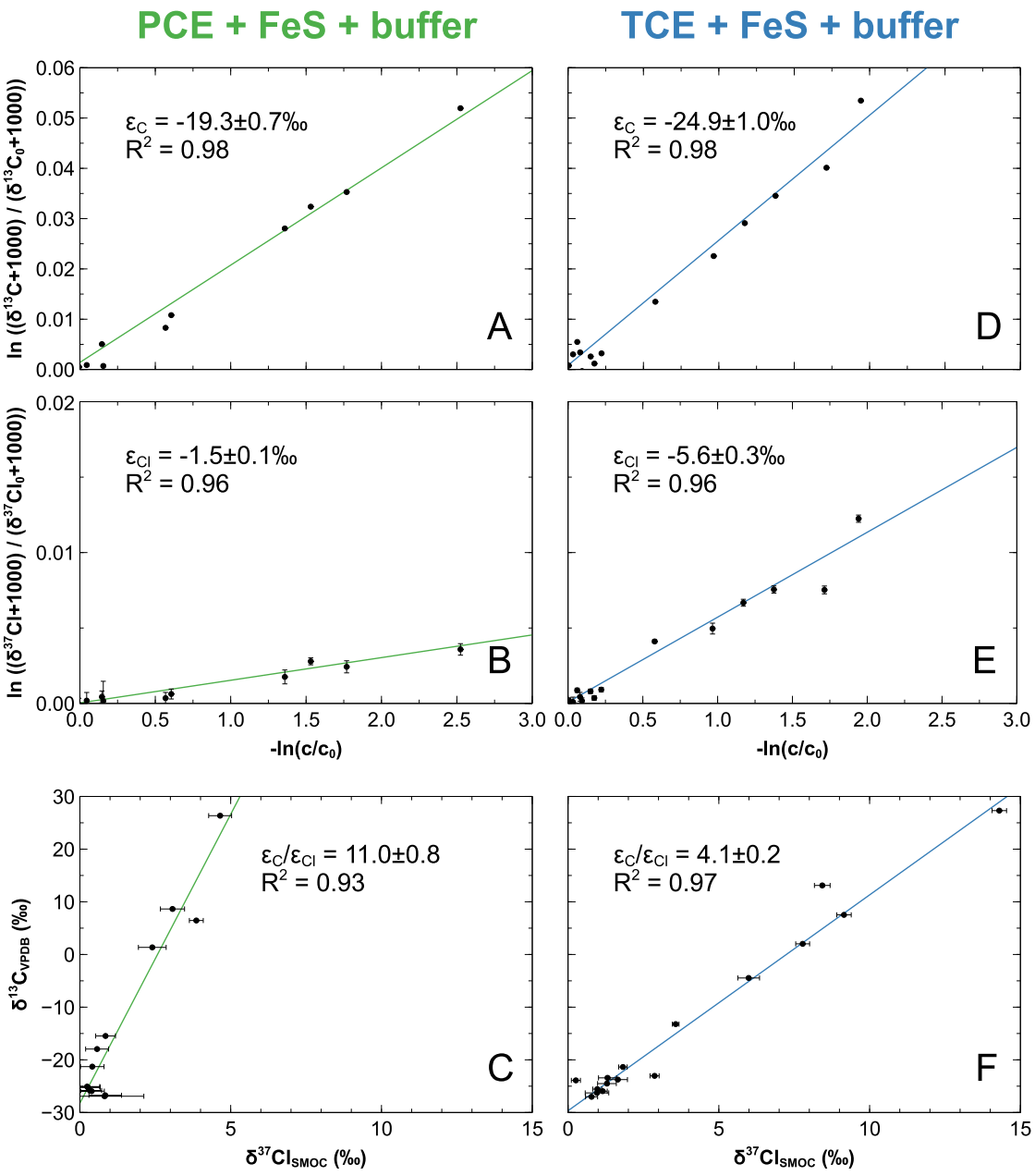

Figure 5.2.: Linearized Rayleigh plots, bulk carbon enrichment factors ε_C (A, D) and bulk chlorine enrichment factors ε_{Cl} (B, E) for PCE (left panels) and TCE (right panels) for the degradation by FeS. Dual carbon-chlorine isotope plots and $\varepsilon_C/\varepsilon_{Cl}$ slopes for PCE (C) and TCE (F).

Tetrachloroethene

The carbon isotopic signature of PCE changed from −27.6‰ to +26.3‰ VPDB over the course of the reaction, yielding an ε_C of -19.3 ± 0.7‰ (Figure 5.2A). Dayan et al. (1999) obtained an ε_C value of −25.3‰ for the reaction of PCE with ZVI, which however took a hydrogenolysis pathway, as only chlorinated ethenes were detected as degradation products. For the reaction with FeS, Liang et al. (2007) measured ε_C values for PCE of -30.2 ± 4.3‰ at pH 7, -29.54 ± 0.83‰ at pH 8, and -24.6 ± 1.1‰ at pH 9. The authors suspected that PCE degradation mainly took a dichloroelimination pathway, but could not confirm this due to difficulties in quantifying acetylene. For abiotic degradation, ε_C values are in general larger in magnitude compared to biotic degradation. The highest PCE ε_C reported for biotic degradation is -19.0 ± 0.9‰ by Cretnik et al. (2014), this however being measured for a hydrogenolysis pathway to TCE.

As for the chlorine isotope enrichment, a PCE ε_{Cl} value of -1.5 ± 0.1‰ (Figure 5.2B) was obtained. This is similar to many ε_{Cl} values measured for biotic degradation of PCE (Figure 5.3). However, the resulting dual $\Delta\delta^{13}C/\Delta\delta^{37}Cl$ slope of 11.0 ± 0.8 (Figure 5.2C) is significantly higher than all slopes reported so far in the literature for biotic degradation (Figure 5.3A), with the maximum slope reported at 3.8 ± 0.2 (Cretnik et al. 2014). Hence, while our obtained ε_C of -19.3 ± 0.7‰ by itself would not be sufficiently indicative of abiotic degradation by FeS, the $\Delta\delta^{13}C/\Delta\delta^{37}Cl$ slope is unambiguous.

Trichloroethene

The $\delta^{13}C$ value for TCE reacting with FeS changed from the initial value of −27.0‰ to +27.3‰ VPDB over the course of the experiment. This results in a bulk enrichment factor ε_C of -24.9 ± 1.0‰ (Figure 5.2D). For biotic degradation of TCE, which typically proceeds via sequential hydrogenolysis, the largest negative ε_C has been reported as −20.2‰ (Renpenning et al. 2014).

One might suspect that the reaction pathway for a degradation of TCE by FeS is the same as the ones observed for reactions with zero-valent iron (ZVI). However, our measured ε_C is larger in magnitude than most ε_C reported in the literature for ZVI, with reported values ranging from −2.4‰ (Sakaguchi-Söder et al. 2007) to −8.6‰ (Dayan et al. 1999), −10.1‰ (Schüth et al. 2003) and -14.8 ± 0.6 (Audí-Miró et al. 2013). Indeed, Audí-Miró et al. (2013) have identified a sequential hydrogenolysis pathway in addition to the dichloroelimination pathway for the reaction with ZVI. Only certain nanoscale ZVI (Elsner et al. 2008) or a surface treatment of the ZVI (Slater et al. 2002) have yielded TCE ε_C values comparable to ours. Slater et al. (2002) obtained ε_C values starting from −16.4‰

that increased to −24.8‰ after acid cleaning of the ZVI to remove surface oxidation. Elsner et al. (2008) have measured ε_C values of up to -26.5 ± 1.5‰ (TCE) with nanoscale ZVI, the reaction being characterized by a 90% contribution of the dichloroelimination pathway and a 10% contribution of the hydrogenolysis pathway. For FeS, Liang et al. (2007) have measured ε_C values for TCE reacting of -33.4 ± 1.5‰ at pH 8 and -27.9 ± 1.3‰ at pH 9, identifying only a minor hydrogenolysis pathway, which is in good agreement with our ε_C values.

We also measured a pronounced chlorine isotope effect; with a bulk enrichment factor ε_{Cl} of -5.6 ± 0.3‰ (Figure 5.2E). The δ^{37}Cl SMOC value increased from 0.8‰ to 14.3‰ over the course of the experiment (Figure 5.2F). The ε_{Cl} value is higher in magnitude than all ε_{Cl} values for biotic degradation of TCE compiled by Ojeda et al. (2019a) and Zimmermann et al. (2020). The value is also higher in magnitude than those measured by Audí-Miró et al. (2013) for TCE degradation with ZVI, ε_{Cl} of -2.6 ± 0.1‰. For the dual carbon-chlorine isotope plots, we determined a $\Delta\delta^{13}$C/ $\Delta\delta^{37}$Cl slope of 4.1 ± 0.2 (Figure 5.2F).

Figure 5.3B shows how our carbon and chlorine isotope enrichment factors for TCE compare to those measured in other studies for biotic and abiotic degradation. The $\varepsilon_C/\varepsilon_{Cl}$ ratio is similar to what has been reported for other TCE degradation experiments. As a consequence, it appears that is not the slope, but instead the large magnitudes of both the carbon and chlorine enrichment factors that are specific to this dichloroelimination reaction mechanism by FeS.

5.3.2. Proposed reaction mechanisms for TCE and PCE degradation by FeS

The ε_{Cl} for PCE for the degradation by FeS is smaller in magnitude than that observed for TCE, leading to a vastly larger dual C-Cl slope, although our evidence shows that both solvents are degraded via a dichloroelimination pathway. This prompts us to bring forth a discussion of possible differences in rate-limiting steps between the reaction mechanisms.

The abiotic dechlorination of TCE and PCE is a surface-mediated, not an aqueous phase process (Elsner et al. 2004). The hydrophobic character of FeS enhances sorption of chlorinated ethenes (He et al. 2010). The large ε_{Cl} and ε_C for TCE indicate that a carbon-chlorine bond is cleaved in the rate-limiting step. As the $\varepsilon_C/\varepsilon_{Cl}$ ratio is similar to other TCE degradation pathways where hydrogenolysis has been observed, we suspect that the rate-limiting steps for both dichloroelimination and hydrogenolysis are the same carbon-chlorine bond cleavage. A possible dichloroelimination pathway is sketched in Figure 5.4 (bottom) as proposed by Butler and Hayes (1999, 2001). Initially, ethenyl (vinyl)

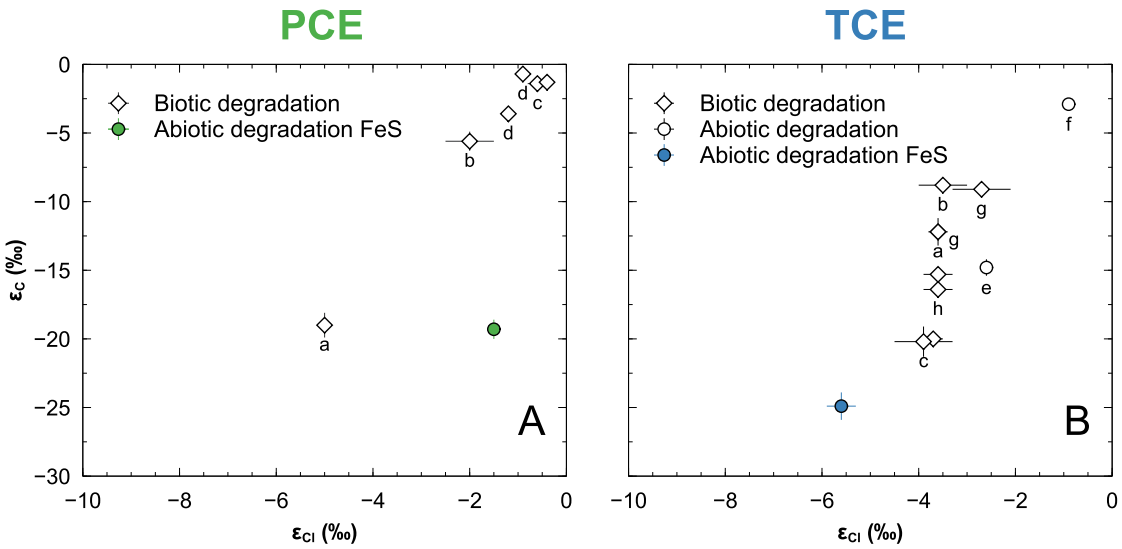

Figure 5.3.: Comparison of carbon (ε_C) and chlorine (ε_{Cl}) bulk enrichment factors for biotic degradation (diamonds) and abiotic degradation (circles) of PCE (A) and TCE (B). Filled-in symbols represent results from our present study. Data from a Cretnik et al. (2014); b Wiegert et al. (2013); c Renpenning et al. (2014); d Badin et al. (2014); e Audí-Miró et al. (2013); f Liu et al. (2014); g Cretnik et al. (2013).

intermediates are formed through cleavage of the C-Cl bond, while the C=C double bond remains intact. For PCE, the dichloroelimination may instead proceed as suggested by Arnold and Roberts (2000) for ZVI by formation of σ-bonds to the reactant surface (Figure 5.4 top). In this rate-limiting step, the C=C double bond is cleaved leading to a primary carbon isotope effect, while the chlorine isotope effect would only be secondary. The underlying effect that causes the difference in dichloroelimination pathways between TCE and PCE may be a difference in sorption behavior, due to a higher aqueous solubility of TCE versus PCE. Additionally, it has been shown for ZVI that electron charges that are transmitted from the reactive surface are higher for PCE versus TCE (Luo and Farrell 2013).

5.4. Environmental significance

The role of abiotic degradation for attenuation of chlorinated ethene contaminations in the subsurface is currently not well understood. Dual carbon-chlorine compound-specific isotope analysis can help in identifying to what extent abiotic degradation occurs in the subsurface environment. Our results indicate that for PCE, ε_C on its own is not indicative of the

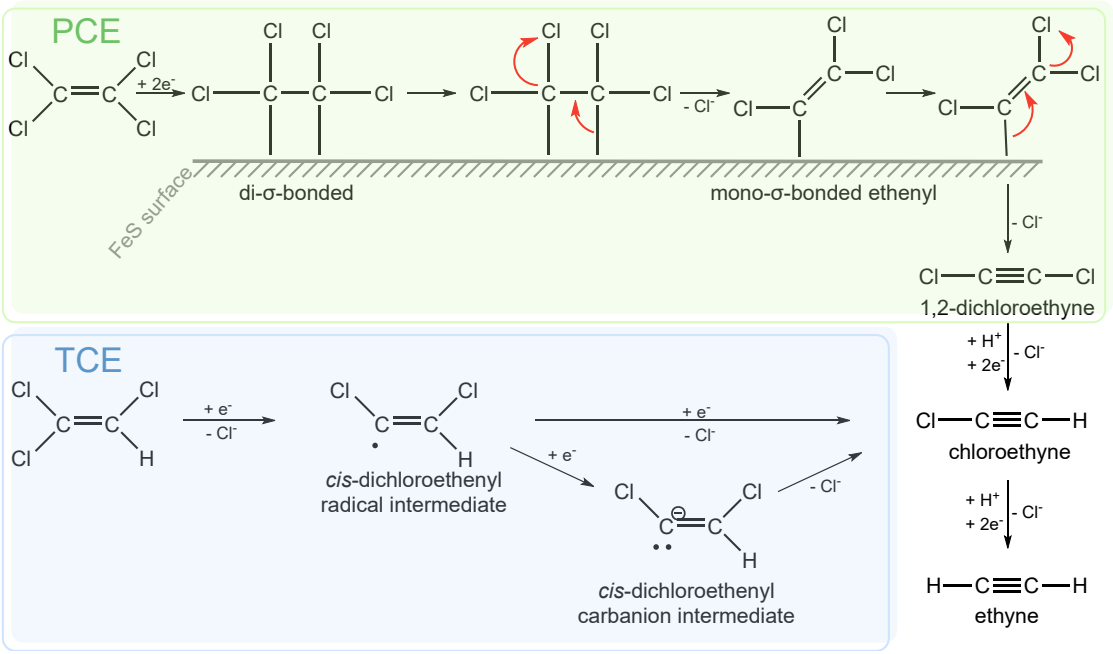

Figure 5.4.: Hypothesized dichloroelimination pathways for the abiotic reductive dechlorination of PCE, modified after Arnold and Roberts (2000), and TCE, modified after Butler and Hayes (1999, 2001). The pathway for PCE proceeds via di-σ-bonded and mono-σ-bonded intermediates, involving cleavage of the C=C double bond, to yield 1,2-dichloroethyne, which is then further reduced via hydrogenolysis to chloroethyne and finally ethyne. TCE is reduced via radical ethenyl (vinyl) intermediate and possibly a carbanion intermediate to yield chloroethyne, which is further reduced to ethyne. Another possible pathway that is caused by a concerted two-electron reduction through nucleophilic addition is not shown, but deemed unlikely (Butler and Hayes 1999).

abiotic degradation pathway, while in combination with chlorine isotopic data, the $\Delta\delta^{13}C/\Delta\delta^{37}Cl$ slope is very distinctive from biotic pathways. For TCE, the large bulk carbon and chlorine enrichment factors ε_C and ε_{Cl} are indicative of abiotic degradation by FeS.

In order to determine whether this abiotic pathway occurs at a field site, compound-specific isotope analysis has an important advantage over the monitoring of non-chlorinated degradation products. The gaseous degradation products acetylene, ethene and ethane do not typically accumulate in groundwater due to their volatility, and acetylene may be further degraded biotically (Akob et al. 2018).

While FeS, or mackinawite in its highly crystalline form, is not the thermodynamically favorable iron sulfide phase in most of the natural environment, it is however metastable and can persist for long time periods under ambient conditions (Butler and Hayes 2001; Jeong et al. 2011). Berns et al. (2019) have recently shown that abiotic degradation processes may strongly contribute to chlorinated contaminant attenuation at sites where the availability of electron donors for biotic degradation is limited. As opposed to bacteria cultures or the ZVI used in engineered remediation, our study has shown that FeS reduces PCE and TCE to non-toxic degradation products, with no accumulation of chlorinated degradation products.

Acknowledgments

We would like to thank the Swiss National Science Foundation (SNSF) [grant number 166233] for supporting this work.

6. Assessing the impact of reactive back-diffusion on a complex chlorohydrocarbon plume using compound-specific isotope analysis

Jeremy Zimmermann[1], Daniel Hunkeler[1]
In preparation

Abstract

The effect of source isolation on contaminant longevity was assessed at a site contaminated by a complex mixture of BTEX and chlorinated ethanes, ethenes and methanes. Through soil and groundwater concentration profiles over time and space, we highlight the importance of forward diffusion into low-permeability zones, degradation, and back-diffusion of initial contaminants and degradation products after source isolation. Compound-specific carbon and chlorine isotope analysis of groundwater and soil extracts shows that chloroform is degraded to dichloromethane through hydrogenolysis, while 1,1,2,2-tetrachloroethane is degraded to trichloroethene through dehydrochlorination and to *cis*-1,2-dichloroethene through dichloroelimination. The study highlights the potential of applying compound-specific isotope analysis not only to groundwater, but also to soil.

[1]Centre for Hydrogeology and Geothermics, University of Neuchâtel, Rue Emile-Argand 11, 2000 Neuchâtel, Switzerland

6.1. Introduction

Chlorinated hydrocarbons have found many industrial uses (Zimmermann et al. 2020) and are common subsurface contaminants (Panagos et al. 2013). Typically they have been released as dense non-aqueous phase liquids (DNAPL), distribute in complex patterns as a function of geological heterogeneity, and often accumulate on top of lower-permeability layers. These contaminants may diffuse into lower-permeability layers where storage is enhanced by sorption (Parker et al. 2004). Even if the NAPL source is completely removed, back-diffusion from these layers can lead to persistent contaminant plumes (Liu and Ball 2002; Chapman and Parker 2005; Tatti et al. 2016), often rendering unfeasible any engineered remediation efforts that aim to restore the affected aquifers to background conditions (Kent and Mosquera 2001). The back-diffusion flux is strongly influenced by contaminant degradation in the lower-permeability layers (Wanner et al. 2016). However, it is challenging to demonstrate degradation in lower-permeability units, especially at sites with complex contaminant mixtures.

Compound-specific isotope analysis (CSIA) is an established method to demonstrate contaminant degradation in the subsurface and is often applied to volatile organic compounds (VOC) in groundwater samples. The principle is based on monitoring the isotopic ratio of one (δ^{13}C) or more elements (δ^{37}Cl, δ^{2}H) of the parent compounds and/or degradation products. Chemical bonds involving the heavier isotope(s) are slightly stronger than those involving the light isotope, leading to a heavy isotope enrichment in the residual compound pool and a depletion in the degradation products. CSIA can be applied to identify different degradation mechanisms, to quantify the degree of degradation, and to differentiate contaminant sources (Wiegert et al. 2012; Zimmermann et al. 2020). Degradation mechanisms can be better constrained when using dual element isotope analysis.

An important scenario for CSIA arises when investigating the effect of remediation on the long-term behavior of complex contaminant plumes. The degradation of complex mixtures is challenging to track through simple monitoring of degradation products, as different initial contaminants may lead to the same degradation products or be further degraded. Here, CSIA offers a distinct advantage.

We present a follow-up study to the results published by Wanner et al. (2018) at a well-characterized field site contaminated by a complex contaminant mixture. Ten years after source removal and isolation, we monitor the effect of the remediation efforts and evolution of the contaminant plume using CSIA. Our study aims to track degradation pathways and examine the importance of reactive aquitards in post-remediation scenarios. To this end, we present spatially and temporally resolved concentration and carbon isotopic

data for contaminants in both groundwater and soil as well as chlorine isotopic data for better constraining degradation processes.

6.2. Site description

The investigated field site is the location of a former manufacturing plant located at an altitude of 30 m ASL on a coastal plain. Here, sandy clay and clayey sand form an unconsolidated aquifer with a thickness of about 8 m, which is underlain by a 1 m thick clay aquitard, right above it a layer of clean sand with a high hydraulic conductivity (Gilmore 2010; Isenschmid 2018). Below the aquitard, sand and clay form another aquifer. Figure 6.1B shows a geological cross section of the site approximately along the groundwater flow direction.

A complex mixture of chlorinated and petroleum hydrocarbons was disposed of below ground in the 1960s, forming a downgradient plume in the heterogeneous sandy aquifer, with diffusion occurring into a thin underlying aquitard. The NAPL source was isolated from the active groundwater flow system by soil mixing with bentonite and zero-valent iron (Figure 6.1A and B) in December of 2007 (Wanner et al. 2018). The bentonite is meant to lower the hydraulic conductivity, while the zero-valent iron (ZVI) donates electrons for enhanced chlorohydrocarbon reduction. The initial contaminant mixture consisted of 1,1,2,2-tetrachloroethane (1,1,2,2-TeCA), tetrachloroethene/perchloroethene (PCE), carbon tetrachloride/tetrachloromethane (CT), chloroform/trichloromethane (CF), and, additionally, petroleum hydrocarbons (BTEX). Multilevel wells CMT-5, CMT-8 and CMT-10 with three ports each were installed along a longsect in the direction of groundwater flow to capture the supposed center line of the plume (Figure 6.1A and B).

The initial chlorinated contaminants can take different degradation pathways. These may partially overlap, i.e. lead to identical degradation products. Figure 6.2 shows possible degradation pathways for the initial contaminants, which are printed in bold. The pathways for the chlorinated C_2-hydrocarbons, the chlorinated ethanes and ethenes, are partially intertwined, while the pathway for the degradation of CT to CF to DCM is independent. 1,1,2,2-TeCA can follow a sequential hydrogenolysis pathway to lesser chlorinated ethanes, but can also take dehydrochlorination (dehydrohalogenation) or dichloroelimination pathways to form chlorinated ethenes. The dichloroelimination pathway is possible during abiotic degradation by ZVI, yielding *cis*-1,2-DCE and *trans*-1,2-DCE at a ratio of approximately 2:1 (Arnold et al. 2002). The dehydrochlorination or hydrolysis/elimination pathway of 1,1,2,2-TeCA is not a redox reaction and does not require specialized dehalogenating cultures, but

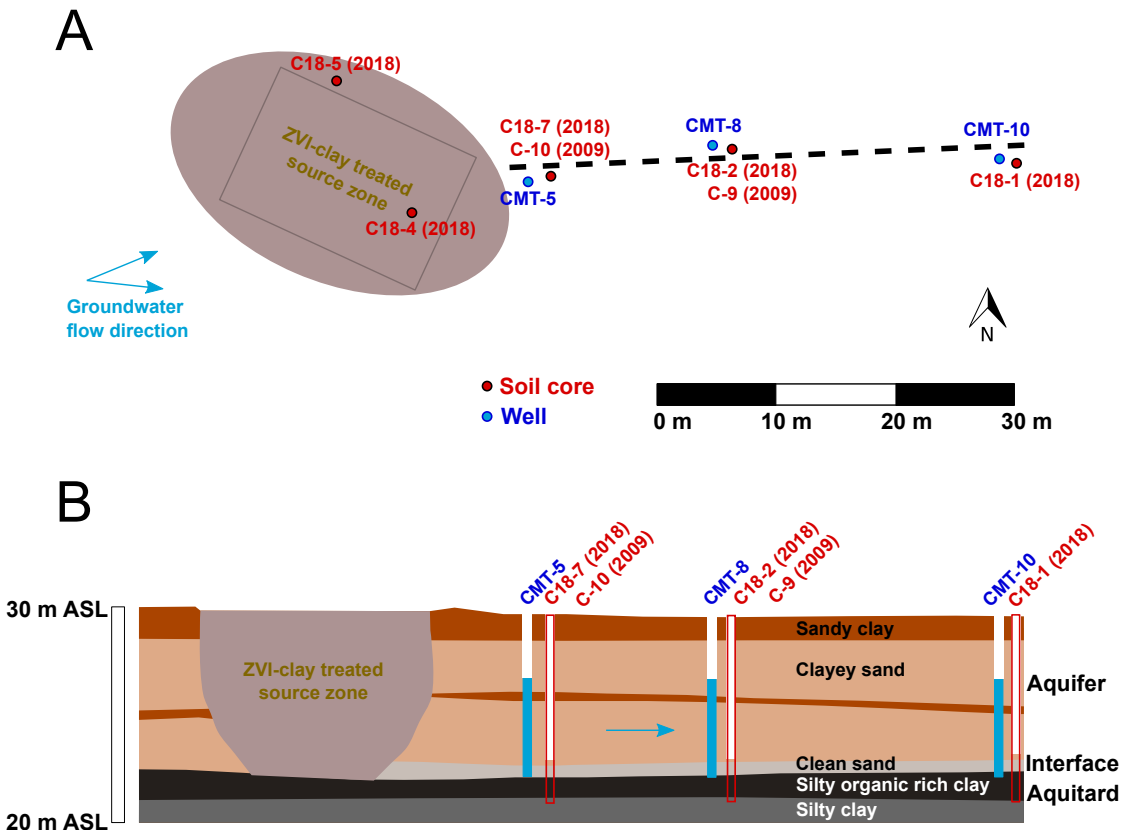

Figure 6.1.: (A) Map of the study site showing the ZVI-clay treated source zone, the longsect as dashed line, the groundwater flow direction with a seasonal variation of 30° and the locations of multilevel wells and soil cores and (B) Geological cross section of the longsect with locations of wells and soil cores taken in March of 2018. Vertical scale exaggerated. Modified after Wanner et al. (2018) and Isenschmid (2018).

instead is made possible by the simple presence of hydroxide anions (Elsner et al. 2007). As such, the process is strongly dependent on pH, with degradation favored at neutral to alkaline pH. The chlorinated ethenes can in turn also follow a sequential hydrogenolysis pathway, but may also be degraded to chlorinated and non-chlorinated ethynes. The volatility of these compounds increases with decreasing degree of chlorination, which complicates field sampling and analysis of degradation products. Nevertheless, TCE, *cis*-1,2-DCE and DCM have all been observed in downgradient wells over the years (Isenschmid 2018), showing that degradation is taking place.

The site was the subject of a field campaign in March of 2009, with soil cores and water samples taken at several locations (Wanner et al. 2018), including wells CMT-5, CMT-8 and CMT-10. Concentration measurements of target contaminants in groundwater and aqueous soil extracts were performed and contaminants analyzed for compound-specific carbon isotope ratios (soil cores C-10 and C-9). Contaminants were found to have diffused up to 1.8 m into the aquitard (Isenschmid 2018). In addition, concentration measurements of target contaminants in groundwater were performed in July of 2008 as well as March of 2010 and 2014.

6.3. Material and methods

6.3.1. Field sampling

A sampling campaign was conducted in March of 2018. The locations of wells and soil cores are shown in Figure 1 A and B. Groundwater was sampled from the three ports each of wells CMT-5, CMT-8 and CMT-10 using a peristaltic pump (Isenschmid 2018).

Soil cores were drilled at locations C18-4 and C18-5 within the source zone, and C18-7, C18-2 and C18-1 along the longsect (Figure 6.1A). As described in Chapter 4, a direct-push rig was used, followed by subsampling of the low-permeability zones with tube-and-piston subsamplers (Isenschmid 2018). Soil samples were extracted in methanol, tetraethylene glycol dimethyl ether (TGDE) or water. The soil samples, weighing 10 g to 15 g, were dispersed in 42 mL glass vials capped with PTFE-coated silicone septa and screw caps containing 20 mL of the extraction medium (Parker et al. 2004). The vials were weighed empty, with the extraction medium, and with the extraction medium plus the soil sample (Isenschmid 2018). The vials containing soil and extraction medium were sonicated, shaken, and centrifuged.

Concentrations of VOC in groundwater and soil extracts were measured using a gas chromatograph coupled to a mass spectrometer (GC-qMS) based on EPA method 8260B,

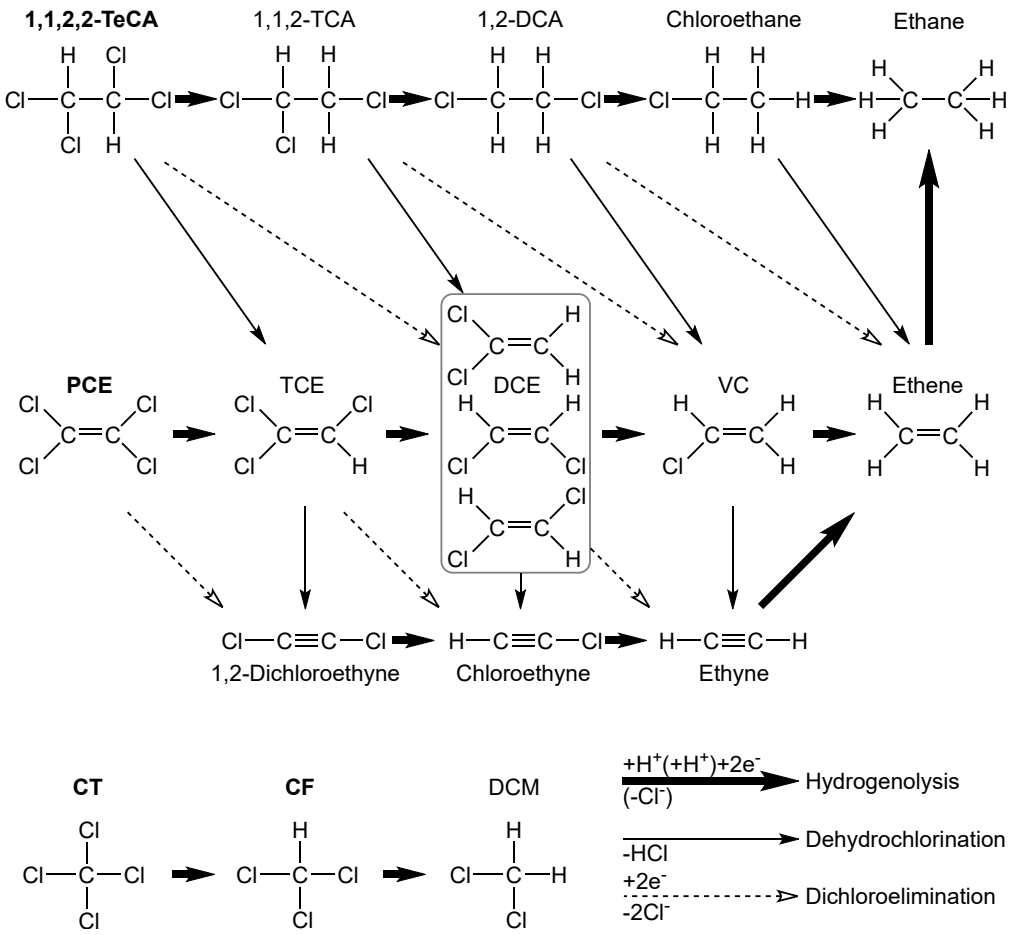

Figure 6.2.: Possible reductive degradation pathways for the initial contaminants (in **bold**) 1,1,2,2-tetrachloroethane, tetrachloroethene, carbon tetrachloride and chloroform. TeCA, tetrachloroethane; TCA, trichloroethane; DCA, dichloroethane; PCE, tetrachloroethene; TCE, trichloroethene; DCE, dichloroethene; VC, vinyl chloride; CT, carbon tetrachloride (tetrachloromethane); CF, chloroform (trichloromethane); DCM, dichloromethane. Modified after Wanner et al. (2018) and Zimmermann et al. (2020).

following concentration with a purge & trap system. VOC concentrations in soil are reported relative to the wet sample weight.

6.3.2. Compound-specific isotope analysis

Compound-specific carbon isotope analysis of target analytes was performed using an Elementar Isoprime 100 continuous flow isotope-ratio mass spectrometer (IRMS) as described in Chapter 4. Soil extracts and groundwater samples were diluted in ultrapure water, acidified with HNO_3 to inhibit hydrolysis of chlorinated ethanes, and concentrated with a Teledyne Tekmar Stratum purge & trap system and Vocarb K 3000 trap. The maximum permissible proportion of soil extract in water was limited to 3% (v/v) for methanol extracts and 10% (v/v) for TGDE extracts.

For carbon isotopes, the ratio of ^{13}C to ^{12}C of a sample R_{sample} is expressed using the delta (δ) notation as per mille (‰) difference from the isotope ratio R_{VPDB} in the reference standard Vienna Pee Dee Belemnite (VPDB):

$$\delta^{13}C = \frac{R_{sample}}{R_{VPDB}} - 1 \qquad (‰) \tag{6.1}$$

The compounds were cryofocused at −120 °C and injected splitlessly into an Agilent 7890A gas chromatograph, and separated using heart-cutting two-dimensional chromatography with two different columns connected in series through a two-way valve (Deans' switch) that allows diversion of non-target peaks. Hydrocarbons were converted to CO_2 in an Elementar Isoprime GC5 combustion furnace, and the CO_2 was detected in the IRMS. Samples were analyzed in duplicate. Standards that had been isotopically characterized with an elemental analyzer (EA) were analyzed during each sequence to correct for isotopic fractionation in the analytical setup. Concentrations were kept within previously determined isotopic linearity limits. Isotopic $\delta^{13}C$ standard deviations 1σ for repeat measurements were below 0.5‰.

Compound-specific chlorine isotope analysis was performed for chloroform. Methanol soil extracts were diluted in 15 mL ultrapure water in 20 mL glass headspace vials capped with PTFE-coated septa. After injection of 1 mL headspace using a PAL3 (CTC Analytics) autosampler into an Agilent 7890B at a split ratio of 1:50, peaks were separated on a HP-5MS column (30 m × 0.25 mm, 0.25 µm, Agilent J & W) and detected with an Agilent 5977B quadrupole mass spectrometer (qMS) in selected-ion mode. For CF, m/z 83 and 85 were measured. Chloroform chlorine isotope ratios R were calculated from the mass intensities I using Equation (6.2):

$$R = \frac{1}{2} \times \frac{I_{85}}{I_{83}} \tag{6.2}$$

For chlorine isotopes, the ratio of ^{37}Cl to ^{35}Cl of a sample R_{sample} is expressed using the delta (δ) notation as permille (‰) difference from the isotope ratio R_{SMOC} in the reference standard Standard Mean Ocean Chloride (SMOC):

$$\delta^{37}Cl = \frac{R_{sample}}{R_{SMOC}} - 1 \qquad (‰) \tag{6.3}$$

In order to obtain SMOC-referenced values, a set of two compound-specific standards of differing $\delta^{37}Cl$ values, CF-A (-5.41‰) and CF-F (-3.02‰), were analyzed during the sequence. Using a two-point isotopic calibration, SMOC-referenced $\delta^{37}Cl$ values were calculated from the chlorine isotope ratios. Each sample and standard was analyzed ten times, removing five times 1 mL headspace from two vials each.

The isotope fractionation during a specific transformation process can be described by the Rayleigh Equation (Abe and Hunkeler 2006). The compound-specific isotope enrichment factor ε_C for carbon or ε_{Cl} for chlorine is related to the initial isotope ratio at the beginning of the transformation process R_0, the isotope ratio R_t and the remaining fraction f at a point in time t according to Equation (6.4).

$$\frac{R_t}{R_0} = f^{\varepsilon} \tag{6.4}$$

6.4. Results and discussion

6.4.1. VOC concentrations in the aquifer-aquitard system

BTEX represent the bulk of the complex mixture of contaminants detected in groundwater at the field site (data not shown), but are not the focus of the following discussion. Among the chlorinated compounds, especially the chlorinated methanes CT, CF and DCM and the chlorinated C_2-hydrocarbons 1,1,2,2-TeCA, TCE, *cis*- and *trans*-1,2-DCE were detected at elevated concentrations in groundwater downgradient of the source zone over the years. Figure 6.3 shows the contaminant evolution of the initial contaminants CT and CF in the aquifer, while Figure 6.4 shows the contaminant evolution of the independent 1,1,2,2-TeCA system. The initial contaminant PCE is not shown due to its generally low levels compared to 1,1,2,2-TeCA.

As mentioned, the NAPL source was isolated in December of 2007. From this point on, the contaminant mass remaining in the downgradient aquifer-aquitard system was expected to not further increase. During 40 years of contaminant leaching, the extent of the CT and CF plume has reached at least 50 m downgradient from the source zone. Figure 6.3 (bottom row) shows the extent of the plume, CT and CF being detected at elevated concentrations

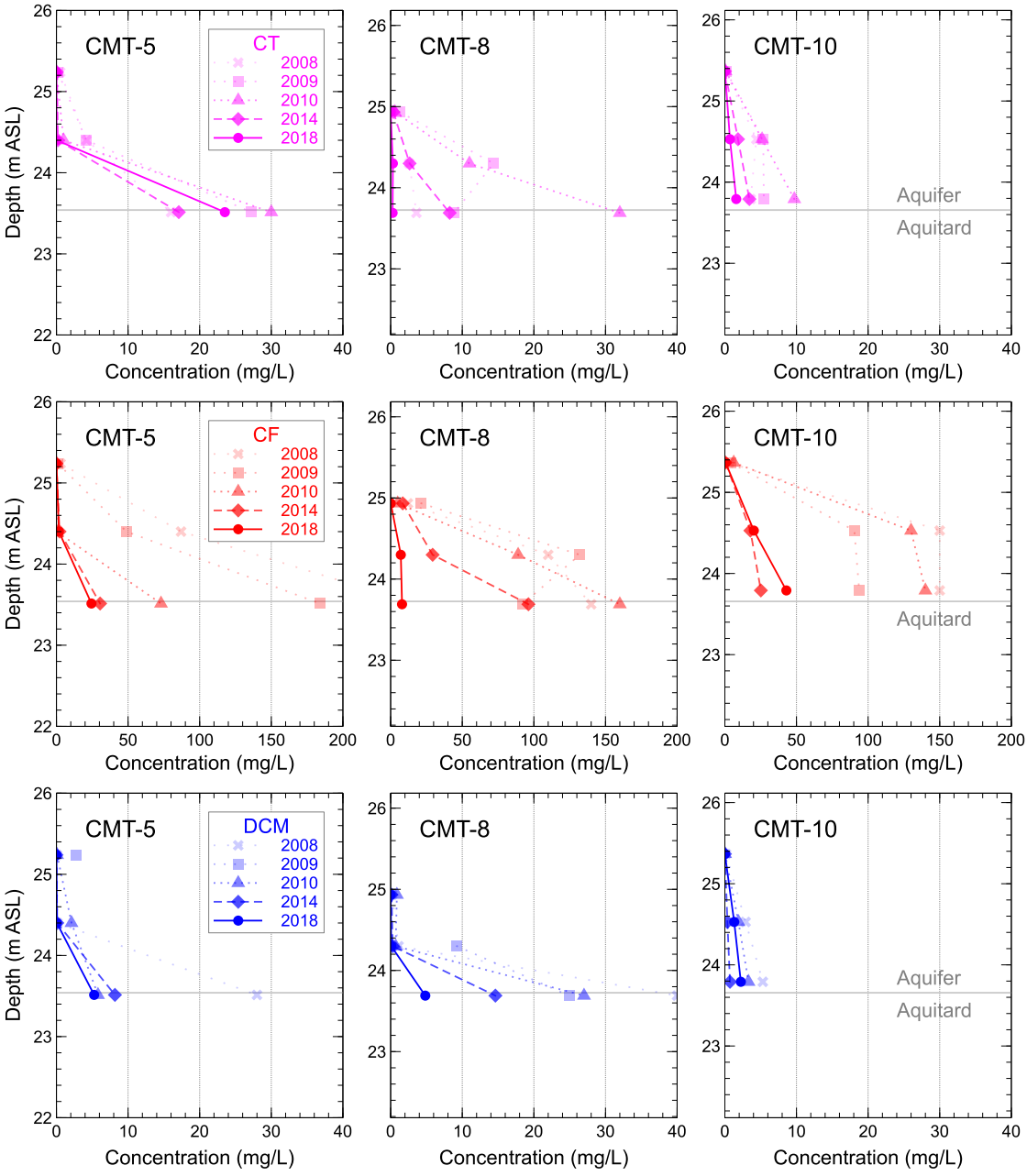

Figure 6.3.: Aqueous concentrations of initial contaminants CT and CF and degradation product DCM over three depths in the multilevel wells installed in the aquifer downgradient of the source zone. Spatial evolution in wells CMT-5, CMT-8 and CMT-10 at increasing distance from the source, and temporal evolution in July of 2008 and March of 2009, 2010, 2014 and 2018.

near the aquifer-aquitard interface, with a sharp decrease toward the top of the saturated zone. CF represents the main contaminant at concentrations of up to 250 mg L^{-1} in 2008. In the following years, the CF concentrations decrease noticeably in the well closest to the source zone. In 2018, the concentration of CF increases in well CMT-10 over 2014, indicating that the main extent of the plume has now migrated. The degradation product DCM appears in all wells with a maximum in the year 2008. The concentration of CT reaches its highest level in well CMT-8 in the year 2010, over two years after source isolation. The release is thought to have been caused by the remediation measures. In well CMT-5 closest to the source, concentrations of CT have increased in 2018 over 2014.

The temporal and spatial evolution of 1,1,2,2-TeCA follows a similar pattern (Figure 6.4). From a maximum concentration of 73 mg L^{-1} in the year 2009 in well CMT-5 close to the source zone, the concentration gradually decreases downgradient. In 2018, a slight increase in 1,1,2,2-TeCA concentration is visible in well CMT-10 compared to 2014. The degradation product is mainly TCE, followed by *cis*-1,2-DCE and a minor contribution of *trans*-1,2-DCE. In 2018, these were detected in all wells. The TCE concentration has increased in 2018 over 2014 in well CMT-5 closest to the source.

The persistence of the initial contaminants CT, CF and 1,1,2,2-TeCA is manifest in their consistently elevated aqueous concentrations in well CMT-5 near the source zone over the years. When we come to examine the aquifer-aquitard system in detail, we cannot but suspect a major influence of the underlying aquitard. To understand the role of the aquitard in plume persistence, we assess the contaminant evolution in spatially and temporally resolved soil profiles downgradient of the source zone. In the source zone itself, contaminant concentrations in soil are about one order of magnitude lower than in the downgradient core C18-7 (Figures S1 and S2 in supporting information Appendix D).

Figure 6.5 shows the soil concentrations for CF and DCM in the three soil cores C18-7, C18-2 and C18-1 taken from the aquitard and part of the aquifer in 2018 and the two soil cores C-10 and C-9 taken in 2009 at the same locations. CT has been omitted because of its low concentration in soil in both years (Wanner et al. 2018). In 2009, CF concentrations in soil have reached up 1170 µg g^{-1} of wet soil. The bulk of CF has accumulated right below the aquifer-aquitard interface and decreases sharply about 60 cm into the aquitard. The degradation product DCM is thought to stem from reductive dechlorination within the aquitard and has diffused even further into the aquitard. While the soil concentration of CF has decreased in 2018, the concentration of DCM remains at the same elevated level. Further downgradient in core C18-2, the concentration of DCM has surpassed that of CF.

Figure 6.6 gives an insight into the fate of 1,1,2,2-TeCA in the aquitard. The soil concentration of the initial contaminant has decreased close to the source zone by an order

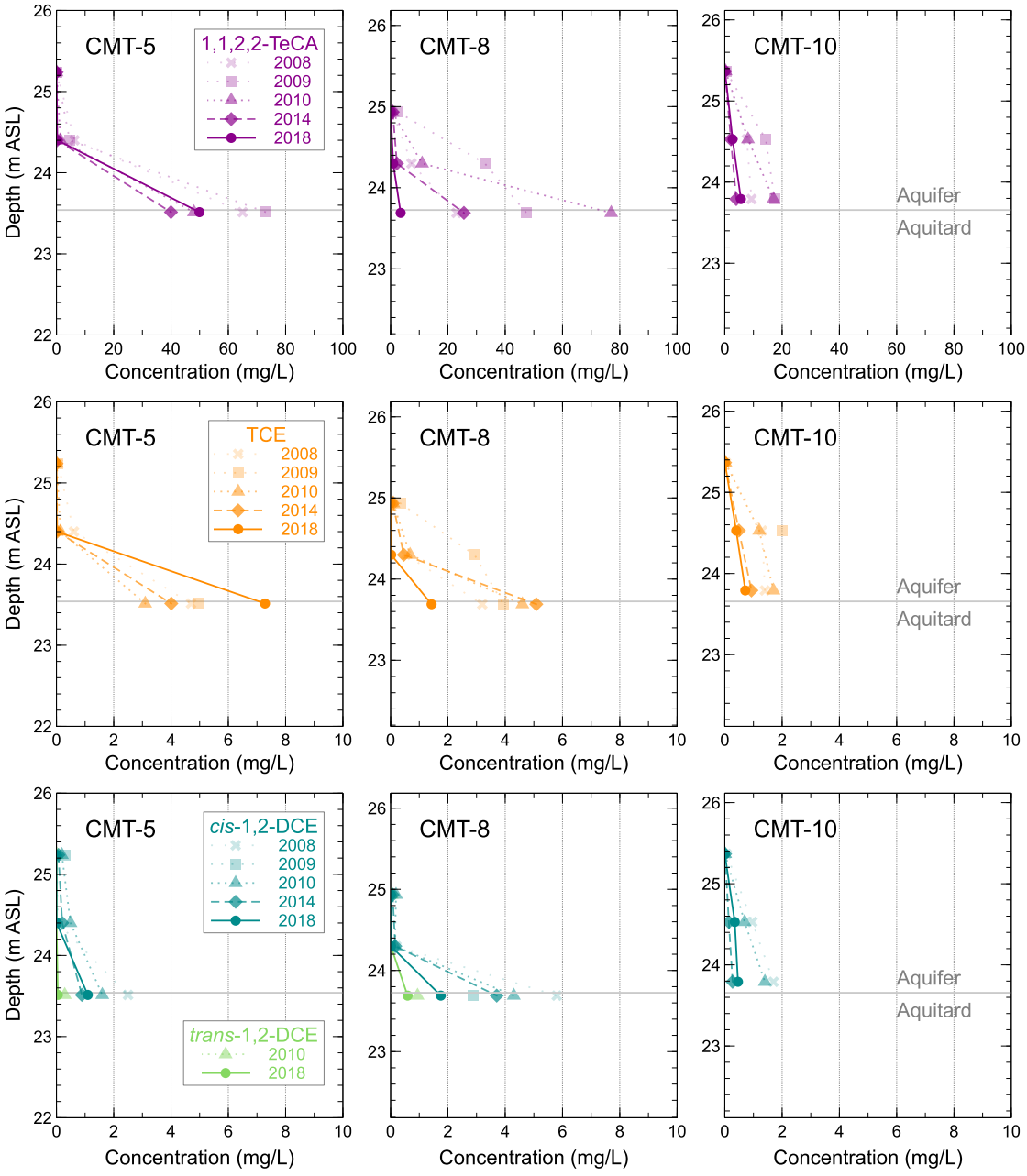

Figure 6.4.: Aqueous concentrations of initial contaminant 1,1,2,2-TeCA and degradation products TCE, *cis*- and *trans*-1,2-DCE over three depths in the multilevel wells installed in the aquifer downgradient of the source zone. Spatial evolution in wells CMT-5, CMT-8 and CMT-10 at increasing distance from the source, and temporal evolution in July of 2008 and March of 2009, 2010, 2014 and 2018.

of magnitude over the span of nine years (C-10 2009 versus C18-7 2018). However, the more recent sampling shows that the highest soil concentration now occurs at location C18-2 at a distance of about 20 m from the source zone, in contrast to the highest aqueous concentrations, which are recorded at the location close to the source (Figure 6.4). Degradation to TCE, *cis*- and *trans*-1,2-DCE is ongoing at all downgradient coring locations in the aquitard.

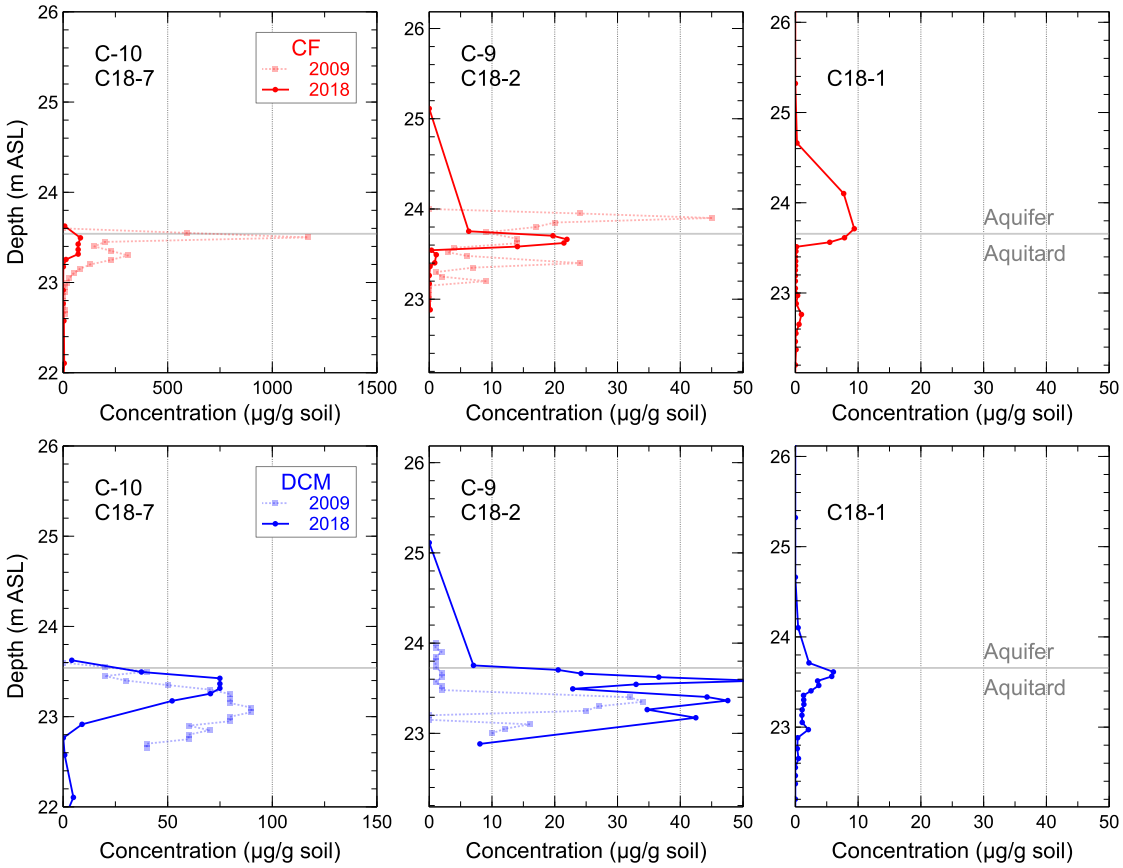

Figure 6.5.: Soil concentrations of initial contaminant and degradation product CF and degradation product DCM in the cores taken across the aquifer-aquitard interface downgradient of the source zone. Spatial evolution in cores C18-7, C18-2 and C18-1 taken at increasing distance from the source in March of 2018 compared to spatial evolution in cores C-10 and C-9 taken in March of 2009.

A closer look at the contaminant concentrations in both the aquifer and aquitard shows the typical picture found at many aquifer-aquitard systems characterized by the contrast of low-permeability zones (aquitards) to high-permeability zones (aquifers) (Liu and Ball 2002;

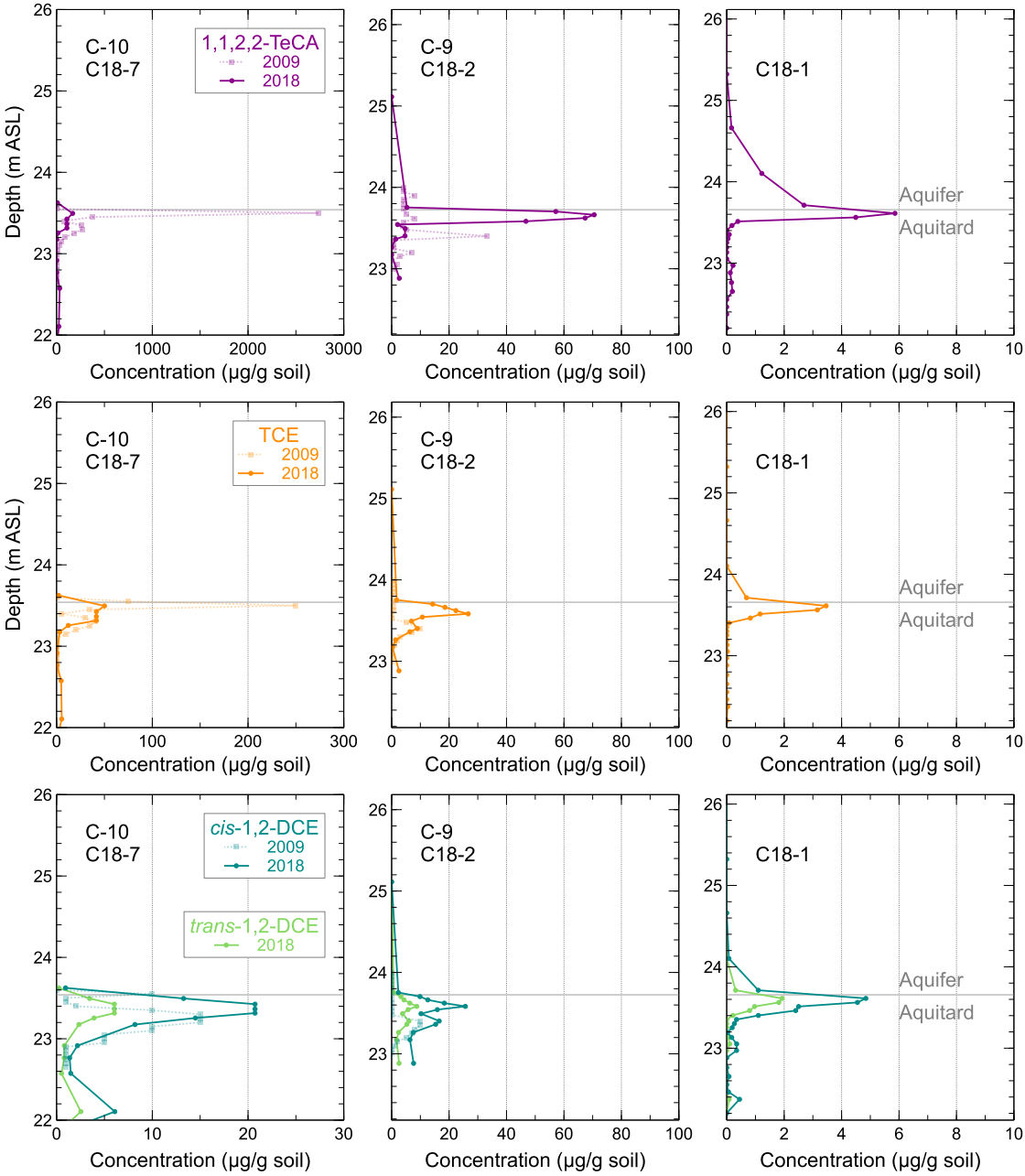

Figure 6.6.: Soil concentrations of initial contaminant 1,1,2,2-TeCA and degradation products TCE, *cis*- and trans-1,2-DCE in the cores taken across the aquifer-aquitard interface downgradient of the source zone. Spatial evolution in cores C18-7, C18-2 and C18-1 taken at increasing distance from the source in March of 2018 compared to spatial evolution in cores C-10 and C-9 taken in March of 2009.

Chapman and Parker 2005; Yang et al. 2015; Tatti et al. 2016; Halloran and Hunkeler 2020; You et al. 2020). During ongoing contamination, the contaminants will diffuse from the source, typically located in the low-permeability zones, into the high-permeability zones. After source isolation, the contaminant flux is then reversed. The force driving the contaminant distribution is the difference in concentrations between low- and high-permeability zones. At this field site, the gradient reversal after source isolation is well visible in the concentration profiles and still ongoing.

6.4.2. Compound-specific carbon isotope analysis of VOC in the aquifer-aquitard system

One must not assume, however, that back-diffusion commences immediately after source isolation. There are two important caveats to consider: (1) Without any further remediation efforts downgradient of the source, the concentration level of contaminants in the aquifer will only subside slowly through dilution and lateral diffusion and dispersion. (2) The diffusive fluxes between aquifer and aquitard depend on the concentrations of specific compounds. While for example the concentration of initial compounds is still elevated in the aquifer, the back-diffusion of degradation products stemming from the aquitard may very well already have begun prior to source isolation.

The question we confront is hence the role of degradation processes in the aquitard in the years following source isolation. These processes are not only demonstrated by occurrence of degradation products, but can be tracked using compound-specific isotope analysis.

Figure 6.7 shows a comparison between 2009 and 2018 of compound-specific $\delta^{13}C$ profiles over depth for the CF-DCM system. For obtaining these, soil extracts were analyzed from the aquitard, while groundwater was analyzed from the aquifer. Concentrations of CT were not sufficiently high to perform CSIA. It is evident that CF becomes enriched in ^{13}C over depth within the aquitard, while DCM becomes depleted, i.e. the $\delta^{13}C$ shifts in the negative direction. In the cores closes to the source zone, the soil concentration of DCM has remained on the same level in 2018 (core C18-7) versus 2009 (core C-10), although it has become further depleted in ^{13}C, which would indicate ongoing formation and accumulation. Instead, this may be the effect of the isotopically depleted DCM peak back-diffusing upward, which is also visible in the concentration profile (Figure 6.5). CF has become isotopically enriched over the years (Figure 6.7), which is either evidence for its ongoing degradation or the result of upward back-diffusion of enriched CF. The more negative $\delta^{13}C$ value of CF in groundwater versus the aquitard may be characteristic for initial CF that is not being degraded or CF originating from the degradation of CT.

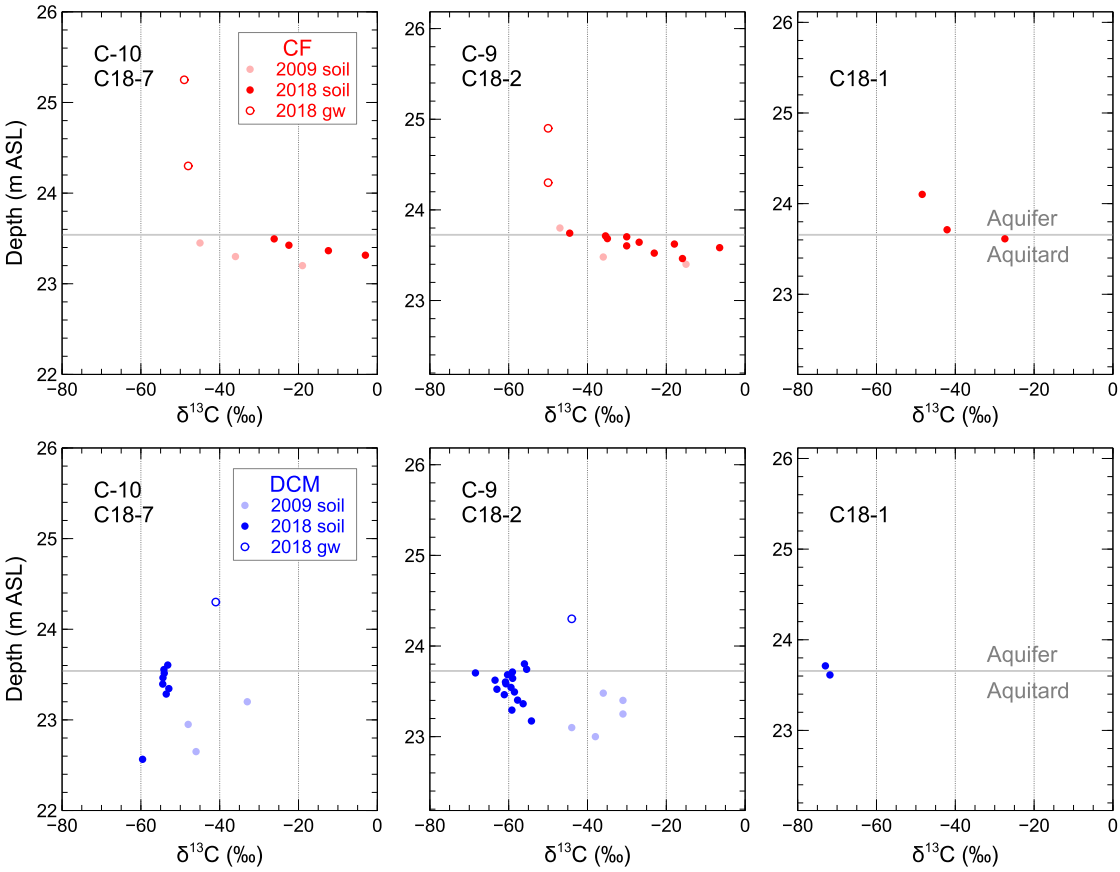

Figure 6.7.: Compound-specific carbon isotope values ($\delta^{13}C$) over depth in groundwater (aquifer) and soil (aquitard) of initial contaminant and degradation product CF and degradation product DCM in the cores taken across the aquifer-aquitard interface downgradient of the source zone. Spatial evolution in cores C18-7, C18-2 and C18-1 taken at increasing distance from the source in March of 2018 compared to spatial evolution in cores C-10 and C-9 taken in March of 2009.

Figure 6.8 shows a comparison between 2009 and 2018 of compound-specific $\delta^{13}C$ profiles over depth for the degradation of 1,1,2,2-TeCA. In core C18-7 closest to the source, all compounds show a slight carbon isotopic enrichment in 2018 over 2009. The initial contaminant becomes isotopically enriched with depth in the aquitard. While the degradation products TCE and *cis*-1,2-DCE are isotopically lighter, they too show this trend. This could either mean that the degradation products themselves are being degraded, or else that they reflect the pronounced enrichment of the parent compound with increasing depth.

One point that can be clarified with the CSIA data is the degradation pathway for 1,1,2,2-TeCA. At all points, *cis*-1,2-DCE is isotopically lighter than 1,1,2,2-TeCA, but heavier than TCE. This means that *cis*-1,2-DCE is not a hydrogenolysis degradation product of TCE, but instead stems from 1,1,2,2-TeCA that is degraded by dichloroelimination (Figure 6.2), which is in accordance with Wanner et al. (2018)'s findings at this field site. The question whether the observed concentration profiles of initial contaminants are the result of limited forward diffusion, or whether degradation increases with depth in the aquitard, cannot be answered without additional microbial data.

6.4.3. Dual carbon-chlorine isotope analysis of chloroform in the aquitard

Chloroform soil extracts in methanol across multiple cores of the 2018 campaign were analyzed for $\delta^{37}Cl$ to gain insight into the degradation pathway. Figure 6.9 shows the obtained dual carbon-chlorine isotope plot and the least-squares regression with slope and uncertainty. The measured slope is characteristic for this CF degradation pathway and is an approximation of the ratio of bulk carbon enrichment factor ε_C to the bulk chlorine enrichment factor ε_{Cl}. CF at this field site is both produced and degraded. This would complicate the evaluation of degradation pathways by comparing our slope with literature values. However, as CT has all but disappeared from the aquitard in the latest sampling campaign, we assume the slope to mainly reflect the degradation of CF to DCM. The value for $\varepsilon_C/\varepsilon_{Cl}$ of 5.5 ± 0.5 is lower than the values of 17 ± 2 and 13 ± 0.8 reported by Torrentó et al. (2017) for abiotic oxidation or abiotic hydrolysis of CF, respectively. It is also lower than the slope of 8 ± 1 measured by Rodríguez-Fernández et al. (2018a) for abiotic hydrogenolysis by zero-valent iron.

Chloroform is however also known to transform biotically (Cappelletti et al. 2012), under both aerobic or anaerobic conditions. Our $\varepsilon_C/\varepsilon_{Cl}$ slope is similar to the slope 7 ± 1 obtained by Rodríguez-Fernández et al. (2018c) for reductive biotic degradation catalyzed by Vitamin

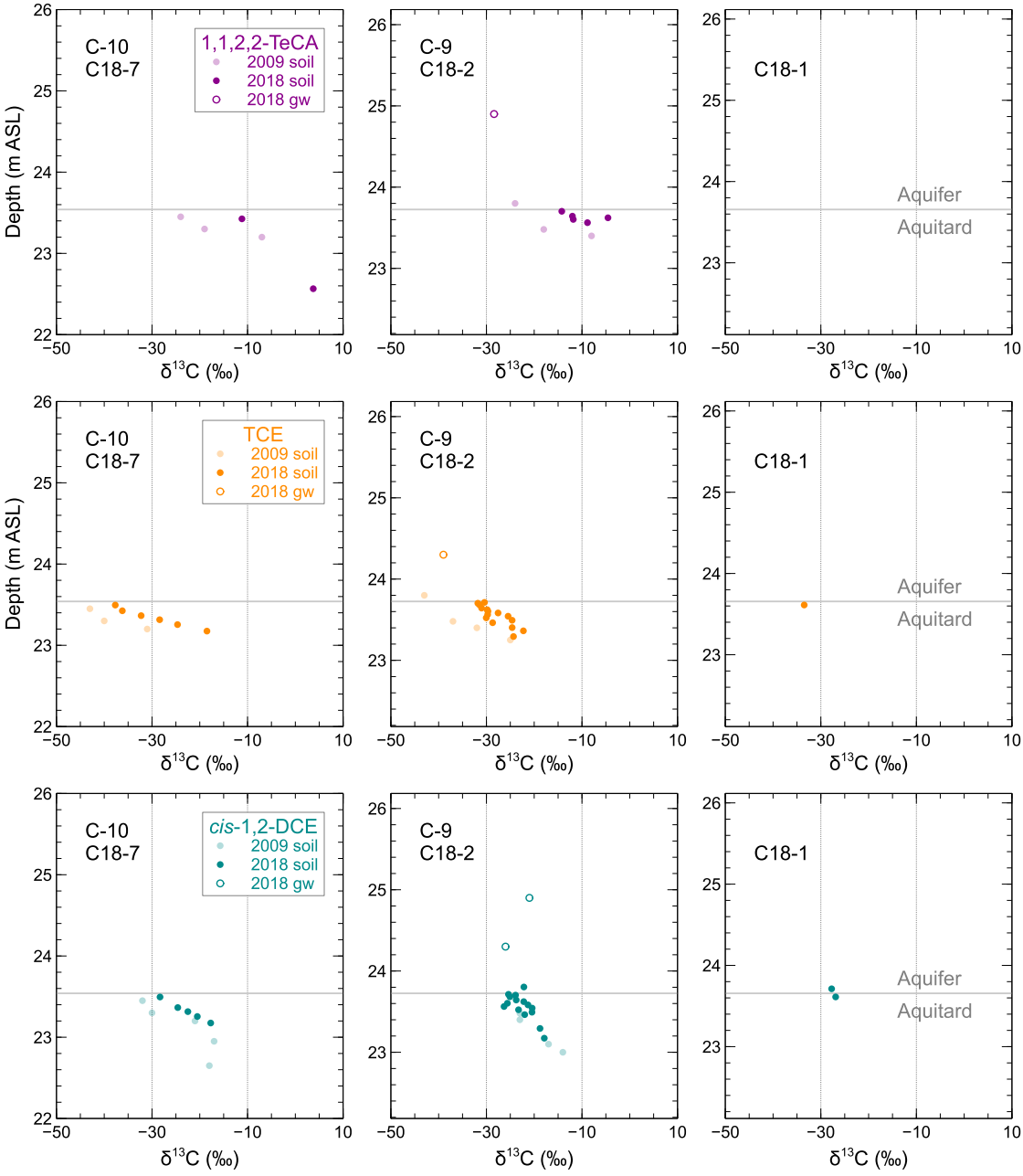

Figure 6.8.: Compound-specific carbon isotope values ($\delta^{13}C$) over depth in groundwater (aquifer) and soil (aquitard) of initial contaminant 1,1,2,2-TeCA and degradation products TCE and *cis*-1,2-DCE in the cores taken across the aquifer-aquitard interface downgradient of the source zone. Spatial evolution in cores C18-7, C18-2 and C18-1 taken at increasing distance from the source in March of 2018 compared to spatial evolution in cores C-10 and C-9 taken in March of 2009.

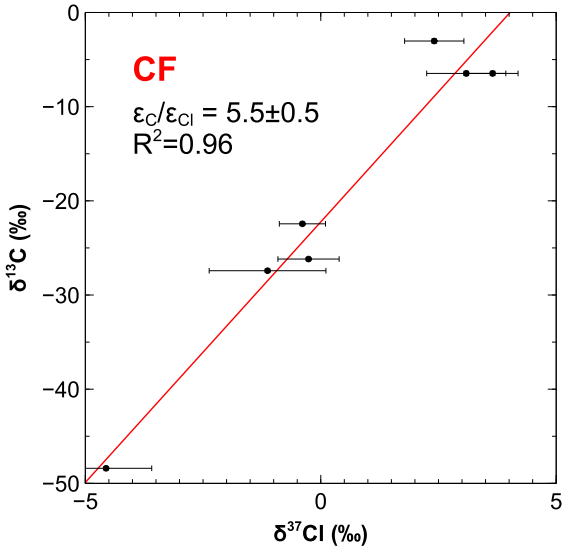

Figure 6.9.: Dual carbon-chlorine isotope plot and linear fit of chloroform (CF) for select soil extracts from profiles C18-1, C18-2 and C18-7.

B_{12}. At parts of an aquifer characterized by reductive redox conditions, Rodríguez-Fernández et al. (2018b) obtained slopes of 3.3 ± 0.8 and 4 ± 1 for CF degradation.

Our relatively low $\varepsilon_C/\varepsilon_{Cl}$ slope is suggestive of a relatively high ε_{Cl} and hence a primary chlorine isotope effect in the rate-limiting step, indicating a C-Cl bond cleavage, not a C-H bond cleavage as observed for abiotic oxidation (Torrentó et al. 2017).

6.5. Conclusions

The investigated field site is a highly complex system due to the plethora of subsurface contaminants remaining in the aquifer-aquitard system even after source isolation. The comparison of soil and groundwater concentration profiles for initial contaminants and degradation products highlights the important role of the aquitard for not only storage, but also degradation, as many of the investigated compounds are degraded reductively under anaerobic conditions. In addition to the concentration data, compound-specific isotope analysis of several target analytes in the aquitard gave an insight into the degradation processes, showing for the chlorinated methanes a carbon isotopic enrichment of CF and an isotopic depletion of the degradation product DCM. The initial contaminant 1,1,2,2-TeCA continues to be degraded over the years as shown by its carbon isotopic enrichment. CSIA of the degradation products indicates that 1,1,2,2-TeCA is degraded by both dehydrochlo-

rination and dichloroelimination. Dual carbon-chlorine isotope analysis of CF resulted in $\varepsilon_C/\varepsilon_{Cl}$ slopes similar to those reported in the literature for reductive dechlorination.

A further understanding of degradation processes will be reached by taking into account microbial data. While some of the contaminants may be transformed by specific degraders, chlorinated methanes are thought to be degraded through co-metabolism.

Acknowledgments

We would like to thank Ramon Aravena, Beth L. Parker and Philipp Wanner from G360 Institute for Groundwater Research (College of Engineering & Physical Sciences, University of Guelph, Canada) for technical and financial support. We would also like to thank the field crew who collected the soil samples: Steven Chapman, Nathan Glas, Flavia Isenschmid, Ryan Kroeker and Philipp Wanner. This work was supported by the Swiss National Science Foundation (SNSF) [grant number 166233].

7. General conclusions and outlook

Chlorinated and petroleum hydrocarbons are widespread subsurface contaminants. Fortunately, compound-specific isotope analysis can provide unique insights into their origin and fate. Different aspects of compound-specific isotope analysis have been addressed in this thesis: analytical aspects, isotope fractionation processes and field applications. The thesis contributed new fundamental knowledge about isotope behavior in the subsurface and addressed an issue of high societal importance: the long-term evolution of the quality of groundwater, an important drinking water resource. As CHC are highly persistent and DNAPL source zones difficult to remediate, CSIA is required in order to gain a better understanding of transformation processes.

Compound-specific isotope analysis has a lot of potential, as illustrated in the review (Chapter 2), but there are some analytical hurdles that prevent its more widespread implementation, including inadequate sensitivity for chlorine isotope analysis and a shortage of CSIA methods for soil samples. Furthermore, a more extensive application of dual carbon-chlorine isotope analysis requires laboratory-derived dual element slopes for different compounds and degradation pathways.

Chapter 3 demonstrated an online chlorine isotope analysis method combining quadrupole mass spectrometry, using a high-efficiency electron ionization source, with solid-phase microextraction for improved sensitivity. The novel SPME Arrow method used has the advantage of an increased sorptive phase volume over standard SPME. The design of experiments approach offered a way to identify critical factors that affect SPME performance. The method is easily automated, which is a key requirement for qMS due to the high number of replicate measurements necessary. As the SPME Arrow can be retrofitted to existing autosampler systems the method could be potentially implemented at many environmental chemistry labs to expand the application of chlorine CSIA as a routine method. The method detection limits for PCE and TCE chlorine isotope ratio measurements are on par with those generally assumed for carbon isotope ratio measurements using IRMS, in the low microgram per liter range in aqueous solution. However, an important caveat of the developed SPME method is the narrow isotopic linearity range. The signal intensity of standards and samples must be closely matched, and this requires assessing and correcting for possible matrix

effects. The intensity will also be influenced by competitive sorption on the SPME fiber if several volatile compounds are found in the samples. The design of experiments approach could possibly be applied to investigate this effect for simple mixtures of target compounds. The method still requires proper validation by applying it to samples from a field site that have been measured by a different method offering a similar sensitivity, e.g. purge & trap and an IRMS with a dedicated cup configuration for chlorine isotope analysis.

An analytical aspect of carbon CSIA of complex mixtures in soil was investigated in Chapter 4. As baseline peak separation is essential for carbon isotope ratio mass spectrometry in conjunction with a combustion step, a heart-cutting two-dimensional chromatography method was developed. A thick-film column in the first dimension ensured reproducible retention times for exact heart-cutting. This not only enabled separation of target peaks from interfering non-target peaks, but also from the extraction solvent peak. The novel use of tetraglyme as soil extraction solvent promises an improved sensitivity for carbon CSIA of soil, as it is less volatile than methanol and thus does not interfere with the sorption of target compounds on the trap. Although the method allows for high proportions of extractions solvents to be purged, the results showed that cosolvent effects must not be disregarded, as the purge efficiency of target compounds decreased with increasing amounts of extraction solvent. Nevertheless, the successful development of a method for carbon IRMS of complex mixtures in soil is a key aspect, as soil and especially low-permeability zones are important areas in the subsurface for storage and degradation of contaminants.

This thesis provided an important contribution to an important research gap revealed in the review: the lack of knowledge about abiotic transformation processes mediated by reactive phases found in the natural environment. The dual carbon-chlorine approach is of particular interest to demonstrate these processes, and its potential was shown in Chapter 5 for the degradation of chlorinated ethenes. The abiotic dual carbon-chlorine slope for PCE was shown to be distinct from that observed for biotic pathways, thus offering an important contribution to the implementation of dual element compound-specific isotope analysis in the field. Additionally, the pronounced difference in dual carbon-chlorine slopes between PCE and TCE made it possible to distinguish possible elementary reactions in the dichloroelimination pathway. For both PCE and TCE, the large carbon isotope enrichment factors make this a highly sensitive method for detecting abiotic processes even during initial stages of degradation. The experimental approach could possibly be extended to additional compounds, and compared to dual element slopes observed in the field for insights into the prevalence of natural abiotic degradation, which is still up for debate.

Finally, the field site in Chapter 6 demonstrated how to apply CSIA in the field for delineating degradation pathways and for evaluating the role of low-permeability zones on

contaminant persistence after source isolation. Initial contaminants became further enriched over the years, indicating that natural degradation in the aquitard is still ongoing. The study highlighted the importance of soil isotopic data in addition to groundwater isotopic data. The investigated field site is an extremely complex system that would lend itself to numerical modelling that combines concentration and isotopic data in order to gain a full understanding of the different degradation and back-diffusion processes.

The analytical improvements developed within this work, as well as the dual carbon-chlorine isotope fractionation insights gained for abiotic degradation, offer an important contribution to the more widespread use of CSIA for tracking contaminant degradation processes in the field. Still, the methods presented here reveal that CSIA is a method that is very susceptible to analytical interferences, hence requiring careful evaluation of analytical factors and isotopic linearity limits. In the future, the focus should be set on improving standardization of CSIA methods across laboratories, especially for measuring chlorine isotope ratios. One shortcoming of compound-specific chlorine isotope analysis exposed in the review could not be considered. A simple way of producing sets of isotopically different standards for chlorine isotopic analysis using quadrupole mass spectrometry still needs to be developed. An experimental setup that allows for controlled and reproducible gaseous phase diffusion could be a viable method for enriching compounds for them to then be isotopically referenced offline and used for bracketing. May this unresolved challenge give impetus to future research.

Bibliography

Abe, Y. and D. Hunkeler (2006): "Does the Rayleigh equation apply to evaluate field isotope data in contaminant hydrogeology?" In: *Environmental Science & Technology* 40.5, pp. 1588–1596. DOI: 10.1021/es051128p.

Abe, Y., R. Aravena, J. Zopfi, O. Shouakar-Stash, E. Cox, J. D. Roberts, and D. Hunkeler (2009a): "Carbon and chlorine isotope fractionation during aerobic oxidation and reductive dechlorination of vinyl chloride and *cis*-1,2-dichloroethene". In: *Environmental Science & Technology* 43.1, pp. 101–107. DOI: 10.1021/es801759k.

Abe, Y., R. Aravena, J. Zopfi, B. L. Parker, and D. Hunkeler (2009b): "Evaluating the fate of chlorinated ethenes in streambed sediments by combining stable isotope, geochemical and microbial methods". In: *Journal of Contaminant Hydrology* 107.1, pp. 10–21. DOI: 10.1016/j.jconhyd.2009.03.002.

Acker, M. R. M. D. van, A. Shahar, E. D. Young, and M. L. Coleman (2006): "GC/multiple collector-ICPMS method for chlorine stable isotope analysis of chlorinated aliphatic hydrocarbons". In: *Analytical Chemistry* 78.13, pp. 4663–4667. DOI: 10.1021/ac0602120.

Aelion, C. M., ed. (2010): *Environmental Isotopes in Biodegradation and Bioremediation*. Boca Raton, FL, USA: CRC Press. 450 pp.

Aeppli, C., M. Berg, O. A. Cirpka, C. Holliger, R. P. Schwarzenbach, and T. B. Hofstetter (2009): "Influence of mass-transfer limitations on carbon isotope fractionation during microbial dechlorination of trichloroethene". In: *Environmental Science & Technology* 43.23, pp. 8813–8820. DOI: 10.1021/es901481b.

Aeppli, C., H. Holmstrand, P. Andersson, and Ö. Gustafsson (2010): "Direct compound-specific stable chlorine isotope analysis of organic compounds with quadrupole GC/MS using standard isotope bracketing". In: *Analytical Chemistry* 82.1, pp. 420–426. DOI: 10.1021/ac902445f.

Akob, D. M., J. M. Sutton, J. L. Fierst, K. B. Haase, S. Baesman, G. W. Luther, L. G. Miller, and R. S. Oremland (2018): "Acetylenotrophy: A hidden but ubiquitous microbial metabolism?" In: *FEMS Microbiology Ecology* 94.8. DOI: 10.1093/femsec/fiy103.

Alder, B. J., W. E. Alley, and J. H. Dymond (1974): "Studies in molecular dynamics. XIV. Mass and size dependence of the binary diffusion coefficient". In: *The Journal of Chemical Physics* 61.4, pp. 1415–1420. DOI: 10.1063/1.1682067.

Ali, S. M., A. Samanta, and S. K. Ghosh (2001): "Mode coupling theory of self and cross diffusivity in a binary fluid mixture: Application to Lennard-Jones systems". In: *The Journal of Chemical Physics* 114.23, pp. 10419–10429. DOI: 10.1063/1.1371261.

Arnold, W. A. and A. L. Roberts (2000): "Pathways and kinetics of chlorinated ethylene and chlorinated acetylene reaction with Fe(0) particles". In: *Environmental Science & Technology* 34.9, pp. 1794–1805. DOI: 10.1021/es990884q.

Arnold, W. A., P. Winget, and C. J. Cramer (2002): "Reductive dechlorination of 1,1,2,2-tetrachloroethane". In: *Environmental Science & Technology* 36.16, pp. 3536–3541. DOI: 10.1021/es025655+.

Audí-Miró, C., S. Cretnik, N. Otero, J. Palau, O. Shouakar-Stash, A. Soler, and M. Elsner (2013): "Cl and C isotope analysis to assess the effectiveness of chlorinated ethene degradation by zero-valent iron: Evidence from dual element and product isotope values". In: *Applied Geochemistry* 32, pp. 175–183. DOI: 10.1016/j.apgeochem.2012.08.025.

Azurad SAS (2020): *Azurad 1.3.2 - Logiciel de plans d'expériences*. Marseille, France. URL: http://www.azurad.fr/logiciel-plans-experiences.php (visited on Feb. 5, 2021).

Badin, A., G. Buttet, J. Maillard, C. Holliger, and D. Hunkeler (2014): "Multiple dual C-Cl isotope patterns associated with reductive dechlorination of tetrachloroethene". In: *Environmental Science & Technology* 48.16, pp. 9179–9186. DOI: 10.1021/es500822d.

Badin, A., M. M. Broholm, C. S. Jacobsen, J. Palau, P. Dennis, and D. Hunkeler (2016): "Identification of abiotic and biotic reductive dechlorination in a chlorinated ethene plume after thermal source remediation by means of isotopic and molecular biology tools". In: *Journal of Contaminant Hydrology* 192, pp. 1–19. DOI: 10.1016/j.jconhyd.2016.05.003.

Badin, A., F. Braun, L. J. S. Halloran, J. Maillard, and D. Hunkeler (2018): "Modelling of C/Cl isotopic behaviour during chloroethene biotic reductive dechlorination: Capabilities and limitations of simplified and comprehensive models". In: *PLOS ONE* 13.8. Ed. by A. Franzetti, e0202416. DOI: 10.1371/journal.pone.0202416.

Baertschi, P., W. Kuhn, and H. Kuhn (1953): "Fractionation of isotopes by distillation of some organic substances". In: *Nature* 171.4362, pp. 1018–1020. DOI: 10.1038/1711018a0.

Ball, W. P., G. Xia, D. P. Durfee, R. D. Wilson, M. J. Brown, and D. M. Mackay (1997): "Hot methanol extraction for the analysis of volatile organic chemicals in subsurface core samples from Dover Air Force Base, Delaware". In: *Groundwater Monitoring & Remediation* 17.1, pp. 104–121. DOI: 10.1111/j.1745-6592.1997.tb01190.x.

Barani, F., N. Dell'Amico, L. Griffone, M. Santoro, and C. Tarabella (2006): "Determination of volatile organic compounds by headspace trap". In: *Journal of Chromatographic Science* 44.10, pp. 625–630. DOI: 10.1093/chromsci/44.10.625.

Barth, J. A. C., G. Slater, C. Schuth, M. Bill, A. Downey, M. Larkin, and R. M. Kalin (2002): "Carbon isotope fractionation during aerobic biodegradation of trichloroethene by *Burkholderia cepacia* g4: A tool to map degradation mechanisms". In: *Applied and Environmental Microbiology* 68.4, pp. 1728–1734. DOI: 10.1128/AEM.68.4.1728-1734.2002.

Bartholomew, R. M., F. Brown, and M. Lounsbury (1954): "Chlorine isotope effect in reactions of *tert*-butyl chloride". In: *Canadian Journal of Chemistry* 32.10, pp. 979–983. DOI: 10.1139/v54-124.

Belardi, R. P. and J. B. Pawliszyn (1989): "The application of chemically modified fused silica fibers in the extraction of organics from water matrix samples and their rapid transfer to capillary columns". In: *Water Quality Research Journal* 24.1, pp. 179–191. DOI: 10.2166/wqrj.1989.010.

Beneteau, K. M., R. Aravena, and S. K. Frape (1999): "Isotopic characterization of chlorinated solvents – Laboratory and field results". In: *Organic Geochemistry* 30.8, pp. 739–753. DOI: 10.1016/S0146-6380(99)00057-1.

Berns, E. C., R. A. Sanford, A. J. Valocchi, T. J. Strathmann, C. E. Schaefer, and C. J. Werth (2019): "Contributions of biotic and abiotic pathways to anaerobic trichloroethene transformation in low permeability source zones". In: *Journal of Contaminant Hydrology* 224, p. 103480. DOI: 10.1016/j.jconhyd.2019.04.003.

Bernstein, A., O. Shouakar-Stash, K. Ebert, C. Laskov, D. Hunkeler, S. Jeannottat, K. Sakaguchi-Söder, J. Laaks, M. A. Jochmann, S. Cretnik, J. Jager, S. B. Haderlein, T. C. Schmidt, R. Aravena, and M. Elsner (2011): "Compound-specific chlorine isotope analysis: A comparison of gas chromatography/isotope ratio mass spectrometry and gas chromatography/quadrupole mass spectrometry methods in an interlaboratory study". In: *Analytical Chemistry* 83.20, pp. 7624–7634. DOI: 10.1021/ac200516c.

Bhattacharyya, S. and B. Bagchi (1997): "Anomalous diffusion of small particles in dense liquids". In: *The Journal of Chemical Physics* 106.5, pp. 1757–1763. DOI: 10.1063/1.473316.

Bhave, C. and S. Shejwalkar (2018): "A review on the synthesis and applications of green rust for environmental pollutant remediation". In: *International Journal of Environmental Science and Technology* 15, pp. 1243–1248. DOI: 10.1007/s13762-017-1468-y.

Blessing, M. (2008): "Compound-specific isotope analysis to delineate the sources and fate of organic contaminants in complex aquifer systems". PhD Thesis. Tübingen, Germany: Universität Tübingen, pp. 44–45. URL: https://publikationen.uni-tuebingen.de/xmlui/handle/10900/49213 (visited on Nov. 26, 2020).

Blessing, M., M. A. Jochmann, S. B. Haderlein, and T. C. Schmidt (2015): "Optimization of a large-volume injection method for compound-specific isotope analysis of polycyclic aromatic compounds at trace concentrations: Optimized large-volume injection method for isotopic analyses of PAHs". In: *Rapid Communications in Mass Spectrometry* 29.24, pp. 2349–2360. DOI: 10.1002/rcm.7389.

Boeker, P., J. Leppert, B. Mysliwietz, and P. S. Lammers (2013): "Comprehensive theory of the Deans' switch as a variable flow splitter: fluid mechanics, mass balance, and system behavior". In: *Analytical Chemistry* 85.19, pp. 9021–9030. DOI: 10.1021/ac401419j.

Bosch, C., A. Andersson, M. Kruså, C. Bandh, I. Hovorková, J. Klánová, T. D. J. Knowles, R. D. Pancost, R. P. Evershed, and Ö. Gustafsson (2015): "Source apportionment of polycyclic aromatic hydrocarbons in Central European soils with compound-specific triple isotopes (δ^{13}c, δ^{14}c, and δ^{2}h)". In: *Environmental Science & Technology* 49.13, pp. 7657–7665. DOI: 10.1021/acs.est.5b01190.

Bouchard, D., P. Wanner, H. Luo, P. W. McLoughlin, J. K. Henderson, R. J. Pirkle, and D. Hunkeler (2017): "Optimization of the solvent-based dissolution method to sample volatile organic compound vapors for compound-specific isotope analysis". In: *Journal of Chromatography A* 1520, pp. 23–34. DOI: 10.1016/j.chroma.2017.08.059.

Bourg, I. C. and G. Sposito (2007): "Molecular dynamics simulations of kinetic isotope fractionation during the diffusion of ionic species in liquid water". In: *Geochimica et Cosmochimica Acta* 71.23, pp. 5583–5589. DOI: 10.1016/j.gca.2007.01.021.

Bradley, D. C. (1954): "Fractionation of isotopes by distillation of some organic substances". In: *Nature* 173.4397, pp. 260–261. DOI: 10.1038/173260a0.

Bradley, P. M. (2003): "History and ecology of chloroethene biodegradation: A review". In: *Bioremediation Journal* 7.2, pp. 81–109. DOI: 10.1080/713607980.

Braeckevelt, M., A. Fischer, and M. Kästner (2012): "Field applicability of compound-specific isotope analysis (CSIA) for characterization and quantification of in situ contaminant degradation in aquifers". In: *Applied Microbiology and Biotechnology* 94.6, pp. 1401–1421. DOI: 10.1007/s00253-012-4077-1.

Brailsford, A. D., I. Gavrilović, R. J. Ansell, D. A. Cowan, and A. T. Kicman (2012): "Two-dimensional gas chromatography with heart-cutting for isotope ratio mass spectrometry analysis of steroids in doping control". In: *Drug Testing and Analysis* 4.12, pp. 962–969. DOI: 10.1002/dta.1379.

Brand, W. A. (1996): "High precision isotope ratio monitoring techniques in mass spectrometry". In: *Journal of Mass Spectrometry* 31.3, pp. 225–235. DOI: 10.1002/(SICI)1096-9888(199603)31:3<225::AID-JMS319>3.0.CO;2-L.

Breukelen, B. M. van, H. A. Thouement, P. E. Stack, M. Vanderford, P. Philp, and T. Kuder (2017): "Modeling 3D-CSIA data: Carbon, chlorine, and hydrogen isotope fractionation during reductive dechlorination of TCE to ethene". In: *Journal of Contaminant Hydrology* 204, pp. 79–89. DOI: 10.1016/j.jconhyd.2017.07.003.

Brown, R. A., R. Hines, M. C. Leahy, and J. Cho (2006): "Abiotic and biotic pathways in chlorinated solvent natural attenuation". In: *Fifth International Conference on Remediation of Chlorinated and Recalcitrant Compounds. Monterey, CA*. URL: https://pdfs.semanticscholar.org/039f/d60c2714398ad6a620108202e28938f885fb.pdf (visited on Apr. 27, 2017).

Buchner, D., B. Jin, K. Ebert, M. Rolle, M. Elsner, and S. B. Haderlein (2017): "Experimental determination of isotope enrichment factors – Bias from mass removal by repetitive sampling". In: *Environmental Science & Technology* 51.3, pp. 1527–1536. DOI: 10.1021/acs.est.6b03689.

Butler, E. C. and K. F. Hayes (1998): "Effects of solution composition and pH on the reductive dechlorination of hexachloroethane by iron sulfide". In: *Environmental Science & Technology* 32.9, pp. 1276–1284. DOI: 10.1021/es9706864.

Butler, E. C. and K. F. Hayes (1999): "Kinetics of the transformation of trichloroethylene and tetrachloroethylene by iron sulfide". In: *Environmental Science & Technology* 33.12, pp. 2021–2027. DOI: 10.1021/es9809455.

Butler, E. C. and K. F. Hayes (2001): "Factors influencing rates and products in the transformation of trichloroethylene by iron sulfide and iron metal". In: *Environmental Science & Technology* 35.19, pp. 3884–3891. DOI: 10.1021/es010620f.

Butler, E. C., Y. Dong, X. Liang, T. Kuder, R. P. Philp, and L. R. Krumholz (2009): *Abiotic Reductive Dechlorination of Tetrachloroethylene and Trichloroethylene in Anaerobic Environments*. Defense Technical Information Center. URL: https://apps.dtic.mil/sti/citations/ADA512772 (visited on Apr. 27, 2017).

Butler, I. B., M. A. Schoonen, and D. T. Rickard (1994): "Removal of dissolved oxygen from water: A comparison of four common techniques". In: *Talanta* 41.2, pp. 211–215.

Cappelletti, M., D. Frascari, D. Zannoni, and S. Fedi (2012): "Microbial degradation of chloroform". In: *Applied Microbiology and Biotechnology* 96.6, pp. 1395–1409. DOI: 10.1007/s00253-012-4494-1.

Chan, J., A. R. Lewis, M. Gilbert, M. F. Karwaski, and A. J. Bennet (2010): "A direct NMR method for the measurement of competitive kinetic isotope effects". In: *Nature Chemical Biology* 6.6, pp. 405–407. DOI: 10.1038/nchembio.352.

Chapelle, F. H., M. A. Widdowson, J. S. Brauner, E. Mendez III, and C. C. Casey (2003): *Methodology for Estimating Times of Remediation Associated with Monitored Natural Attenuation*. U.S. Geological Survey Water-Resources Investigation Report 03-4057. 51 pp. URL: https://toxics.usgs.gov/pubs/wri03-4057/index.html (visited on Apr. 21, 2021).

Chapman, S. W. and B. L. Parker (2005): "Plume persistence due to aquitard back diffusion following dense nonaqueous phase liquid source removal or isolation". In: *Water Resources Research* 41.12. DOI: 10.1029/2005WR004224.

Chapman, S. and T. G. Cowling (1970): *The mathematical theory of non-uniform gases: An account of the kinetic theory of viscosity, thermal conduction and diffusion in gases*. Cambridge, UK: Cambridge University Press. 423 pp.

Charles, M. J. and M. S. Simmons (1987): "Recovery studies of volatile organics in sediments using purge/trap methods". In: *Analytical Chemistry* 59.8, pp. 1217–1221. DOI: 10.1021/ac00135a031.

Chen, F., D. L. Freedman, R. W. Falta, and L. C. Murdoch (2012): "Henry's law constants of chlorinated solvents at elevated temperatures". In: *Chemosphere* 86.2, pp. 156–165. DOI: 10.1016/j.chemosphere.2011.10.004.

Choi, J., B. Batchelor, and J. Chung (2010): "Reductive dechlorination of tetrachloroethylene by green rusts modified with copper". In: *Water, Air, & Soil Pollution* 212.1, pp. 407–417. DOI: 10.1007/s11270-010-0354-8.

Cincinelli, A., F. Pieri, Y. Zhang, M. Seed, and K. C. Jones (2012): "Compound specific isotope analysis (CSIA) for chlorine and bromine: A review of techniques and applications to elucidate environmental sources and processes". In: *Environmental Pollution* 169, pp. 112–127. DOI: 10.1016/j.envpol.2012.05.006.

Clayton, C. (1991): "Carbon isotope fractionation during natural gas generation from kerogen". In: *Marine and Petroleum Geology* 8.2, pp. 232–240. DOI: 10.1016/0264-8172(91)90010-X.

Coplen, T. B. (2011): "Guidelines and recommended terms for expression of stable-isotope-ratio and gas-ratio measurement results: Guidelines and recommended terms for expressing stable isotope results". In: *Rapid Communications in Mass Spectrometry* 25.17, pp. 2538–2560. DOI: 10.1002/rcm.5129.

Cramer, B., B. M. Krooss, and R. Littke (1998): "Modelling isotope fractionation during primary cracking of natural gas: A reaction kinetic approach". In: *Chemical Geology* 149.3-4, pp. 235–250. DOI: 10.1016/S0009-2541(98)00042-4.

Crane, R. and T. Scott (2012): "Nanoscale zero-valent iron: Future prospects for an emerging water treatment technology". In: *Journal of Hazardous Materials* 211-212, pp. 112–125. DOI: 10.1016/j.jhazmat.2011.11.073.

Cretnik, S., K. A. Thoreson, A. Bernstein, K. Ebert, D. Buchner, C. Laskov, S. Haderlein, O. Shouakar-Stash, S. Kliegman, K. McNeill, and M. Elsner (2013): "Reductive dechlorination of TCE by chemical model systems in comparison to dehalogenating bacteria: Insights from dual element isotope analysis ($^{13}C/^{12}C$, $^{37}Cl/^{35}Cl$)". In: *Environmental Science & Technology* 47.13, pp. 6855–6863. DOI: 10.1021/es400107n.

Cretnik, S., A. Bernstein, O. Shouakar-Stash, F. Löffler, and M. Elsner (2014): "Chlorine isotope effects from isotope ratio mass spectrometry suggest intramolecular C-Cl bond competition in trichloroethene (TCE) reductive dehalogenation". In: *Molecules* 19.5, pp. 6450–6473. DOI: 10.3390/molecules19056450.

Dass, C. (2007): *Fundamentals of Contemporary Mass Spectrometry*. New York, NY, USA: John Wiley & Sons. 610 pp. DOI: 10.1002/0470118490.

Dayan, H., T. Abrajano, N. C. Sturchio, and L. Winsor (1999): "Carbon isotopic fractionation during reductive dehalogenation of chlorinated ethenes by metallic iron". In: *Organic Geochemistry* 30.8, pp. 755–763. DOI: 10.1016/S0146-6380(99)00058-3.

Deans, D. R. (1968): "A new technique for heart cutting in gas chromatography". In: *Chromatographia* 1.1, pp. 18–22. DOI: 10.1007/BF02259005.

Derringer, G. and R. Suich (1980): "Simultaneous optimization of several response variables". In: *Journal of Quality Technology* 12.4, pp. 214–219. DOI: 10.1080/00224065.1980.11980968.

Dettmer-Wilde, K. and W. Engewald, eds. (2014): *Practical gas chromatography: A comprehensive reference*. New York, NY, USA: Springer. DOI: 10.1007/978-3-642-54640-2.

Doherty, R. E. (2000): "A history of the production and use of carbon tetrachloride, tetrachloroethylene, trichloroethylene and 1,1,1-trichloroethane in the United States: Part 1 – historical background; carbon tetrachloride and tetrachloroethylene". In: *Environmental Forensics* 1.2, pp. 69–81. DOI: 10.1006/enfo.2000.0010.

Dolinová, I., M. Štrojsová, M. Černík, J. Němeček, J. Macháčková, and A. Ševců (2017): "Microbial degradation of chloroethenes: A review". In: *Environmental Science and Pollution Research* 24, pp. 13262–13283. DOI: 10.1007/s11356-017-8867-y.

Dong, Y., X. Liang, L. R. Krumholz, R. P. Philp, and E. C. Butler (2009): "The relative contributions of abiotic and microbial processes to the transformation of tetrachloroethylene and trichloroethylene in anaerobic microcosms". In: *Environmental Science & Technology* 43.3, pp. 690–697. DOI: 10.1021/es801917p.

Dreher, E.-L., T. R. Torkelson, and K. K. Beutel (2011): "Chlorethanes and chloroethylenes". In: *Ullmann's Encyclopedia of Industrial Chemistry*. Weinheim, Germany: Wiley-VCH. DOI: 10.1002/14356007.o06_o01.

Dries, J., L. Bastiaens, D. Springael, S. N. Agathos, and L. Diels (2007): "Competition for sorption and degradation of chlorinated ethenes in batch zero-valent iron systems". In: *Environmental Science & Technology* 38.10, pp. 2879–2884. DOI: 10.1021/es034933h.

Dron, J., R. Garcia, and E. Millán (2002): "Optimization of headspace solid-phase microextraction by means of an experimental design for the determination of methyl *tert.*-butyl ether in water by gas chromatography-flame ionization detection". In: *Journal of Chromatography. A* 963.1, pp. 259–264. DOI: 10.1016/s0021-9673(02)00359-x.

Ebert, K. A., C. Laskov, M. Elsner, and S. B. Haderlein (2017): "Calibration bias of experimentally determined chlorine isotope enrichment factors: The need for a two-point calibration in compound-specific chlorine isotope analysis". In: *Rapid Communications in Mass Spectrometry* 31.1, pp. 68–74. DOI: 10.1002/rcm.7752.

Eggenkamp, H. (2014): *The Geochemistry of Stable Chlorine and Bromine Isotopes*. Berlin, Heidelberg, Germany: Springer. DOI: 10.1007/978-3-642-28506-6.

Eiler, J. M. (2007): ""Clumped-isotope" geochemistry – The study of naturally-occurring, multiply-substituted isotopologues". In: *Earth and Planetary Science Letters* 262.3, pp. 309–327. DOI: 10.1016/j.epsl.2007.08.020.

Einstein, A. (1905): "Über die von der molekularkinetischen Theorie der Wärme geforderte Bewegung von in ruhenden Flüssigkeiten suspendierten Teilchen". In: *Annalen der Physik* 322.8, pp. 549–560. DOI: 10.1002/andp.19053220806.

Elsner, M., R. P. Schwarzenbach, and S. B. Haderlein (2004): "Reactivity of Fe(II)-bearing minerals toward reductive transformation of organic contaminants". In: *Environmental science & technology* 38.3, pp. 799–807. DOI: 10.1021/es0345569.

Elsner, M., L. Zwank, D. Hunkeler, and R. P. Schwarzenbach (2005): "A new concept linking observable stable isotope fractionation to transformation pathways of organic pollutants". In: *Environmental Science & Technology* 39.18, pp. 6896–6916. DOI: 10.1021/es0504587.

Elsner, M., D. M. Cwiertny, A. L. Roberts, and B. Sherwood Lollar (2007): "1,1,2,2-tetrachloroethane reactions with OH-, cr(II), granular iron, and a copper–iron bimetal: Insights from product formation and associated carbon isotope fractionation". In: *Environmental Science & Technology* 41.11, pp. 4111–4117. DOI: 10.1021/es063040x.

Elsner, M. and D. Hunkeler (2008): "Evaluating chlorine isotope effects from isotope ratios and mass spectra of polychlorinated molecules". In: *Analytical Chemistry* 80.12, pp. 4731–4740. DOI: 10.1021/ac702543y.

Elsner, M., M. Chartrand, N. VanStone, G. Lacrampe Couloume, and B. Sherwood Lollar (2008): "Identifying abiotic chlorinated ethene degradation: Characteristic isotope patterns in reaction products with nanoscale zero-valent iron". In: *Environmental Science & Technology* 42.16, pp. 5963–5970. DOI: 10.1021/es8001986.

Elsner, M. (2010): "Stable isotope fractionation to investigate natural transformation mechanisms of organic contaminants: Principles, prospects and limitations". In: *Journal of Environmental Monitoring* 12.11, p. 2005. DOI: 10.1039/c0em00277a.

Elsner, M., M. A. Jochmann, T. B. Hofstetter, D. Hunkeler, A. Bernstein, T. C. Schmidt, and A. Schimmelmann (2012): "Current challenges in compound-specific stable isotope analysis of environmental organic contaminants". In: *Analytical and Bioanalytical Chemistry* 403.9, pp. 2471–2491. DOI: 10.1007/s00216-011-5683-y.

Erickson, M. D., M. K. Alsup, and P. A. Hyldburg (1981): "Foam prevention in purge and trap analysis". In: *Analytical Chemistry* 53.8, pp. 1265–1269. DOI: 10.1021/ac00231a031.

European Chemicals Agency (2020): *Registration dossier*. URL: http://echa.europa.eu/ (visited on July 28, 2020).

Ferrey, M. L., R. T. Wilkin, R. G. Ford, and J. T. Wilson (2004): "Nonbiological removal of *cis*-dichloroethylene and 1,1-dichloroethylene in aquifer sediment containing magnetite". In: *Environmental Science & Technology* 38.6, pp. 1746–1752. DOI: 10.1021/es0305609.

Fick, A. (1855): "Ueber Diffusion". In: *Annalen der Physik und Chemie* 170.1, pp. 59–86. DOI: 10.1002/andp.18551700105.

Fitts, C. R. (2013): "Groundwater contamination". In: *Groundwater Science*. Ed. by C. R. Fitts. 2nd Edition. Boston, MA, USA: Academic Press, pp. 499–585. DOI: 10.1016/B978-0-12-384705-8.00011-X.

Gilevska, T., N. Ivdra, M. Bonifacie, and H.-H. Richnow (2015): "Improvement of analytical method for chlorine dual-inlet isotope ratio mass spectrometry of organochlorines: Chlorine stable isotope analyses of organic compounds". In: *Rapid Communications in Mass Spectrometry* 29.14, pp. 1343–1350. DOI: 10.1002/rcm.7220.

Gilmore, A. M. (2010): "High resolution investigation in a heterogeneous aquifer and evaluation of the membrane interface probe to assess back diffusion potential". Master's thesis. Guelph, ON, Canada: University of Guelph. URL: https://www.collectionscanada.gc.ca/obj/thesescanada/vol2/002/MR71506.PDF?oclc_number=791137918 (visited on Apr. 28, 2021).

Graham, M. C., R. Allan, A. E. Fallick, and J. G. Farmer (2006): "Investigation of extraction and clean-up procedures used in the quantification and stable isotopic characterisation of PAHs in contaminated urban soils". In: *Science of The Total Environment*. Urban Environmental Research in the UK: The Urban Regeneration and the Environment (NERC URGENT) Programme and associated studies. 360.1, pp. 81–89. DOI: 10.1016/j.scitotenv.2005.08.026.

Gribble, G. W. (2010): *Naturally Occurring Organohalogen Compounds – A Comprehensive Update*. Vol. 91. Fortschritte der Chemie organischer Naturstoffe / Progress in the Chemistry of Organic Natural Products. Vienna, Austria: Springer Vienna. DOI: 10.1007/978-3-211-99323-1.

Guha, N., D. Loomis, Y. Grosse, B. Lauby-Secretan, F. E. Ghissassi, V. Bouvard, L. Benbrahim-Tallaa, R. Baan, H. Mattock, and K. Straif (2012): "Carcinogenicity of trichloroethylene, tetrachloroethylene, some other chlorinated solvents, and their metabolites". In: *The Lancet Oncology* 13.12, pp. 1192–1193. DOI: 10.1016/S1470-2045(12)70485-0.

Häggblom, M. M. and I. D. Bossert (2004): "Halogenated organic compounds – A global perspective". In: *Dehalogenation*. Ed. by M. M. Häggblom and I. D. Bossert. Boston, MA, USA: Kluwer Academic Publishers, pp. 3–29. DOI: 10.1007/0-306-48011-5_1.

Halloran, L. J. S. and D. Hunkeler (2020): "Controls on the persistence of aqueous-phase groundwater contaminants in the presence of reactive back-diffusion". In: *Science of The Total Environment* 722, p. 137749. DOI: 10.1016/j.scitotenv.2020.137749.

Halloran, L. J., P. Brunner, and D. Hunkeler (2019): "COMPEST, a PEST-COMSOL interface for inverse multiphysics modelling: Development and application to isotopic fractionation of groundwater contaminants". In: *Computers & Geosciences* 126, pp. 107–119. DOI: 10.1016/j.cageo.2019.02.001.

Han, Y.-S., S. P. Hyun, H. Y. Jeong, and K. F. Hayes (2012): "Kinetic study of *cis*-dichloroethylene (*cis*-DCE) and vinyl chloride (VC) dechlorination using green rusts formed under varying conditions". In: *Water Research* 46.19, pp. 6339–6350. DOI: 10.1016/j.watres.2012.08.041.

Hara, J. (2012): "Chemical degradation of chlorinated organic pollutants for in situ remediation and evaluation of natural attenuation". In: *Organic Pollutants Ten Years After the Stockholm Convention*. Ed. by T. Puzyn and A. Mostrag-Szlichtyng. Rijeka, Croatia: INTECH Open Access Publisher. DOI: 10.5772/31775.

Harrington, E. C. (1965): "The desirability function". In: *Industrial quality control* 21.10, pp. 494–498.

He, Y. T., J. T. Wilson, C. Su, and R. T. Wilkin (2015): "Review of abiotic degradation of chlorinated solvents by reactive iron minerals in aquifers". In: *Groundwater Monitoring & Remediation* 35.3, pp. 57–75. DOI: 10.1111/gwmr.12111.

He, Y. T., J. T. Wilson, and R. T. Wilkin (2010): "Impact of iron sulfide transformation on trichloroethylene degradation". In: *Geochimica et Cosmochimica Acta* 74.7, pp. 2025–2039. DOI: 10.1016/j.gca.2010.01.013.

Heckel, B., D. Rodríguez-Fernández, C. Torrentó, A. Meyer, J. Palau, C. Domènech, M. Rosell, A. Soler, D. Hunkeler, and M. Elsner (2017): "Compound-specific chlorine isotope analysis of tetrachloromethane and trichloromethane by gas chromatography-isotope ratio mass spectrometry vs gas chromatography-quadrupole mass spectrometry: Method development and evaluation of precision and trueness". In: *Analytical Chemistry* 89.6, pp. 3411–3420. DOI: 10.1021/acs.analchem.6b04129.

Heraty, L. J., M. E. Fuller, L. Huang, T. Abrajano, and N. C. Sturchio (1999): "Isotopic fractionation of carbon and chlorine by microbial degradation of dichloromethane". In: *Organic Geochemistry* 30.8, pp. 793–799. DOI: 10.1016/S0146-6380(99)00062-5.

Herrero, J., D. Puigserver, B. L. Parker, and J. M. Carmona (2021): "A new method for determining compound specific carbon isotope of chlorinated solvents in porewater". In: *Groundwater Monitoring & Remediation* n/a (n/a). DOI: 10.1111/gwmr.12435.

Hewitt, A. D. (1998): "Comparison of sample preparation methods for the analysis of volatile organic compounds in soil samples: Solvent extraction vs vapor partitioning". In: *Environmental Science & Technology* 32.1, pp. 143–149. DOI: 10.1021/es970431q.

Hitzfeld, K. L., M. Gehre, and H.-H. Richnow (2011): "A novel online approach to the determination of isotopic ratios for organically bound chlorine, bromine and sulphur: Isotopic ratios for organically bound chlorine, bromine and sulphur". In: *Rapid Communications in Mass Spectrometry* 25.20, pp. 3114–3122. DOI: 10.1002/rcm.5203.

Höhener, P. (2016): "Simulating stable carbon and chlorine isotope ratios in dissolved chlorinated groundwater pollutants with BIOCHLOR-ISO". In: *Journal of Contaminant Hydrology* 195, pp. 52–61. DOI: 10.1016/j.jconhyd.2016.11.002.

Holmstrand, H., P. Andersson, and Ö. Gustafsson (2004): "Chlorine isotope analysis of submicromole organochlorine samples by sealed tube combustion and thermal ionization mass spectrometry". In: *Analytical Chemistry* 76.8, pp. 2336–2342. DOI: 10.1021/ac0354802.

Holmstrand, H., M. Mandalakis, Z. Zencak, Ö. Gustafsson, and P. Andersson (2006): "Chlorine isotope fractionation of a semi-volatile organochlorine compound during preparative megabore-column capillary gas chromatography". In: *Journal of Chromatography A* 1103.1, pp. 133–138. DOI: 10.1016/j.chroma.2005.11.009.

Holt, B. D., N. Sturchio, T. Abrajano, and L. Heraty (1997): "Conversion of chlorinated volatile organic compounds to carbon dioxide and methyl chloride for isotopic analysis of carbon and chlorine". In: *Analytical Chemistry* 69. DOI: 10.1021/ac961096b.

Horii, Y., K. Kannan, G. Petrick, T. Gamo, J. Falandysz, and N. Yamashita (2005): "Congener-specific carbon isotopic analysis of technical PCB and PCN mixtures using two-dimensional gas chromatography–isotope ratio mass spectrometry". In: *Environmental Science & Technology* 39.11, pp. 4206–4212. DOI: 10.1021/es050133q.

Horst, A., G. Lacrampe-Couloume, and B. Sherwood Lollar (2016): "Vapor pressure isotope effects in halogenated organic compounds and alcohols dissolved in water". In: *Analytical Chemistry* 88.24, pp. 12066–12071. DOI: 10.1021/acs.analchem.6b02597.

Horst, A., J. Renpenning, H.-H. Richnow, and M. Gehre (2017): "Compound specific stable chlorine isotopic analysis of volatile aliphatic compounds using gas chromatography hyphenated with multiple collector inductively coupled plasma mass spectrometry". In: *Analytical Chemistry* 89.17, pp. 9131–9138. DOI: 10.1021/acs.analchem.7b01875.

Huang, L., N. Sturchio, T. Abrajano, L. Heraty, and B. Holt (1999): "Carbon and chlorine isotope fractionation of chlorinated aliphatic hydrocarbons by evaporation". In: *Organic Geochemistry* 30.8, pp. 777–785. DOI: 10.1016/S0146-6380(99)00060-1.

Hunkeler, D. and R. Aravena (2000): "Determination of compound-specific carbon isotope ratios of chlorinated methanes, ethanes, and ethenes in aqueous samples". In: *Environmental Science & Technology* 34.13, pp. 2839–2844. DOI: 10.1021/es991178s.

Hunkeler, D., R. U. Meckenstock, B. Sherwood Lollar, T. C. Schmidt, and J. T. Wilson (2008): *A Guide for Assessing Biodegradation and Source Identification of Organic Ground Water Contaminants using Compound Specific Isotope Analysis (CSIA)*. Tech. rep. Washington, DC, USA: Office of Research and Development, National Risk Management Research Laboratory, US Environmental Protection Agency. URL: https://cfpub.epa.gov/si/si_public_record_report.cfm?Lab=NRMRL&dirEntryId=202171.

Hunkeler, D., B. M. van Breukelen, and M. Elsner (2009): "Modeling chlorine isotope trends during sequential transformation of chlorinated ethenes". In: *Environmental Science & Technology* 43.17, pp. 6750–6756. DOI: 10.1021/es900579z.

Hunkeler, D., Y. Abe, M. M. Broholm, S. Jeannottat, C. Westergaard, C. S. Jacobsen, R. Aravena, and P. L. Bjerg (2011a): "Assessing chlorinated ethene degradation in a large scale contaminant plume by dual carbon-chlorine isotope analysis and quantitative PCR". In: *Journal of Contaminant Hydrology* 119.1, pp. 69–79. DOI: 10.1016/j.jconhyd.2010.09.009.

Hunkeler, D., R. Aravena, O. Shouakar-Stash, N. Weisbrod, A. Nasser, L. Netzer, and D. Ronen (2011b): "Carbon and chlorine isotope ratios of chlorinated ethenes migrating through a thick unsaturated zone of a sandy aquifer". In: *Environmental Science & Technology* 45.19, pp. 8247–8253. DOI: 10.1021/es201415k.

Hunkeler, D., T. Laier, F. Breider, and O. S. Jacobsen (2012): "Demonstrating a natural origin of chloroform in groundwater using stable carbon isotopes". In: *Environmental Science & Technology* 46.11, pp. 6096–6101. DOI: 10.1021/es204585d.

Huybrechts, T., J. Dewulf, K. Van Craeynest, and H. Van Langenhove (2001): "Evaluation of tetraglyme for the enrichment and analysis of volatile organic compounds in air". In: *Journal of Chromatography A* 922.1, pp. 207–218. DOI: 10.1016/S0021-9673(01)00930-X.

Ingram, J. C., M. M. Cortez, D. L. Bates, and M. O. McCurry (2000): "Reductive dechlorination of trichloroethylene and carbon tetrachloride at iron oxides and basalt minerals". In: *Nuclear Site Remediation*. Vol. 778. ACS Symposium Series. Washington, DC, USA: American Chemical Society, pp. 267–281. DOI: 10.1021/bk-2001-0778.ch016.

Isenschmid, F. (2018): "Assessing the remediation of an aquifer - aquitard system contaminated by chlorinated hydrocarbons". Master's thesis. Neuchâtel, NE, Switzerland: Université de Neuchâtel.

Jakubowska, N., B. Zygmunt, Ż. Polkowska, B. Zabiegała, and J. Namieśnik (2009): "Sample preparation for gas chromatographic determination of halogenated volatile organic compounds in environmental and biological samples". In: *Journal of Chromatography A* 1216.3, pp. 422–441. DOI: 10.1016/j.chroma.2008.08.092.

Jancsó, G. and W. A. Van Hook (1974): "Condensed phase isotope effects". In: *Chemical Reviews* 74.6, pp. 689–750. DOI: 10.1021/cr60292a004.

Jeannottat, S. and D. Hunkeler (2012): "Chlorine and carbon isotopes fractionation during volatilization and diffusive transport of trichloroethene in the unsaturated zone". In: *Environmental Science & Technology* 46.6, pp. 3169–3176. DOI: 10.1021/es203547p.

Jendrzejewski, N., H. G. M. Eggenkamp, and M. L. Coleman (1997): "Sequential determination of chlorine and carbon isotopic composition in single microliter samples of chlorinated solvent". In: *Analytical Chemistry* 69.20, pp. 4259–4266. DOI: 10.1021/ac970447z.

Jenkins, T. F. and P. W. Schumacher (1987): *Comparison of Methanol and Tetraglyme as Extraction Solvents for Determination of Volatile Organics in Soil*. Special Report 87-22. Hanover, NH, USA: U.S. Army Cold Regions Research and Engineering Laboratory. URL: http://www.dtic.mil/docs/citations/ADA189028 (visited on Nov. 19, 2018).

Jeong, H. Y., H. Kim, and K. F. Hayes (2007): "Reductive dechlorination pathways of tetrachloroethylene and trichloroethylene and subsequent transformation of their dechlorination products by mackinawite (FeS) in the presence of metals". In: *Environmental Science & Technology* 41.22, pp. 7736–7743. DOI: 10.1021/es0708518.

Jeong, H. Y., K. Anantharaman, Y.-S. Han, and K. F. Hayes (2011): "Abiotic reductive dechlorination of *cis*-dichloroethylene by Fe species formed during iron- or sulfate-reduction". In: *Environmental Science & Technology* 45.12, pp. 5186–5194. DOI: 10.1021/es104387w.

Jeong, H. Y., K. Anantharaman, S. P. Hyun, M. Son, and K. F. Hayes (2013): "pH impact on reductive dechlorination of *cis*-dichloroethylene by Fe precipitates: An X-ray absorption spectroscopy study". In: *Water Research* 47.17, pp. 6639–6649. DOI: 10.1016/j.watres.2013.08.035.

Jin, B., C. Laskov, M. Rolle, and S. B. Haderlein (2011): "Chlorine isotope analysis of organic contaminants using GC-qMS: Method optimization and comparison of different evaluation schemes". In: *Environmental Science & Technology* 45.12, pp. 5279–5286. DOI: 10.1021/es200749d.

Jin, B., S. B. Haderlein, and M. Rolle (2013): "Integrated carbon and chlorine isotope modeling: Applications to chlorinated aliphatic hydrocarbons dechlorination". In: *Environmental Science and Technology* 47.3, pp. 1443–1451. DOI: 10.1021/es304053h.

Jin, B., M. Rolle, T. Li, and S. B. Haderlein (2014): "Diffusive fractionation of BTEX and chlorinated ethenes in aqueous solution: Quantification of spatial isotope gradients". In: *Environmental Science and Technology* 48.11, pp. 6141–6150. DOI: 10.1021/es4046956.

Jochmann, M. A., M. Blessing, S. B. Haderlein, and T. C. Schmidt (2006): "A new approach to determine method detection limits for compound-specific isotope analysis of volatile organic compounds". In: *Rapid Communications in Mass Spectrometry* 20.24, pp. 3639–3648. DOI: 10.1002/rcm.2784.

Jochmann, M. A. and T. C. Schmidt (2015): *Compound-specific Stable Isotope Analysis*. Cambridge, UK: Royal Society of Chemistry. 331 pp.

Kent, B. and G. C. B. Mosquera (2001): "Remediation of NAPL-contaminated aquifers: Is the cure worth the cost?" In: *Journal of Environmental Science and Health, Part A* 36.8, pp. 1559–1569. DOI: 10.1081/ESE-100105731.

Khoder, K. (2011): "Optimisation de composants hyperfréquences par la technique des plans à surfaces de réponses". PhD Thesis. Limoges, France: Université de Limoges. URL: http://aurore.unilim.fr/ori-oai-search/notice/view/unilim-ori-28713 (visited on Jan. 5, 2021).

Kim, M., M. C. Kennicutt, and Y. Qian (2005): "Polycyclic aromatic hydrocarbon purification procedures for compound specific isotope analysis". In: *Environmental Science & Technology* 39.17, pp. 6770–6776. DOI: 10.1021/es050577m.

Koenig, J., M. Lee, and M. Manefield (2015): "Aliphatic organochlorine degradation in subsurface environments". In: *Reviews in Environmental Science and Bio/Technology* 14.1, pp. 49–71. DOI: 10.1007/s11157-014-9345-3.

Kompala, D. S., D. Ramkrishna, and G. T. Tsao (1984): "Cybernetic modeling of microbial growth on multiple substrates". In: *Biotechnology and Bioengineering* 26.11, pp. 1272–1281. DOI: 10.1002/bit.260261103.

Kremser, A., M. A. Jochmann, and T. C. Schmidt (2016): "Systematic comparison of static and dynamic headspace sampling techniques for gas chromatography". In: *Analytical and Bioanalytical Chemistry* 408.24, pp. 6567–6579. DOI: 10.1007/s00216-016-9843-y.

Kuder, T., B. M. van Breukelen, M. Vanderford, and P. Philp (2013): "3D-CSIA: Carbon, chlorine, and hydrogen isotope fractionation in transformation of TCE to ethene by a *Dehalococcoides* culture". In: *Environmental Science & Technology* 47.17, pp. 9668–9677. DOI: 10.1021/es400463p.

Lan, Y., A. S. Elwood Madden, and E. C. Butler (2016): "Transformation of mackinawite to greigite by trichloroethylene and tetrachloroethylene". In: *Environmental Science: Processes & Impacts* 18.10, pp. 1266–1273. DOI: 10.1039/C6EM00461J.

Langevin, P. (1908): "Sur la théorie du mouvement brownien". In: *Comptes rendus de l'académie des sciences* 146, pp. 530–533. URL: https://gallica.bnf.fr/ark:/12148/bpt6k3100t/f530.image (visited on Jan. 5, 2021).

Langvad, T., H. Richtzenhain, V. Salakivi, and A. I. Virtanen (1954): "Separation of chlorine isotopes by ion-exchange chromatography." In: *Acta Chemica Scandinavica* 8, pp. 526–527. DOI: 10.3891/acta.chem.scand.08-0526.

Lawrence, S. J. (2006): *Description, Properties, and Degradation of Selected Volatile Organic Compounds Detected in Ground Water – A Review of Selected Literature*. Open-File Report 2006-1338. 62 pp. DOI: 10.3133/ofr20061338.

Leardi, R. (2009): "Experimental design in chemistry: A tutorial". In: *Analytica Chimica Acta* 652.1, pp. 161–172. DOI: 10.1016/j.aca.2009.06.015.

Lecloux, A. (2003): "Scientific activities of Euro Chlor in monitoring and assessing naturally and man-made organohalogens". In: *Chemosphere* 52.2, pp. 521–529. DOI: 10.1016/S0045-6535(03)00205-4.

Lee, K.-J., H. Pyo, S.-J. Park, E.-A. Yoo, and D.-W. Lee (2001): "A study on purge efficiency in purge and trap analysis of VOCs in water". In: *Bulletin of the Korean Chemical Society* 22.2, pp. 171–178. URL: https://www.koreascience.or.kr/article/JAKO200113464477510.

Lee, W. and B. Batchelor (2002a): "Abiotic reductive dechlorination of chlorinated ethylenes by iron-bearing soil minerals. 1. Pyrite and magnetite". In: *Environmental Science & Technology* 36.23, pp. 5147–5154. DOI: 10.1021/es025836b.

Lee, W. and B. Batchelor (2002b): "Abiotic reductive dechlorination of chlorinated ethylenes by iron-bearing soil minerals. 2. Green rust". In: *Environmental Science & Technology* 36.24, pp. 5348–5354. DOI: 10.1021/es0258374.

Lee, W. and B. Batchelor (2004): "Abiotic reductive dechlorination of chlorinated ethylenes by iron-bearing phyllosilicates". In: *Chemosphere* 56.10, pp. 999–1009. DOI: 10.1016/j.chemosphere.2004.05.015.

Leeuwen, K. A. v., P. D. Prenzler, D. Ryan, and F. Camin (2014): "Gas chromatography-combustion-isotope ratio mass spectrometry for traceability and authenticity in foods and beverages". In: *Comprehensive Reviews in Food Science and Food Safety* 13.5, pp. 814–837. DOI: 10.1111/1541-4337.12096.

Lennie, A. R. (1995): "Synthesis and Rietveld crystal structure refinement of mackinawite, tetragonal FeS". In: *Mineralogical Magazine* 59.397, pp. 677–683. DOI: 10.1180/minmag.1995.059.397.10.

Liang, X., Y. Dong, T. Kuder, L. R. Krumholz, R. P. Philp, and E. C. Butler (2007): "Distinguishing abiotic and biotic transformation of tetrachloroethylene and trichloroethylene by stable carbon isotope fractionation". In: *Environmental Science & Technology* 41.20, pp. 7094–7100. DOI: 10.1021/es070970n.

Liang, X., R. P. Philp, and E. C. Butler (2009): "Kinetic and isotope analyses of tetrachloroethylene and trichloroethylene degradation by model Fe(II)-bearing minerals". In: *Chemosphere* 75.1, pp. 63–69. DOI: 10.1016/j.chemosphere.2008.11.042.

Liu, C. and W. P. Ball (2002): "Back diffusion of chlorinated solvent contaminants from a natural aquitard to a remediated aquifer under well-controlled field conditions: Predictions and measurements". In: *Ground Water* 40.2, pp. 175–184. DOI: 10.1111/j.1745-6584.2002.tb02502.x.

Liu, Y., Y. Gan, A. Zhou, C. Liu, X. Li, and T. Yu (2014): "Carbon and chlorine isotope fractionation during Fenton-like degradation of trichloroethene". In: *Chemosphere* 107, pp. 94–100. DOI: 10.1016/j.chemosphere.2014.03.011.

Long, A., C. J. Eastoe, R. S. Kaufmann, J. G. Martin, L. Wirt, and J. B. Finley (1993): "High-precision measurement of chlorine stable isotope ratios". In: *Geochimica et Cosmochimica Acta* 57.12, pp. 2907–2912. DOI: 10.1016/0016-7037(93)90398-G.

Luo, J. and J. Farrell (2013): "Understanding pH effects on trichloroethylene and perchloroethylene adsorption to iron in permeable reactive barriers for groundwater remediation". In: *International Journal of Environmental Science and Technology* 10.1, pp. 77–84. DOI: 10.1007/s13762-012-0082-2.

Magenheim, A., A. Spivack, C. Volpe, and B. Ransom (1994): "Precise determination of stable chlorine isotopic ratios in low-concentration natural samples". In: *Geochimica et Cosmochimica Acta* 58.14, pp. 3117–3121. DOI: 10.1016/0016-7037(94)90183-X.

Maithreepala, R. A. and R.-a. Doong (2005): "Enhanced dechlorination of chlorinated methanes and ethenes by chloride green rust in the presence of copper(II)". In: *Environmental Science & Technology* 39.11, pp. 4082–4090. DOI: 10.1021/es048428b.

Mandalakis, M., H. Holmstrand, P. Andersson, and Ö. Gustafsson (2008): "Compound-specific chlorine isotope analysis of polychlorinated biphenyls isolated from Aroclor and Clophen technical mixtures". In: *Chemosphere* 71.2, pp. 299–305. DOI: 10.1016/j.chemosphere.2007.09.004.

Mangayayam, M. C., K. Dideriksen, and D. J. Tobler (2018): "Can or cannot green rust reduce chlorinated ethenes?" In: *Energy Procedia*. Carbon in natural and engineered processes: Selected contributions from the 2018 International Carbon Conference 146, pp. 173–178. DOI: 10.1016/j.egypro.2018.07.022.

Manickum, T. and W. John (2011): "Trace analysis of taste-odor compounds in water by salt-free purge-and-trap sampling with GC-MS detection". In: *Journal of Waste Water Treatment & Analysis* 2.5. DOI: 10.4172/2157-7587.1000121.

Marrubini, G., S. Dugheri, G. Cappelli, G. Arcangeli, N. Mucci, P. Appelblad, C. Melzi, and A. Speltini (2020): "Experimental designs for solid-phase microextraction method development in bioanalysis: A review". In: *Analytica Chimica Acta* 1119, pp. 77–100. DOI: 10.1016/j.aca.2020.04.012.

Maxwell, J. C. (1867): "On the dynamical theory of gases". In: *Philosophical Transactions of the Royal Society of London* 157, pp. 49–88. DOI: 10.1098/rstl.1867.0004.

Meckenstock, R. U., B. Morasch, C. Griebler, and H.-H. Richnow (2004): "Stable isotope fractionation analysis as a tool to monitor biodegradation in contaminated aquifers". In: *Journal of Contaminant Hydrology* 75.3, pp. 215–255. DOI: 10.1016/j.jconhyd.2004.06.003.

Meier-Augenstein, W., P. W. Watt, and C.-D. Langhans (1996): "Influence of gas chromatographic parameters on measurement of $^{13}C/^{12}C$ isotope ratios by gas-liquid chromatography-combustion isotope ratio mass spectrometry. I". In: *Journal of Chromatography A* 752.1, pp. 233–241. DOI: 10.1016/S0021-9673(96)00498-0.

Michot, L. J. (1991): "Adsorption of chlorinated phenols from aqueous solution by surfactant-modified pillared clays". In: *Clays and Clay Minerals* 39.6, pp. 634–641. DOI: 10.1346/CCMN.1991.0390609.

Minnich, M. M., B. A. Schumacher, and J. H. Zimmerman (1997): "Comparison of soil VOCs measured by soil gas, heated headspace, and methanol extraction techniques". In: *Journal of Soil Contamination* 6.2, pp. 187–203. DOI: 10.1080/15320389709383556.

Murray, A. M., C. B. Ottosen, J. Maillard, C. Holliger, A. Johansen, L. Brabæk, I. L. Kristensen, J. Zimmermann, D. Hunkeler, and M. M. Broholm (2019): "Chlorinated ethene plume evolution after source thermal remediation: Determination of degradation rates and mechanisms". In: *Journal of Contaminant Hydrology* 227, p. 103551. DOI: 10.1016/j.jconhyd.2019.103551.

Nara, H., F. Nakagawa, and N. Yoshida (2006): "Development of two-dimensional gas chromatography/isotope ratio mass spectrometry for the stable carbon isotopic analysis of C_2-C_5 non-methane hydrocarbons emitted from biomass burning". In: *Rapid Communications in Mass Spectrometry* 20.2, pp. 241–247. DOI: 10.1002/rcm.2302.

Numata, M., N. Nakamura, H. Koshikawa, and Y. Terashima (2002a): "Chlorine isotope fractionation during reductive dechlorination of chlorinated ethenes by anaerobic bacteria". In: *Environmental Science & Technology* 36.20, pp. 4389–4394. DOI: 10.1021/es025547n.

Numata, M., N. Nakamura, H. Koshikawa, and Y. Terashima (2002b): "Chlorine stable isotope measurements of chlorinated aliphatic hydrocarbons by thermal ionization mass spectrometry". In: *Analytica Chimica Acta* 455.1, pp. 1–9. DOI: 10.1016/S0003-2670(01)01566-5.

O'Loughlin, E. J., K. M. Kemner, and D. R. Burris (2003): "Effects of Ag(I) , Au(III), and Cu(II) on the reductive dechlorination of carbon tetrachloride by green rust". In: *Environmental Science & Technology* 37.13, pp. 2905–2912. DOI: 10.1021/es030304w.

O'Loughlin, E. J. and D. R. Burris (2004): "Reduction of halogenated ethanes by green rust". In: *Environmental Toxicology and Chemistry* 23.1, p. 41. DOI: 10.1897/03-45.

Oh, S., W. S. Shin, and H. T. Kim (2016): "Effects of pH, dissolved organic matter, and salinity on ibuprofen sorption on sediment". In: *Environmental Science and Pollution Research* 23.22, pp. 22882–22889. DOI: 10.1007/s11356-016-7503-6.

Ohlsson, K. E. A. and P. H. Wallmark (1999): "Novel calibration with correction for drift and non-linear response for continuous flow isotope ratio mass spectrometry applied to the determination of δ^{15}N, total nitrogen, δ^{14}C and total carbon in biological material". In: *Analyst* 124.4, pp. 571–577. DOI: 10.1039/A900855A.

Ojeda, A. S., E. Phillips, and B. S. Lollar (2019a): "Multi-element (C, H, Cl, Br) stable isotope fractionation as a tool to investigate transformation processes for halogenated hydrocarbons". In: *Environmental Science: Processes & Impacts* 22.3, pp. 567–582. DOI: 10.1039/C9EM00498J.

Ojeda, A. S., E. Phillips, S. A. Mancini, and B. S. Lollar (2019b): "Sources of uncertainty in biotransformation mechanistic interpretations and remediation studies using CSIA". In: *Analytical Chemistry* 91.14, pp. 9147–9153. DOI: 10.1021/acs.analchem.9b01756.

Ottosen, C. B., P. L. Bjerg, D. Hunkeler, J. Zimmermann, N. Tuxen, D. Harrekilde, L. Bennedsen, G. Leonard, L. Brabæk, I. L. Kristensen, and M. M. Broholm (2021): "Assessment of chlorinated ethenes degradation after field scale injection of activated carbon and bioamendments: Application of isotopic and microbial analyses". In: *Journal of Contaminant Hydrology* 240, p. 103794. DOI: 10.1016/j.jconhyd.2021.103794.

Owen, H. R. and O. A. Schaeffer (1955): "The isotope abundances of chlorine from various sources". In: *Journal of the American Chemical Society* 77.4, pp. 898–899. DOI: 10.1021/ja01609a026.

Page, B. D. and G. Lacroix (2000): "Analysis of volatile contaminants in vegetable oils by headspace solid-phase microextraction with carboxen-based fibres". In: *Journal of Chromatography A* 873.1, pp. 79–94. DOI: 10.1016/S0021-9673(99)01201-7.

Palau, J., A. Soler, P. Teixidor, and R. Aravena (2007): "Compound-specific carbon isotope analysis of volatile organic compounds in water using solid-phase microextraction". In: *Journal of Chromatography A* 1163.1, pp. 260–268. DOI: 10.1016/j.chroma.2007.06.050.

Palau, J., R. Yu, S. Hatijah Mortan, O. Shouakar-Stash, M. Rosell, D. L. Freedman, C. Sbarbati, S. Fiorenza, R. Aravena, E. Marco-Urrea, M. Elsner, A. Soler, and D. Hunkeler (2017a): "Distinct dual C-Cl isotope fractionation patterns during anaerobic biodegradation of 1,2-dichloroethane: Potential to characterize microbial degradation in the field". In: *Environmental Science & Technology* 51.5, pp. 2685–2694. DOI: 10.1021/acs.est.6b04998.

Palau, J., S. Cretnik, O. Shouakar-Stash, M. Höche, M. Elsner, and D. Hunkeler (2014a): "C and Cl isotope fractionation of 1,2-dichloroethane displays unique $\delta^{13}C/\delta^{37}Cl$ patterns for pathway identification and reveals surprising C-Cl bond involvement in microbial oxidation". In: *Environmental Science & Technology* 48.16, pp. 9430–9437. DOI: 10.1021/es5031917.

Palau, J., O. Shouakar-Stash, and D. Hunkeler (2014b): "Carbon and chlorine isotope analysis to identify abiotic degradation pathways of 1,1,1-trichloroethane". In: *Environmental Science & Technology* 48.24, pp. 14400–14408. DOI: 10.1021/es504252z.

Palau, J., M. Marchesi, J. C. Chambon, R. Aravena, A. Canals, P. J. Binning, P. L. Bjerg, N. Otero, and A. Soler (2014c): "Multi-isotope (carbon and chlorine) analysis for fingerprinting and site characterization at a fractured bedrock aquifer contaminated by chlorinated ethenes". In: *Science of The Total Environment* 475, pp. 61–70. DOI: 10.1016/j.scitotenv.2013.12.059.

Palau, J., P. Jamin, A. Badin, N. Vanhecke, B. Haerens, S. Brouyère, and D. Hunkeler (2016): "Use of dual carbon-chlorine isotope analysis to assess the degradation pathways of 1,1,1-trichloroethane in groundwater". In: *Water Research* 92, pp. 235–243. DOI: 10.1016/j.watres.2016.01.057.

Palau, J., O. Shouakar-Stash, S. Hatijah Mortan, R. Yu, M. Rosell, E. Marco-Urrea, D. L. Freedman, R. Aravena, A. Soler, and D. Hunkeler (2017b): "Hydrogen isotope fractionation during the biodegradation of 1,2-dichloroethane: Potential for pathway identification using a multi-element (C, Cl, and H) isotope approach". In: *Environmental Science & Technology* 51.18, pp. 10526–10535. DOI: 10.1021/acs.est.7b02906.

Panagos, P., M. Van Liedekerke, Y. Yigini, and L. Montanarella (2013): "Contaminated sites in Europe: Review of the current situation based on data collected through a European network". In: *Journal of Environmental and Public Health* 2013, e158764. DOI: 10.1155/2013/158764.

Parker, B. L., J. A. Cherry, and S. W. Chapman (2004): "Field study of TCE diffusion profiles below DNAPL to assess aquitard integrity". In: *Journal of Contaminant Hydrology* 74.1, pp. 197–230. DOI: 10.1016/j.jconhyd.2004.02.011.

Parker, B. L., S. W. Chapman, and M. A. Guilbeault (2008): "Plume persistence caused by back diffusion from thin clay layers in a sand aquifer following TCE source-zone hydraulic isolation". In: *Journal of Contaminant Hydrology* 102.1-2, pp. 86–104. DOI: 10.1016/j.jconhyd.2008.07.003.

Paul, D., G. Skrzypek, and I. Fórizs (2007): "Normalization of measured stable isotopic compositions to isotope reference scales – A review". In: *Rapid Communications in Mass Spectrometry* 21.18, pp. 3006–3014. DOI: 10.1002/rcm.3185.

Pawliszyn, J., ed. (2012): *Handbook of Solid Phase Microextraction*. London, UK: Elsevier. DOI: 10.1016/C2011-0-04297-7.

Pham, H. T., M. Kitsuneduka, J. Hara, K. Suto, and C. Inoue (2008): "Trichloroethylene transformation by natural mineral pyrite: The deciding role of oxygen". In: *Environmental Science & Technology* 42.19, pp. 7470–7475. DOI: 10.1021/es801310y.

Philp, R. P. (2007): "The emergence of stable isotopes in environmental and forensic geochemistry studies: A review". In: *Environmental Chemistry Letters* 5.2, pp. 57–66. DOI: 10.1007/s10311-006-0081-y.

Ponsin, V., T. E. Buscheck, and D. Hunkeler (2017): "Heart-cutting two-dimensional gas chromatography-isotope ratio mass spectrometry analysis of monoaromatic hydrocarbons in complex groundwater and gas-phase samples". In: *Journal of Chromatography A* 1492, pp. 117–128. DOI: 10.1016/j.chroma.2017.02.060.

Popp, P. and A. Paschke (1997): "Solid phase microextraction of volatile organic compounds using carboxen-polydimethylsiloxane fibers". In: *Chromatographia* 46.7, pp. 419–424. DOI: 10.1007/BF02490880.

Poulson, S. R. and J. I. Drever (1999): "Stable isotope (C, Cl, and H) fractionation during vaporization of trichloroethylene". In: *Environmental Science & Technology* 33.20, pp. 3689–3694. DOI: 10.1021/es990406f.

Reddy, C., L. Heraty, B. Holt, N. Sturchio, T. Eglinton, N. Drenzek, L. Xu, J. Lake, and K. Maruya (2000): "Stable chlorine isotopic compositions of Aroclors and Aroclor-contaminated sediments". In: *Environmental Science & Technology* 34. DOI: 10.1021/es9908220.

Renpenning, J., S. Keller, S. Cretnik, O. Shouakar-Stash, M. Elsner, T. Schubert, and I. Nijenhuis (2014): "Combined C and Cl isotope effects indicate differences between corrinoids and enzyme (*Sulfurospirillum multivorans* PceA) in reductive dehalogenation of tetrachloroethene, but not trichloroethene". In: *Environmental Science & Technology* 48.20, pp. 11837–11845. DOI: 10.1021/es503306g.

Renpenning, J., K. L. Hitzfeld, T. Gilevska, I. Nijenhuis, M. Gehre, and H.-H. Richnow (2015): "Development and validation of an universal interface for compound-specific stable isotope analysis of chlorine (^{37}Cl/^{35}Cl) by GC-high-temperature conversion (HTC)-MS/IRMS". In: *Analytical Chemistry* 87.5, pp. 2832–2839. DOI: 10.1021/ac504232u.

Ricci, M. P., D. A. Merritt, K. H. Freeman, and J. M. Hayes (1994): "Acquisition and processing of data for isotope-ratio-monitoring mass spectrometry". In: *Organic Geochemistry* 21.6, pp. 561–571. DOI: 10.1016/0146-6380(94)90002-7.

Rickard, D. (1969): "The chemistry of iron sulphide formation at low temperatures". In: *Stockhom Contributions to Geology* 20, pp. 67–95. URL: http://orca.cf.ac.uk/92418/ (visited on Sept. 13, 2017).

Rodríguez-Fernández, D., B. Heckel, C. Torrentó, A. Meyer, M. Elsner, D. Hunkeler, A. Soler, M. Rosell, and C. Domènech (2018a): "Dual element (C Cl) isotope approach to distinguish abiotic reactions of chlorinated methanes by Fe(0) and by Fe(II) on iron minerals at neutral and alkaline pH". In: *Chemosphere* 206, pp. 447–456. DOI: 10.1016/j.chemosphere.2018.05.036.

Rodríguez-Fernández, D., C. Torrentó, J. Palau, M. Marchesi, A. Soler, D. Hunkeler, C. Domènech, and M. Rosell (2018b): "Unravelling long-term source removal effects and chlorinated methanes natural attenuation processes by C and Cl stable isotopic patterns at a complex field site". In: *Science of The Total Environment* 645, pp. 286–296. DOI: 10.1016/j.scitotenv.2018.07.130.

Rodríguez-Fernández, D., C. Torrentó, M. Guivernau, M. Viñas, D. Hunkeler, A. Soler, C. Domènech, and M. Rosell (2018c): "Vitamin B_{12} effects on chlorinated methanes-degrading microcosms: Dual isotope and metabolically active microbial populations assessment". In: *Science of The Total Environment* 621, pp. 1615–1625. DOI: 10.1016/j.scitotenv.2017.10.067.

Rosell, M., J. Palau, S. H. Mortan, G. Caminal, A. Soler, O. Shouakar-Stash, and E. Marco-Urrea (2019): "Dual carbon - chlorine isotope fractionation during dichloroelimination of 1,1,2-trichloroethane by an enrichment culture containing *Dehalogenimonas* sp." In: *Science of The Total Environment* 648, pp. 422–429. DOI: 10.1016/j.scitotenv.2018.08.071.

Sakaguchi-Söder, K., J. Jager, H. Grund, F. Matthäus, and C. Schüth (2007): "Monitoring and evaluation of dechlorination processes using compound-specific chlorine isotope analysis". In: *Rapid Communications in Mass Spectrometry* 21.18, pp. 3077–3084. DOI: 10.1002/rcm.3170.

Schaefer, C. E., R. M. Towne, D. R. Lippincott, V. Lazouskaya, T. B. Fischer, M. E. Bishop, and H. Dong (2013): "Coupled diffusion and abiotic reaction of trichlorethene in minimally disturbed rock matrices". In: *Environmental Science & Technology* 47.9, pp. 4291–4298. DOI: 10.1021/es400457s.

Scherer, M. M., E. O'Loughlin, G. F. Parkin, R. Valentine, H. Al-Hosney, R. Handler, C. Just, P. Larese-Casanova, T. Pasakarnis, and S. L. Smith (2007): *Sustainability of Long-Term Abiotic Attenuation of Chlorinated Ethenes*. Iowa City, IA, USA: The University of Iowa. URL: http://www.dtic.mil/docs/citations/ADA476323 (visited on Sept. 12, 2017).

Schmidt, T. C. and M. A. Jochmann (2012): "Origin and fate of organic compounds in water: Characterization by compound-specific stable isotope analysis". In: *Annual Review of Analytical Chemistry* 5.1, pp. 133–155. DOI: 10.1146/annurev-anchem-062011-143143.

Schüth, C., M. Bill, J. A. C. Barth, G. F. Slater, and R. M. Kalin (2003): "Carbon isotope fractionation during reductive dechlorination of TCE in batch experiments with iron samples from reactive barriers". In: *Journal of Contaminant Hydrology* 66.1, pp. 25–37. DOI: 10.1016/S0169-7722(03)00026-3.

Schwarzenbach, R. P., P. M. Gschwend, and D. M. Imboden (2003): *Environmental Organic Chemistry*. 2nd Edition. Hoboken, NJ, USA: John Wiley & Sons. 1330 pp.

Sciarrone, D., A. Schepis, M. Zoccali, P. Donato, F. Vita, D. Creti, A. Alpi, and L. Mondello (2018): "Multidimensional gas chromatography coupled to combustion-isotope ratio mass spectrometry/quadrupole MS with a low-bleed ionic liquid secondary column for the authentication of truffles and products containing truffle". In: *Analytical Chemistry* 90.11, pp. 6610–6617. DOI: 10.1021/acs.analchem.8b00386.

Scott, K. M., X. Lu, C. M. Cavanaugh, and J. S. Liu (2004): "Optimal methods for estimating kinetic isotope effects from different forms of the Rayleigh distillation equation". In: *Geochimica et Cosmochimica Acta* 68.3, pp. 433–442. DOI: 10.1016/S0016-7037(03)00459-9.

Sherwood Lollar, B., S. K. Hirschorn, M. M. G. Chartrand, and G. Lacrampe-Couloume (2007): "An approach for assessing total instrumental uncertainty in compound-specific carbon isotope analysis: Implications for environmental remediation studies". In: *Analytical Chemistry* 79.9, pp. 3469–3475. DOI: 10.1021/ac062299v.

Shouakar-Stash, O., S. K. Frape, and R. J. Drimmie (2003): "Stable hydrogen, carbon and chlorine isotope measurements of selected chlorinated organic solvents". In: *Journal of Contaminant Hydrology* 60.3, pp. 211–228. DOI: 10.1016/S0169-7722(02)00085-2.

Shouakar-Stash, O., R. J. Drimmie, M. Zhang, and S. K. Frape (2006): "Compound-specific chlorine isotope ratios of TCE, PCE and DCE isomers by direct injection using CF-IRMS". In: *Applied Geochemistry* 21.5, pp. 766–781. DOI: 10.1016/j.apgeochem.2006.02.006.

Shouakar-Stash, O., S. K. Frape, R. Aravena, A. Gargini, M. Pasini, and R. J. Drimmie (2009): "Analysis of compound-specific chlorine stable isotopes of vinyl chloride by continuous flow–isotope ratio mass spectrometry (CF–IRMS)". In: *Environmental Forensics* 10.4, pp. 299–306. DOI: 10.1080/15275920903347628.

Slater, G. F., J. M. Ahad, B. Sherwood Lollar, R. Allen-King, and B. Sleep (2000): "Carbon isotope effects resulting from equilibrium sorption of dissolved VOCs". In: *Analytical Chemistry* 72.22, pp. 5669–5672. DOI: 10.1021/ac000691h.

Slater, G. F., B. Sherwood Lollar, R. Allen King, and S. O'Hannesin (2002): "Isotopic fractionation during reductive dechlorination of trichloroethene by zero-valent iron: Influence of surface treatment". In: *Chemosphere* 49.6, pp. 587–596. DOI: 10.1016/S0045-6535(02)00327-2.

Slater, G. F., B. S. Lollar, S. Lesage, and S. Brown (2003): "Carbon isotope fractionation of PCE and TCE during dechlorination by vitamin B_{12}". In: *Ground Water Monitoring & Remediation* 23.4, pp. 59–67. DOI: 10.1111/j.1745-6592.2003.tb00695.x.

Sparkman, O. D., Z. Penton, and F. G. Kitson (2011): *Gas Chromatography and Mass Spectrometry: A Practical Guide*. 2nd Edition. Cambridge, MA, USA: Academic Press. 633 pp.

Spietelun, A., A. Kloskowski, W. Chrzanowski, and J. Namieśnik (2013): "Understanding solid-phase microextraction: Key factors influencing the extraction process and trends in improving the technique". In: *Chemical Reviews* 113.3, pp. 1667–1685. DOI: 10.1021/cr300148j.

Staudinger, J. and P. V. Roberts (1996): "A critical review of Henry's law constants for environmental applications". In: *Critical Reviews in Environmental Science and Technology* 26.3, pp. 205–297. DOI: 10.1080/10643389609388492.

Stroo, H. F. and C. H. Ward, eds. (2010): *In Situ Remediation of Chlorinated Solvent Plumes*. New York, NY, USA: Springer New York. DOI: 10.1007/978-1-4419-1401-9.

Sturchio, N. C., J. L. Clausen, L. J. Heraty, L. Huang, B. D. Holt, and T. A. Abrajano (1998): "Chlorine isotope investigation of natural attenuation of trichloroethene in an aerobic aquifer". In: *Environmental Science & Technology* 32.20, pp. 3037–3042. DOI: 10.1021/es9802605.

Tanaka, N. and D. M. Rye (1991): "Chlorine in the stratosphere". In: *Nature* 353.6346, pp. 707–707. DOI: 10.1038/353707a0.

Tang, C., J. Tan, S. Xiong, J. Liu, Y. Fan, and X. Peng (2017): "Chlorine and bromine isotope fractionation of halogenated organic pollutants on gas chromatography columns". In: *Journal of Chromatography A* 1514, pp. 103–109. DOI: 10.1016/j.chroma.2017.07.058.

Tang, C., J. Tan, Z. Shi, Y. Fan, Z. Yu, and X. Peng (2019): "Chlorine and bromine isotope fractionations of halogenated organic compounds in fragmentation by gas chromatography-electron ionization high resolution mass spectrometry". In: *Journal of Chromatography A* 1603, pp. 278–287. DOI: 10.1016/j.chroma.2019.06.017.

Tatti, F., M. P. Papini, M. Raboni, and P. Viotti (2016): "Image analysis procedure for studying back-diffusion phenomena from low-permeability layers in laboratory tests". In: *Scientific Reports* 6.1, p. 30400. DOI: 10.1038/srep30400.

Taylor, J. W. and E. P. Grimsrud (1969): "Chlorine isotopic ratios by negative ion mass spectrometry". In: *Analytical Chemistry* 41.6, pp. 805–810. DOI: 10.1021/ac60275a002.

Tiehm, A. and K. R. Schmidt (2011): "Sequential anaerobic/aerobic biodegradation of chloroethenes – Aspects of field application". In: *Current Opinion in Biotechnology* 22.3, pp. 415–421. DOI: 10.1016/j.copbio.2011.02.003.

Tobiszewski, M. and J. Namieśnik (2012): "Abiotic degradation of chlorinated ethanes and ethenes in water". In: *Environmental Science and Pollution Research* 19.6, pp. 1994–2006. DOI: 10.1007/s11356-012-0764-9.

Torrentó, C., J. Palau, D. Rodríguez-Fernández, B. Heckel, A. Meyer, C. Domènech, M. Rosell, A. Soler, M. Elsner, and D. Hunkeler (2017): "Carbon and chlorine isotope fractionation patterns associated with different engineered chloroform transformation reactions". In: *Environmental Science & Technology* 51.11, pp. 6174–6184. DOI: 10.1021/acs.est.7b00679.

Tranchida, P. Q., D. Sciarrone, P. Dugo, and L. Mondello (2012): "Heart-cutting multidimensional gas chromatography: A review of recent evolution, applications, and future prospects". In: *Analytica Chimica Acta* 716, pp. 66–75. DOI: 10.1016/j.aca.2011.12.015.

Troost, J. (1999): "An air to water bridge: Air sampling and analysis using tetraglyme". In: *Analytical Chemistry* 71.7, pp. 1474–1478. DOI: 10.1021/ac981316g.

US EPA (2004): *Standard operating procedure: Sample preparation and calculations for dissolved gas analysis in water samples using a GC headspace equilibration technique*. RSKSOP-175. URL: https://archive.epa.gov/region1/info/testmethods/web/pdf/rsksop175v2.pdf (visited on Apr. 28, 2020).

Vakili, F. (2017): "Stable isotope fractionations of chlorinated ethenes associated with physical processes". PhD thesis. Waterloo, ON, Canada: University of Waterloo. URL: https://uwspace.uwaterloo.ca/handle/10012/11268.

Van Hook, W. A. (2005): "Condensed matter isotope effects". In: *Isotope Effects In Chemistry and Biology*. Ed. by A. Kohen and H.-H. Limbach. Boca Raton, FL, USA: CRC Press. DOI: 10.1201/9781420028027.

Wang, Z., E. A. Schauble, and J. M. Eiler (2004): "Equilibrium thermodynamics of multiply substituted isotopologues of molecular gases". In: *Geochimica et Cosmochimica Acta* 68.23, pp. 4779–4797. DOI: 10.1016/j.gca.2004.05.039.

Wanner, P. and D. Hunkeler (2015): "Carbon and chlorine isotopologue fractionation of chlorinated hydrocarbons during diffusion in water and low permeability sediments". In: *Geochimica et Cosmochimica Acta* 157, pp. 198–212. DOI: 10.1016/j.gca.2015.02.034.

Wanner, P., B. L. Parker, S. W. Chapman, R. Aravena, and D. Hunkeler (2016): "Quantification of degradation of chlorinated hydrocarbons in saturated low permeability sediments using compound-specific isotope analysis". In: *Environmental Science & Technology* 50.11, pp. 5622–5630. DOI: 10.1021/acs.est.5b06330.

Wanner, P., B. L. Parker, S. W. Chapman, R. Aravena, and D. Hunkeler (2017): "Does sorption influence isotope ratios of chlorinated hydrocarbons under field conditions?" In: *Applied Geochemistry* 84, pp. 348–359. DOI: 10.1016/j.apgeochem.2017.07.016.

Wanner, P., B. L. Parker, S. W. Chapman, G. Lima, A. Gilmore, E. E. Mack, and R. Aravena (2018): "Identification of degradation pathways of chlorohydrocarbons in saturated low-permeability sediments using compound-specific isotope analysis". In: *Environmental Science & Technology* 52.13, pp. 7296–7306. DOI: 10.1021/acs.est.8b01173.

Wanner, P. and D. Hunkeler (2019): "Isotope fractionation due to aqueous phase diffusion – What do diffusion models and experiments tell? – A review". In: *Chemosphere* 219, pp. 1032–1043. DOI: 10.1016/j.chemosphere.2018.12.038.

Warmerdam, E. van, S. Frape, R. Aravena, R. Drimmie, H. Flatt, and J. Cherry (1995): "Stable chlorine and carbon isotope measurements of selected chlorinated organic solvents". In: *Applied Geochemistry* 10.5, pp. 547–552. DOI: 10.1016/0883-2927(95)00025-9.

Weerasooriya, R. and B. Dharmasena (2001): "Pyrite-assisted degradation of trichloroethene (TCE)". In: *Chemosphere* 42.4, pp. 389–396. DOI: 10.1016/S0045-6535(00)00160-0.

Wejnerowska, G. and J. Gaca (2008): "Application of headspace solid-phase microextraction for determination of chloro-organic compounds in sewage samples". In: *Toxicology Mechanisms and Methods* 18.6, pp. 543–550. DOI: 10.1080/15376510701624084.

Wercinski, S. A. (1999): *Solid Phase Microextraction: A PRACTICAL GUIDE*. Boca Raton, FL, USA: CRC Press. 274 pp.

Westman-Brinkmalm, A. and G. Brinkmalm (2008): "A mass spectrometer's building blocks". In: *Mass Spectrometry*. Hoboken, NJ, USA: John Wiley & Sons, Ltd, pp. 15–87. DOI: 10.1002/9780470395813.ch2.

Wiegert, C., C. Aeppli, T. Knowles, H. Holmstrand, R. Evershed, R. D. Pancost, J. Macháčková, and Ö. Gustafsson (2012): "Dual carbon-chlorine stable isotope investigation of sources and fate of chlorinated ethenes in contaminated groundwater". In: *Environmental Science & Technology* 46.20, pp. 10918–10925. DOI: 10.1021/es3016843.

Wiegert, C., M. Mandalakis, T. Knowles, P. N. Polymenakou, C. Aeppli, J. Macháčková, H. Holmstrand, R. P. Evershed, R. D. Pancost, and Ö. Gustafsson (2013): "Carbon and chlorine isotope fractionation during microbial degradation of tetra- and trichloroethene". In: *Environmental Science & Technology*, p. 130604132217008. DOI: 10.1021/es305236y.

Wilcke, W., M. Krauss, and W. Amelung (2002): "Carbon isotope signature of polycyclic aromatic hydrocarbons (PAHs): Evidence for different sources in tropical and temperate environments?" In: *Environmental Science & Technology* 36.16, pp. 3530–3535. DOI: 10.1021/es020032h.

Yang, M., M. D. Annable, and J. W. Jawitz (2015): "Back diffusion from thin low permeability zones". In: *Environmental Science & Technology* 49.1, pp. 415–422. DOI: 10.1021/es5045634.

You, X., S. Liu, C. Dai, Y. Guo, G. Zhong, and Y. Duan (2020): "Contaminant occurrence and migration between high- and low-permeability zones in groundwater systems: A review". In: *Science of The Total Environment* 743, p. 140703. DOI: 10.1016/j.scitotenv.2020.140703.

Yu, S. and L. Semprini (2004): "Kinetics and modeling of reductive dechlorination at high PCE and TCE concentrations". In: *Biotechnology and Bioengineering* 88.4, pp. 451–464. DOI: 10.1002/bit.20260.

Zhang, Y., H. J. Tobias, G. L. Sacks, and J. Thomas Brenna (2012): "Calibration and data processing in gas chromatography combustion isotope ratio mass spectrometry: Calibration in IRMS". In: *Drug Testing and Analysis* 4.12, pp. 912–922. DOI: 10.1002/dta.394.

Zimmermann, J., L. J. S. Halloran, and D. Hunkeler (2020): "Tracking chlorinated contaminants in the subsurface using compound-specific chlorine isotope analysis: A review of principles, current challenges and applications". In: *Chemosphere* 244, p. 125476. DOI: 10.1016/j.chemosphere.2019.125476.

Zimmermann, J., P. Wanner, and D. Hunkeler (2021): "Compound-specific carbon isotope analysis of volatile organic compounds in complex soil extracts using purge and trap concentration coupled to heart-cutting two-dimensional gas chromatography–isotope ratio mass spectrometry". In: *Journal of Chromatography A* 1655, p. 462480. DOI: 10.1016/j.chroma.2021.462480.

Ziv-El, M., T. Kalinowski, R. Krajmalnik-Brown, and R. U. Halden (2014): "Simultaneous determination of chlorinated ethenes and ethene in groundwater using headspace solid-phase microextraction with gas chromatography". In: *Journal of Chromatographic Science* 52.2, pp. 137–142. DOI: 10.1093/chromsci/bms258.

Zwank, L., M. Berg, T. C. Schmidt, and S. B. Haderlein (2003): "Compound-specific carbon isotope analysis of volatile organic compounds in the low-microgram per liter range". In: *Analytical Chemistry* 75.20, pp. 5575–5583. DOI: 10.1021/ac034230i.

Zwank, L., M. Elsner, A. Aeberhard, R. P. Schwarzenbach, and S. B. Haderlein (2005a): "Carbon isotope fractionation in the reductive dehalogenation of carbon tetrachloride at iron (hydr)oxide and iron sulfide minerals". In: *Environmental Science & Technology* 39.15, pp. 5634–5641. DOI: 10.1021/es0487776.

Zwank, L., M. Berg, M. Elsner, T. C. Schmidt, R. P. Schwarzenbach, and S. B. Haderlein (2005b): "New evaluation scheme for two-dimensional isotope analysis to decipher biodegradation processes: Application to groundwater contamination by MTBE". In: *Environmental Science & Technology* 39.4, pp. 1018–1029. DOI: 10.1021/es049650j.

Appendix

A. Supporting Information for Chapter 2

Tracking chlorinated contaminants in the subsurface using compound-specific chlorine isotope analysis: A review of principles, current challenges and applications

Jeremy Zimmermann[1], Landon J.S. Halloran[1], Daniel Hunkeler[1]

Chemosphere 244 (2020) 125476

[1]Centre for Hydrogeology and Geothermics, University of Neuchâtel, Rue Emile-Argand 11, 2000 Neuchâtel, Switzerland

A.1. Supplementary tables

Table S1.: Reported range of δ^{37}Cl SMOC values for different chlorinated compounds with corresponding δ^{13}C VPDB values if measured.

Compound	δ^{13}C (‰)	δ^{37}Cl (‰)	Reference
Chloromethane		-6.00 ± 0.14	Tanaka and Rye (1991)
DCM		-0.26 ± 0.17	Numata et al. (2002b)
DCM		$+0.64 \pm 0.26$	Numata et al. (2002b)
CF		-2.9 ± 0.05	Numata et al. (2002b)
CT		-4.33 ± 0.12	Numata et al. (2002b)
CT		$+0.87 \pm 0.15$	Tanaka and Rye (1991)
1,2-DCA		-1.11 ± 0.26	Numata et al. (2002b)
1,2-DCA		$+1.07 \pm 0.15$	Tanaka and Rye (1991)
1,1,1-TCA		-5.0 ± 0.16	Numata et al. (2002b)
1,1,1-TCA	-26.17 ± 0.12	-3.54 ± 0.08	Shouakar-Stash et al. (2003)
1,1,1-TCA	-26.84 ± 0.18	$+1.39 \pm 0.07$	Shouakar-Stash et al. (2003)
1,1-DCE		$+2.9 \pm 0.40$	Numata et al. (2002b)
cis-1,2-DCE		$+0.08 \pm 0.20$	Numata et al. (2002b)
trans-1,2-DCE		-0.14 ± 0.23	Numata et al. (2002b)
TCE	-29.19 ± 0.14	-3.19 ± 0.07	Shouakar-Stash et al. (2003)
TCE	-31.90 ± 0.05	$+4.08 \pm 0.34$	van Warmerdam et al. (1995)
PCE	-33.84 ± 0.03	-2.54 ± 0.33	van Warmerdam et al. (1995)
PCE	-27.59 ± 0.08	$+0.29 \pm 0.01$	Beneteau et al. (1999)
PCB congeners		-3.5 ± 0.46	Mandalakis et al. (2008)
PCB congeners		-1.9 ± 0.46	Mandalakis et al. (2008)

A.2. Supplementary figures

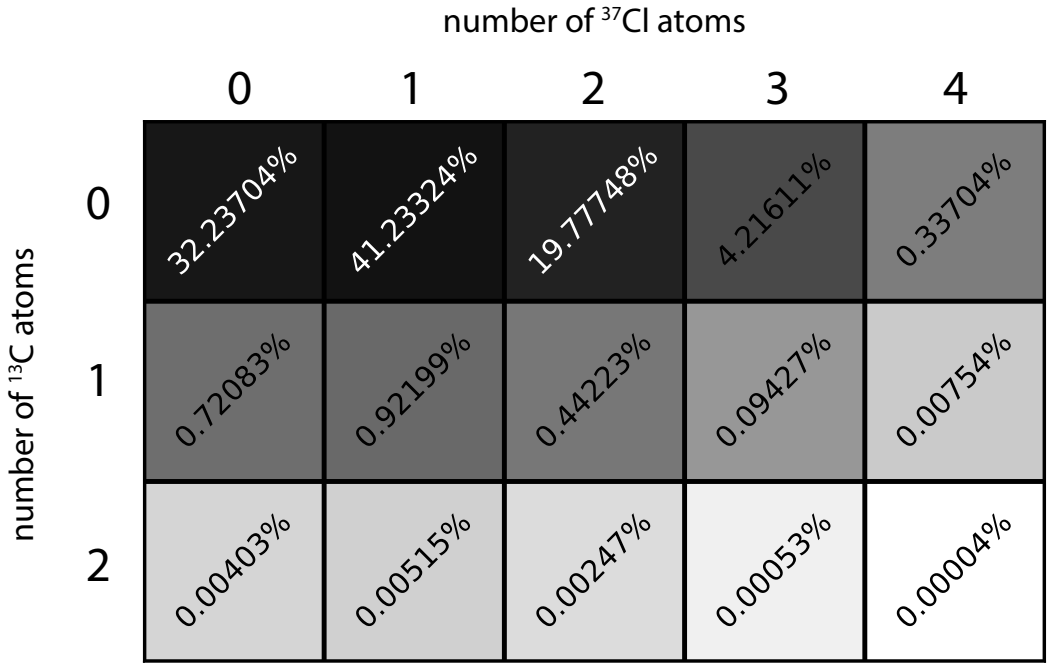

Figure S1.: Relative proportions of each isotopologue of PCE with $\delta^{13}C = 0‰$ (relative to VPDB) and $\delta^{37}Cl = 0‰$ (relative to SMOC). For information on TCE and *cis*-1,2-DCE isotopologue proportions, see Halloran et al. (2019).

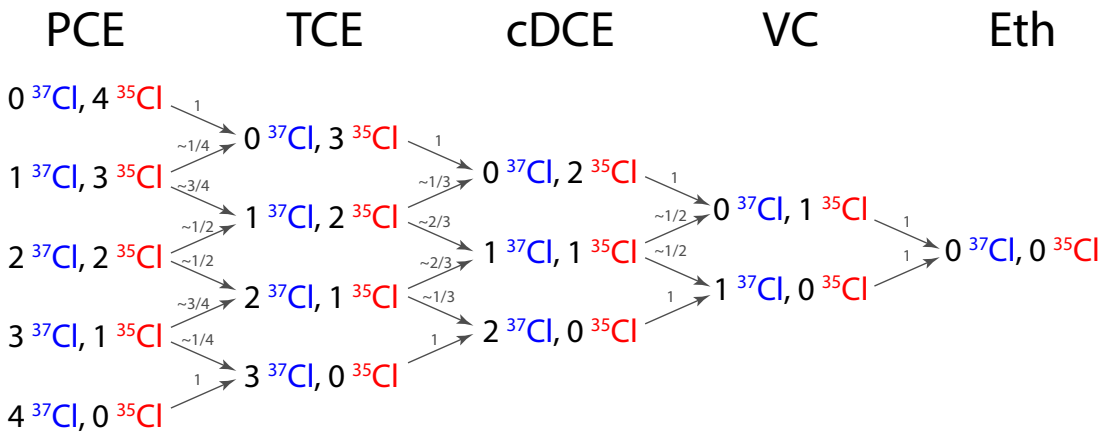

Figure S2.: Schematic for progressive dechlorination of PCE to ethene, considering chlorine isotopologues of each molecule. The approximate proportions of each reaction pathway are indicated in grey. The true values are modified by the apparent kinetic isotope effect (Badin et al. 2018). This results in, for example, slightly more than 1/2 of *cis*-1,2-DCE with 1 ^{37}Cl and 1 ^{35}Cl being degraded to VC with 1 ^{35}Cl and slightly less than 1/2 being degraded to VC with 1 ^{37}Cl. Adapted from Hunkeler et al. (2009) and van Breukelen et al. (2017).

B. Supporting Information for Chapter 3

A design of experiments to optimize solid-phase microextraction for compound-specific chlorine isotope analysis of chlorinated ethenes

Jeremy Zimmermann[1,a], Ouassim M. Boukaroum[1,2,a], Daniel Hunkeler[1]

In preparation

[1]Centre for Hydrogeology and Geothermics, University of Neuchâtel, Rue Emile-Argand 11, 2000 Neuchâtel, Switzerland

[2]Laboratoire de Chimie Environnement, Aix-Marseille University, 3 Place Victor Hugo, 13331 Marseille, France

[a]These authors contributed equally to the work

B.1. Modified multiple ion method

Tetrachloroethene – Calculation of weighting factors a, b, c, d according to the modified multiple ion method (Jin et al. 2011):

$$a = \frac{I_{166} + I_{164}}{(I_{166} + I_{164}) + (I_{131} + I_{129}) + (I_{96} + I_{94}) + (I_{61} + I_{59})}$$

$$b = \frac{I_{131} + I_{129}}{(I_{166} + I_{164}) + (I_{131} + I_{129}) + (I_{96} + I_{94}) + (I_{61} + I_{59})}$$

$$c = \frac{I_{96} + I_{94}}{(I_{166} + I_{164}) + (I_{131} + I_{129}) + (I_{96} + I_{94}) + (I_{61} + I_{59})}$$

$$d = \frac{I_{61} + I_{59}}{(I_{166} + I_{164}) + (I_{131} + I_{129}) + (I_{96} + I_{94}) + (I_{61} + I_{59})}$$

Trichloroethene – Calculation of weighting factors a, b, c according to the modified multiple ion method (Jin et al. 2011):

$$a = \frac{I_{132} + I_{130}}{(I_{132} + I_{130}) + (I_{97} + I_{95}) + (I_{62} + I_{60})}$$

$$b = \frac{I_{97} + I_{95}}{(I_{132} + I_{130}) + (I_{97} + I_{95}) + (I_{62} + I_{60})}$$

$$c = \frac{I_{62} + I_{60}}{(I_{132} + I_{130}) + (I_{97} + I_{95}) + (I_{62} + I_{60})}$$

B.2. Influence of split ratio on peak shape for SPME injection

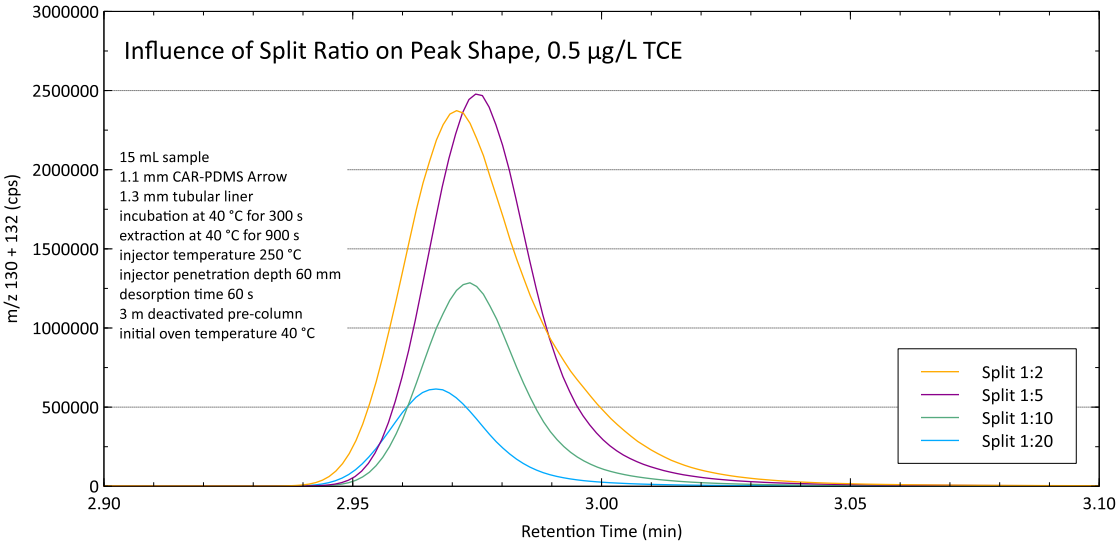

Figure S1.: Influence of split ratio on TCE peak shape for SPME injection.

B.3. Central composite design

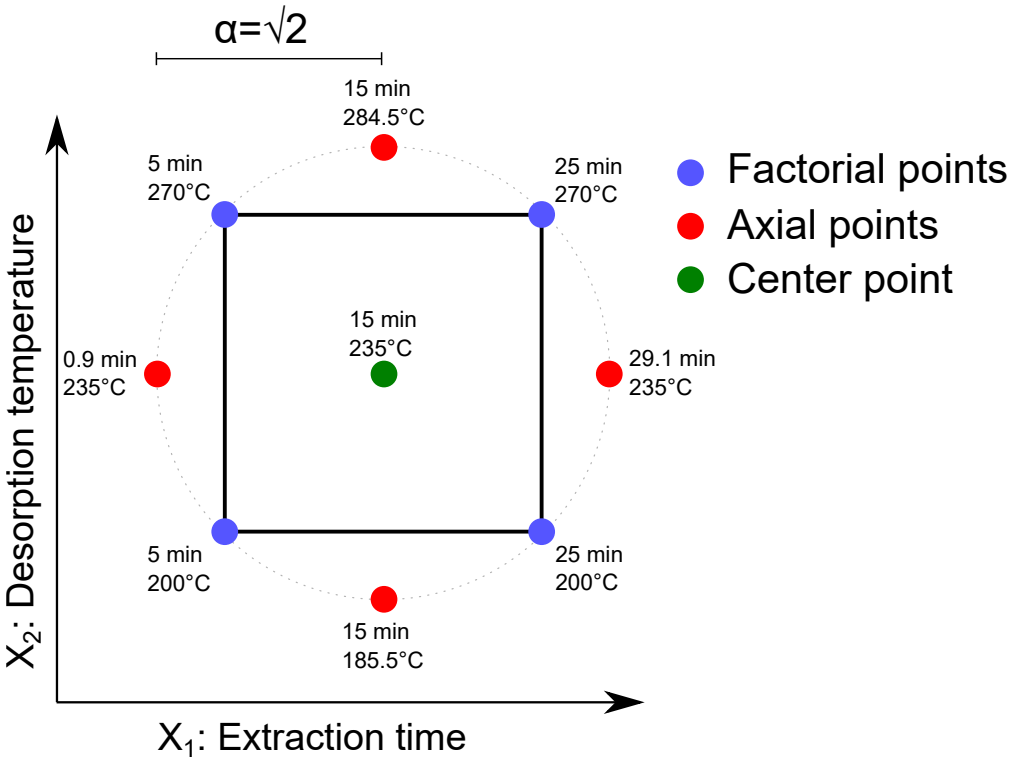

Figure S2.: Central composite design factors for two levels each of the two factors extraction time and desorption time and an α of $\sqrt{2} \sim 1.414$.

B.4. Response surface validation

Table S1.: Resulting intensity for measurements of three random samples compared to calculated responses, as a function of extraction time and desorption temperature. No significant difference according to a 95% confidence interval is observed between measured responses and responses predicted by the response surface. The response surface correctly predicts the intensity for SPME.

M.	Factors		Responses		Difference	Standard deviation 1σ	p-value
	Extraction time X_1 (min)	Desorption temp. X_2 (°C)	Measured intensity PCE m/z 164 + 166 (cps)	Calculated intensity PCE m/z 164 + 166 (cps)	(cps)	(cps)	(%)
10	8.88	222.63	9 540 051	8 872 661	667 390	526 712	22.9
11	21.12	222.63	11 701 383	12 489 157	−787 775	526 712	16.1
12	15	259.75	11 871 806	11 486 707	385 099	526 712	47.9

C. Supporting Information for Chapter 4

Compound-specific carbon isotope analysis of volatile organic compounds in complex soil extracts using purge and trap concentration coupled to heart-cutting two-dimensional gas chromatography–isotope ratio mass spectrometry

Jeremy Zimmermann[1], Philipp Wanner[2], Daniel Hunkeler[1]

Journal of Chromatography A 1655 (2021) 462480

[1]Centre for Hydrogeology and Geothermics, University of Neuchâtel, Rue Emile-Argand 11, 2000 Neuchâtel, Switzerland

[2]Department of Earth Sciences, University of Gothenburg, Guldhedsgatan 5a, 41320 Göteborg, Sweden

C.1. Concentration measurement

Table S1.: Parameters for measuring VOC concentrations in soil extracts.

Parameter	Unit	Value
Method		Purge & trap with GC-MS
Sample volume	(mL)	5
Purge time	(min)	11
Column		DB-VRX
Column diameter	(mm)	0.18
Column length	(m)	20
Film thickness	(µm)	1
Detection limits *trans*-1,2-DCE, *cis*-1,2-DCE PCE, DCM, CF, BTEX	($\mu g\,L^{-1}$)	0.1
Detection limits 1,1,2,2-TeCA, CT, TCE	($\mu g\,L^{-1}$)	0.2

C.2. Purge & trap parameters

Table S2.: Parameters for the Teledyne Tekmar Stratum purge & trap system.

Parameter	Unit	Value	Parameter	Unit	Value
Valve oven temperature	(°C)	150	Desorb temperature	(°C)	250
Transfer line temperature	(°C)	150	Desorb flow	($mL\,min^{-1}$)	400
Sample mount temperature	(°C)	90	Bake time	(min)	15
Purge ready temperature	(°C)	35	Bake temperature	(°C)	260
Condenser ready temperature	(°C)	40	Bake flow	($mL\,min^{-1}$)	300
Standby flow	($mL\,min^{-1}$)	0	Condenser bake temperature	(°C)	200
Purge time	(min)	10 to 20	Focus temperature	(°C)	−120
Purge flow	($mL\,min^{-1}$)	40	Inject time	(min)	1
Dry purge time	(min)	0 to 1	Inject temperature	(°C)	180
Dry purge temperature	(°C)	35	Standby temperature	(°C)	120
Dry purge flow	($mL\,min^{-1}$)	40 to 100	Number of bake rinses		3
Desorb preheat temperature	(°C)	245			
Desorb time	(min)	2			

C.3. GC-GC parameters

Table S3.: GC-GC parameters used to calculate pressures for 2D setup. Calculated outputs in **bold**.

Parameter	Unit	Value
Carrier gas		Helium
Initial oven temperature	(°C)	70
Primary flow	(mL min^{-1})	1.5
Primary column diameter	(mm)	0.32
Primary column length	(m)	30
Inlet pressure (first column)	(psi)	**14.75**
Secondary flow	(mL min^{-1})	2.5
Secondary column diameter	(mm)	0.32
Secondary column length	(m)	15
Secondary detector outlet pressure	(psi)	17.196
(here: combustion furnace, set to 2.5 psi above atmospheric pressure)		
PCM pressure (secondary column)	(psi)	**9.94**
Primary detector outlet pressure (FID) at atmospheric pressure	(psi)	14.696
Restrictor flow (same as secondary column)	(mL min^{-1})	2.5
Restrictor diameter	(mm)	0.15
Restrictor length	(m)	**0.947**

C.4. Physical properties of the extraction solvents

Table S4.: Physicochemical properties of the extraction solvents. Data from European Chemicals Agency (2020).

Systematic name	Abbrv.	Density ρ ($g\,cm^{-3}$)	Boiling point T_b (°C)	Vapor pressure (25 °C) (Pa)	Misc. in H_2O (20 °C)
Methanol	MeOH	0.79	65	16927	Miscible
Tetraethylene glycol dimethyl ether / 2,5,8,11,14-Penta-oxapentadecane	TGDE	1.01	275	0.25	Miscible

C.5. Method detection limit determination

The stop criteria for the MDLs are exemplified for TCE (Figure S1) and PCE (Figure S2) for a 10 minute purge at 25 °C over 7 concentration levels with 5 replicates each ranging from about 6 µg L^{-1} to 80 µg L^{-1}. For TCE, the MDL corresponds to the lowest concentration level for which the $\delta^{13}C$ value is still within the ±0.5‰ range around the moving mean of the higher concentration levels. For PCE, the MDL corresponds to the lowest concentration level for which $1\sigma \leq 0.5‰$. As well as depicting the isotopic linearity, Figures S1 and S2 also illustrate the concept of linearity as it is usually defined in analytical chemistry; that is the linear relationship between signal intensity and concentration.

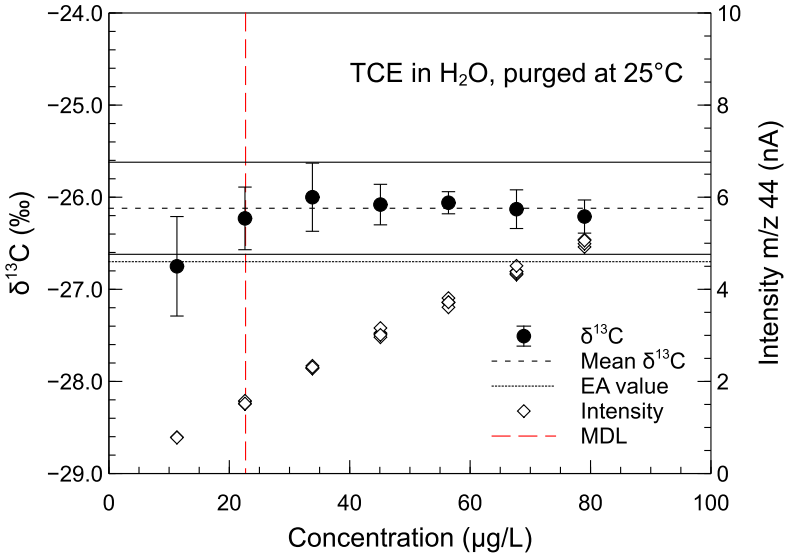

Figure S1.: Procedure for carbon isotope MDL determination of TCE in water. The dashed line is the mean $\delta^{13}C$ value for the six highest concentration levels. The $\delta^{13}C$ value for the lowest concentration level is outside the ±0.5‰ interval around the mean value.

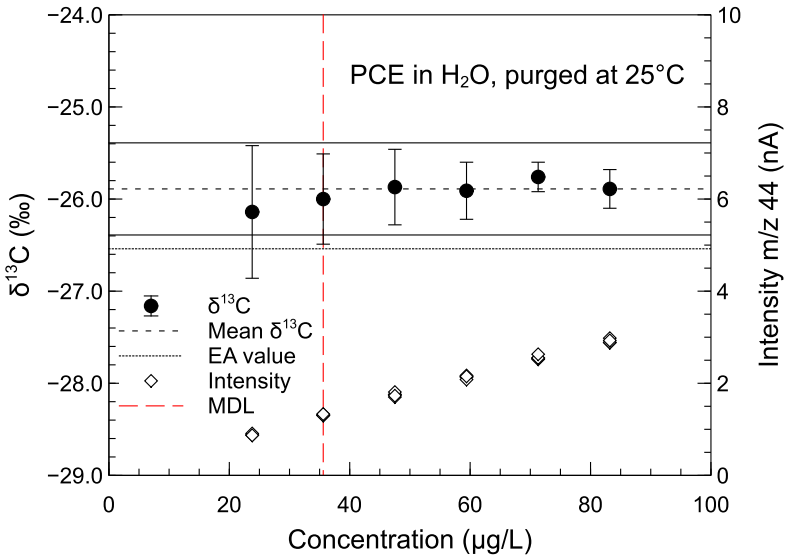

Figure S2.: Procedure for carbon isotope MDL determination of PCE in water. Here, the $\delta^{13}C$ value for the lowest concentration level has a standard deviation that exceeds ±0.5‰.

C.6. Calculation of soil MDL

The samples from the field site were taken at a soil-to-extraction-solvent ratio of 10 g to 15 g of wet soil in 20 mL of solvent. To obtain the concentration of VOC in soil in $\mu g\,g^{-1}$, the concentrations in solvent in $\mu g\,L^{-1}$ are multiplied by this ratio, i.e. the MDL for soil concentrations is a factor of $0.020\,L/0.010\,kg = 2$ higher than the MDL in solvent. Multiplied by the necessary dilution by 10 (v/v) for TGDE, this will yield an MDL in soil, e.g. for TCE, of $11\,\mu g\,L^{-1} \times 2\,L\,kg^{-1} \times 10\,L\,L^{-1} = 220\,\mu g\,kg^{-1}$ or $0.22\,\mu g\,g^{-1}$.

D. Supporting Information for Chapter 6

Assessing the impact of reactive back-diffusion on a complex chlorohydrocarbon plume using compound-specific isotope analysis

Jeremy Zimmermann[1], Daniel Hunkeler[1]

In preparation

[1]Centre for Hydrogeology and Geothermics, University of Neuchâtel, Rue Emile-Argand 11, 2000 Neuchâtel, Switzerland

D.1. Soil profiles from source zone

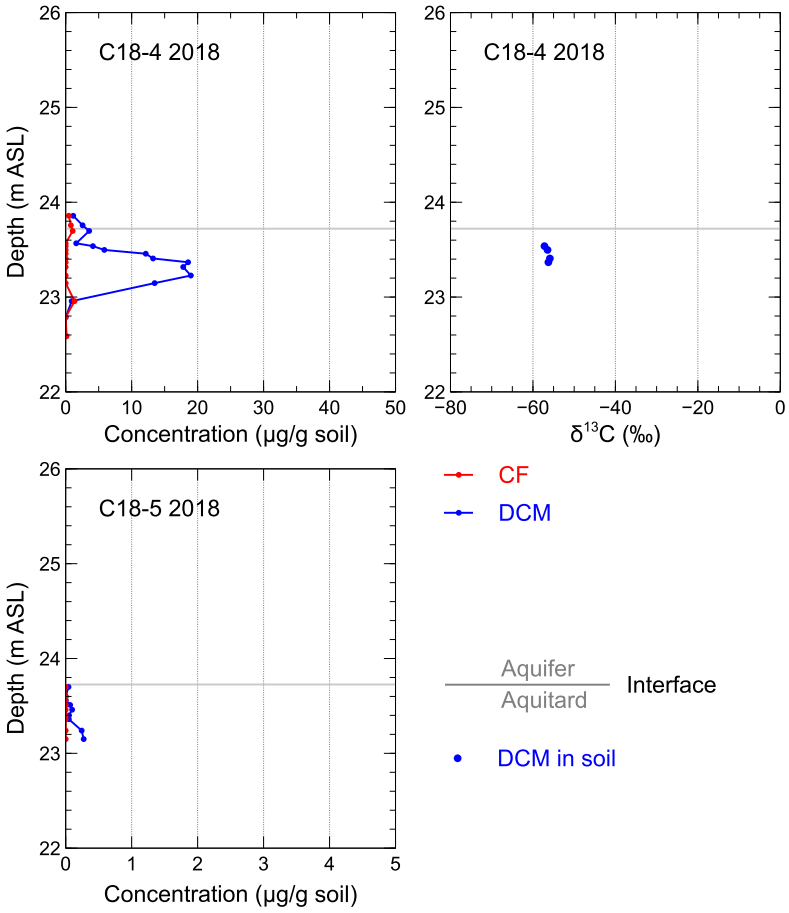

Figure S1.: Soil concentrations of initial contaminant and degradation product CF, and soil concentrations and compound-specific carbon isotope values ($\delta^{13}C$) of degradation product DCM over depth. Cores C18-4 and C18-5 taken within the source zone in March of 2018.

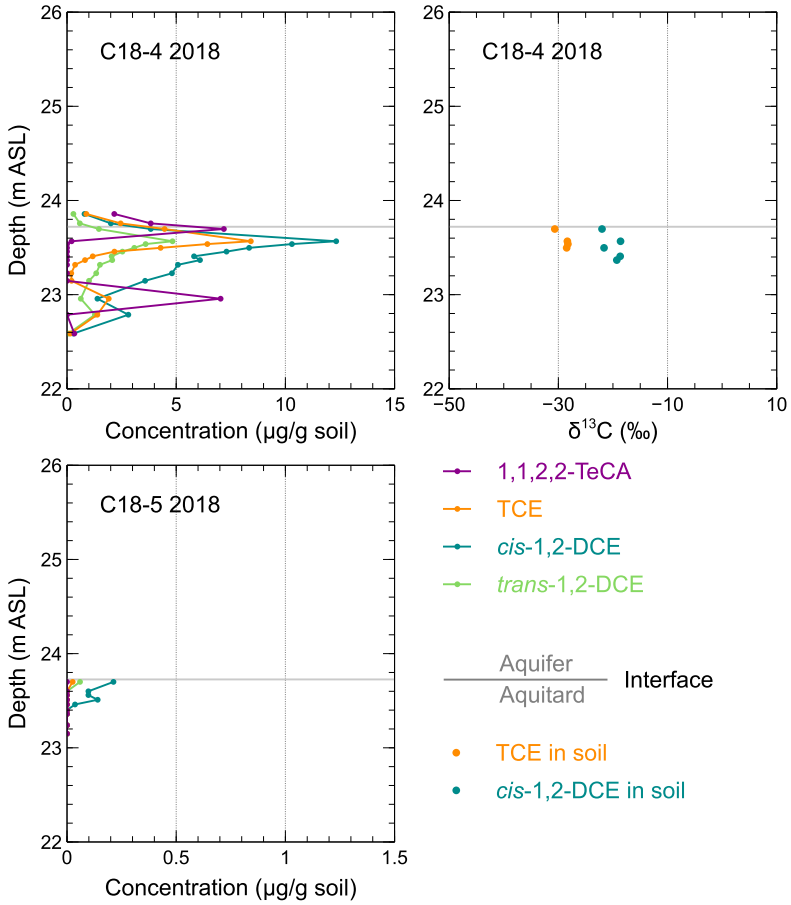

Figure S2.: Soil concentrations of initial contaminant 1,1,2,2-TeCA and degradation product *trans*-1,2-DCE, and soil concentrations and compound-specific carbon isotope values ($\delta^{13}C$) of degradation products TCE and *cis*-1,2-DCE over depth. Cores C18-4 and C18-5 taken within the source zone in March of 2018.